Optimizing cultivated meat techno-economics:

Cell growth modeling review and recommendations

Bert Frohlich*, PhD, BioFarm Designs, LLC.
Faraz Harsini, MSc, PhD, DipACLM, Good Food Institute
Elliot Swartz, PhD, Good Food Institute

*Corresponding author: bert@biopharmdesigns.com

Suggested citation: Frohlich, B., F. Harsini, and E. Swartz. *Optimizing cultivated meat techno-economics: Cell growth modeling review and recommendations*. Washington D.C.: Good Food Institute. 2025. https://doi.org//10.62468/xcjx6040.

Abstract

Improved digital tools and models are needed to accelerate cultivated meat toward commercialization through enabling more efficient bioreactor designs and operation.

Cultivated meat (CM) offers promise as a sustainable protein source, but reaching cost parity with conventional meat remains a challenge. Scaling production will require very large bioreactors, which are expensive to design and build; therefore, accurate predictive models are essential to guide investment and design choices. These large systems will inherently exhibit heterogeneous environments, especially as high cell concentrations increase culture viscosity. Simplified but biologically informed models are needed to integrate with computational fluid dynamics simulations. This sets our framework apart from flux-based or genome-scale models, which are better suited for media optimization rather than reactor design at an industrial scale. Leveraging modern digital tools is therefore critical to move the industry toward economic viability and achieve industrial-scale production.

A central part of the push toward cost-effective scale-up is building performance models, which are mathematical frameworks used to estimate how cells and bioreactors behave under different conditions. The performance model framework is most useful when structured to separate intracellular processes from extracellular and environmental ones, so each part of the system can be examined and improved independently. The framework includes three components: the cell growth model, the bioreactor environment model, and the system-level model that simulates operational controls. In this report, we focus on the cell growth model, which covers predictions of biomass accumulation, substrate use, and metabolite formation, because cell-level processes set the foundation for predicting productivity, costs, and product characteristics, and are a prerequisite for building the other model components.

Current modeling approaches face major limitations. Most techno-economic assessments assume static and homogeneous conditions, which do not reflect the gradients and heterogeneity of large-scale bioreactors. Empirical and semi-empirical models often fail to capture dynamic cellular behavior, particularly the complex relationships between substrates like glucose and glutamine, or the impact of metabolite accumulation, such as lactate and ammonium. Missing baseline data, including cell mass and biomass composition, further complicate normalization across cell lines. Together, these gaps limit predictive power and reduce the usefulness of digital twins for guiding process design.

To address the lack of dynamic, biologically informed models and the shortage of CM-relevant data, we analyzed decades of biopharma data alongside the limited CM-specific data available to evaluate how well biopharma cell lines reflect the behavior of CM-relevant cells. Our analysis identified key parameters, modeling needs, and data gaps, such as dry cell mass, biomass composition, and the effects of environmental variables like temperature, pH, and osmolality on cell growth. We reviewed existing techno-economic models and the biological assumptions behind them, evaluated published data across biopharma and CM-relevant cell lines, and identified where data are missing or incompatible.

These insights lay the groundwork for developing structured models of cell growth that improve predictions for bioreactor performance. Unlike empirical models, structured models account for intracellular and extracellular processes separately, which can include explicit representation of metabolite pools and energy carriers such as ATP and NADH. Our findings show that energetics-based models are especially useful because ATP and NADH yields remain consistent across cell lines. They provide reliable anchors for describing growth kinetics, substrate use, and metabolite formation. These models also point to strategies such as improved feeding, cell line adaptation, or genetic modification to enhance efficiency. Energetics-based modeling provides a tractable and scalable path toward predictive digital twins of CM processes.

In addition, opportunities in genetic engineering, such as circumventing the Warburg Effect and adaptation strategies to reduce the inherent inefficiencies of animal cell metabolism, offer promising avenues to improve productivity and reduce costs. More empirical data will be needed to validate and refine these models, particularly time-series measurements of nutrient use, waste accumulation, energetics, and adaptive responses under relevant culture conditions.

Table of contents

Introduction

Cultivated meat (CM) is a new form of meat production that involves the cultivation of animal cells in a safe and controlled environment. This approach presents society with the opportunity to feed more people with fewer resources, meeting the growing global demand for protein in a more humane way. While the biological knowledge and techniques to culture muscle, fat, and other cell types are well established, transforming animal cell culture into a viable platform for large-scale food production presents a multifaceted challenge. This transformation hinges not only on solving engineering problems that lower costs and enhance scale, efficiency, and productivity, but also on developing a deeper understanding of the complex interactions between cells, cell culture media, scaffolds (in some cases), and bioreactor environments. To make any significant impact on conventional meat consumption, CM will need to be manufactured at massive scales to, in turn, capture the economies of scale needed to achieve cost parity. Therefore, tools are needed to predict the performance of cell culture processes at scales that have never been attempted. As with other complex systems, computational models offer powerful tools to understand, predict, and optimize the CM production process—ultimately accelerating development and reducing costs.

Techno-economic models (TEMs) combine mathematical models of the underlying biological and physical (or physicochemical) processes with analyses of key financial parameters to evaluate the performance and economics of a given technology. TEMs are particularly useful in early technology development, as they enable the identification of cost drivers to inform decision-making, test hypotheses, and guide research. Several published TEMs of hypothetical, scaled CM processes have illuminated cost drivers such as the cell culture media and manufacturing equipment used in CM production (Goodwin, Aimutis, and Shirwaiker 2024). However, these TEMs have been based on a set of assumptions rather than a true prediction of performance. We suggest that an underlying performance model is needed to support TEMs to overcome their current limitations:

1. Most models have focused on evaluating the economics of a limited set of predefined processes (e.g., stirred-tank reactors limited to 10-20K liter scale). These models largely ignore the many other processes being trialed in the industry, including other bioreactor types (e.g., air-lift, hollow fiber, fixed bed), operational modalities, and scales of production (Harsini and Swartz 2024; Laura Pasitka et al. 2024).
2. The underlying models for cell growth and bioreactors feature static stoichiometries, homogenous bioreactor mixing, and fixed feeding strategies and growth rates that limit performance optimization and evaluation of trade-offs. In short, more complex models may be necessary to increase predictive power and interrogate different question sets or use cases.
3. The underlying models feature layers of assumptions taken from other industries (e.g., biopharma), and it remains an open question to what extent these assumptions apply to the different cell types, species, and process settings used in CM production.
4. The framing of TEMs is often, “hypothetical process X is not economically viable, therefore cultivated meat is not economically viable.” This framing ignores the reality that meat products

vary significantly in cost and complexity, and different processes will be better suited to certain product types versus others.

Our collective experience led us to conclude that the most economically viable method of CM manufacturing for any given product is not yet known. Consequently, developing a model for such a process is not possible at this time. Instead, models should be constructed to serve as tools that enable more efficient discovery of economically viable paths forward while the industry remains small and nimble. To accomplish this, models should not simply evaluate one-off hypothetical processes. Rather than asking what level of performance is required to achieve favorable unit economics for a given product, a performance model can be framed and constructed to evaluate which bioreactor design will be more productive and estimate the consumption of raw material and utilities quantitatively. Model development also builds an understanding of the critical parameters for predicting the overall performance of any given bioprocess, with the ultimate goal of creating a digital twin.

In this report, we describe a modeling approach centered on the evaluation of the performance-to-cost ratio (PCR) to enable a future bioprocess optimization strategy. We present a modeling framework that consists of a performance model incorporated with an underlying cell growth model, a physical bioreactor environment model, and a bioreactor system model. The performance model will be integrated alongside a cost model for a given bioreactor, process, or full facility to derive a PCR that can be used as a tool for testing hypotheses for performance improvement and cost reduction.

Given the number of variables and considerations for each component model, this report focuses solely on the cell growth model. We present the governing equations important for cell growth and review the literature that describes the key parameters and considerations of the equation set, including cell size, mass, composition, proliferation and differentiation kinetics, metabolite inhibition, and stoichiometry. Where possible, we compare data from cells used in biopharma with those used in CM production and assumptions made in prior TEMs. Lastly, we describe the key data gaps and incomplete information surrounding these parameters. Throughout, we provide clear direction for the CM research community by describing cell growth knowledge and gaps alongside a guiding modeling framework.

Future reports will replicate this process for the other component models, culminating in model construction and outputs centered on comparative evaluation of the performance of different bioreactor systems. Ultimately, the work presented here and future models that build on it will need to be validated and/or refined through iterative, empirical experimentation at increasingly larger scales. As more data become publicly available, open models created from this work will evolve in complexity and customization, helping end users answer new questions as the technological readiness of the CM sector matures. This work lays the foundation for a more complete understanding of large-scale animal cell culture and the techno-economics of CM production.

Report organization

The report consists of four sections that outline the development and assessment of an improved cell growth and performance-to-cost modeling framework for CM production.

- **Section 1 describes the performance modeling framework**, which is structured in three nested components: a cell growth model, a bioreactor environment model, and a bioreactor system model. It explains the rationale for focusing first on cell growth as the core driver of productivity before layering on bioreactor and system-level considerations, which will be the focus of separate studies.
- **Section 2 describes the cell growth model,** outlining the mathematical equations and modeling approaches to simulate cell proliferation, differentiation, death, nutrient consumption, metabolite formation, and inhibition. It explains options for modeling these processes, including empirical equations and structured energetics-based models.
- **Section 3 provides a critical review of the data** available to define each parameter required by the modeling approaches in Section 2. It evaluates the strength and consistency of existing evidence, highlights areas where assumptions rely on limited information, and identifies specific gaps that researchers must address to build reliable models.
- **Section 4 examines the big picture and broader challenges** in modeling CM cell growth, including the limitations of current approaches described in Section 2 and the data gaps identified in Section 3. It explores opportunities to improve modeling frameworks and outlines directions for developing more robust and adaptable tools.
- **Section 5 summarizes key conclusions and recommendations,** based on decades of animal cell culture research and their relevance to CM. It emphasizes the inefficiency of animal cell metabolism, suggests ATP and NADH as a unifying basis for modeling, and notes the ability of cells to adapt under stress or use alternative substrates. It identifies major data gaps, particularly for dry cell mass, continuous culture, and energetics, and outlines priorities for experimental work and cell line and process development.

Section 1. Modeling framework for techno-economic assessment

The modeling framework presented here provides the basis for a future bioprocess optimization strategy. At the highest level, the model system consists of a performance component and a cost component (**Figure 1.1**). Together, these components allow the PCR to be evaluated for a given process technology. The concept of the PCR can be applied to the cell culture bioreactor design itself as well as the overall manufacturing facility.

The PCR can be defined as:

$$PCR = \frac{U_X V_w}{P} = U_X \frac{V_w}{P}$$ **Equation 1**

Symbol	Definition	Typical units
U_x	Volumetric productivity of the bioreactor	g product/L/day or kg WCW/m^3/day
V_w	The working volume of the bioreactor	m^3 or L
P	Price of the bioreactor	Dollars ($)

As depicted in Figure 1.1, the PCR can be used to gauge whether a manufacturing technology is economically viable and permits comparison between alternative approaches. In essence, the PCR can serve as an optimization function to be maximized. To improve the PCR, either the performance must be enhanced, the cost reduced, or both.

In the cost model component, various layers or levels are depicted that enable assessments to be conducted at granularities for different use cases. A PCR can be focused solely on the bioreactor, or it could cover the entire facility, including all upstream process (USP) and downstream process (DSP) areas. **Table 1.1** lists examples of PCRs for various levels.

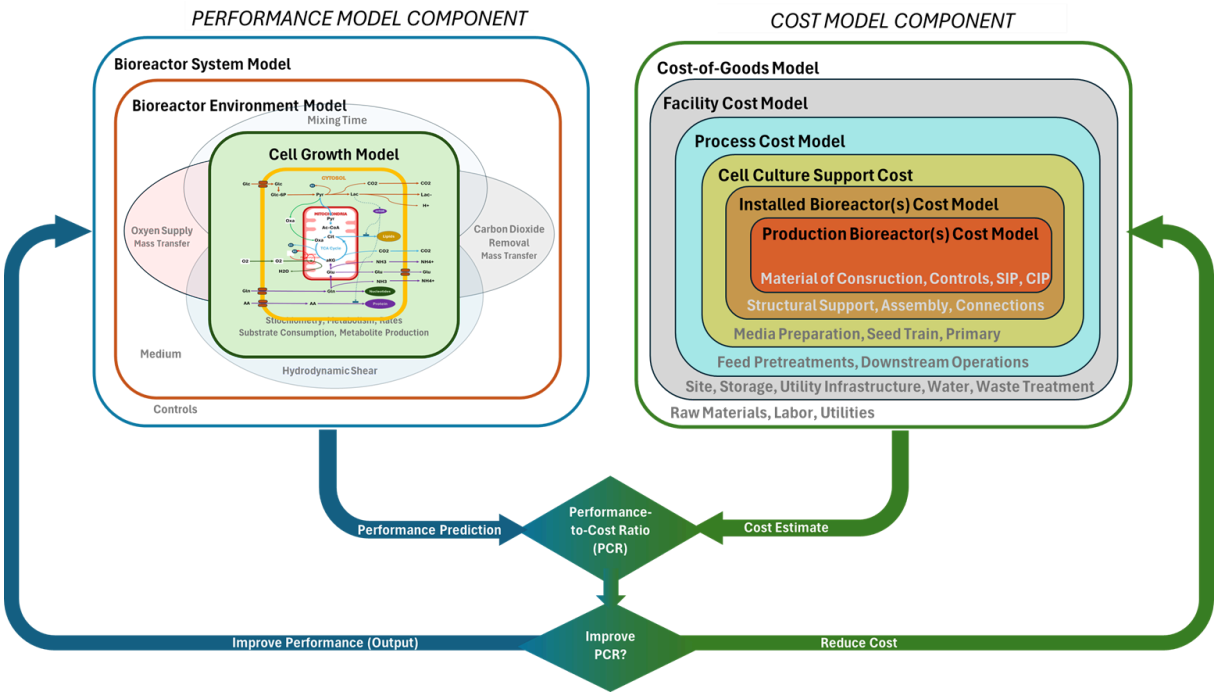

Figure 1.1. Schematic of the overall modeling framework consisting of a bioreactor performance and cost model component to assess the performance-to-cost ratio.

Table 1.1: Examples of PCR ratios at various levels of technology or business evaluation. Metrics can be based on total biomass as wet cell weight (WCW) or dry cell weight (DCW), or even a specific biomass component like protein.

Level	Performance Parameter	Cost Parameter	PCR
Enterprise	Profit Margin	Total Operating Expenses	Profitability (e.g., $ Profit / $ Cost)
Manufacturing	Total Product Output	Cost of Goods Sold (COGS, includes depreciation)	Net Margin (e.g., kg WCW / $ Cost)
Facility	Overall Facility Output	Total Facility Cost	Capital Efficiency (e.g., kTon DCW/yr / $1,000,000 Facility)
Overall Process	Final Product Output	Installed Process Cost (USP + DSP)	Capacity to Cost Ratio (e.g., kTon DCW/yr / $ Installed Cost)
Cell Culture Process	Biomass Output	Installed Process Cost (Upstream Only)	Upstream Capital Efficiency (e.g., kTon DCW/yr / $ USP Installed Cost)
Installed Bioreactor	Bioreactor Volumetric Productivity	Bioreactor Installed Cost	Productivity-to-Cost Ratio (e.g., kg WCW/m3 BR Volume / $)
Bioreactor	Bioreactor Volumetric Productivity	Bioreactor Purchase Price	Productivity-to-Cost Ratio (e.g., kg WCW/m3 BR Volume / $)

A significant challenge of this ongoing work will be identifying the simplest biological models that will be compatible with complex physical models of large-scale bioreactors. This will require balancing a model's predictive power for a given application with its mathematical complexity and computational intensity so that the various components can be coupled without system overload. **Figure 1.2** depicts how the various model components might be overlapped to perform a given function. The greater the overlap, the greater the model's complexity and the number of parameters required. Highly complex genome-scale models and metabolic flux analyses will be indispensable in generating more productive cell lines and high-performing, low-cost media. However, it is doubtful that they should be (or can feasibly be) coupled with the more sophisticated physics-based models that govern the bioreactor environment. We speculate that once the most salient aspects of a cell line's growth and metabolism are deduced, a simpler model can be used downstream for process optimization. However, nothing precludes breaking down a design challenge into small components and using more specialized models individually before attempting to build a larger interconnected digital twin.

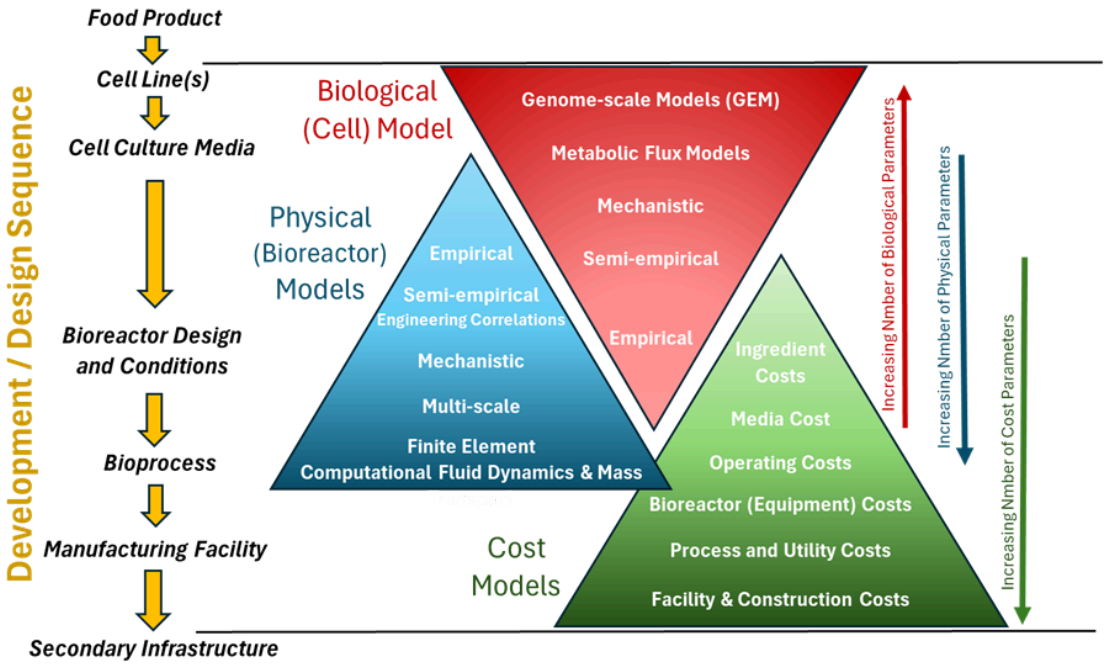

Figure 1.2: Coupling of model types to create systems of tractable complexity for bioreactor and bioprocess design. The degree of overlap between the biological, physical, and cost models represents the total model system's computational intensity.

1.1 The performance model

The performance model is composed of three distinct, nested components: the cell growth model, the bioreactor environment model, and the bioreactor system model (**Figure 1.3**). With this approach, the cellular response to prevailing conditions can be applied to multiple potential microenvironments in the bioreactor while the overall operating mode and control dynamics of the bioreactor are captured computationally by the bioreactor system model. The focus of this report is on the cell growth model.

Future work will describe the remaining model components and how they are coupled, culminating in a performance model that can be adapted to different cell lines and bioreactor designs.

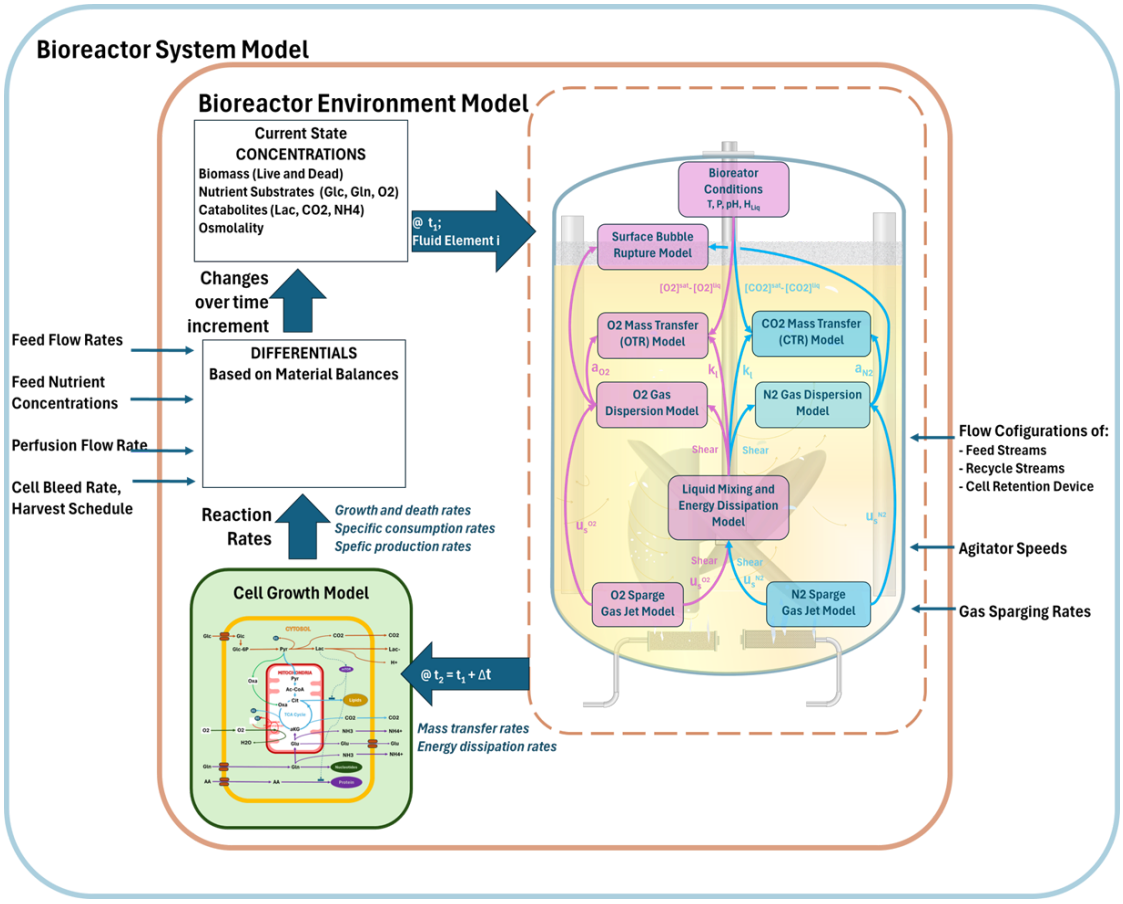

Figure 1.3. Overview schematic of the performance model, consisting of three individual component models.

The cell growth model

The cell growth model predicts cell growth, metabolism, and viability based on substrate and metabolite concentrations as well as physical forces (e.g., shear) that are simulated by the bioreactor environment model. For CM production, the primary goal of the cell growth model is to capture the predominant processes driving the accumulation of cell mass and cellular composition. The equations and parameters that describe these processes are primarily aimed at cell line characteristics and the surrounding liquid medium, which defines the cells' immediate environment. How they interact during cell proliferation and/or differentiation is crucial to predicting rates of biomass accumulation and substrate consumption, as well as the resulting shift in the composition of the extracellular medium. The cell growth model is discussed in detail in Section 2.

The bioreactor environment model

The bioreactor model simulates the internal environment of the bioreactor, including substrate and metabolite concentrations, gas dispersion, mass transfer, and shear forces that dictate the conditions to which the cells are exposed. There are important trade-offs that must be considered, such as the

delivery of oxygen and nutrients to the cell through mixing and gas sparging, which can also adversely impact the cells if too vigorous. The biopharmaceutical industry is well aware that induced stress due to bubble collapse can be the primary factor influencing cell viability and that the success of industrial cell culture can largely be attributed to the use of shear protectants added to the medium. Modeling the environment within the bioreactor is complex, involving the distribution of liquid shear rates, gas bubble sizes and interfacial shear associated with gas jets around the sparger element, and the effects of shear protectants that still need to be optimized for food applications. Also, physical conditions can change with different bioreactor designs, and heterogeneity becomes more pronounced at larger working volumes. Thus, the industry needs models that can account for the various physicochemical microenvironments and predict the global performance of a bioreactor. When coupled with the cell model, they will enable prediction of the bioreactor's internal environment impact on the rates of cell growth, inhibition, death, and even lysis. However, accounting for spatiotemporal aspects of the bioreactor environment will increase complexity and computational requirements.

The bioreactor system model

The bioreactor system model governs the operation of the bioreactor, including feeding rates of nutrients, gas flow for aeration and stripping, power for mixing, perfusion streams, cell bleed, and harvest schedule. This component of the performance model acts as the outer envelope of the system that dictates the material balance equations describing the desired mode of operation (e.g., fed-batch, perfusion, continuous). It can be envisaged as the control system surrounding the bioreactor, whether it is a stirred tank, airlift, hollow fiber, or some other design. The bioreactor environment and system models will be further defined in future reports.

1.2 The cost model

A cost model can fundamentally examine production costs at different levels of capital and operational expenditures. This flexibility permits users to evaluate aspects ranging from profitability of the entire enterprise, capital efficiency, or bioreactor volumetric productivity (**Table 1.1**).

We envisage the cost model as a separate component to the overall model system supporting TEMs. The cost model would take the same design specifications as those given to the cell and bioreactor component models to determine performance. A cost estimate would then be assembled based on these specifications, presumably drawing from a cost database for equipment, materials of construction, and infrastructure tied to various scaling factors. Together with the performance metric and the cost estimate, the PCR can be determined.

As a cautionary note, comparing PCRs of design options at different levels may not yield the same conclusion. Capital efficiency can be a surrogate for total running cost only if the facility or equipment design does not significantly impact non-capital expenses such as construction times, labor, utilities, or material requirements. For example, an airlift bioreactor may be less expensive to build for a similar capacity than a stirred-tank reactor but may require substantially more gas consumption, which may result in its apparent PCR offset by increased utility costs. Similarly, continuous unit operations may also reduce the labor and utilities required for repeatedly cleaning and sterilizing process equipment.

Section 2. The cell growth model: key components, inputs, and equations

2.1 Approach to cell growth modeling

In CM manufacturing, a key determinant of the volumetric productivity and overall economics is the rate and efficiency of biomass generation. Beyond productivity, the cellular nutritional composition, including protein and lipid content, will also be important determinants of sensory attributes and, ultimately, market value. Therefore, a cell growth model for CM manufacturing should aim to describe the predominant processes that influence the growth of cell mass and its composition in a large-scale bioreactor.

Biological processes are highly complex, so different modeling approaches have been developed to describe, predict, and understand them. The most common ways to model cell growth are empirical models that describe patterns in observed experimental data and mechanistic models that rely on causal theories of how biological functions work. A core challenge in modeling biological processes is that many of the mechanisms governing a given process are only partially understood and remain active areas of research. As our understanding of biology improves, mechanistic models become increasingly complex, incorporating more parameters, pathways, and multi-scale interactions. While statistical approaches such as machine learning can cut through complexity and draw predictive inferences, they are limited by the need for vast amounts of data. In short, there is tension in selecting a modeling approach for CM that balances ease of use, prediction, flexibility, data availability, and complexity.[1]

Improving models for cultivated meat manufacturing

Previous TEMs of CM have relied on sets of assumptions for cell growth, the bioreactor environment, and the overall process. In simplifying complexity through these assumptions (e.g., fixed growth rate, homogenous mixing, static stoichiometry), the dynamic nature of how a cell responds to its environment during production is lost. As a consequence, the model's utility is limited by its inability to test or predict the impact of changes to a process that a practitioner may wish to make, such as alternative feeding strategies, scales of production, and bioreactor designs. While we acknowledge that the full dynamic complexity cannot yet be completely captured, we suggest that cell growth models for CM can be improved, which in turn can inform future TEMs.

It is highly unlikely that any single model can satisfy all future needs as CM technology continues to develop, particularly with the anticipated variety of CM products. Rather than a single tool, such mathematical models should be viewed as a toolbox from which the appropriate tool can be selected. In any case, we believe that the toolbox for the cell growth component should accommodate the following needs:

[1] While a full review of different modeling approaches is out of the scope of this report, additional discussion in relation to complexity is provided in Section 4.

1. **Predict bioreactor volumetric productivity** as a function of controlled growth conditions, operating mode, primary substrate concentrations in the starting medium, and addition of concentrated feeds and/or perfusion medium. The availability of the primary carbon, nitrogen, and energy substrates has a direct impact on their consumption and the formation rate of inhibitory metabolites, which can restrict the bioreactor's performance envelope by suppressing growth rates. Estimating system productivity is the first step in establishing, comparing, and ultimately improving PCRs. Physical factors such as shear can also limit bioreactor productivity but will be addressed in subsequent work.
2. **Optimize bioreactor feeding strategies and operating modes** from the standpoint of raw material costs and bioreactor performance as a function of the rate and timing of substrate addition. Once bioreactor volumetric productivity can be predicted, the model should enable the evaluation of the quantitative trade-offs between the cost of medium components and their relative contribution to overall productivity through the accurate prediction of substrate consumption and feed conversion ratios. Moreover, the effect of restricting the supply of a substrate will often increase the efficiency of its use as well as reduce the formation of inhibitory metabolites.
3. **Enable bioreactor design and evaluation by capturing the effects of heterogeneous conditions on overall performance.** Localized depletion of substrates can occur as a result of insufficient mixing or control overshoot, resulting in concentration gradients or transients. Of primary importance is oxygen due to its low solubility and therefore high potential for depletion zones in a large bioreactor, as well as other potential non-idealities.
4. **Improve bioprocesses.** Study the impact of and trade-offs between various physical and biochemical conditions on the overall system performance in addition to substrate feeding strategies and operating modes. Ideally, the model parameters would include temperature and pH, which have broader optimization potential.
5. **Evaluate cellular adaptation strategies and alternative primary substrates**, such as the inclusion of pyruvate and alpha-ketoglutarate, and their impact on PCR.
6. **Predict quantitative benefits of altered biochemical pathways** as a result of adaptation and/or genetic manipulation.

Notably absent from this list is media optimization. While the development of efficient, low-cost media for the proliferation and differentiation of animal cells will be critical to the success of CM, evaluating media composition is not the subject of this paper. It is assumed here that the bulk of media design will be conducted at small scale and probably not in fully controlled bioreactors. Typically consisting of well over 40 individual components, the basal media composition would be too complex to represent all interactions mathematically, in addition to those associated with high cell density bioreactor culture. Not only is the maximum growth rate in a given medium a function of factors such as pH, temperature, and substrate concentrations, but it can also be affected by the ratios between certain amino acids, trace elements, and growth factors. Models for media optimization applications are

certainly of value but would emphasize multicomponent metabolic flux analysis and highly specific cell::factor interactions.

For the models proposed in this paper, the base medium and the maximum growth rate it can support are considered inputs, not outputs. Our focus instead is on the major changes in substrate concentrations as a consequence of their consumption, the associated accumulation of the major waste metabolites, and their overall effect on bioreactor process performance. Inherent in these assumptions is that (1) the basal medium's minor components do not change significantly or their consumption is predictable by a constant yield factor and (2) the intrinsic maximal growth rate does not change appreciably. Most animal cell culture media contain the full complement of essential and nonessential amino acids in addition to the major substrates to support the highest possible growth rates, and their uptake contributes to a significant fraction of final cell mass (Hosios et al. 2016). However, they are assumed not to limit growth, alter growth rate, or change the consumption pattern of the primary substrates. As we show in this report, this last assumption may not always be valid.

Modeling approaches for animal cell growth and metabolism

Animal cell metabolism is considerably more complex than that of microorganisms, both in the number of biochemical pathways at work and the number of required nutrients. A brief overview of animal cell metabolism is offered in **Appendix A1**. A diagram of the associated biochemical pathways is also provided in **Figure A1.1,** showing the metabolite species that change to the greatest degree during growth.

In short, the energy required for animal cell growth is naturally provided by the catabolism of carbon and energy substrates, glucose, a sugar, and glutamine, an amino acid. Under conditions of rapid growth, glycolysis is the primary contributor to energy production from the consumption of glucose, resulting in the production of lactic acid. Glycolysis occurs even though the greatest energy is produced via oxidative phosphorylation through the TCA cycle, ending in the formation of carbon dioxide. This phenomenon is known as the Warburg Effect, which occurs even if oxygen is available in excess. Glucose also has an anabolic role in contributing 5-carbon sugars (pentoses) to the synthesis of nucleotides.

Glutamine is typically the main contributor to the nitrogenous base of nucleotides and to the synthesis of nonessential amino acids and protein synthesis more generally, but can also be consumed as an energy substrate, resulting in the release of free ammonia. It is well established that glucose and glutamine are partially substitutable as energy sources in mammalian cell culture media (DiMasi and Swartz 1995). Each provides unique biosynthetic precursors but is complementary for the production of other metabolites and energy (Miller, Wilke, and Blanch 1989). Thus, glycolysis and glutaminolysis are jointly regulated to provide sufficient energy required by cells, depending on the availability of these major energy substrates (Jeong and Wang 1995).

The rate of glucose and glutamine consumption directly determines the production rates of their main waste products of lactic acid, ammonium, and carbon dioxide. It is also well established that all three of these metabolites can inhibit the growth of most animal cells if allowed to accumulate and can even result in cell death at higher concentrations.

To be of predictive value, any model will need to address most if not all of the following key factors governing animal cell growth in a bioreactor. The approach presented is primarily empirical, relying on observed correlations between related variables, and reflects the most common mathematical approach to modeling the key factors that dictate cell growth.

- **Nutritional factors:** the principal energy substrates that are consumed by the cell during growth processes and are deterministic of cell growth rates. The main natural substrates include glucose, which is the main substrate for ATP production via glycolysis, and glutamine, which supplies nitrogen for the synthesis of other amino acids as well as energy when needed. Additionally, oxygen is consumed to support ATP production via oxidative phosphorylation and cycling of NADH, a critical energy carrier and reducing agent. The relative uptake and metabolism of these substrates depend strongly on their availability to the growing cells.
- **Inhibitory and cytotoxic factors:** the metabolic by-products known to inhibit cell growth or viability. These include lactate produced as the by-product of glycolysis, ammonium produced as the by-product of glutaminolysis, and carbon dioxide as the by-product of cellular respiration. Accounting for the osmolality of the cell culture media is also important, as fluctuations in osmolality have been shown to inhibit cell growth. In addition to quantifying growth inhibition, modeling cell death is also relevant in predicting viable biomass accumulation and culture viability. Viability of the proliferation stage culture is critical when followed by a cell differentiation step, especially under stressed conditions of nutrient starvation, inhibitor toxicity, and shear that may be expected in high-density, large-scale CM manufacturing.
- **Temperature and pH**: these factors can influence the growth rate by altering the kinetics of chemical reactions, the solubility of inhibitory factors, protein stability, and the cell's overall metabolism. Temperature and pH also have an overarching impact on bioreactor dynamics.
- **Cellular response times and dynamics**: the time it takes cells to respond to a sudden change in conditions will shed light on transient conditions that may occur in a large-scale bioreactor. The cells may be moving through different zones with various degrees of mixing and substrate concentrations, including oxygen. Understanding cellular response to such conditions that recur at high frequency will be necessary to quantify the effects of large-scale cell culture.

In this section, we describe the simplest mathematical cell growth model that attempts to capture major aspects of cell growth dynamics, leading to the formation of biomass, and the consumption of the primary substrates that contribute most to cost. In addition to the primary substrates, other macrometabolites would be included if they have a significant effect on the physical chemical environment as they are formed or consumed and/or have a direct impact on the cells' rate of growth or metabolism during cultivation in a given medium. This approach creates an initial framework to clarify cause and effect as well as to allow identification of the most relevant parameters.

However, to address all of the above aspects, more complex models may be required. Examples are introduced later in the report with additional details presented in **Appendix A2**. In Section 3, we will review the literature to assess how experimental data fit with the proposed equations and discuss

data gaps and limitations. Knowledge of typical cell sizes, mass, and composition is also discussed, as this information is essential to normalizing data across studies.

It is important to note that the models outlined in this report should not be interpreted as the totality of cell growth modeling but rather as an improved foundation on which to build. For many of the above factors, complexity can be added by accounting for other parameters or interaction effects, which are discussed where appropriate. This complexity may be included in future models tailored to different use cases and production scenarios, or to interrogate different questions or trade-offs.

2.2 Biomass generation and bioreactor productivity

Understanding the rate of biomass accumulation in cell culture is critical to quantify key process metrics. Biomass is typically quantified on the basis of hydrated (wet) or dry cell mass, but it can also be quantified in terms of protein or lipid content, if these are critical quality attributes.

Cell concentrations have historically been expressed as a number of cells per unit volume (e.g., millions of cells/mL). However, during growth, the rate of increase of biomass and cell number may diverge, thus cell count may be a poor proxy for cell size and mass. Moreover, the composition (e.g., lipid or protein content) of the cell can change independently of biomass or cell number, such that the rate of product formation may not align with total biomass formation either.

To account for these variables, biomass accumulation is commonly measured by the metric of volumetric productivity of the bioreactor, which represents the amount of product mass generated per unit time per unit of bioreactor volume. In the case of CM where biomass is the product, this can be defined as the total wet cell weight (WCW), dry cell weight (DCW), or just protein mass, depending on the desired output.

The bioreactor volume can be defined as either the working volume or total volume, with the former more commonly used in practice and applied in Equation 2.2a. Thus, the volumetric productivity is the overall reaction rate of product formation divided by the bioreactor's volume, which can be applied to any bioreactor type:

$$U_X = r_X * V_{culture} / V_w$$ **Equation 2.2a**

Symbol	Definition	Typical units
U_x	Volumetric productivity of the bioreactor	g product/Lr/day, where Lr = reactor volume
X	Biomass concentration or product mass	g WCW/L, g DCW/L, g protein/L
r_x	Overall rate of product formation	g DCW/L/day
$V_{culture}$	Total volume of the cell culture	L or m^3
V_w	Working volume of the bioreactor	L or m^3

Batch culture

Depending on how a bioprocess is operated, Equation 2.2a may appear different. For example, during a constant-volume process such as batch culture, the ratio $V_{culture}/V_w$ will reduce to 1 as the culture volume equals the working volume, reducing Equation 2.2a to:

$$U_X = r_X$$

During exponential growth in a constant-volume culture, the rate of biomass formation is proportional to the product of the specific growth rate (μ) and biomass concentration (X) such that:

$$r_X = \mu * X_v$$

Thus, volumetric productivity is governed by both how fast cells grow and how many viable cells (X_v) are present at any point in time. Typically, a batch bioreactor is harvested when volumetric productivity reaches its highest value.

The **specific growth rate (μ)** of a given cell line represents the rate of growth (typically per hour or day for animal cells) of a population of cells normalized to the population size. Most animal cell culture practitioners measure and report doubling time, which is the time it takes for a population of cells to double. The doubling time (t_d) can be transformed to the specific growth rate (μ) by the equation: $\mu = ln(2) / t_d$

Callout box 1. Relationship between doubling time and specific growth rate.

Continuous (chemostat) culture

In a chemostat bioreactor, fresh nutrients are continuously added while spent media and cells are removed simultaneously. This maintains a steady-state condition in which the biomass and nutrient concentrations remain constant over time. Under steady-state conditions, the volumetric productivity can be expressed as the product of the specific growth rate and the steady-state biomass concentration:

$$U_X = \mu_X * X_v$$ **Equation 2.2b**

Symbol	Definition	Typical units
μ	Specific growth rate of cells	1/day or 1/hour
X_v	Concentration of viable biomass at steady state	g WCW/L or g DCW/L

In a chemostat operating at steady state, the specific growth rate is equal to the dilution rate, which is defined as the feed flow rate divided by the working volume:

$$\mu = D = F / V_w$$ **Equation 2.2c**

Symbol	Definition	Typical units
D	Dilution rate	1/hr or 1/day
F	Feed flow rate	L/hr or m^3/day

To maximize volumetric productivity in a chemostat, it is desirable to maximize both the viable biomass concentration and specific growth rate. However, there is typically a trade-off between these two factors. For example, at high dilution rates, cells may wash out before reaching high biomass concentrations. And at high biomass concentrations, nutrient limitations or accumulation of inhibitory by-products may reduce growth rates. Thus, the maximum attainable productivity in a chemostat or bioreactor under continuous operation is a combination of the biomass concentration that can be maintained *and* the maximum specific growth rate that can be sustained at steady-state.

Differentiation and maturation

For processes involving cellular differentiation and/or maturation to achieve tissue-like structures, assumptions of exponential growth do not necessarily apply. In these cases, alternative growth models are required. In the proliferation stage, biomass concentration increases by cell division, where each daughter cell is the same size and mass as its parent. In contrast, during differentiation, the cells can increase in size and mass, but cell number may remain constant. There may also be a maturation stage where additional mass may be gained (e.g., by deposition of extracellular matrix to form the final tissue). Certain CM processes may incorporate differentiation and maturation; however, existing TEMs have not modeled mass gain during this stage.

In its simplest form, biomass production during differentiation or maturation can be modeled by a constant linear growth rate; however, more complex models may be appropriate in some cases:

$$r_{Xv} = k_{growth}$$ **Equation 2.2d**

Symbol	Definition	Typical units
r_{Xv}	Rate of viable biomass increase	g DCW/day or cells/day
k_{growth}	Linear growth rate constant	g DCW/day or cells/day

For a differentiation stage cell culture with linear growth, Equation 2.2a still applies to determine the volumetric productivity at any point in time. However, at the point of harvest, the volumetric productivity is simply determined by the final state, corrected for the nominal reactor volume:

$$U_X = X_{final} / t_{final} * V_{culture} / V_w$$ **Equation 2.2e**

It is also important to note that only viable cells contribute to ongoing growth. While Equation 2.2d describes growth in terms of viable biomass, the total biomass produced may include both live and

dead cells, as well as non-cellular components such as extracellular matrix. It is therefore also important to account for cell death rates.

Accounting for cell death

While maintaining high rates of viability is always sought after, cell death is an inherent part of any culture process. Despite this, cell death has not yet been modeled in CM TEMs. Distinguishing living from dead cells may be important in CM processes, as shear stress, inhibitory by-products, and nutrient depletion are likely to occur in large-scale and high-density cell cultures. While all cells are expected to be dead by the time of final product consumption, high death rates may be particularly difficult to tolerate in a two-stage process where cells are seeded onto a scaffold for continued differentiation and maturation.

For exponential growth, the true specific growth rate (μ) is applied to the instantaneous viable biomass concentration (X_v). However, a fraction of viable cells is lost over time due to cell death, which reduces the actual rate of biomass accumulation. Thus, the net rate of viable biomass accumulation becomes the difference between the true specific growth rate and the specific death rate (δ):

$$r_{Xv} = (\mu - \delta) * X_v = \mu_{app} * X_v$$ **Equation 2.2f**

Symbol	Definition	Typical units
δ	Specific death rate (assumed to be 1st order with respect to viable cell concentration)	1/day
μ	True specific growth rate (1st order)	1/day
μ_{app}	Apparent specific growth rate	1/day
r_{Xv}	Net rate of viable biomass formation	g DCW/day or cells/day

Similarly, for a non-exponential stage such as differentiation, the net rate of viable biomass change is:

$$r_{Xv} = \left(k_{growth} - k_{death}\right) = k_{app} * X_v$$ **Equation 2.2g**

Symbol	Definition	Typical units
k_{growth}	Constant (linear) growth rate	g DCW/day or cells/day
k_{death}	Constant (linear) death rate	g DCW/day or cells/day
k_{app}	Apparent linear growth rate after subtracting the death rate	g DCW/day or cells/day
r_{Xv}	Net rate of viable biomass formation (differentiation phase)	g DCW/day or cells/day

Therefore, the apparent growth rate is always less than the true growth rate.

Dead cell accumulation and lysis

The accumulation of dead biomass (X_d) results from the death of viable cells and is offset by lysis, which is the degradation or removal of dead biomass:

$$r_{Xd} = \delta * X_v - \lambda * X_d$$ **Equation 2.2h**

Symbol	Definition	Typical units
δ	Specific death rate (assumed to be 1st order with respect to viable cell concentration)	1/day
X_d	Concentration of dead biomass	g WCW/L or g DCW/L
λ	Specific lysis rate	1/day
r_{Xd}	Net rate of dead biomass accumulation	g DCW/L/day, g WCW/L/day, or cells/L/day

The lysis rate factor can be used to determine the amount of cell debris and/or lysate that may appear in the extracellular medium, some of which may be recovered with the product.

Total biomass

Taken together, the total biomass (X_t) in the bioreactor at any time is the sum of the viable (X_v) and dead (X_d) cells:

$$X_t = X_v + X_d$$ **Equation 2.2i**

2.3 Kinetic expressions for cell proliferation and differentiation

The kinetics of cell proliferation and differentiation are the primary drivers of bioreactor productivity, and understanding the key factors influencing these rates is paramount to effective process design and modeling. What are the key factors that should be included in a model?

Temperature and pH are critical factors affecting growth rate and other physical and chemical processes. Although each is typically tightly controlled near its respective optima for a given cell line, real bioreactor conditions such as incomplete mixing can result in cells being exposed to suboptimal microenvironments. Additionally, some processes may be better controlled at conditions that are suboptimal for maximizing growth rate but enhance other physical factors such as oxygen solubility or mass transfer. For these reasons, a model that can account for some of these trade-offs would be useful.

Substrate concentrations may also vary and impact growth rates, especially as the substrate is depleted. This is particularly true when the main carbon and energy substrates are controlled at low

concentrations to minimize waste metabolite formation. However, this strategy is sensitive to control overshoot or poor mixing, which may result in cells experiencing nutrient starvation or excessive inhibitory metabolite production. Lastly, shear forces in a bioreactor from agitation, mixing, sparging, and bubble entrainment and rupture can also impact growth, inhibition, death, and lysis rates. Capturing the dynamics of each of these factors is also important for modeling purposes.

Taken together, a cell's specific growth rate (μ), introduced earlier, can be considered a state variable, representing the cell's physiological status under certain conditions at a given time. Growth rate is not a constant as assumed in prior TEMs, but rather a function of the many factors described previously. For modeling purposes, only those factors expected to change under the simulated scenario should be included in the model. The multiplication of these factors then represents the total impact on the maximum specific growth rate, reducing it to the true growth rate in the culture at any given time. As a general expression, Equation 2.3a represents the global function of key factors influencing the state of a cell's growth rate, and each of these primary factors can be separately modeled by mathematical equations. Each of these factors is briefly introduced below.

$$\mu = \mu_{max} f(T, pH) * NF * IF * SF \qquad \textbf{Equation 2.3a}$$

Symbol	Definition	Typical units
μ_{max}	The maximum possible specific growth rate for a given cell line under defined conditions[1]	1/day or cells/day
T	Temperature	ºC
pH	pH	–
NF	Nutrition factor representing nutrient substrate concentration effects	Dimensionless (0-1)
IF	Inhibition factor representing the cumulative effect of inhibiting metabolites or by-products	Dimensionless (0-1)
SF[2]	Shear factor representing the overall effect of various types of physical stresses the cell experiences over time	Dimensionless (0-1)

[1] For modeling purposes, it is assumed that the conditions include a medium composition where all nutrients, including growth factors, are available in excess.

[2] Shear factors will be described in more detail in a future report on the bioreactor environment model.

Temperature

Temperature can have a strong influence on a variety of cellular activities that affect cell growth, including metabolism and gene expression. Higher temperatures have been correlated to increased developmental rates that are attributed to faster metabolic and protein synthesis rates (Gillooly et al. 2002), but temperatures significantly above the optimal growth temperature can result in heat shock. Mildly hypothermic conditions have also shown enhanced expression of recombinant proteins, which is believed to be due to the lower growth rates allowing more expression of non-growth-associated

proteins (Sunley, Tharmalingam, and Butler 2008). However, no model of CM has yet accounted for temperature's important influence on growth rate.

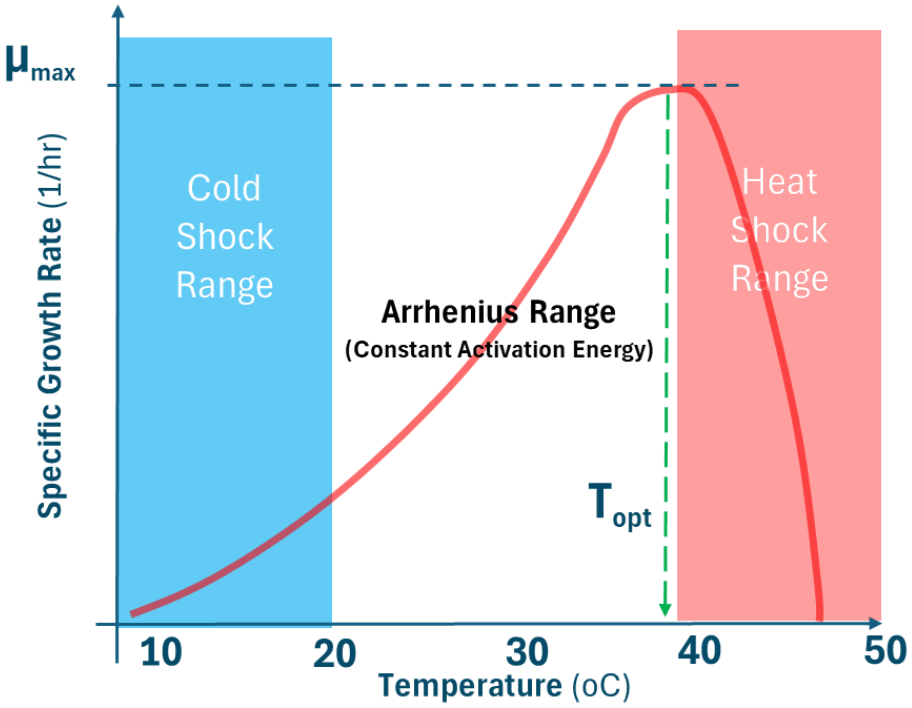

Figure 2.3a: Typical profile of specific growth rate as a function of temperature for most mammalian cells.

Between the extremes of heat shock and cold shock lies the Arrhenius range, where the relationship between reaction (i.e., growth) rate and temperature can be modeled using the Arrhenius equation (**Figure 2.3a**). Arrhenius's law describes how chemical reaction rates vary with temperature when the activation energy is constant. For biological systems, the specific growth rate can be approximated within the Arrhenius range by the Arrhenius equation:

$$\mu = A\, e^{\frac{-E_a}{RT}}$$ **Equation 2.3b**

Symbol	Definition	Typical units
μ	Specific growth rate at temperature T	1/day
A	Pre-exponential or "Frequency Factor"	1/day
E_a	The energy needed for activation of the reaction	J/mol
R	Universal gas constant	8.314 J/mol*K
T	Absolute temperature	Kelvin (K)

As we will show in Section 3, this relationship is useful for experimentally determining the Frequency Factor (A) and the Activation Energy (E_a) by fitting growth rate data to the linearized form of the Arrhenius equation. By plotting the natural logarithm of the specific growth rate versus the reciprocal of absolute temperature, a straight line can be obtained:

$$ln(\mu) = ln(A) - E_a/R * 1/T$$

In this linear form, the slope of the line equals $-E_a/R$, from which the activation energy can be calculated. The y-intercept corresponds to ln(A), allowing determination of the Frequency Factor (A). Once these parameters are determined for a given cell line, the specific growth rate can be well-predicted for the temperatures within the Arrhenius range, which can be useful for process optimization. It is also likely that the same parameters could be applied to multiple cell lines by expressing growth rate as a fraction of specific growth rate at each cell line's respective optimal temperature (T_{opt}). This could enable broader predictive modeling with fewer parameters.

pH

Similar to temperature, most animal cell cultures are maintained at pH values at or near the physiological pH of the organism's blood supply. For most species relevant to CM, this means pH will be held between 7.0 and 7.6, with the more alkaline pH used for the culture of some aquatic species (Rubio et al. 2019). The shape of the pH tolerance profile is generally broader than that of temperature but can be highly cell line-dependent. Some cell lines are more sensitive to alkaline conditions and others are more sensitive to acidic conditions, but most cell lines are more tolerant of alkaline conditions than acidic conditions.

Unlike temperature, there is no readily available model to describe the effects of pH on cell growth based on first principles because there are several mechanisms at play. For example, pH can influence the cell's metabolism as well as the buffering capacity of the media, which can have numerous and complex downstream effects, such as changes in osmolality. For this reason, pH effects are often modeled using empirical equations that are fit to experimental growth data.

The nutrition factor: Substrate effects on growth rate

The nutrition factor (NF) collectively accounts for the effects of several key substrates that the cell relies on for growth: oxygen, glucose, and glutamine. These substrates are typically consumed in the greatest quantities in animal cell culture and are also most likely to become depleted or limiting.

The NF can be mathematically described using Monod-type kinetics where each substrate is represented by saturation kinetic terms using a parameter referred to as the Monod constant, originally adopted from Michaelis-Menton enzyme kinetics. **Figure 2.3b** graphically depicts different Monod kinetic models. The first model represents classical Monod kinetics where growth rate increases proportionally with increases in substrate concentrations at low concentrations, but exhibits saturation at higher substrate concentrations where the reaction rate is limited by the cells' ability to absorb and metabolize the substrate. This single-parameter model can be extended to include

substrate inhibition at high concentrations (Model 2). Finally, Model 3 is a two-parameter model that represents a maximum substrate concentration at which there is a complete cessation of cell growth.

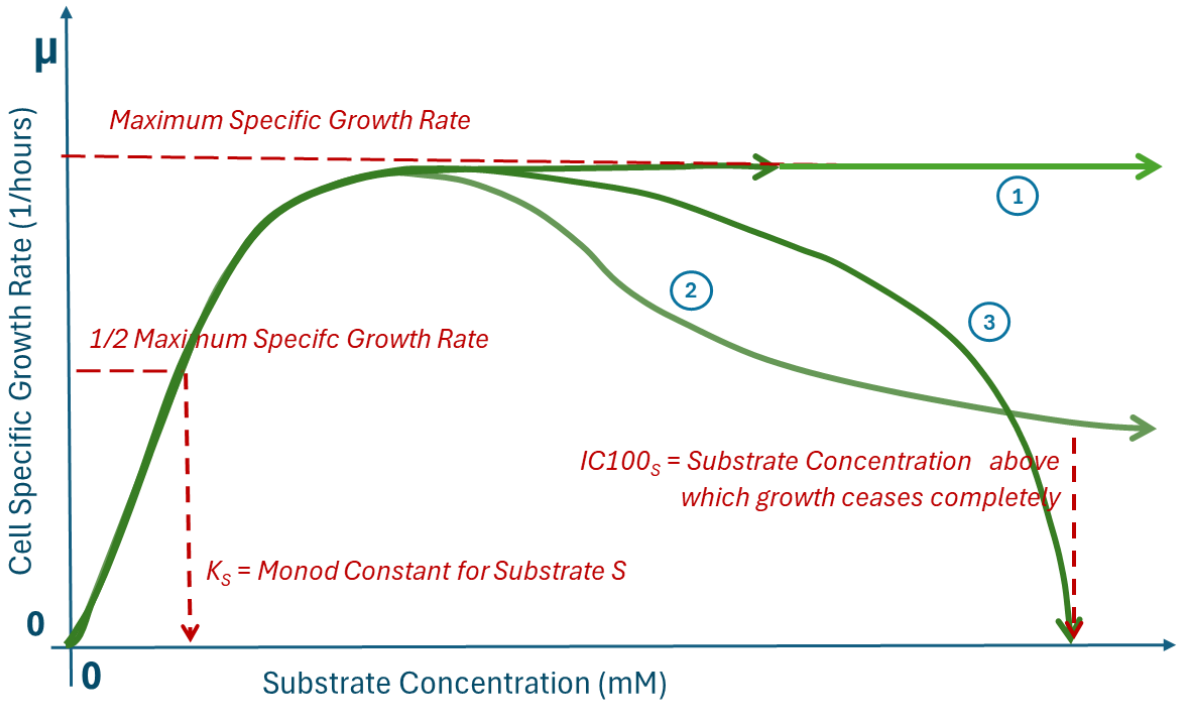

Figure 2.3b: Monod-type models of the effect of substrate concentration on cellular growth rate. **Model 1**: original Monod model for saturation kinetics; **Model 2**: single-parameter model for substrate inhibition; **Model 3**: two-parameter model for substrate inhibition.

In bioreactor systems, multiple substrates can become limited simultaneously. In such cases, the NF can be expressed as the product of independent saturation terms, assuming noncompetitive interactions among the substrates:

$$NF = NF_{O2} * NF_{Glc} * NF_{Gln}$$
$$= \left[\frac{O2}{O2 + K_{O2}}\right]\left[\frac{Glc}{Glc + K_{Glc}}\right]\left[\frac{Gln}{Gln + K_{Gln}}\right]$$

Equation 2.3c

Symbol	Definition	Typical units
NF_{O2}, NF_{Glc}, NF_{Gln}	Nutrition factor for oxygen, glucose, and glutamine substrates	Dimensionless
[O2], [Glc], [Gln]	Concentration of oxygen, glucose, and glutamine in the liquid phase (extracellular media)	mM
K_{O2}, K_{Glc}, K_{Gln}	The half-saturation (Monod) constant for oxygen, glucose, and glutamine	mM

While glucose and glutamine can likely be modeled using classical Monod kinetics, high concentrations of oxygen can inflict oxidative stress and become inhibitory at higher concentrations. In this case, the NF_{O2} in Equation 2.3c can be substituted with:

$$NF_{O2} = \left[\frac{O2}{O2 + K_{O2}}\right]\left[1 - \frac{O2}{IC100_{O2}}\right]^{a}$$ **Equation 2.3d**

Symbol	Definition	Typical units
$IC100_{O2}$	The concentration of oxygen in the liquid phase at which total growth inhibition is observed	mM
a	Model exponent that determines the curvature of the relationship	Dimensionless

These equations collectively offer a more robust and dynamic modeling approach to substrates compared to previous TEMs that assumed no growth-limiting substrates, a well-mixed reactor with no substrate-deficient zones, and subinhibitory concentrations of waste metabolites such that the growth rate was constant.

As described previously in the overall cell growth model (Equation 2.3a), the non-energy substrates, including growth factors, are assumed to be available in excess and therefore do not impact the growth rate. However, this model can be customized to include other substrates if they are involved in important kinetic or stoichiometric trade-offs. For example, a model of avian cells may include NF_{asp}, as avian cells tend to use asparagine rather than glutamine as a principal energy substrate (Lohr et al. 2014).

Substrate starvation effect on death rate

For most essential nutrients or substrates, at very low concentrations, cells can undergo substrate starvation, leading to cell death. The rate of death under starvation is not constant but depends on the specific substrate and its concentration. For example, oxygen and glucose starvation may lead to rapid death, whereas depletion of certain amino acids may have a more delayed response.

Models have been proposed to represent this concentration-dependent death rate. The most common kinetic model is an inverse-Monod relationship, which assumes that the death rate increases with decreasing substrate concentrations, reaching a maximum death rate at a substrate concentration of zero:

$$\delta_S = \delta_{S,max} * \left[\frac{K_{S,D}}{K_{S,D} + S}\right]$$ **Equation 2.3e**

Symbol	Definition	Typical units
δ_S	Death rate due to depletion of substrate S	1/hr or 1/day
$\delta_{S,max}$	Maximum death rate observed upon starvation of substrate S	1/hr or 1/day
$K_{S,D}$	Death rate half-saturation constant for substrate S	mM
[S]	Concentration of substrate S	mM

However, other empirical models have used either a simple linear relationship (Equation 2.3f) or a Monod-like model modified by Hill (Equation 2.3g) to include an additional exponent to make it a two-parameter model. These models are useful when experimental data suggest a different pattern of response or provide a better fit to the data:

$$\delta_S = \delta_{S,max} - \alpha S$$ **Equation 2.3f**

$$\delta_S = \delta_{S,max} * \left[\frac{K_{S,D}^{n}}{K_{S,D}^{n} + [S]^{n}} \right]$$ **Equation 2.3g**

Symbol	Definition	Typical units
α	Inhibition coefficient to inhibition parameter	1/(mM•day)
n	Hill coefficient (exponent) that controls sigmoidal steepness	Dimensionless

The inhibition factor: Waste metabolite effects on growth rate

The inhibition factor (IF) collectively accounts for the effects of several key inhibitory by-products on cell growth, namely lactate, ammonia, and carbon dioxide. Although previous TEMs have accounted for these factors, they did so by assuming strict limits where growth does not occur above a certain boundary, which may be an oversimplification of inhibitory effects. Additionally, the inhibition effects of osmolality have been well-characterized, but have yet to be incorporated into CM TEMs.

Similar to the NF, the IF can be represented by multiplying the effects of individual inhibition factors, assuming noncompetitive interactions among them:

$$IF = IF_{Lac} * IF_{Osm} * IF_{CO2} * IF_{NH4}$$ **Equation 2.3h**

Symbol	Definition	Typical units
IF_{lac}	Inhibition factor for lactate	Dimensionless (0-1)
IF_{osm}	Inhibition factor for osmolality	Dimensionless (0-1)
IF_{NH4}	Inhibition factor for ammonia/ammonium	Dimensionless (0-1)
IF_{CO2}	Inhibition factor for carbon dioxide	Dimensionless (0-1)

In reality, this relationship may be an oversimplification if significant synergistic or antagonistic interactions exist between inhibitors. In such cases, interaction terms, weighting coefficients, or additional parameters may need to be added to the model.

Various expressions have been used in the past to represent the degree of inhibition caused by a specified concentration of inhibitor. A commonly used expression to describe a single inhibitor is based on a half-maximal inhibition (IC50) function, where growth rates decline as inhibitor concentration increases:

$$IF_I = \left[\frac{K_I}{I + K_I}\right] = \left[\frac{IC50_I}{I + IC50_I}\right]$$

Equation 2.3i

Symbol	Definition	Typical units
IF_I	Inhibition factor for inhibitor I	Dimensionless
K_I	Inhibition parameter for inhibitor I	mM
$IC50_I$	Concentration of inhibitor I that reduces growth rate by 50%	mM

Alternative models may be used when inhibition follows a different profile. Ultimately, the choice of inhibition model will depend on experimental data fit, mechanistic understanding, and trade-offs around simplicity versus accuracy. **Figure 2.3c** shows various models (functions) used in the literature to model inhibition.

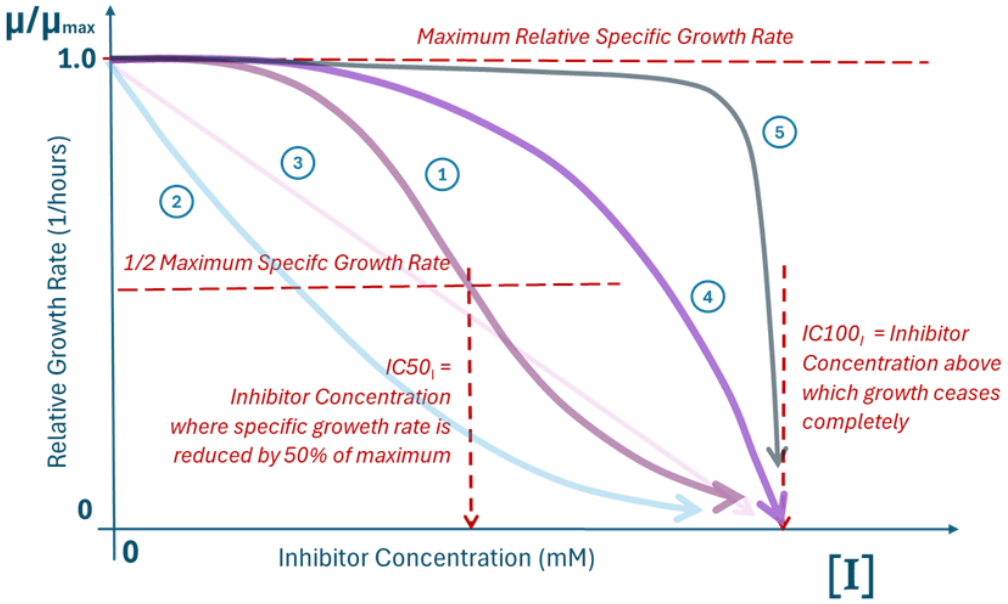

Figure 2.3c: Various models of growth inhibition. **Model 1** is an inverse Monod relationship (Equation 2.3i); **Model 2,** using Equation 2.3j, is also a single-parameter model; **Model 3** is simply a straight line; **Model 4** is a two-component model using Equation 2.3k; **Model 5** is a three-parameter model that uses an additional exponent to Model 4 to give more control of the curvature.

The single-parameter models have some shortcomings in that their representation at high inhibitor concentrations is not realistic. Typically, there is a concentration at which growth is fully arrested, which is represented as the IC100. Equations 2.3i (Model 1) and 2.3j (Model 2, where the IF decays exponentially) are widely used but do not predict zero growth at any concentration and would underestimate inhibition at very high concentrations:

$$IF_I = e^{-kI}$$ **Equation 2.3j**

Symbol	Definition	Typical units
IF_I	Inhibition factor for inhibitor I	Dimensionless
k	Decay coefficient that determines steepness of inhibition	1/mM
I	Concentration of inhibitor I	mM

A more flexible, two-parameter empirical approach can also be used (Model 4 in Figure 2.3c; Equation 2.3k). This model is useful when experimental data show a threshold effect:

$$IF_I = \left[1 - \frac{I}{IC100_I}\right]^{\varphi}$$ **Equation 2.3k**

Symbol	Definition	Typical units
$IC100_I$	Concentration of inhibitor I that fully stops growth	mM
φ	Inhibition exponent that controls curve steepness	dimensionless
I	Concentration of inhibitor I	mM

Model 5 in Figure 2.3c is a three-parameter model giving more control of the curvature where there may be a very abrupt transition but requires another parameter. Still more models can be borrowed from the microbial end-product inhibition literature, depending on the mechanism (Straathof 2023). Any of these models offers a more realistic representation of growth inhibition than a binary threshold that cannot be exceeded, as assumed in TEMs published to date. These models at least allow some optimization of the cell culture system to be performed *in silico* to account for trade-offs.

Effect of cytotoxic waste metabolites on cell death rates

If certain waste metabolites are cytotoxic at high enough concentrations, they will cause cell death in addition to slowing the growth rate. Typically, these concentrations are higher than those leading to a reduction in the growth rate, but there can be an overlap in which cells grow more slowly and die simultaneously (Cooper and Youle 2012).

Monod-type kinetics can be used to model cytotoxic death similarly to substrate or metabolite inhibition. The following commonly used model is similar to Equation 2.3e proposed for substrate starvation, except that the death rate increases with rising inhibitor concentrations instead of decreasing substrate concentrations:

$$\delta_I = \delta_{I,max} * \left[\frac{I}{K_{I,D} + I} \right]$$ **Equation 2.3l**

Symbol	Definition	Typical units
δ_I	Death rate caused by inhibitor I	1/day or 1/hr
$\delta_{I,max}$	Maximum death rate caused by inhibitor I	1/day or 1/hr
$K_{I,D}$	Half-maximum death rate parameter for inhibitor I	mM
I	Concentration of inhibitor I	mM

If the death kinetics are nonlinear or threshold-like, a sigmoidal expression similar to Equation 2.3g can be constructed, providing greater flexibility by introducing an exponent that adjusts the curvature of the death response:

$$\delta_I = \delta_{I,max} * \left[\frac{I^n}{K_{I,D}^n + I^n} \right]$$ **Equation 2.3m**

Symbol	Definition	Typical units
n	Hill coefficient that controls sigmoidal steepness	Dimensionless

When multiple media components and/or metabolites independently contribute to cell death, the total death rate is the sum of the individual death rates, assuming no interactions among them:

$$\delta = \delta_{Lac} + \delta_{CO2} + \delta_{Amm} + \delta_{Osm}$$ **Equation 2.3n**

Symbol	Definition	Typical units
δ	Total death rate	1/day or 1/hr
$\delta_{Lac}, \delta_{CO2}, \delta_{amm}, \delta_{osm}$	Death rate by individual waste metabolites	1/day or 1/hr

Similar to growth inhibition, this death relationship may be an oversimplification if significant synergistic or antagonistic interactions exist between inhibitors. In such cases, interaction terms, weighting coefficients, or additional parameters may also need to be added to the model.

2.4 Substrate consumption and metabolite production rates

To formulate material balances for critical nutrients and by-products in cell culture, mathematical models are typically employed to predict the rate of nutrient consumption and waste generation per unit of cell growth. Thus far, existing CM TEMs have assumed fixed amounts of substrate consumed per unit of cell number or cell mass generated. In these models, cell-specific substrate consumption and waste metabolite production are strictly and linearly proportional to growth rate. However, this is not realistic, especially at low growth rates when cells still need to expend energy to maintain homeostasis even though they are not rapidly proliferating.

A semi-empirical model used in the biochemical engineering field is represented by Equation 2.4a and is based on (Pirt 1965)) work on microbial cultures. Here, a cell's consumption of a carbon and energy substrate (q_s) is a function of its specific growth rate, a yield factor, and a maintenance term that accounts for substrate consumption even if the cell is not actively growing:

$$q_S = (\mu / Y_{X/S}) + m_S$$ **Equation 2.4a**

Symbol	Definition	Typical units
μ	Specific growth rate	1/day or 1/hr
q_s	Cell-specific consumption rate of substrate S	mmol/cell/day or mmol/gDCW/day
$Y_{X/S}$	The true growth-associated cell mass yield of substrate S	gDCW/mmol or gDCW/g
m_S	Specific consumption of substrate S for non-growth cell maintenance	mmol/cell/day or mmol/gDCW/day

In this semi-empirical model, the maintenance term is normally associated with carbon and energy substrates such as glucose and glutamine, since the cell requires energy to maintain homeostasis. For non-energy substrates such as amino acids used solely for biosynthesis, the maintenance term is assumed to be zero, meaning that these are only consumed during active cell growth.

When Equation 2.4a is plotted on linear coordinates, the relationship between specific substrate consumption (q_s) and specific growth rate (μ) forms a straight line:

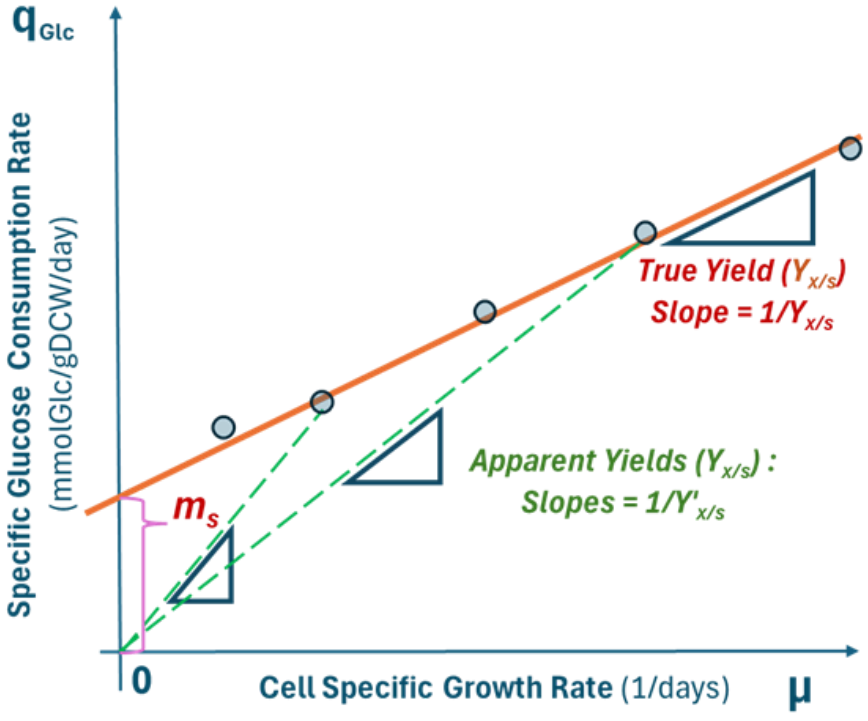

Figure 2.4a: Graphical representation of the linear model (Equation 2.4a) for substrate consumption.

The slope of the line is equivalent to the inverse of the true yield coefficient (1/Y) and the y-intercept is equal to the maintenance term. This linear behavior, represented by these two factors, fits experimental data for a single carbon and energy substrate. Thus, this relationship offers a practical method to determine yield and maintenance requirements for most cell types, including

microorganisms, although they have a significantly lower maintenance requirement as a percentage of total substrate consumption than animal cells, which are larger and more complex.

Apparent yield

Because data and multiple growth rates are required to determine a true yield, apparent yield ($Y'_{X/S}$) is often reported in the literature because it is easier to determine. Apparent yield is defined as the observed ratio of biomass formed to substrate consumed, including both growth and maintenance requirements. It is essentially what has been used by published TEMs. These coefficients are valid if they are measured at similar growth rates that are assumed in the model. The apparent yield is represented by the equation:

$$q_S = \mu / Y'_{X/S}$$ **Equation 2.4b**

The apparent yield can be related to the true yield by deriving Equation 2.4c from Equations 2.4a and 2.4b:

$$Y_{X/S} = Y'_{X/S} \left(1 + m_s / \mu\right)$$ **Equation 2.4c**

The apparent yield can vary with the growth rate and is less consistent than the true yield. As depicted in Figure 2.4a, the apparent yield can be visualized graphically as the slope of the line from the origin (rather than the y-intercept) to the data point representing the measured specific consumption rate for a given growth rate. Therefore, the true yield ($Y_{X/S}$) is larger than the apparent yield ($Y'_{X/S}$) by the term m_S/μ. Because the slope is the reciprocal of yield, the true yield line has a shallower slope than the apparent yield. The higher the data points and/or the slope on the graph, the more substrate is required to make cell mass, and the lower the biomass yield. The literature review of experimental data in Section 3.5 will add more clarity to these points.

Metabolite formation as a function of growth rate

The formation rates of the key metabolites are often modeled as a proportional function of cell growth rate. If little is known of the origins of metabolite formation or if it is derived from multiple substrates, its specific production rate can simply be described as:

$$q_I = \mu * Y_{I/X}$$ **Equation 2.4d**

Symbol	Definition	Typical units
q_I	Specific formation rate of inhibitor I	mmol/cell/day or mmol/gDCW/day
$Y_{I/X}$	Yield of metabolite I per biomass formed	mmol I/10^6 cells or g I/gDCW

When the bulk of a waste metabolite is derived from a single substrate (e.g., lactate from glucose or ammonia from glutamine), then its production can be modeled as a function of substrate consumption using a yield factor that reflects the stoichiometry of the metabolic pathway:

$$q_I = Y_{I/S} * q_S$$ **Equation 2.4e**

Symbol	Definition	Typical units
q_S	Specific substrate consumption rate	mmol/cell/day or mmol/gDCW/day
$Y_{I/S}$	Yield of metabolite I from substrate S	mmol I/mmol S or gI/gS

Equation 2.4e can be used when the stoichiometry is mechanistically known. For example, 1 mol glucose → 2 mol lactate in anaerobic glycolysis, while 1 mol glutamine → 2 mol ammonia via glutaminolysis and full deamination.

Osmolality changes with metabolite accumulation

As cells consume nutrients and produce waste by-products, the total osmolality of the cell culture medium changes. As discussed previously, osmolality changes are also important to model, as osmolality can influence overall growth rate and viability.

The osmolality can be estimated at any time in the process by summing the molar concentrations of dominant solutes, including ions from base addition and counterions used to control pH:

$$Osmo = Osmo_{base} + [Glc] + [Gln] + [Lac] + [NH4] + [Na+]$$ **Equation 2.4f**

Symbol	Definition	Typical units
$Osmo_{base}$	Osmolality of the fresh culture medium excluding glucose and glutamine	mOsm/kg
[Glc], [Gln], [Lac], [Amm]	Molar concentrations of glucose, glutamine, lactate, and ammonia	mM
[Na+]	Concentration of the counter-ion in the extracellular medium as a result of base addition for pH control	mM

As discussed further in Section 3.5, it is desirable to minimize the consumption rates of substrates (q_S) and the yields of inhibitory metabolites from an efficiency and cost standpoint, as bioreactor volumetric productivity will be affected.

Models of ATP and energy balance

Throughout the development of this report, we realized that unstructured empirical models based solely on external substrates, such as those presented above (Equations 2.4a-2.4e), suffer from limitations that could affect their ability to capture all of the phenomena that have been observed in the literature. While linear models and fixed-yield coefficients of substrates are effective under defined conditions, they do not account for intracellular phenomena, which can lead to significant errors when applied to changing environments and growth rates. This is especially true during batch culture when substrate and metabolite concentrations change rapidly. ATP is the primary energy carrier in most cells and is derived from the catabolism of the primary substrates supplied externally.

In effect, ATP is an internal substrate. Using the same rationale for external substrates, the specific rate of ATP production to provide the necessary energy for growth and cell maintenance can be described similarly to Equation 2.4a:

$$q_{ATP} = (\mu / Y_{ATP/S}) + m_{ATP}$$ **Equation 2.4g**

Symbol	Definition	Typical units
μ	Specific growth rate	1/day or 1/hr
q_{ATP}	Cell-specific production rate of ATP from substrate S	mmol/cell/day or mmol/gDCW/day
Y_{ATP}	The yield of ATP from substrate S	mmol/mmol
m_{ATP}	The maintenance requirement for ATP	mmol/cell/day or mmol/gDCW/day

Such a model based on ATP production and overall energy balance could serve as the unifying currency for anabolic and catabolic processes. Similarly, the primary intracellular reducing agent, NADH, can also be viewed as a common product of substrate catabolism. Another way energy homeostasis is represented in the literature is by the metric adenylate energy charge (AEC), which tracks ratios of ATP, ADP, and AMP as proxies for metabolic health. AEC tends to stay in the range of 0.8 to 0.95 in metabolically "healthy" cells across prokaryotes and eukaryotes (De la Fuente et al. 2014). However, using AEC in a model requires the inclusion of AMP and ADP in addition to ATP.

ATP and NADH production can both be measured in cell cultures, and quantified data from studies are included in Section 3.5. The use of pooled or pseudo-metabolites is discussed in Section 4.4 along with structured energetics models. Additional substrate and energy-based modeling approaches are included in Appendix A2.

The systems of equations presented in Section 2 provided a framework for the literature review presented in the next section. We focused our search on data and parameters that are directly relevant to the relationships representing key phenomena and interactions in bioreactor culture.

Section 3. Cell growth model: Critical review and data gaps for model parameters

A comprehensive literature review was conducted using the modeling framework outlined in Section 2 as a guide to finding the most relevant parameters.

3.1 Overview

This section reviews the literature, supplemented with survey data collected for this project, to summarize existing data and contextualize information for the key factors and parameters in the modeling framework and equations presented in Sections 1 and 2. We examine data availability, quality, and gaps, as well as the extent to which existing data from biopharmaceutical-relevant cell lines could be used as a starting point for modeling cell lines relevant to CM applications. While the literature review primarily examines steady-state interactions among macronutrients, metabolites, and rates of cell growth, inhibition, and substrate consumption, we include data on cellular response times and the effects of temperature and pH. Metabolite influences are summarized individually where possible, though their complex interactions sometimes necessitated combined discussion or separate sections. Section 3 is intended to mirror the structure of Section 2, where literature is reviewed and discussed for:

- Cell mass and composition (3.2)
- Cell proliferation and differentiation kinetics (3.3)
- Growth inhibition and death rates due to waste metabolites (3.4)
- Overall cell growth stoichiometry, including substrate consumption and metabolic by-product production as indicators of metabolic efficiency (3.5)

This section also serves as a systematic guide for CM researchers to understand the types of experiments to perform, data to collect, and how these data plug into models that inform scale-up and optimization of commercial processes.

3.2 Cell size, mass, and composition

As discussed in Section 2.2, the volumetric productivity of a bioreactor is defined as the amount of product mass generated per unit of time per unit of bioreactor volume. In CM, where biomass is the product, it can be defined as WCW or DCW, or in some cases by the mass of certain nutritional components. Understanding and measuring cell mass and composition is therefore crucial to accurately model the productivity of CM processes. What do we know about the mass and composition of animal cells?

A variety of cell types, including pluripotent stem cells, myoblasts, fibroblasts, fibro-adipogenic progenitors, and mesenchymal stem cells, are used as starting material in the production of CM. The cell types vary in their stemness and potency, which influences many downstream characteristics that can affect manufacturing outcomes.

Cells can also vary significantly in their size, mass, density, and composition. Accordingly, we cite the type of cell that corresponds to the data being discussed throughout this section. Future models should be tailored to the specific cell type being used in production, with data collection guided by the recommendations throughout this report.

For a detailed review of cultivated meat cell lines, we direct readers to the following resources (Deep dive: cultivated meat cell lines; Cell line development and utilization trends in the cultivated meat industry). Please visit our cell lines database to locate cultivated meat cell lines to use in your research program.

Callout box 2. Cell types used in cultivated meat production.

Deriving cell mass based on cell size

Mass is often estimated based on cell size (i.e., diameter) and density. Assuming a spherical shape and a common cytoplasmic density of 1.06 g/cm^3, mass can be approximated by the equation:

$$\text{cell mass} = \text{cell density} * 4/3\pi(d/2)^3$$

In our review of the literature, we found that most animal cells (in suspension) are between 10-20 µm in diameter, which was also validated by survey data received from CM companies (**Figure 3.2a**). An exception to this may be adipocytes, which can accumulate lipids during maturation processes and grow to sizes beyond 100 µm in diameter. However, as discussed below, the size of a hydrated cell is a poor proxy for its overall mass or relevant compositional makeup. Therefore, we do not recommend using the above approach to derive accurate values for cell mass.

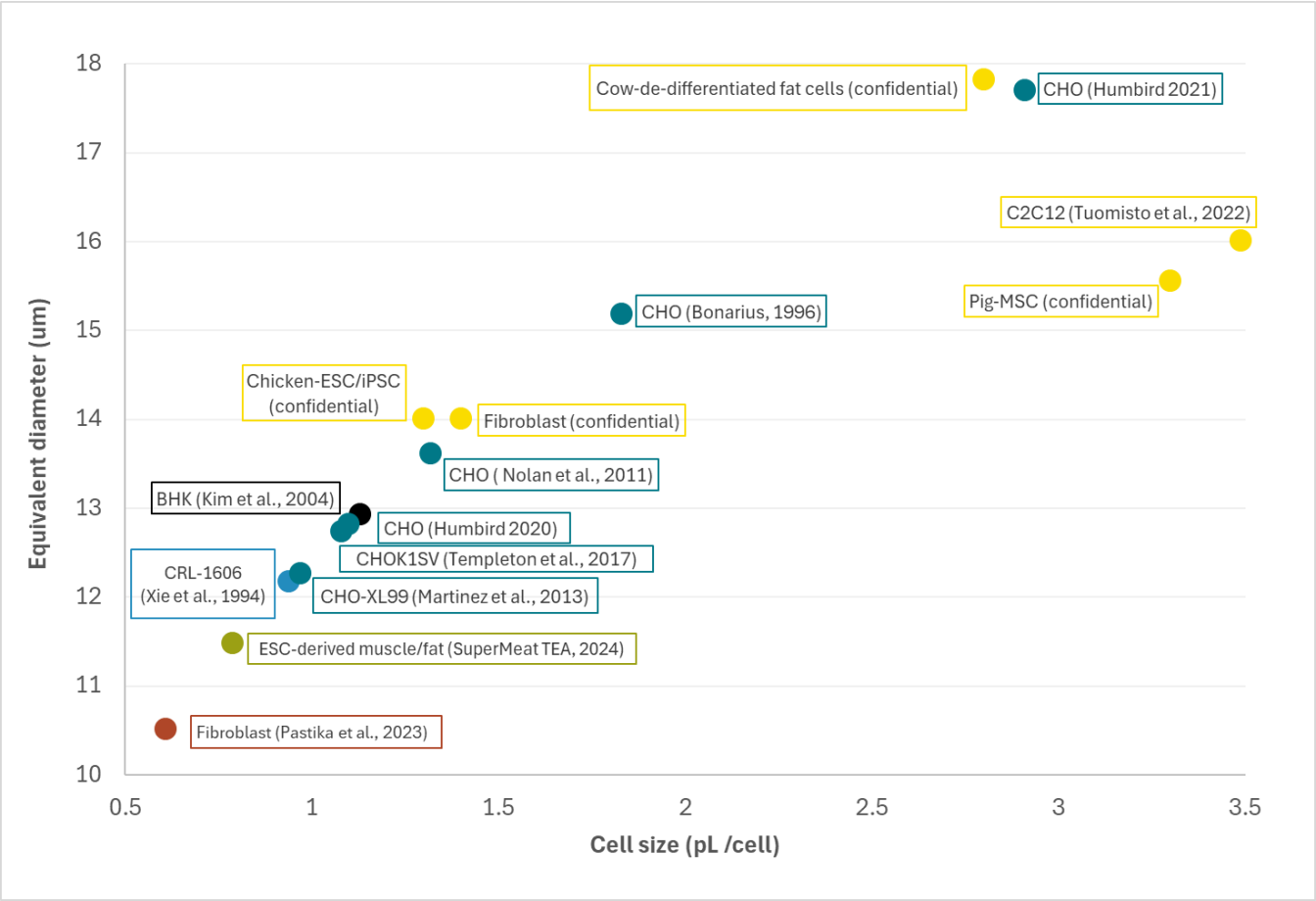

Fig. 3.2a: Summary of cell size data from our literature research. Cell size and mass data were rarely reported directly and these values were calculated from reported cell mass (dry or hydrated), assuming 75% cell water content unless otherwise stated, cell density (specific gravity) of 1.06 (except for Humbird, which used 1.03), and assuming a spherical shape. The dry mass was often the reported value. Three experimental data points from CM companies were not shown in the figure to prevent crowding and due to the lack of cell mass data. These were: Cow Myoblast, 14.5 µm; Cow Pluripotent ESC/iPSC, 10.0 µm; and Cow Mesenchymal MSC, 20.0 µm. Caution is advised in over-interpreting these data. As we will see in the next section, dry cell mass has a weak relationship with cell volume.

Key takeaway

The size of a hydrated cell is a poor proxy for its overall mass or composition, making cell size and diameter measurements lower value for modeling efforts.

Hydrated (wet) cell mass (WCW)

The overall mass of a cell is highly dependent on its water content, which in turn is influenced by the composition and osmolality of the surrounding medium. Several CM modeling studies have assumed the intracellular water content of cells to be 70%, which is intended to approximate that of conventional meat (Humbird 2021; Tuomisto, Allan, and Ellis 2022). However, survey data collected from companies suggest intracellular water content in their products may be as high as 83%. Furthermore, water content in multiple approved CM products spanned 75-96% (**Table 3.2a**).

Study or product	Water content assumed or measured	Notes
Humbird, 2021; Tuomisto, 2023	70%	Assumed from textbooks
Sinke, 2023	70-80%	Assumed based on values provided by collaborating companies
Mattick, 2015	83%	Assumed by authors
Mission Barns: cultivated pork fat	86%	Measured moisture content in product evaluated by regulators
Vow: cultivated quail	>80%	Moisture content specification in product evaluated by regulators
GOOD Meat: cultivated chicken	89%	Measured moisture content in product evaluated by regulators
UPSIDE Foods: cultivated chicken	75-80%	Measured moisture content in product evaluated by regulators
Wildtype: cultivated salmon	75-90%	Moisture content specification in product evaluated by regulators
Believer Meats: cultivated chicken	95-96%	Measured moisture content in product evaluated by regulators
Other company data	70-83%	Survey data collected as part of this project

Table 3.2a. Water content assumed in prior CM models and reported in real-world products.

The variance in reported values for water content may be based on differences in harvesting and measurement techniques that may result in excess extracellular water being carried over, especially when measurements are taken directly from harvested cell pellets. Nevertheless, initial data indicate that the water content of cultivated cells is likely not a fixed number and may be higher than assumed in previous TEMs. Research efforts that measure the dry mass of cultivated cells directly can prevent

the need to make error-prone assumptions for water content in future TEMs. Product developers should also consider the effect of water content on the nutritional density of the end product, and how it may influence equivalence to conventional meat, consumer perception, and market value.

Key takeaways and data gaps

- The reported water content of cells and real-world products varies between ~70-95%, likely due to differences in methods for weighing cell mass post-harvest.
- A 10% error in total mass could significantly affect techno-economics.
- Future research should measure dry cell mass of CM cells and products to avoid making error-prone assumptions for hydrated cell mass.

Dry cell mass (DCW)

While the DCW measurement provides the best means to normalize data across studies (see Section 3.5), these measurements are infrequently provided in the literature. A study by Széliová et al. represents the best available dataset for the dry mass and composition of animal cells (Széliová et al. 2020). The study evaluated the dry mass and biomass composition of 13 different CHO cell lines. The dry cell mass ranged between 199 and 293 picograms per cell line, with an average of 264 pg. These values correspond with the range of dry cell mass measured during the growth phase of L1210 (mouse lymphocytic leukemia) cells, where values reported were between ~125 and 300 pg per cell (Miettinen et al. 2022), as well as hybridoma cells reported between 250 and 470 pg per cell (Széliová et al. 2020). Importantly, the authors also noted that there is only a weak correlation between dry cell mass and cell volume, implying that dry mass needs to be quantified rather than attempting to estimate it from cell volume or diameter (**Figure 3.2b**).

Assuming a water composition of 75% for an average CHO cell with a mass of 264 pg, it can be calculated that the hydrated CHO cell mass would be 1,056 pg, roughly one-third of the 3,000 pg hydrated mass assumed in prior CM modeling (LCA/TEA) studies (Humbird 2021; Sinke et al. 2023). Measurements from C2C12 (mouse myoblast) cells suggest a hydrated mass closer to 4,000 pg (Tuomisto, Allan, and Ellis 2022), with other modeling efforts choosing 3,300 pg or 3,500 pg (Mattick et al. 2015; Tuomisto and de Mattos 2011). To test whether or not CM modeling studies overestimated the mass of cells, we plotted data from CM modeling studies and studies where DCW was actually measured. Overall, the data show that DCW and WCW assumptions in CM modeling studies display a large discrepancy with real measurements from animal cells of a similar size (**Figure 3.2c**).

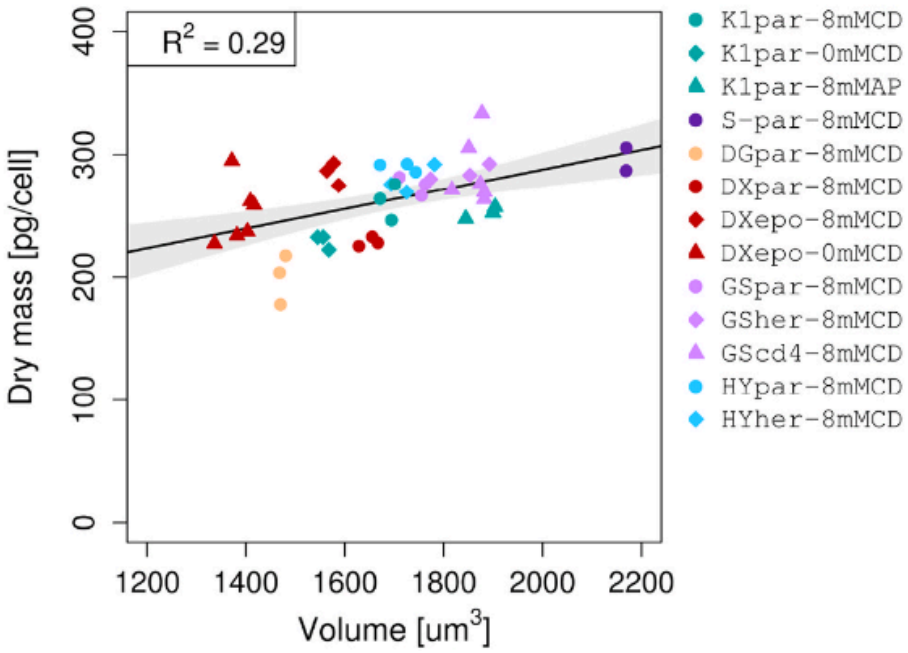

Figure 3.2b. Dry cell mass has a weak relationship with overall cell volume across 13 different CHO cell lines. Data from (Széliová et al. 2020). Re-printed according to CC BY 4.0 license.

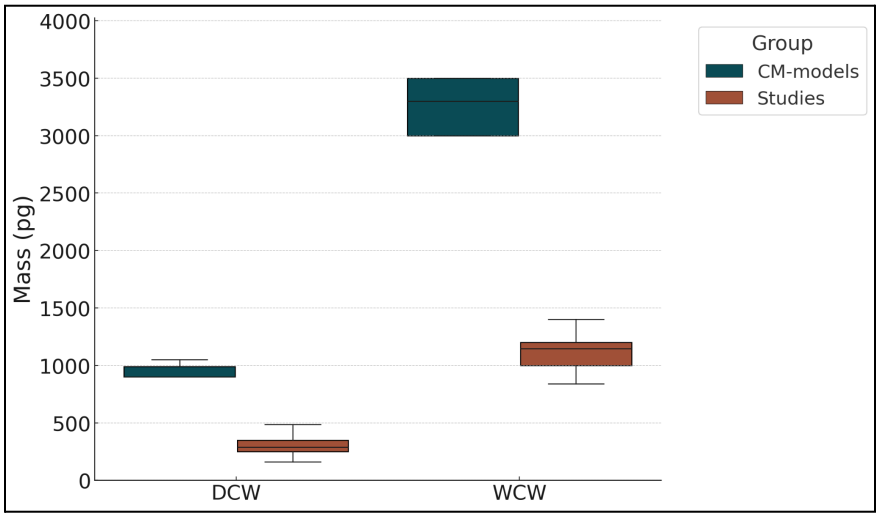

Figure 3.2c. Comparison of DCW and WCW values between five CM LCA and TEM models alongside other studies where DCW of animal cells was actually measured (WCW values for these studies were calculated assuming 75% hydration). Data from Studies included mouse hybridoma, BHK, CHO, and chicken fibroblast and embryonic stem cells.

We were unable to collect additional dry mass data from companies or researchers, which highlights the need for dry cell mass measurements across species and cell types as a major data gap in the field. It is strongly recommended that researchers and companies in the sector report measurements of both hydrated and dry cell mass of their cells. Because hydrated cell mass measurements may be

variable, dry cell mass measurements are crucial to ensuring mass quantification is consistent and comparable across research groups.

Key takeaways and data gaps

- Prior TEMs have assumed a single cell's WCW is ~3,000 pg, however, data from animal cells suggest this may be overestimated by a factor of 2-3x.
- The DCW of CM-relevant cell lines is a major data gap.
- DCW needs to be quantified rather than attempting to estimate it from cell volume or diameter. The following publications contain protocols that may be used for dry mass measurements of single cells in suspension (Széliová, Ruckerbauer, et al. 2020; Széliová, Schoeny, et al. 2020; Miettinen et al. 2022) and as adherent cells (Liu et al. 2020).

Biomass composition

Biomass composition refers to the relative proportions of macromolecules such as proteins, lipids, carbohydrates, and nucleic acids within a cell, in addition to water. Composition is a key determinant of the nutritional value of CM and is important to capture in modeling, as it affects stoichiometric calculations, nutrient demands, and yield estimates. Humbird reported the composition of animal cell dry mass as approximately 70% protein, 15% lipids, 10% carbohydrates, and 5% nucleic acids (Humbird 2020)).[2] More recent data from 13 different CHO cell lines suggest an average dry mass composition of approximately 46% protein, 14% lipids, 12% nucleic acids, and 2% carbohydrates, with the remaining 26% being attributed to remaining minerals, metabolites, and small molecules (Széliová et al. 2020). Inorganic constituents, namely minerals and salts, are often referred to as ash in proximate analyses by combustion. Ash content is sometimes included and sometimes not in compositional data, making comparisons more difficult. The only compositional data from cultivated meat-relevant cells (chicken fibroblasts) reported values of 80% protein and 13% fat on a dry mass basis (Laura Pasitka et al. 2024). These data are summarized in **Figure 3.2d**.

[2] Humbird also supplied a molar ratio of elemental carbon, hydrogen, oxygen, and nitrogen (CHON), and we were unable to identify additional data sources that confirm or dispute these values.

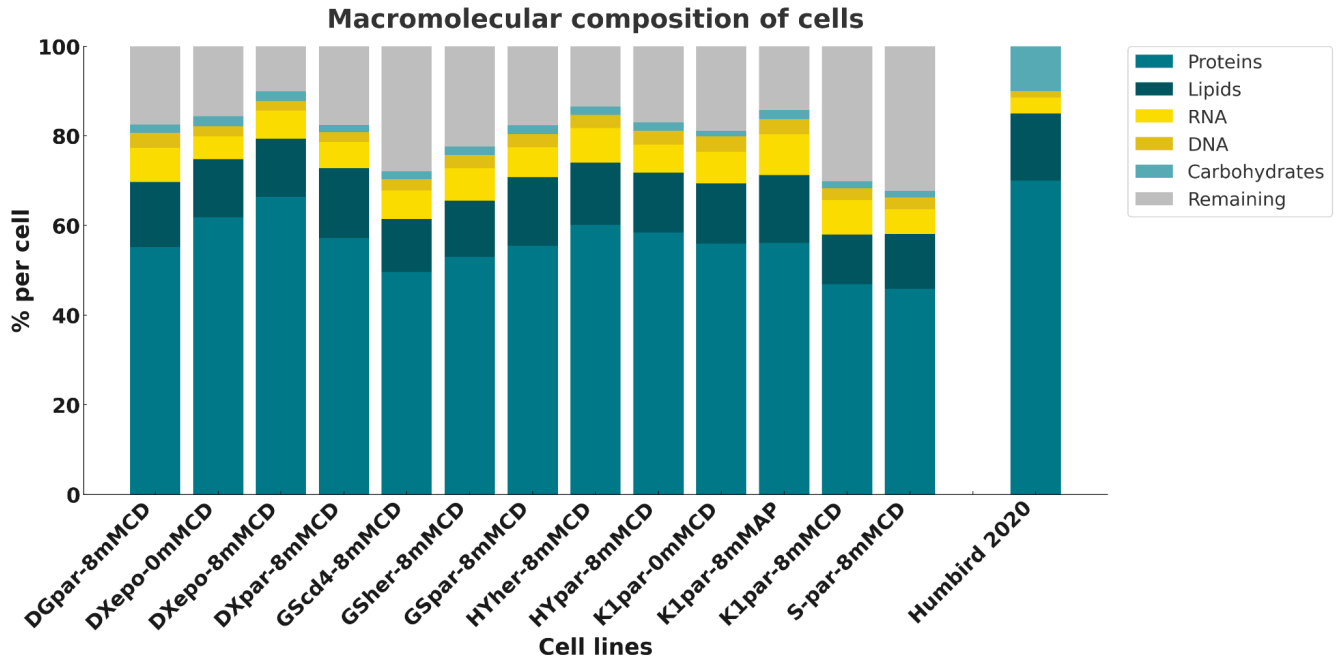

Figure 3.2d: Biomass composition data of CHO cells compared to assumptions in prior TEMs. Humbird noted that the typically reported 5-10% remaining mass fraction of minerals, metabolites, and small molecules was excluded from the total, as this fraction was assumed to have a similar elemental make up and was normalized.

In the CHO cell data from Széliová, it is notable that there is variance even among different cell lines of the same cell type, with protein content varying by 20%, lipids by 5%, RNA by 4%, and DNA and carbohydrates by 1%. Although the samples were collected at mid-exponential phase when cells undergo rapid division in the S and G2 phases of the cell cycle, other studies have documented a strong relationship between dry mass accumulation and cell cycle phase (Miettinen et al. 2022), suggesting that some variance may be accounted for by different populations of cells captured at different points along mitosis.

Another consideration is the overall phase of the culture (**Figure 3.2e**). RNA content is known to increase dramatically to support high rates of cell growth during the exponential phase before returning to baseline levels in the stationary phase (Darzynkiewicz et al. 1979). Nucleotide synthesis can even be rate limiting under conditions of rapid growth. Conversely, DNA content is at its lowest in the exponential phase while total cell mass is at its highest due to the recruitment of additional protein synthesis machinery. Because cells will be cycling throughout each phase of the cell culture, mass changes during the cell cycle must be considered on the individual cellular levels, while mass changes during different culture phases need to be assessed on the population level.

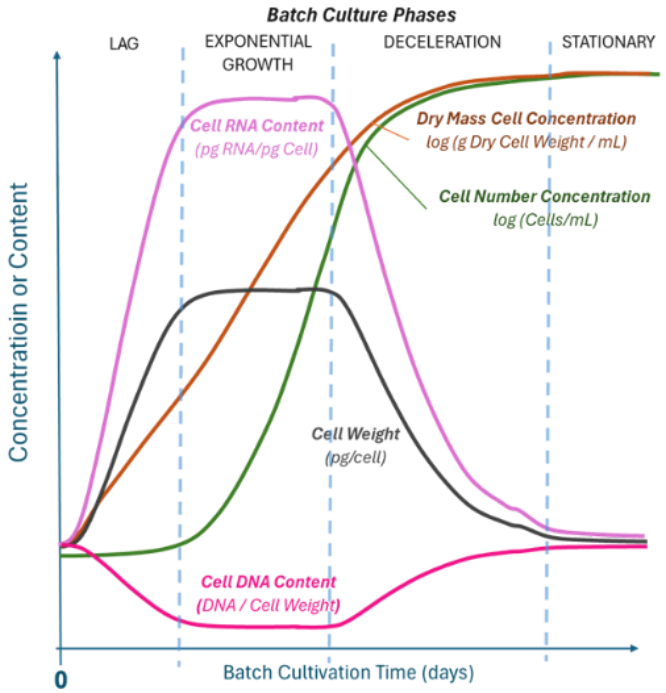

Figure 3.2e: Overview of cellular content changes during cell culture phases. Adapted from Wang et al. 1979.

Changes in cell size

Evidence of the effect of a cell's growth rate on its size has been demonstrated by several research groups. **Figure 3.2f** shows the increase in cell size as measured directly by cell diameter (converted to volume; (Ozturk and Palsson 1991; Frame and Hu 1991a), and dry mass content (Dimasi 1992). While average cell size is related to the cell type, the effect of the cell size of a given type can vary significantly based on growth rate alone. It is apparent that cell volume and mass can change by more than a factor of two over the range of growth rates typically experienced in a cell culture.

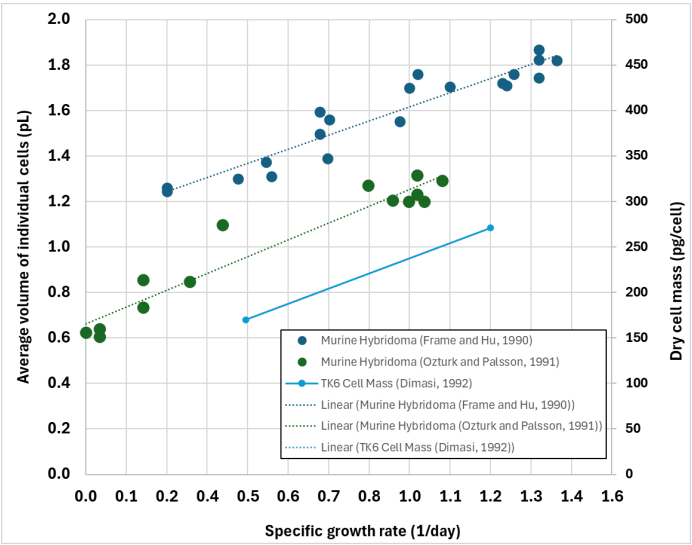

Figure 3.2f: Cell size and mass as a function of specific growth rate.

Cell size appears to be tied to the cell cycle. Cell protein and RNA content have been shown to decrease in cells when their growth slows, consistent with Figure 3.2f (Ozturk and Palsson 1991; Dimasi 1992). Concurrently, the fraction of cells in the G0 + G1 phase increases during the deceleration phase, accompanied with a decrease in the size of the population in the S phase. The fraction of cells in the M phase did not change, suggesting that cells in the M phase do not divide, even though they have enough DNA synthesized.

Liu et al. used computationally enhanced quantitative phase microscopy to study populations of proliferating cells, which enabled highly accurate measurements of cell dry mass of individual cells throughout the cell cycle (Liu et al. 2020). Using this method, they found that the coordination of size-dependent cell cycle regulation and size-dependent growth rate modulation allowed cells to maintain accurate cell mass homeostasis while proliferating. They speculated that the same regulatory processes might also be operative in terminally differentiated cells.

More studies will be needed to disentangle the regulatory mechanisms and interplay between these two phenomena, which are just beginning to be understood (Liu, Yan, and Kirschner 2024). However, developers of CM processes should be cognizant of the relationships between cell cycle status, cell size, and composition, because they are directly relevant to volumetric productivity of biomass components and for determining optimal harvest timepoints.

Outside of the few examples provided in this section, we were not able to find any additional detailed biomass composition data from CM-relevant cell lines. The overall lack of biomass composition data has also been highlighted by other investigators, as composition is also crucial in the related field of genome-scale metabolic modeling (Gomez Romero and Boyle 2023). In their review, the authors noted that accurate biomass measurements taken from cells grown in defined media are needed, as well as biomass compositions of different cell types of the same organism, which can guide additional genome-scale model reconstructions derived from the parent model.

Key takeaways and data gaps

- Optimizing for specific compositional makeup in CM processes will be important, as the product's value will be highly dependent on its nutritional content.
- The field needs a better understanding of compositional variability between species, cell types, and even of the same cell line at various rates of growth. Investigators should consider computationally enhanced quantitative phase microscopy for accurate measurement of cell dry mass of individual cells throughout the cell cycle (Liu et al. 2020).
- Cell mass and composition are major data gaps for the field. Compositional data should be obtained from cells grown in commercially relevant, defined media and as a function of growth rate.

3.3 Kinetics of cell proliferation and differentiation

Overview of doubling time and specific growth rate

As previously described by Equation 2.2a, a key parameter to determine the rate of biomass formation is the specific growth rate (μ) of the cell. There are many factors that influence growth rate, including nutrient and growth factor availability, metabolite inhibition, and environmental conditions such as temperature, pH, and oxygen levels (Equation 2.3a; (Hauser et al. 2024). Accordingly, doubling time (or specific growth rate; **Callout box 1**) is a trait that can vary depending on culture conditions. In modeling biological systems, specific growth rate is commonly viewed as a state variable representing the cell's state.

An example of cell growth flexibility is provided below, where doubling times of eel fibroblasts were shown to vary dramatically depending on the nutrient availability (i.e., serum), temperature, and whether the cells were grown in adherent or suspension conditions (**Figure 3.3a**). As shown by these data, it's important to acknowledge that doubling times can change significantly when moving to suspension culture in the more complex bioreactor environment. Therefore, it is important for researchers to report specific growth rates in relevant bioreactor environments rather than rely on observations solely from adherent cell cultures in plastic dishes, as these may not be as representative for modeling CM manufacturing.

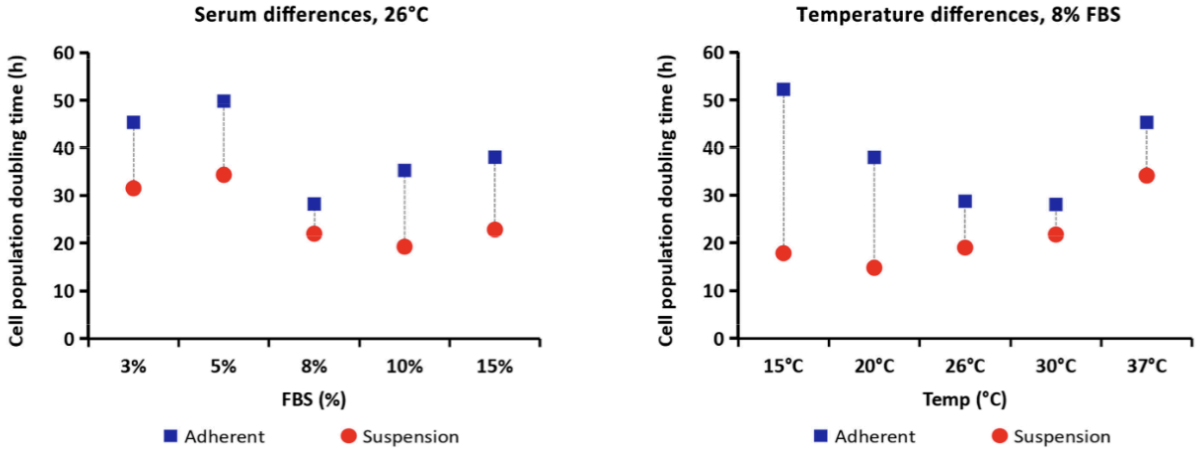

Figure 3.3a: Example of growth rate variability of eel fibroblast cells under different culture conditions. Data from (Zheng et al. 2024). Reprinted according to CC BY 4.0 license.

Intrinsic limits for how fast a cell can grow are likely to exist depending on the cell type and species. For example, cell progenitors (cells with more stemness) tend to grow faster than primary cells. However, these limits have generally not yet been fully characterized. To provide a sense of a potential lower boundary for animal cell doubling time, our review of the literature found that a lung cell line from the Chinese hamster had the shortest reported doubling time (i.e., highest specific growth rate) of an animal cell line in vitro at 8 hours (Yamano-Adachi et al. 2020), while some T-cell populations

reportedly double in vivo at 4-5 hours (Hwang et al. 2006).[3] With this information, alongside previously collected survey data (Ravikumar et al. 2023), it is reasonable to expect most doubling times for CM production will be in the range of 12 to 24 hours (μ = .058 to .029 hr^{-1}) after optimization of culture conditions, with potential for some cell lines to grow at even faster rates.

Key takeaways and data gaps

- The maximum specific growth rate (minimum cell doubling time) at near-optimal temperature and pH is an intrinsic property of a given cell type.
- A cell's actual growth rate is a flexible trait that varies depending on culture conditions and nutrient availability. Researchers should report doubling times or specific growth rates in relevant media and bioreactor environments rather than solely from adherent cell cultures.
- Researchers should report and graph specific growth rate (μ) to show relationships with culture conditions since it is linearly related to growth, rather than doubling time, which has an inverse relationship.
- Most doubling times for cultivated meat production are likely to be in the range of 12 to 24 hours (μ = 0.0578 to 0.0289 hr-1 or 0.138 to 0.693 day-1) after optimization of culture conditions, with potential for some cell lines to grow at even faster rates.

Effect of temperature on cell growth rates

As discussed in Section 2.2, the temperature can have a strong influence on a variety of cellular activities that affect cell growth. Despite this, there is limited experimental data for temperature's effects on animal cell growth rates, especially for cultivated meat-relevant cell lines.

Using available data from a study on mouse lymphoblasts (Watanabe and Okada 1967) plotted in **Figure 3.3b**), we applied the linearized form of the Arrhenius equation previously described (Equation 2.3b) to the six data points from the study. The middle four points in Figure 3.3b (31-37 ºC) fell along a straight line. Thus, growth rate in this range is well modeled using the Arrhenius relationship with temperature. In the study, the authors also determined the activation energy in this range to be 27.5 kcal/mol (or 115 kJ/mol), which likely could apply to other cell lines as well. The study also found that the G_1 and S phases were the most temperature-sensitive, with G_1 being particularly prolonged at reduced temperatures. This suggests that cell growth is regulated primarily by energy-dependent processes in the G_1 phase, and that lower temperatures disproportionately slow these steps, leading to an overall reduction in growth rate from its optimum.

[3] As a point of comparison, the fastest-growing bacteria, *V. natriegens*, has a doubling time of just 14 minutes.

As the CM sector matures, it will be important to collect additional data on temperature effects in the complex environment of a bioreactor. In a bioreactor, the temperature influences crucial aspects tied to productivity, including oxygen and nutrient solubility, and diffusion and mass transfer rates. For example, temperature increases lead to increases in oxygen diffusion but decreases in oxygen solubility, viscosity, and surface tension. Despite lower oxygen solubility, the cumulative effects can outweigh lower solubility, resulting in increased oxygen uptake and kLa values (Muralidharan, Bolduc, and Davis 2024).

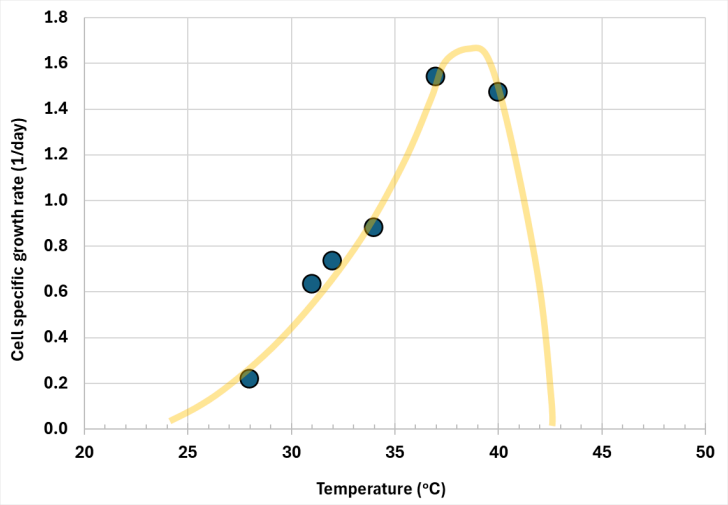

Figure 3.3b: Effect of temperature on specific growth rate of mouse lymphocyte cells (L5178Y) replicates the Arrhenius profile. Data from (Watanabe and Okada 1967).

This may lead to the hypothesis that maintaining cells at higher temperatures will always achieve faster growth rates. However, even small increases above the normal physiological temperature can lead to viability issues due to perturbations in protein folding, proteostasis, and heat shock response pathways, with some studies demonstrating cell-type sensitivity (Dorrity et al. 2023). Lower temperatures can favor certain metabolic processes over others and can change membrane dynamics, potentially enabling greater resistance to culture conditions (Al-Fageeh and Smales 2006). Accordingly, downward temperature shifts during the exponential phase are now commonly practiced in the biopharmaceutical field, as this has been shown to achieve an improved balance of cell growth rates and prolonged periods of productivity (Xu et al. 2019).

Taken together, while the optimal growth temperature may be static in a small-scale adherent culture, the optimal growth temperature in a bioreactor environment could be a moving target. CM manufacturers will need to determine if similar downward temperature shifts could improve productivity in their bioprocesses, which can be assisted with modeling approaches (Wang, Wang, and Chen 2022).

Key takeaways and data gaps

- The optimal growth temperature in a bioreactor process is not necessarily the temperature that supports the maximum specific growth rate of the cell (T_{opt}) at tissue culture scale. In the biopharmaceutical sector, for example, downward temperature shifts can enhance the productivity of recombinant proteins.
- Thus, the impact of temperature (and pH) on specific growth rates should be understood so that biomass productivity can be optimized along with other physical conditions in a bioreactor. For example, lower temperatures can increase membrane rigidity and increase resistance to certain culture conditions (Al-Fageeh and Smales 2006).
- Limited data exist for the effect of temperature on the growth rate of CM-relevant cell lines. Researchers can repeat experiments by Watanabe and Okada and use the linearized form of the Arrhenius equation (Section 2.3) to describe the relationship.

Effect of pH on specific growth rate

Optimizing pH is another important factor to consider. pH is typically maintained at or near the physiological pH of the organism. For example, human cell cultures are typically maintained at pH 7.4, while chicken cell cultures have been maintained at pH 7.1 (Laura Pasitka et al. 2024) and bovine cell cultures at pH 7.1 to 7.3 (Hanga et al. 2021; Tzimorotas et al. 2023). Data collected for this study supports this, with reported optimal pH values ranging between 7.0 to 7.6. Divergence in pH is only observed in insect cell cultures, which are typically held at more acidic pH levels between 6.0 to 6.4 (Letcher et al. 2024).

Similar to temperature, there are limited data available on the effects of pH on growth rate, especially for CM-relevant cell lines. **Figure 3.3c** shows the approximate pH effects on growth rate for different mouse and human cell lines. There are too few points to fit any mathematical model, but the data suggest a bell-shaped curve that is skewed to either the basic or acidic side. Such a complex relationship is probably best handled with an empirical correlation. Additionally, the study of pH on the growth of over 20 different cell types by Eagle provides an excellent relative comparison of the pH-μ profiles (Eagle 1973). However, it is difficult to discern absolute growth rates since growth measurements were based on protein accumulation.

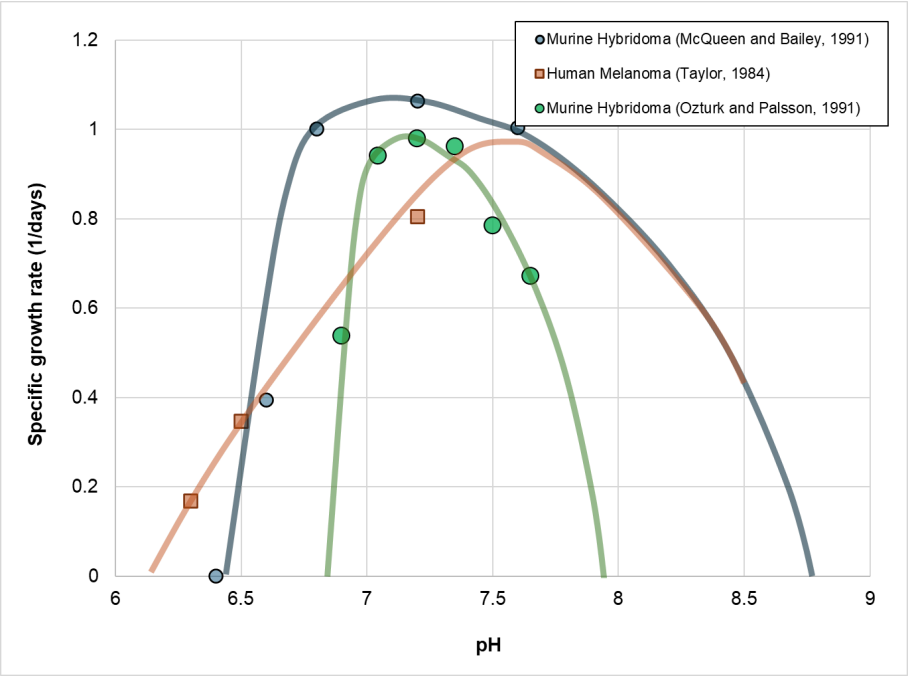

Figure 3.3c: Effect of pH on the specific growth rate of various cell lines. The trend lines are presumed based on the literature. Data from (McQueen and Bailey 1990; Ozturk and Palsson 1991; Taylor, Los, and Robinson 1984).

Looking forward, tightly controlling pH will be important in CM manufacturing, as deviations in pH can influence protein folding and metabolism, which can impact the growth rate and cell viability. In small-scale cell cultures, pH is controlled by buffers, which typically consist of CO_2-bicarbonate systems or buffering agents such as HEPES. In larger and higher-density systems, the pH can become altered via the accumulation of metabolic by-products such as lactate and CO_2, which form lactic acid and carbonic acid in solution and usually necessitate further control.

In larger reactors, pH can be controlled via the addition of base and gas sparging. The addition of base is a less preferred method, as mixing inefficiencies at larger scales can lead to localized pH heterogeneity that may impact viability and increase the osmolality of the culture. However, it is often required because a bicarbonate buffering system and controlled sparging cannot sufficiently counter the shifts in pH. Sparging itself requires optimization and balancing of trade-offs related to agitation rates, bubble size, gas rates, reactor design (e.g., available headspace), and process operation (e.g., perfusion vs. fed-batch).

Taken together, understanding the impact of pH on growth rate is an important consideration, but data and representative mathematical models are limited. Added difficulty for modeling pH effects is introduced when metabolic and/or physical trade-offs occur, and when calculating shifts in pH with the multiple buffering components normally contained in cell culture media. These considerations will be discussed in more detail in a future report on the bioreactor environment model.

Key takeaways and data gaps

- Like temperature, optimal pH in a bioreactor process is not necessarily the pH corresponding to the one supporting the maximum rate of growth at tissue culture scale.
- Thus, the impact of pH (and temperature) on specific growth rates should be understood so that biomass productivity can be optimized along with other physical conditions in a bioreactor.
- Selecting an optimal pH for a bioreactor process is a challenge due to the many biological and physical parameters it can interact with.
- Mathematically modeling changes in pH in a cell culture is especially difficult because of the complex buffering dynamics of multiple medium components.

Differentiation kinetics and mass gain

According to a 2023 industry survey, 15/21 respondents said that their company includes or plans to include a differentiation phase in its manufacturing process, with an expected duration of two to ten days (Harsini and Swartz 2024). However, differentiation duration is trending downward as new innovations are introduced. For example, CM companies have published several protocols on fat differentiation (Mitić et al. 2023; Dohmen et al. 2022; L. Pasitka et al. 2022), with timelines for fat differentiation recently demonstrated as short as one day (SuperMeat 2024). Likewise, recent demonstrations in muscle cell differentiation suggest timelines may become shortened to two to three days (Profuse, (Eigler et al. 2021). Statements from other companies suggest muscle and fat differentiation times of four days (Meatable).

Implementing a differentiation stage is highly tractable from a biological perspective, as the pathways underlying the differentiation of stem cells or precursor cells into mature muscle and fat tissue are well understood. However, the necessity of a differentiation and maturation stage (hereafter referred to as differentiation) in CM manufacturing is an open question in the field. On one hand, differentiation may improve product quality aspects such as texture and nutrition, although it may or may not increase overall biomass productivity. For example, a recent study from SuperMeat suggests that a 1.7-fold increase in mass during an averaged two-day differentiation could reduce production costs by approximately 40% (SuperMeat 2024) depending on the relative costs of the proliferation and differentiation stages. On the other hand, the addition of a differentiation step is expected to add time and complexity to the process, as 75% of companies expect to perform differentiation in a separate bioreactor from the proliferation stage (Harsini and Swartz 2024).

Thus far, differentiation has not been thoroughly modeled in existing TEMs, which have focused on the proliferation stage only. To evaluate differentiation trade-offs in future models, it is critical to first

understand the potential rate of mass gain during differentiation, which will determine the volumetric productivity of the differentiation stage bioreactor.

Mass gain during differentiation

The most relevant and complete dataset for mass gain during differentiation can be found in a study by Tuomisto et al. using C2C12 mouse myoblast cells (Tuomisto, Allan, and Ellis 2022). Over a 14-day period of differentiation, protein content (and assumed proportional cell mass) increased (nearly) linearly for the first nine days, with a ~128% mass gain reached by day seven. Linear regression revealed a k_{growth} (Equation 2.2d) equivalent to ~18% mass gain per day relative to the initial biomass. This trend of initial linear mass gain aligns with other studies of C2C12 and immortalized bovine myoblasts grown on fiber scaffolds (X. Li et al. 2024).

Assuming linear growth, as modeled by Equation 2.2d, simplifies the calculation of mass gain in the differentiation stage. This implies that volumetric productivity remains constant over time. However, as the data from Tuomisto et al. show, the rate of mass gain decelerates after about seven days, possibly due to contact inhibition or nutrient limitations. As a result, there is a trade-off between extending the differentiation stage to gain additional mass versus terminating the run due to declining volumetric productivity.

To enable optimization of differentiation duration under more realistic kinetics, we developed a model using an expression similar to saturation kinetics, with the differentiation rate declining as total biomass increases:

$$k_{growth} = k_{growth}^{max} * \left[\frac{K_{decel}^{n}}{X^{n} + K_{decel}^{n}} \right]$$

Equation 3.3a

Symbol	Definition	Typical units
$k_{growth,\ max}$	Maximum specific growth rate at t=0	1/day
K_{decel}	Biomass concentration at which growth decelerates	g WCW/L
n	Saturation exponent controlling curve steepness	Dimensionless
X	Wet cell biomass concentration	g WCW/L

And to represent the increase in protein content (as a fraction of cell mass) during differentiation, we applied a sigmoidal transition:

$$x_p = x_p^{min} + (x_p^{max} - x_p^{min}) * \left[\frac{X}{X + K_p} \right]$$

Equation 3.3b

Symbol	Definition	Typical units
x_p	Mass fraction of protein per unit cell mass	g protein/g cell
x_p^{min}	Initial (undifferentiated) protein content	g protein/g cell
x_p^{max}	Final (differentiated) protein content	g protein/g cell
K_p	Half-max protein saturation constant	g WCW/L

These two equations were fit to the experimental data and provided an excellent match to observed mass and protein accumulation (**Figure 3.3d**), yielding the following set of parameters:

Symbol	Value
$k_{growth,\ max}$	0.22 day^{-1} (22% per day)
K_{decel}	90 g WCW/L
n	6
x_p^{min}	40% DCW (10% WCW)
x_p^{max}	80% DCW (20% WCW)
K_p	200 g WCW/L

This analysis serves as an example of a model that can describe the deceleration of mass gain during differentiation, as would be expected when the wet cell mass concentration approaches the density of muscle tissue (~1,060 gWCW/L). The deceleration that is apparent in Figure 3.3d begins far below this value; however, the data were collected in a 2D tissue culture format, which may not fully represent 3D tissue cultures. Nevertheless, the model illustrates how nonlinear curvature can be applied to fit empirical data, which in this case begins at 22% protein increase per day (nonlinear) compared to 18% per day (linear regression) calculated by Tuomisto.

The model also demonstrates how to account for changes in cellular composition during differentiation. While Tuomisto assumed that the dry mass and protein content increased proportionally, this still needs to be validated experimentally (Tuomisto, Allan, and Ellis 2022). It is more likely that in muscle cells, the rise in cellular mass increases at a different rate compared to the protein fraction. It would be expected that total protein content would accumulate at a higher rate than wet and even dry cell mass as the cells fuse, form fibers, and lay down extracellular protein.

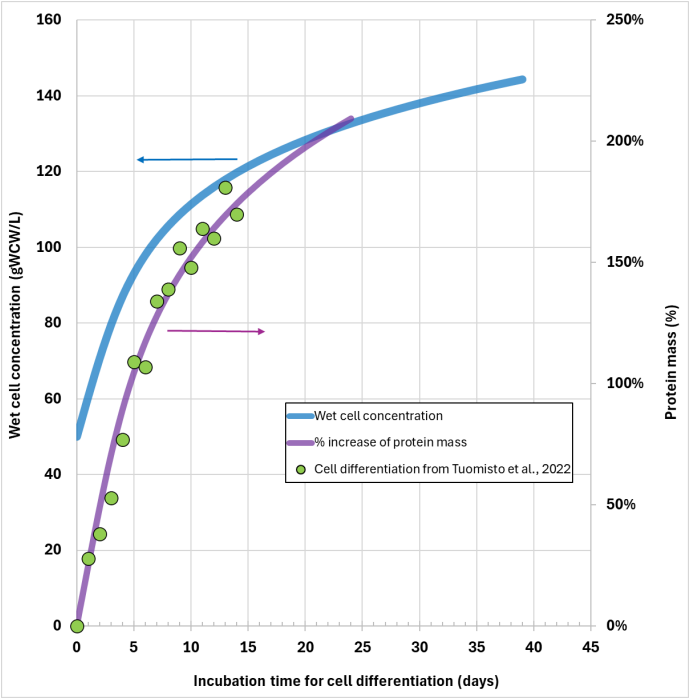

Figure 3.3d: Mouse skeletal muscle cell (C2C12) differentiation model using Equations 3.3a and 3.3b. A value of 50 gWCW/L was arbitrarily selected as the initial seeding density prior to differentiation. Data from (Tuomisto, Allan, and Ellis 2022).

Estimating upper bounds for mass gain during differentiation

One can also attempt to derive an upper bound for mass gain during differentiation based on physiological values observed in vivo. Many studies noted that individual myofibers can increase 20-30% in volume during hypertrophy following resistance training, but this is for mature muscle tissue. Quantifying mass gain throughout the entire developmental timeline from myoblast to myocyte to myotube to myofiber is difficult, as mature myofibers can be composed of hundreds of fused myoblasts, resulting in fibers that grow to several centimeters over many weeks, with variance in these numbers depending on the muscle type and species (Frontera and Ochala 2015). The degree of maturation and the secretion of extracellular matrix proteins are additional variables to consider.

Mass gain can be estimated by taking the length of the myofiber and the diameter of the fiber to calculate the volume, then estimating the mass by the average muscle density of 1.06 g/cm^3, and finally dividing the mass by the number of nuclei or individual myoblasts that fused to make up the fiber. While some AI-generated sources suggested that an over 10-fold mass increase is possible, we were unable to identify specific studies that quantified these numbers throughout the entire developmental process. In the study previously mentioned, the authors noted that differentiation was modeled as a reduction in the number of cells required from the proliferation stage to achieve the same final mass (Tuomisto, Allan, and Ellis 2022). Repeatable and standardized methods for calculating mass gain during muscle differentiation will therefore be essential to ensuring values can be compared across studies.

Fat differentiation involves a single cell accumulating lipids over time, making it more straightforward to model based on volume increase. In humans, mature white adipocytes typically accumulate lipids in a single lipid droplet that can range from 25 to 150 μm in diameter, occupying the majority of the cell's volume (Konige, Wang, and Sztalryd 2014). A meta-analysis in humans suggested that adipocyte diameter was ~80 μm in lean individuals and >120 μm in obese individuals (Q. Li and Spalding 2022).

Experimental data suggest that in vitro adipocyte differentiation protocols can approach in vivo cell sizes. For example, primary bovine mesenchymal stem cells displayed a mean lipid droplet diameter of 50-60 μm following four weeks of differentiation and maturation (Zagury et al. 2022). Similarly, an immortalized porcine mesenchymal stem cell line displayed a six-fold increase in lipid volume per cell from day 11 to day 40, with the largest total volume recorded at nearly 100,000 μm^3, close to in vivo adipocytes (Thrower et al. 2024). While these studies did not quantify mass, they suggested that a large volume of lipids can accumulate over time during adipocyte differentiation. Further data are needed to understand lipid accumulation and mass gain during shorter differentiation intervals. The data also suggest that different modeling assumptions may be needed to analyze the productivity of muscle and fat differentiation.

Key takeaways and data gaps

- More differentiation data are needed from relevant species and cells (e.g., muscle, fat, and extracellular matrix accumulation from fibroblasts) to understand the extent of mass gain that can be achieved under different conditions. There is a dearth of quantitative data, even from in vivo physiology, to help guide CM processes.
- Special attention should be paid to protein and lipid compositional changes during differentiation, as these will have a significant bearing on the nutritional value of CM.
- The accumulation of protein mass in skeletal muscle differentiation could be modeled using saturation kinetics (e.g., Equations 3.3a and 3.3b).
- Repeatable and standardized methods for calculating mass gain during differentiation will be essential to ensuring values can be compared across studies.
- More work is also needed to understand what factors are likely to limit cell differentiation in vitro and whether kinetic relationships (e.g., Monod growth-saturation constants) from suspension cultures are relevant.

Effects of substrate concentrations on cell growth and death rates

The nutrition factor (NF in Equation 2.3a) accounts for the effects of key substrates such as oxygen, glucose, and glutamine on cell growth. To quantify growth kinetics as a function of substrate

concentrations, we looked for published Monod half-saturation constants (K_s) for the model outlined in Equation 2.3c. We also searched for data sets where the growth rate was studied at different substrate concentrations to derive estimated K_s values for each substrate.

Oxygen

In cell culture, shifts in metabolism and decreases in growth rate have been observed at oxygen concentrations below 1% of air saturation. The gas-phase partial pressure of oxygen in air is 0.21 atm at 37ºC, which corresponds to about 0.2 mM oxygen dissolved in the media (DO), reflecting the very limited solubility of oxygen in water. In a salt solution more representative of a cell culture medium, oxygen's solubility is even less, at approximately 0.18 mM (180 µM). Thus, at 1% air saturation, this corresponds to just 0.0018 mM (1.8 µM) DO in the extracellular medium, an extremely low concentration for sustaining growth.

Using hybridoma cells, Ozturk and Palsson saw that growth became oxygen-limited in this range and measured a K_{O2} value of 0.6% dissolved oxygen (~0.001 mM; (Ozturk and Palsson 1990). The same group also examined the effects of serum concentration, dissolved oxygen concentration, and medium pH on hybridoma growth in a batch reactor (Ozturk and Palsson 1991). They observed that growth limitations occurred when DO fell below 5% (0.01 mM) of air saturation, suggesting that the K_{O2} for hybridoma cells is likely below this value. However, from the data presented in the paper, the K_{O2} appears to be further below this but could not be discerned due to low resolution.

Studies by Miller et al. in mouse hybridoma cells provide better data for the effect of oxygen on growth (Miller, Wilke, and Blanch 1987, 1988). In these studies, continuous culture allowed for the best separation of growth rate effects and substrate concentration effects on various metabolic parameters. In this case, oxygen concentrations were varied over a wide range while maintaining the same dilution rate. **Figure 3.3e** shows their data for the whole range tested, which included DO concentrations as high as 100% air saturation. From oxygen uptake rate data, they established an upper limit to the Monod half-saturation constant of 0.5% DO (0.001 mM), in agreement with Ozturk and Palsson, and similar to that observed for yeast. The inset in Figure 3.3e shows the data at tested DO concentrations as low as 0.1% of air saturation. These results highlight the exceptionally low K_{O2} values typical for mammalian cells, reflecting their efficiency in extracting oxygen from their environment even under hypoxic conditions.

It is also readily apparent that growth rate declines from a maximum value at approximately 0.5% DO (0.001 mM) as oxygen concentrations are increased. This behavior reflects substrate toxicity at higher oxygen concentrations, suggesting the need for a substrate inhibition factor to be added to the model proposed in Equation 2.3d. However, we found that bringing the exponent inside the expression, as shown in Equation 3.3c, gave a significantly better fit to the data due to the very sharp transition:

$$NF_{O2} = \left[\frac{O2}{O2 + K_{O2}} \right] \left[\frac{IC50_{O2}^{n}}{O2^{n} + IC50_{O2}^{n}} \right] \qquad \textbf{Equation 3.3c}$$

It is not too surprising that cells may be sensitive to high DO concentrations since they normally are exposed to a physiological range of 2-6% in most animal tissues. For this reason, most animal cells are cultivated at DO concentrations below 30%, which is already a hyperoxic state. Nevertheless, cells can be exposed to much higher (and potentially toxic) oxygen concentrations if not carefully controlled. There is clear evidence in both studies that cell death is associated with both hypoxic and hyperoxic oxygen concentrations. Using a chemostat, Ozturk and Palsson noted significant drops in cell viability below 5% DO (0.01 mM) and above 80% DO (0.16 mM), with similar observations made in other studies (Ozturk and Palsson 1991; Miller, Wilke, and Blanch 1987). However, death rates were not measured in these studies, and there was otherwise very little growth or death rate data available in the literature, signalling a gap that will need to be addressed for CM-relevant cell lines.

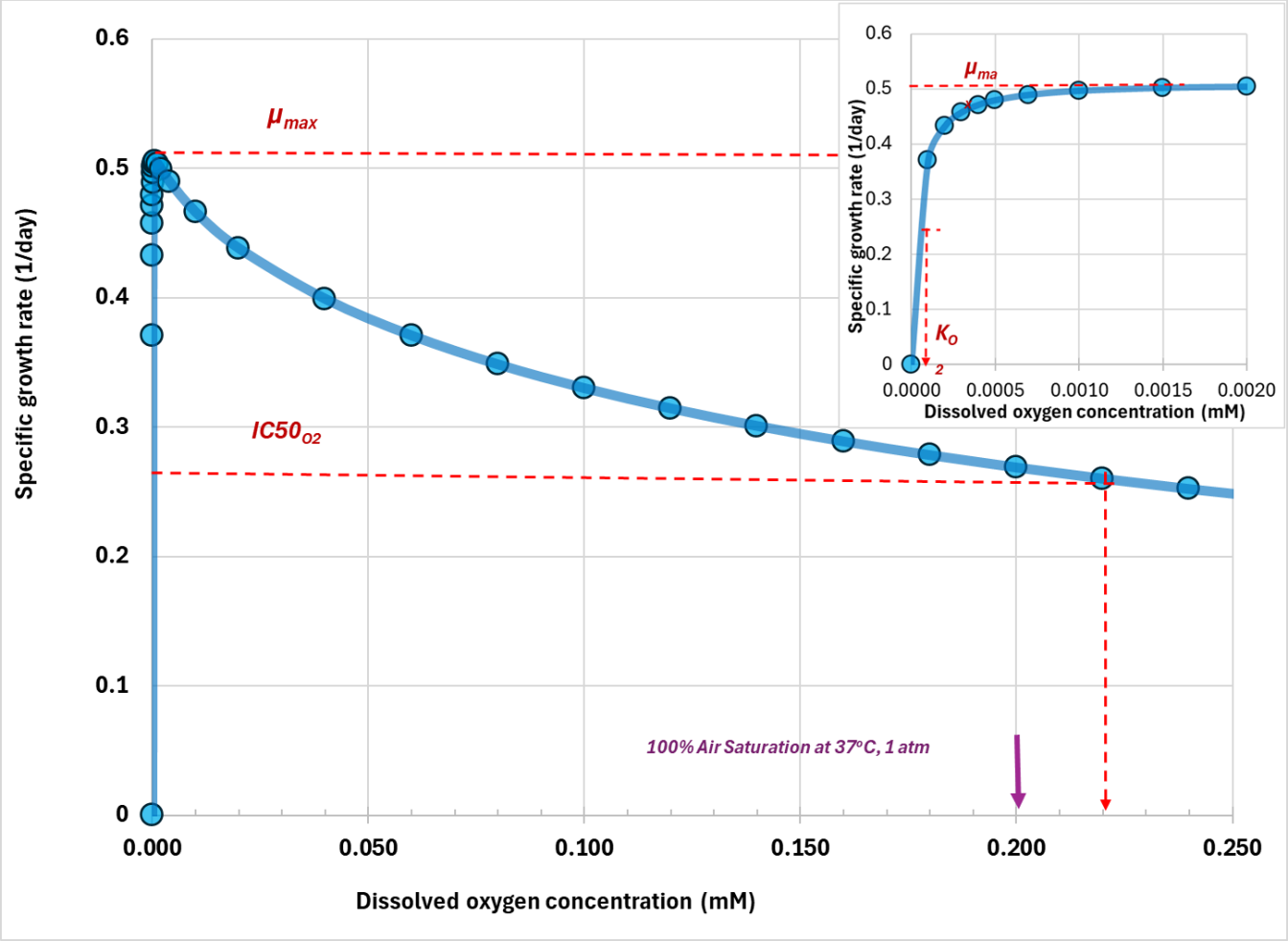

Figure 3.3e: Dissolved oxygen effects on growth rate. The trend line shown uses the modified inhibition model of Equation 3.3c with an IC50 of 0.22 mM and an exponent (n) of 0.7. The growth half-saturation constant(K_{O2}) is shown in the inset because it is exceedingly low (= 0.008 µM). Data from (Miller, Wilke, and Blanch 1987). Additional information for oxygen is available in the Supplementary Spreadsheet.

Key takeaways and data gaps

- Monod growth rate saturation kinetic constants for oxygen (KO2) values were found to be well below 0.01 mM. According to the function fit to the data in Figure 3.3e, KO2 is exceedingly low (below one hundredth of a micromole), suggesting animal cells are highly efficient at extracting oxygen from their environment.
- Growth inhibition can occur in both hypoxic and hyperoxic states and can be modeled using Equation 3.3c. The optimal oxygen concentration for animal cell growth appears to be in the range of 5-20% of air saturation
- More data on oxygen's effects on growth and death rates are needed for CM-relevant cell lines. Data from aquatic animal cell cultures will be particularly important, as environmental differences in oxygen concentrations and temperature may impact oxygen kinetics in cultivated seafood.

Glucose

Taking a similar approach, we found that the reported half-saturation constants for glucose (K_{Glc}) were much more prevalent in the literature compared to oxygen. Although more data were available, there was high variability in K_{Glc} parameters, ranging from as low as 0.02 mM to over 5 mM (**Table 3.3a**).

Most mechanistic or macroscopic models cite values in the range of 0.05–0.75 mM for hybridoma and CHO cells under batch culture conditions. The lower end of this spectrum tends to appear in studies assuming balanced growth or fitting batch data using simplified Monod kinetics (Pörtner and Schäfer 1996; Sanderson et al. 1999). Conversely, studies incorporating more complex or dynamic culture conditions—such as fed-batch or continuous systems—often adopt higher K_{Glc} values. These values have been derived directly from experimental fitting (Dhir et al. 2000) or selected to ensure model alignment with observed data during simulation.

Despite this variability, several studies note that the true growth-limiting behavior in glucose-sufficient cultures does not always correlate with measured glucose concentration. For example, Ljunggren and Häggström observed that growth persisted even when glucose levels were well below published K_{Glc} values, suggesting that glucose may not have been the limiting nutrient (Ljunggren and Häggström 1994). This discrepancy could arise from the presence of other limiting factors, such as essential amino acids or micronutrients, which would obscure the apparent influence of glucose and inflate its estimated K_{Glc} in models.

Table 3.3a: Kinetic parameters for glucose's effect on cell growth and death rates in animal cells. Additional information for each study can be found in the supplementary spreadsheet.

		Half-saturation Rate Constant	Death Rate Model (First-order)	
Source	**Cell Type**	**Glucose Monod Constant: KGlc (mM)**	**Death Rate at Zero DO: δmax (1/day)**	**Critical Concentration: KD (mM)**
Sumbilia et al., 1981	Human Fibroblast	0.4		
Miller et al., 1988	Murine Hydridoma	1.25		
Xiachang, 1992	Murine Hydridoma	0.019	0	
Frame and Hu, 1991	Murine Hydridoma	0.034	0.101	0.0134
	Murine Hydridoma	0.024	0.151	0.2404
de Tremblay et al, 1992		1		
Flickinger et al., 1992	Murine Hydridoma	0.49		
Dhir et al., 2000		4.79		
Jang and Barford, 2000		0.75		
Acosta et al., 2007		0.13		
Xing et al., 2010		0.084		
Borchers et al., 2013		1.45		
López-Meza et al., 2016	CHO - Naive	5.68		
	CHO - recombinant	3.69		
	CHO - Naive	1.59		
	CHO - recombinant	3.69		
Overall		1.57		
With serum		0.82		
Without serum		2.64		

There are numerous considerations for interpreting the data compiled in Table 3.3a, which show no clear correlation between the model constants determined and the conditions under which they were measured. For example, serum content may significantly affect uptake kinetics and K_{Glc} estimates, as serum-free cultures may be lacking transport-facilitating proteins and display altered cell physiology. The mode of cultivation is also important, as the numerical methods used to fit parameters to models of continuous cultures may be different than for batch data, and nonlinearities may further introduce a

bias. It has also been speculated that multiple glucose transporters with varying affinities may be used by cells, and expression patterns may differ depending on glucose availability (Bosdriesz et al. 2015). Lastly, temperature and pH are also likely to affect both the saturation and the death rate constants. While there is insufficient data to quantify these effects, some data in Table 3.3a seem to suggest that the K_{Glc} decreases when the temperature is dropped from 37°C to 33°C (López-Meza et al. 2016). In summary, the measurement systems, experimental conditions, and cell type differences are all likely to play a role in driving variability.

Cell death kinetics due to glucose depletion are even less clear. Frame and Hu's studies were the only ones found to measure death rates as a function of glucose concentration (Frame and Hu 1991a, 1991b); **Figure 3.3f**). This is in contrast to other reports of cells surviving in the absence of glucose. While the relationships resemble Monod-type saturation kinetics, the growth rate curve does not appear to come through zero. Instead, there appears to be a minimum glucose concentration required to support any growth. The authors incorporated a threshold value in a modified Monod equation to obtain a better fit of the data. In doing so, their half-saturation kinetic parameters are shifted and appear to be higher than most of the others. This apparent offset is peculiar but has been observed by others studying glucose kinetics (López-Meza et al. 2016). Various hypotheses have been put forward to explain this, such as the absence of other unidentified limiting nutrients or maintenance energy requirements, but none offer a clear answer.

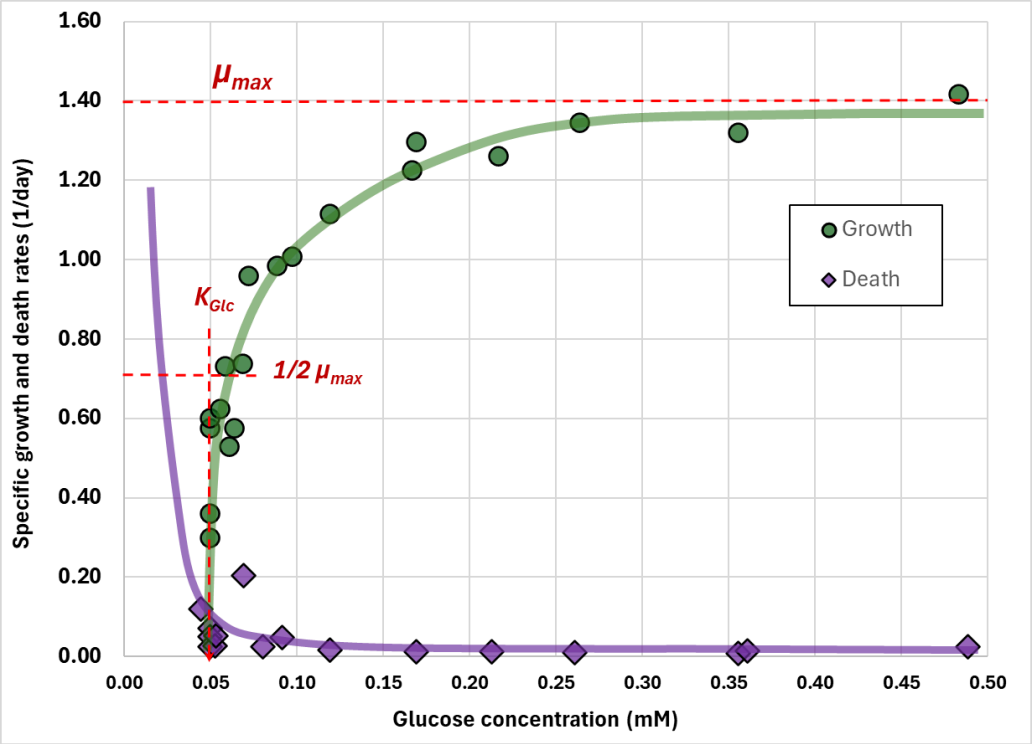

Figure 3.3f: Effects of glucose concentration on specific growth and death rates in a murine hybridoma non-producer cell line as a function of residual glucose concentration. Data from (Frame and Hu 1991a).

Key takeaways and data gaps

- Monod growth rate saturation kinetic constants for glucose (KGlc) values were found to vary over two orders of magnitude, falling between 0.02 to 5 mM. This high variability can be explained by media components, culture conditions, and measurement techniques, as well as cell type differences.
- More data on glucose effects on growth and death rates are needed from CM-relevant cell lines grown in relevant bioreactor conditions and in relation to other substrate concentrations, such as glutamine. Also, if a metabolite like pyruvate is added to provide some of the cell's energy needs, growth kinetics are likely to be affected if any of the substrates become limiting.

Glutamine

K_s values reported for glutamine (K_{Gln}) also span nearly an order of magnitude, from approximately 0.03 to 0.15 mM (**Table 3.3b**). Most values cluster around 0.05 to 0.1 mM, especially in models derived from batch cultures of hybridoma cells (Sanderson et al. 1999). As with glucose, some discrepancies in the literature were observed. For example, Glacken et al. used nonlinear regression to estimate a K_{Gln} of 0.15 mM in CRL-1606 hybridomas (Glacken, Adema, and Sinskey 1988). However, these findings were questioned by others who noted fed-batch cultures maintained robust growth even when glutamine concentrations were well below 0.1 mM (Ljunggren and Häggström 1994). In this study, it was concluded that glutamine was likely not the growth-limiting factor under their conditions and speculated that other nutrients with higher K_s, such as certain essential amino acids, may have been responsible for limiting growth.

Moreover, different cell lines and culture formats (e.g., perfusion vs. fed-batch) exhibit distinct metabolic regulation, including differences in glutamine transporter expression and enzyme activity. Therefore, a fixed K_{Gln} value is unlikely to apply across systems. Like K_{Glc}, K_{Gln} is also influenced by serum concentration and medium composition, although to a lesser extent due to glutamine's central role in nitrogen metabolism. Taken together, the most reasonable consensus value for K_{Gln} in mammalian cell models is approximately 0.1–0.5 mM for batch systems in the presence of serum and probably higher in continuous systems and/or serum-free media.

Table 3.3b: Kinetic parameters for glutamine's effect on cell-specific growth rate in animal cells. Additional information for each study can be found in the supplementary spreadsheet.

		Half-saturation Rate Constant	Death Rate Model (First-order)	
Source	**Cell Type**	**Glutamine Monod Constant: KGln (mM)**	**Death Rate at Zero Concentration: δmax (1/day)**	**Critical Concentration: KC0 (mM)**
Sumbilia et al., 1981	Human Fibroblast	0.350		
Miller et al., 1988	Murine Hydridoma	0.370		
Bree et al., 1988	Murine Hydridom,	0.800		
Glacken et al., 1988	Murine Hydridoma	0.150		
Xiachang et al., 1992	Murine Myeloma	0.496	0.286	0.0367
Frame and Hu, 1991	Human Fibroblast*	0.260		
Jeong and Wang, 1995	Hydridoma	0.089	0.158	0.254
Dhir et al., 2000		0.032		
Jang and Barford, 2000		0.075		
Acosta et al., 2007		0.080		
Xing et al., 2010		0.047		
Nolan and Lee, 2011	CHO	2.5		
Overall		**0.44**		
With serum		**0.25**		
Without serum		**2.50**		
(*) Estimated by Frame and Hu based on the data from Sumbilla et al., 1981				

Figure 3.3g shows an example of death kinetics as a function of ultra-low glutamine concentrations (Jeong and Wang 1995). In the study, the authors explained that although glutamine and glucose are partially substitutable as an energy substrate, they also have other functions independently and thus are still required to support cell growth and even survival. We fit the data to two models: a linear model like Equation 2.2e and an inverse saturation model like Equation 2.3d. Both offer a reasonable fit of the data. Both are two-parameter models, therefore, the curvilinear model is recommended since it is a continuous, non-zero function.

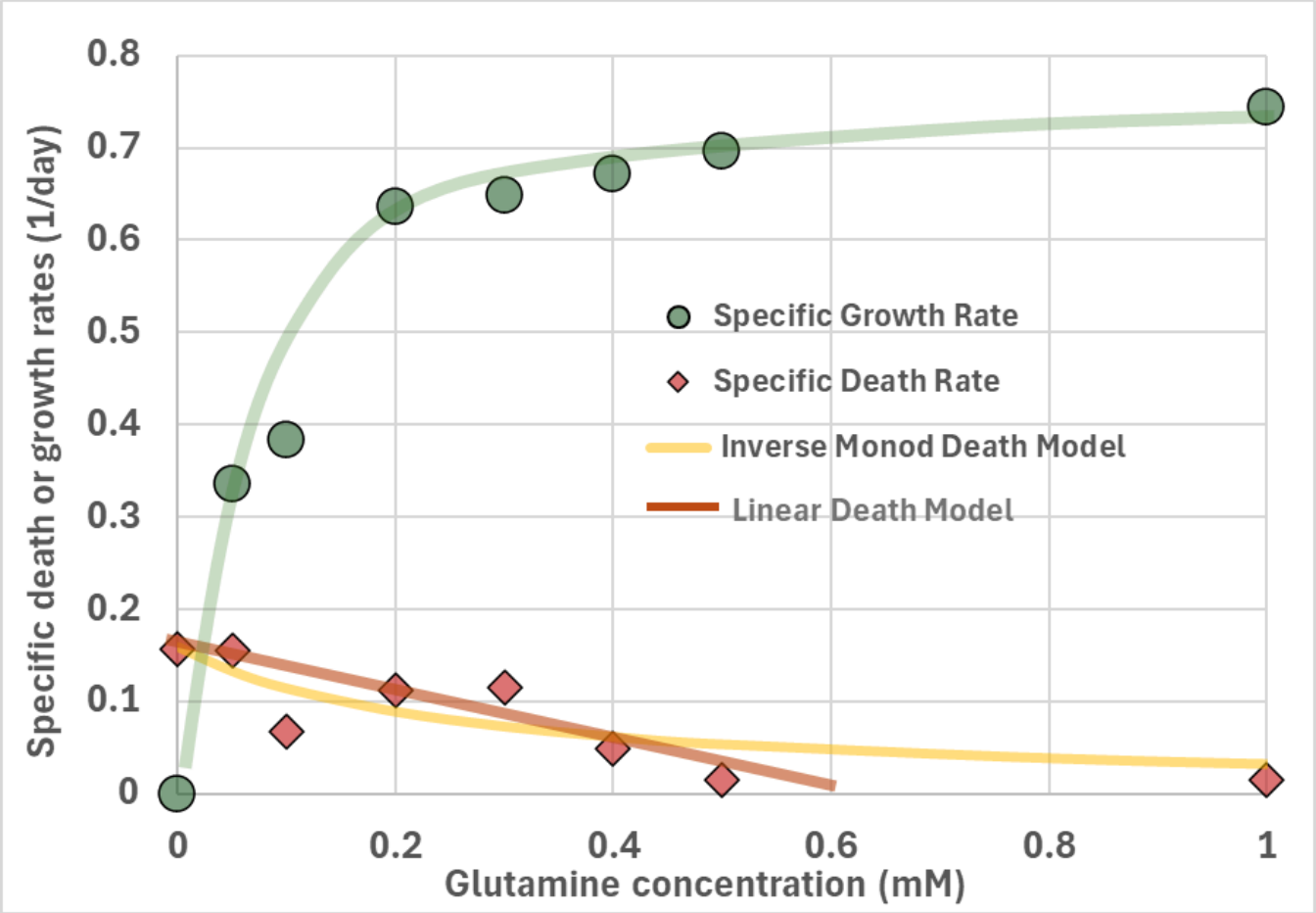

Figure 3.3g: Death kinetics due to glutamine depletion overlaid on growth kinetics in murine hybridoma cells. Data from (Jeong and Wang 1995). Two models are fit to the death kinetics: a simple linear function and an inverse Monod. Both intersect the y-axis at δ_{max} of 0.158 $day^{-1,}$ and the latter model has a death rate constant of 0.254 mM.

The death rate data in Figure 3.3g is overlaid on the growth kinetics, also as a function of glutamine concentration. It is apparent that there is a significant overlap of cell death and substrate limitation. Thus, it appears some cell death is unavoidable if glutamine is also a limiting nutrient in culture. From the overlay, one would need to maintain glutamine concentrations above 0.5 mM to avoid appreciable death rates. However, over most of this range, the specific growth rate is considerably higher than the death rate. Only at very low concentrations of approximately 0.004 mM is the death rate greater than the growth rate

This observation in batch culture is substantiated by the studies conducted by Miller et al. and Boraston et al., where a (continuous) chemostat was used to study the effect of growth rate and substrate concentration on various metabolic quotients (Boraston et al. 1983; Miller, Blanch, and Wilke 2000). Both studies observed that the true cell-specific growth rate was not always equal to the dilution rate for all dilution rates tested, contrary to what theory would predict at steady state. Instead, a declining viability was observed at low dilution rates. Since glutamine was depleted first in these continuous cultures, it is assumed that this substrate was limiting growth. At the lower residual

glutamine concentrations, elevated death rates were apparent. In response, the chemostat preserved a steady state by increasing the true growth rate to compensate for the dying cells.

Key takeaways and data gaps

- Monod growth rate saturation kinetic constants for glutamine (KGln) values are more consistent in the literature compared to glucose. A reasonable consensus for KGln values lies between 0.1-0.5 mM for batch systems with serum and probably higher in continuous systems and/or in serum-free media.
- Two-parameter models can be used to fit death rate kinetics for glutamine. Both a linear relationship and an inverse Monod (Equation 2.3l) provide a reasonable fit for initial modeling purposes.
- However, such kinetic parameters need to be measured for CM-relevant cell lines and in conjunction with the availability of other amino acids and possibly other intermediate metabolites if added to the medium (e.g., alpha-ketoglutarate).

Summary: Effects of substrate concentrations on cell growth and death rates

In summary, empirical models based on Monod-type kinetics effectively capture how substrate concentrations influence specific growth and death rates. However, the model parameters measured over the past 30 years are highly variable. Many studies used murine hybridoma cell lines, and the half-saturation kinetic constants also varied among these studies, suggesting the conditions under which these parameters are determined are important to consider when interpreting results. For future studies, it will be important to understand how best to measure these parameters such that they are representative of the final process. For example, it appears that serum may allow faster growth at low substrate concentrations (i.e., lower K_s). Thus, these measurements need to be made in representative (likely serum-free) conditions for commercially relevant processes. Similarly, continuous processes may have different substrate affinities because they have the opportunity to adapt to low substrate conditions. Ideally, cellular energetics should also be captured in such studies to understand whether any transient effects are at work and if substrate uptake and assimilation are best separated in a structured model.

The average K_s values of approximately 0.001 mM (1 µM) for oxygen, 2 mM for glucose, and 0.5 mM for glutamine should provide a good starting point for model construction and even testing some of the concepts discussed in this paper. These values are not as critical for simple models under non-limiting substrate conditions but become important in understanding system dynamics in ranges where metabolic shifts may occur, which are discussed further in Section 3.5. Lastly, the maximum specific growth rate for a given cell type or line is also a function of temperature and pH, yet little data exist on how these parameters affect the kinetics of growth, death, and thresholds for substrate limitations.

Understanding these effects could reveal opportunities to improve bioreactor performance and process control.

3.4 Kinetics of metabolite-induced growth inhibition and cytotoxic death

As animal cells consume nutrients, they also produce metabolic by-products such as lactate, ammonium, and CO_2 that can inhibit growth and productivity as they accumulate. At high enough concentrations, they can also contribute to cell death. Additionally, these by-products also influence osmolality, which can itself affect growth rates. Some previous TEMs have set absolute thresholds for metabolite inhibition. However, using a binary limit that assumes there can be no growth above this value is an oversimplification of the kinetics of metabolite-induced cell growth inhibition. In this section, we summarize data on metabolite inhibition and cell death kinetics (where available) with a focus on using mathematical expressions to estimate the reduction in growth rates as a function of inhibitor concentration, which can be used to inform more dynamic and representative TEMs.

Inhibition effects of lactate

Lactate is the main by-product of aerobic glycolysis in most animal cell cultures. As lactate accumulates in the extracellular environment, it acidifies the medium, which is typically countered with base addition to control pH, which then increases the culture's osmolality. All of these phenomena, which can negatively impact growth and viability, were once attributed to lactate itself. However, when separated from these other effects, the lactate ion is generally less inhibitory than previously believed. From the modeling perspective, the effects of lactate, pH, and osmolality should be handled separately.

Accordingly, the mechanism of lactate toxicity is thought to be driven by intracellular acidification, disruption of ion gradients, osmotic stress, and calcium chelation, which can inhibit glutaminase activity and reduce ammonium production (Glacken, Fleischaker, and Sinskey 1986). Humbird used an absolute threshold for lactate where growth was fully inhibited at >50 mM, but this is an oversimplification (Humbird 2021). We compiled several studies that reported the specific growth rate of animal cells as a function of extracellular lactate concentration and visualized the results as normalized growth rates relative to control cultures without added lactate (**Table 3.4a, Figure 3.4a**). As shown in the figure, most of the dose-response curves could be fit to the one- or two-parameter models previously presented in Figure 2.3b. For example, the two-parameter model (Equation 2.3k) applied to CHO cells was fit to the data from Lao and Toth using an IC100 of 96 mM and an exponent of 0.40 (Lao and Toth 1997).

The data collectively show considerable variability across different cell types. Growth inhibition typically emerges at concentrations above 20 to 30 mM, with an approximate IC50 range between 10 to 80 mM depending on the cell line and culture conditions. Therefore, growth inhibition for lactate is not a binary function (i.e., growth or no growth) surrounding a single concentration as assumed in prior TEMs. Instead, growth inhibition is a progressive event that can be represented using either anIC50

(as in Equation 2.3i) or an IC100 (as in Equation 2.3k) with an exponent, if desired, to control the curve's steepness.

Table 3.4a. Summary table of lactate inhibition across animal cell lines. The full dataset, including culture conditions, mode of growth, and death kinetics data, can be viewed in the Supplementary Spreadsheet.

Reference	Cell type	IC50 (mM)	IC100 (mM)
Bree, 1988	Murine hybridoma (DuPont)	8	
Glacken, 1987	Murine hybridoma	40	
Hassell, 1990	Murine hybridoma (PQXB1/2)	22	
Ozturk, 1992	Murine hybridoma (167.4G5.3)	70	80
Lao, 1997	CHO	87	96
Cruz, 2000	BHK	43.5 (stirred), 70 (stationary)	76 (stirred), 120 (stationary)
Silvac, 2010	Channel catfish ovary	10	40
Gupta, 2017	Murine ESC	26.5	54
Haraguchi, 2024	Murine myoblast (C2C12)	22	44
Average		39.9	72.9

The variability in the data can be partially explained by differences in conditions between studies, from cell lines, culture modes, adaptation states, and media composition (e.g., use of serum). In our review of the literature, we observed that primary cells tend to be more sensitive to lactate than immortalized or transformed cell lines. While stationary cultures often exhibited greater sensitivity than stirred suspension systems, some have observed the opposite trend for BHK cells, with an IC50 of 44 mM in stirred cultures and 70 mM in stationary conditions (Cruz et al. 2000). Even among hybridoma lines, there is significant variability. For instance, Glacken et al. found little inhibition below 40 mM, whereas Bree et al. reported an IC50 as low as 8 mM in a different hybridoma line (Bree et al. 1988; Glacken, Fleischaker, and Sinskey 1986).

Many studies also used serum-containing media, which may offer some protection against lactate inhibition. Some groups corrected for osmolality by using sodium lactate controls that revealed that true lactate toxicity was often less severe than initially thought. Others found that the gradual accumulation of lactate during culture was better tolerated than sudden additions. Adaptive responses to lactate have also been documented, especially in CHO cells. Some engineered or adapted lines show reduced lactate production and, in some cases, net lactate consumption in

late-stage cultures. This shift, often induced by glucose limitation or galactose supplementation, can increase energy efficiency and product yields. These data point to the many variables that should be taken into consideration when interpreting lactate inhibition and when making assumptions in TEMs.

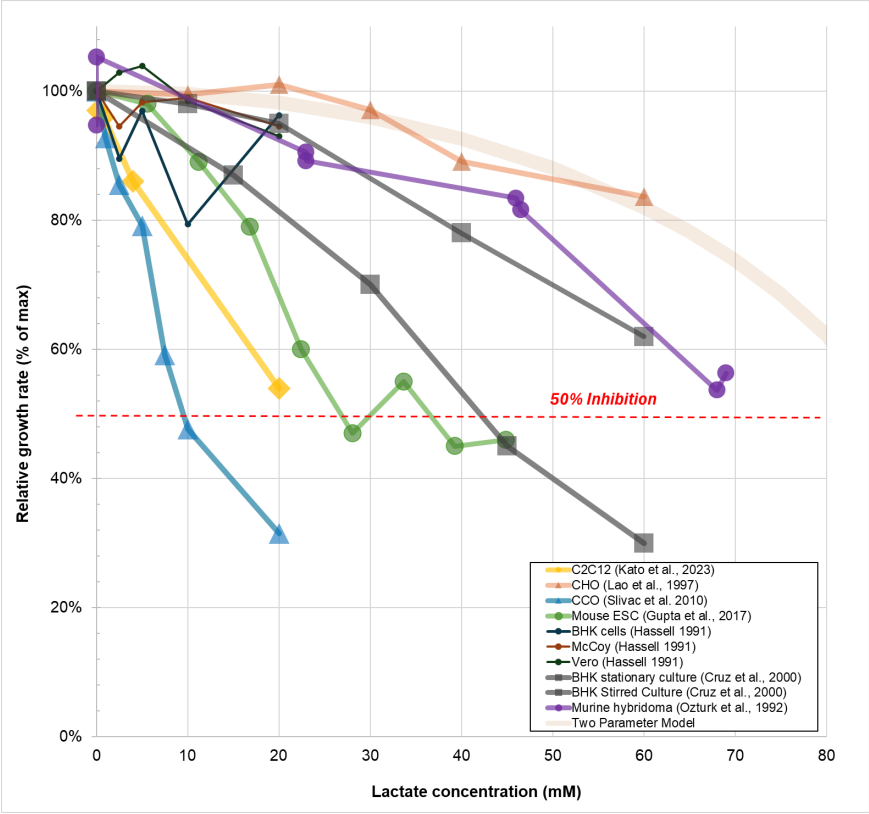

Figure 3.4a: Inhibitory effect of lactate on the growth rate of various animal cells relative to a control culture. The trend line shown was fit to the data from Lao et al. using the two parameter model of Equation 2.3k and adjusting the IC100 to 96 mM and the exponent to 0.4 (Lao and Toth 1997).

In the context of CM, C2C12 murine myoblasts were more sensitive to lactate than CHO or hybridoma cells, showing measurable cytotoxicity at concentrations as low as 20 mM (Chu et al. 2024). In this study, the authors used a co-culture system with lactate-consuming cyanobacteria, showing C2C12 proliferation increased by threefold when lactate concentrations were reduced by 38% ((Chu et al. 2024)). Another study using chicken fibroblasts held lactate below 30 mM to limit inhibition during a continuous process (Laura Pasitka et al. 2024). However, other complete dose-response data for lactate on CM-relevant cell lines were not identified.

Gupta et al. studied the impact of lactate on the pluripotency of mouse pluripotent stem cells (Gupta et al. 2017). No significant effect was found, discrediting earlier studies. However, when the pH was allowed to change, pluripotency was indeed affected, suggesting prior studies did not control for pH. Such phenomena are clearly of interest to CM applications if pluripotent cells are to be used in a subsequent differentiation process.

Lastly, unlike growth inhibition, cell death processes are irreversible. Data describing lactate-induced cell death (i.e., cytotoxicity) are more limited. Xing et al. reported a drop in CHO cell viability when lactate concentrations exceeded 58 mM (Xing et al. 2008). While lactate generally does not trigger apoptosis, very high concentrations can lead to necrosis by overwhelming cellular pH regulation and osmolarity tolerance. For example, necrosis and cytoplasmic leakage were observed in BHK cells exposed to lactate levels greater than 30 mM (Cruz et al. 2000).

Taken together, our literature review showed that lactate inhibition depends on multiple factors, including the cell line, culture mode, adaptation state, and medium composition (e.g., use of serum). Experimental data tended to fit the kinetics of a two-parameter model for substrate inhibition, allowing for the derivation of IC50 and IC100 values. When more experimental data on the growth inhibition of lactate on CM-relevant cell lines becomes available, these models can be incorporated into future TEMs.

Key takeaways and data gaps

- A two-parameter model is best used to describe lactate inhibition on cell growth, with IC50 values varying between 10-80 mM. On average, for the cell lines where data were reported, the IC50 and IC100 are approximately 40 mM and 73 mM, respectively.
- Taking only the three studies that corrected for osmolality, these averages for IC50 and IC100 move up to 67 and 84 mM, respectively, suggesting that sensitivity to lactate is overestimated in many studies.
- More dose-response data are needed on lactate inhibition and cytotoxicity under serum-free conditions, especially for cell lines relevant to CM production.
- Future growth inhibition studies should compare gradual accumulation of lactate with acute lactate addition.
- Exploring metabolic engineering and cell feeding strategies to promote lactate consumption could improve culture performance and cell yields.

Inhibition effects of ammonia

Ammonia is produced from glutamine catabolism and non-enzymatic glutamine degradation, making its accumulation difficult to avoid in cultures that rely on glutamine as a principal nitrogen source. Ammonia is a potent metabolic inhibitor that impairs growth and viability in nearly all animal cells, as it interferes with intracellular pH regulation, membrane potential, glycosylation pathways, and lysosomal function. At physiological pH (~7.4), about 99% of ammonia exists as ammonium (NH_4^+), with only 1% as membrane-permeable ammonia gas (NH_3). After entering the cell, NH_3 re-forms NH_4^+, causing a brief alkalinization followed by acidification that disrupts cell function and can lead to growth arrest or death (Ozturk, Riley, and Palsson 1992). Ammonia can also trigger apoptosis by

disrupting glycoprotein synthesis and lysosomal function (Cruz et al. 2000; Ozturk, Riley, and Palsson 1992; Glacken, Adema, and Sinskey 1988).

Humbird previously used an absolute threshold for ammonia where growth was fully inhibited at >5 mM (Humbird 2021)). Our review of the literature confirmed that ammonia is substantially more toxic than lactate, with inhibitory effects commonly observed at concentrations of 2 to 4 mM (Table 3.4b). We summarized datasets where ammonia-induced growth inhibition was characterized for at least three concentrations, with most cell lines showing IC50 values between 3 to 8 mM ammonium (Figure 3.4b). Similar to lactate inhibition, the dose-response curves generally fit the three-parameter model, although some sensitive cell lines displayed a linear decline in growth beyond 2 mM.

Table 3.4b. Summary table of ammonia inhibition across animal cell lines. The full dataset, including culture conditions, mode of growth, and death kinetics data, can be viewed in the Supplementary Spreadsheet.

Reference	Cell type	IC50 (mM)	IC100 (mM)
Cain, 1986	Murine Fibroblast	7.2	12.4
Miller, 1988	Murine Hybridoma AB2-143.2	5	
Bree, 1988	Murine Hybridoma (Dupont)	1.05	
Glacken et al., 1988	Murine Hybridoma CRL-1606	5.1	
McQueen and Bailey, 1991	Murine Hybridoma	8.35	
	Murine Hybridoma	7.3	
	Murine Hybridoma	5.2	
Hassell, 1991	Hamster (Baby) Kidney (BHK)	1.3	
	Human Fibroblasts (HeLa)	0.8	
	Murine Fibroblast (McCoy)	1.7	
	Canine Kidney (MDCK)	1.8	
	Murine Hybridoma PQXB1/2	5.1	
Ozturk et al., 1992	Murine Hybridoma 167.4G5.3	4.25	4.8
Newland et al., 1994	Murine Hybridoma SP2/0-Ag-14	3.4	7
	Murine Hybridoma SP2/0-Ag-14	4.1	8
Cruz et al., 2000	Hamster (Baby) Kidney (BHK)	4	10
Slivac, 2010	Channel Catfish Ovary	3.65	6.7

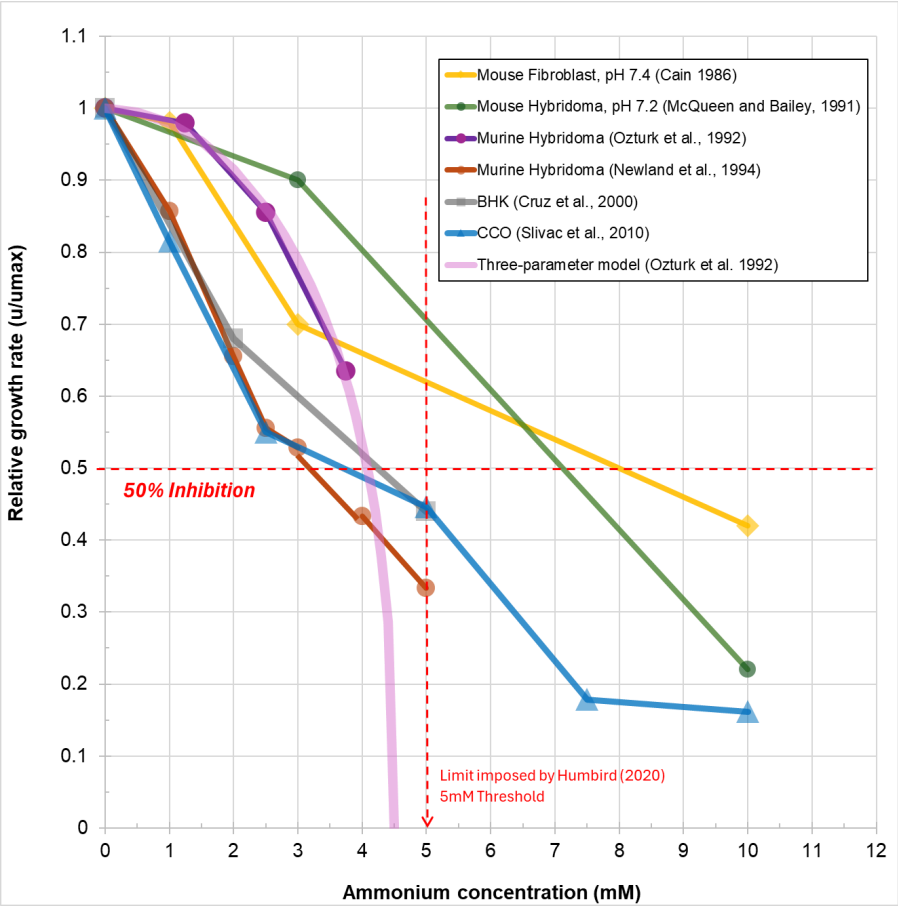

Figure 3.4b: Dose-response curves for growth inhibition of ammonia across various animal cell lines. The trend line shown was fit to the data from Ozturk (1992) using a three-parameter model. The model is a modification of Equation 2.3k including another exponent (n) applied to I and IC100. The fit was accomplished with IC100 = 4.5 mM, Phi = 0.4, and n = 2.

There are several observations that can be made from the data. Most of the early studies were conducted on murine hybridomas, meaning the available data may not represent the effects of ammonia on a broader range of species and cell types, such as those used for CM. Cell type specificity has been observed, as BHK and MDCK cells show IC50 values near 1 to 2 mM, while mouse ascites tumor cells reportedly tolerate up to 40 mM NH_4^+ without inhibition ((Cruz et al. 2000; Ozturk, Riley, and Palsson 1992; Glacken, Adema, and Sinskey 1988). Additionally, most inhibition studies used bolus ammonium chloride addition, which may exaggerate toxicity compared to real-world cultures where ammonia accumulates gradually, permitting cellular adaptation ((Newland et al. 1994; McQueen and Bailey 1990). As observed with lactate, primary cells may be more sensitive than transformed cell lines, and cells grown in stirred suspension generally exhibit less sensitivity compared to stationary cultures ((Cruz et al. 2000; Ozturk, Riley, and Palsson 1992; Glacken, Adema, and Sinskey 1988). Most studies were conducted in serum-containing media, although limited comparisons suggest that serum concentration may not strongly influence ammonia sensitivity. In general, while it is likely that serum offers some protection against ammonium toxicity, more studies are needed under serum-free conditions for CM-relevant cell types.

It is also important to consider pH when interpreting ammonia inhibition. Analysis of the data shows a marked shift in IC50 values as a function of extracellular pH, suggesting ammonia toxicity is strongly pH-dependent (**Figure 3.4c**). Notably, the curve of the relationship matches the general profile of pH on specific growth rate (Figure 3.3c), suggesting a shared underlying inhibition mechanism related to intracellular acidification and disruption of pH homeostasis.

As with lactate, there are fewer studies describing ammonia-induced cell death, although some have noted these mechanisms can trigger apoptosis (Cruz et al. 2000). Overall, the limited data indicate that specific death rates remain relatively stable with increasing ammonia concentration, which suggests that ammonia primarily reduces growth rate and cell yield rather than causing acute cell death (Newland et al. 1994; McQueen and Bailey 1990).

We were unable to identify sufficient dose-response data to characterize ammonia inhibition effects on CM-relevant cells, although one study using chicken fibroblasts held ammonia below 3 mM to limit inhibition during a continuous process (Laura Pasitka et al. 2024). Because the inhibition effects of ammonia are known to be problematic, most of the research to date has focused on methods to minimize its effects, such as non-ammoniagenic feedstocks (Hubalek et al. 2023) and media recycling strategies that remove ammonia (Yang et al. 2025) or remediate ammonia-containing spent media using microalgae (Thyden et al. 2024).

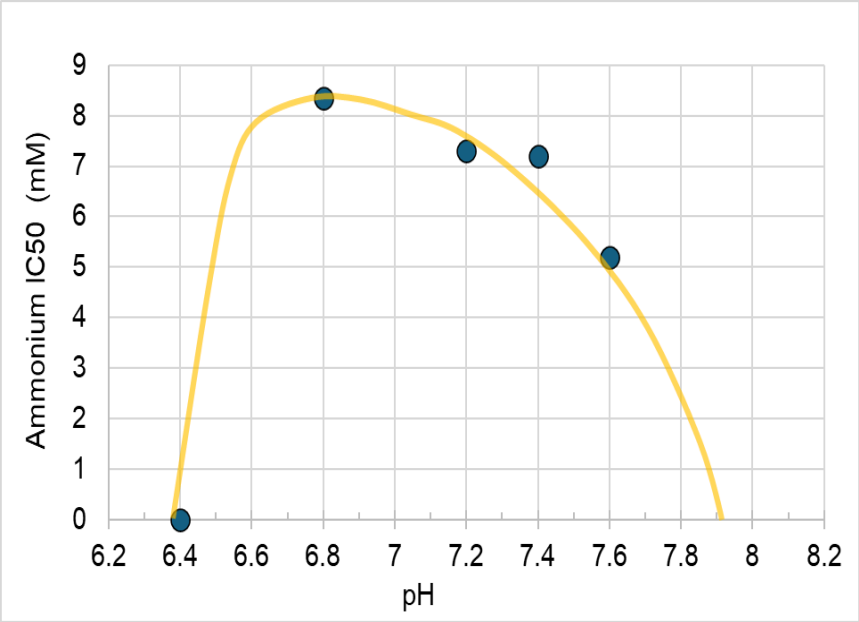

Figure 3.4c: Effect of extracellular pH on the IC50 for ammonia chloride added to a cell culture. Data from ((McQueen and Bailey 1990)).

Key takeaways and data gaps

- A two-parameter model for substrate inhibition can sometimes be used to describe ammonia inhibition on cell growth, with IC50 values between 3-8 mM.
- More dose-response data are needed on ammonia inhibition and cytotoxicity under serum-free conditions, especially for cell lines relevant to cultivated meat production.
- Future studies should pay special attention to pH when interpreting results.
- Future studies should examine gradual adaptation to ammonia as well as continued methods to remove or limit ammonia production.

Effects of osmolality

As lactic acid accumulates during cell growth, it becomes a major contributor to increasing osmolality, especially when base addition is used to control pH. Therefore, some negative effects previously attributed to lactate may be associated with increased osmolality. To determine this, studies were performed using spiked sodium lactate with osmolality-matched controls, finding that the lactate sharply inhibited cell growth in CHO cells (Gagnon et al. 2011). Similarly, Cruz et al. observed that while osmolality accounted for part of the growth inhibition at low to moderate lactate concentrations, lactate-specific effects dominated at higher concentrations (Cruz et al. 2000). Overall, osmotic stress had a measurable but secondary role, while lactate acted as a direct metabolic inhibitor.

With this in mind, it is important for models to account for osmolality as an independent inhibition factor, as described in Equation 2.3h. In CM processes, high osmolality can be a result of the initial medium formulation and whether concentrated nutrients are added, especially during fed-batch processes. In essence, controlling for the inhibition effects of osmolality requires balancing sufficient nutrient concentration for cell growth with the risk of osmotic stress (O'Toole, n.d.).

Across studies on CHO and other mammalian cells, the optimal osmolality range for growth and productivity generally falls between 280 and 320 mOsm/kg, close to serum osmolality (~290 mOsm/kg) (O'Toole, n.d.). Growth typically declines when osmolality drops below ~260 mOsm/kg or exceeds ~380 to 450 mOsm/kg, depending on the cell line and culture system (Alhuthali, Kotidis, and Kontoravdi 2021; Xing et al. 2008). Similar to lactate and ammonia, adherent cells tend to tolerate narrower osmotic ranges compared to suspension-adapted cells (Alhuthali, Kotidis, and Kontoravdi 2021).

In our literature review, we summarized osmolality vs. growth rate data in controlled experiments from CHO and hybridoma cultures (**Figure 3.4d**). Across studies, the growth rate decreased linearly with increasing osmolality above the optimal range, with some cell type specificity observed for the slope of growth inhibition. Based on the data, the estimated IC50 for osmolality was approximately 465 mOsm/kg. In CHO suspension cultures, a critical threshold around 450 mOsm/kg has been observed, while osmolality below 320 mOsm/kg can also reduce specific growth rates due to limited nutrient availability (Alhuthali, Kotidis, and Kontoravdi 2021).

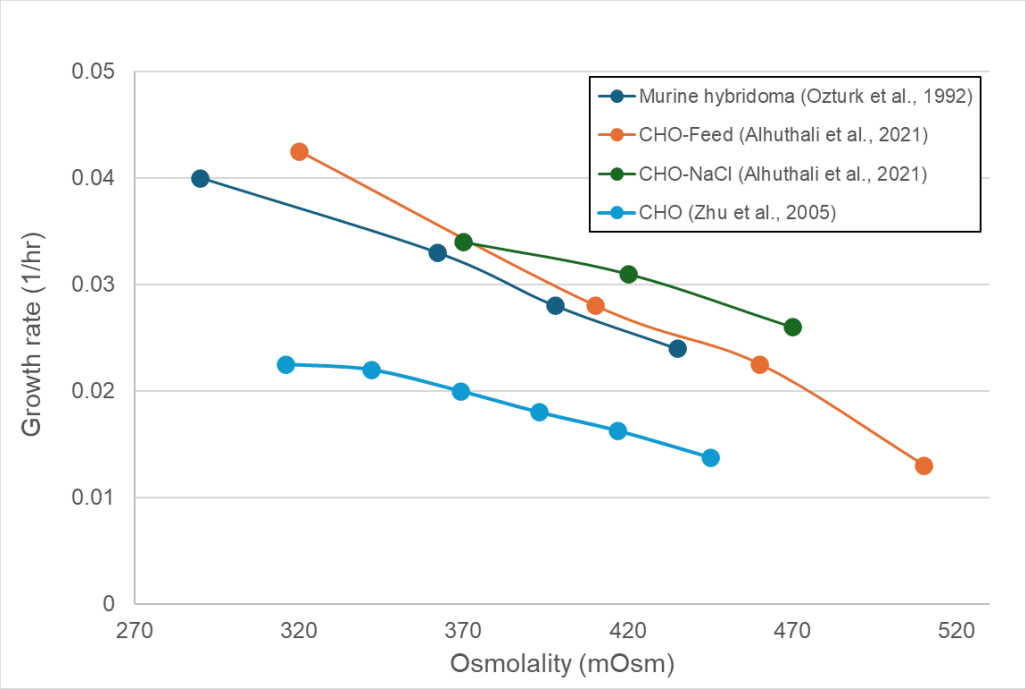

Figure 3.4d: Effect of osmolality on growth rate in CHO and Hybridoma cells.

In the context ofCM, maintaining culture osmolality within the optimal range will be critical for achieving high-density cell growth. Muscle, fat, pluripotent, or fibroblast cells may differ from CHO cells in osmolality tolerance, and additional work is needed to define safe operating windows. Given that both hypo-osmotic and hyper-osmotic stress can impair culture performance, nutrient feeding strategies and by-product control should be carefully designed (Alhuthali, Kotidis, and Kontoravdi 2021).

Key takeaways and data gaps

- The osmolality effect on growth rate was linear, with inhibition observed as osmolality increased.
- An IC50 of 465 mOsm/kg was estimated across studies.
- More data are needed to determine osmolality tolerance across cell types and species for CM production. These studies should distinguish between osmotic stress and metabolite-specific toxicity, especially as it relates to lactate.
- Understanding the effects of gradual osmolality shifts vs. sudden changes can inform optimal feeding strategies that limit growth inhibition.

Effects of dissolved carbon dioxide

Dissolved CO_2 (dCO_2) plays an important role in cell culture as a part of the bicarbonate buffering system that maintains pH ($CO_2 + H_2O \rightleftharpoons H_2CO_3 \rightleftharpoons H^+ + HCO_3^-$). However, accumulation of dCO_2 due to

cellular respiration or limited gas exchange in bioreactors can inhibit growth and impact metabolic pathways. The inhibitory effects are believed to result primarily from intracellular acidification, as CO_2 freely crosses the cell membrane, reacts with water, and dissociates into hydrogen and bicarbonate ions.

Understanding the point at which dCO_2 becomes inhibitory has been challenging for several reasons. First, standard CO_2 sensors measure partial pressure (pCO_2, in mmHg), while cells respond to the molecular concentration of dCO_2 (in mM). Converting pCO_2 to dCO_2 requires the use of Henry's Law and depends on variables such as temperature, pH, and salinity. As a result, two cultures at the same pCO_2 may have different dCO_2 concentrations. This complexity is further compounded in bioreactors by large-scale effects like imperfect mixing and hydrostatic pressure. Second, controlling for interaction effects such as osmolality is difficult. Even at constant pH, an increase in pCO_2 can lead to an increase in osmolality, and osmolality alone can impair growth. As such, it is difficult to distinguish direct CO_2 toxicity from secondary osmotic stress.

Across several studies, inhibitory effects of dCO_2 in CHO and hybridoma cells were observed at concentrations between ~1.0 and 8 mM, with an estimated IC50 of 6.3 mM (**Figure 3.4e**; (Gray et al. 1996; Dezengotita, Kimura, and Miller 1998; Zhu et al. 2005). Humbird previously set a threshold of 75 mmHg (~2.34 mM) for inhibition, although some studies reported high viability even above this point (Zhu et al. 2005). Zhu et al. highlighted the importance of independently controlling CO_2 and osmolality (Zhu et al. 2005). In their study, when osmolality was held constant at 350 mOsm/kg, an increase in dCO_2 from 1.88 to 4.7 mM caused a 9% drop in viability. When osmolality rose to 425 mOsm/kg alongside increased dCO_2, viability dropped by 24%. These findings, supported by others (Brunner et al. 2017), suggest that dCO_2 and osmolality have synergistic impacts on cell growth. While some results emphasize the role of osmolality, others point to intracellular pH as a more critical factor.

In the context of CM, managing dCO_2 accumulation will be important for maintaining growth and productivity, especially at high cell densities. There is a precedent of using inert gas (e.g., nitrogen) stripping in the biopharmaceutical industry to remove excess CO_2 (Pattison et al. 2000). More data are needed to establish tolerance thresholds in CM cell lines, and future experiments should control pH and osmolality independently to identify the primary drivers of inhibition.

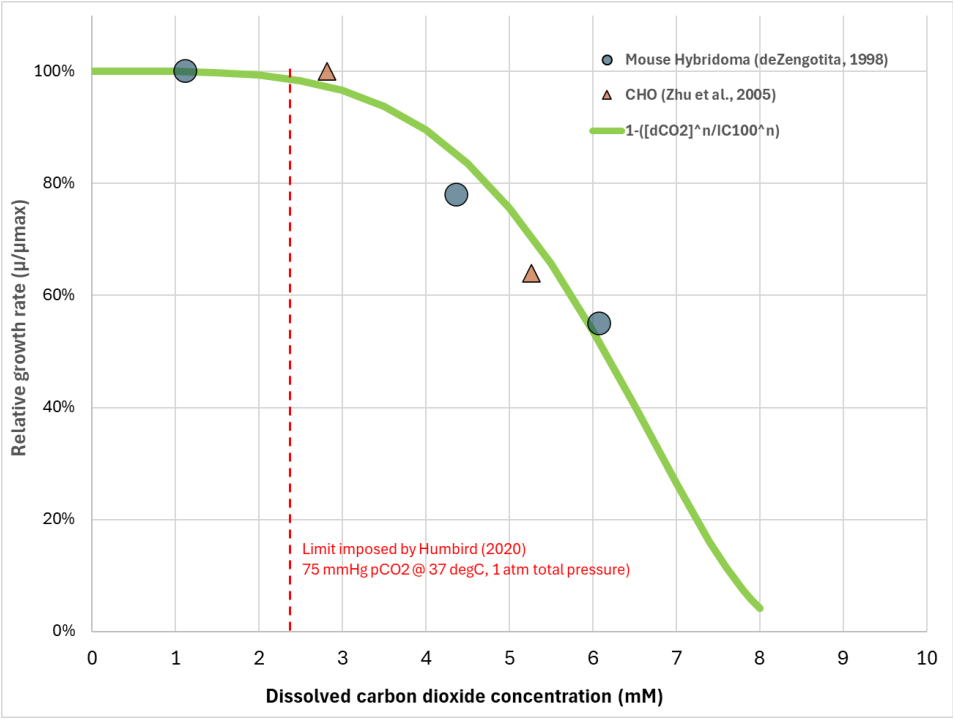

Figure 3.4e: Effect of dissolved CO_2 concentration on cell growth rate (relative to maximum specific growth rate for the given cell line) (Dezengotita, Kimura, and Miller 1998; Zhu et al. 2005). The red line represents the Humbird threshold. The trend line was fit to the combined data using a modified two-parameter model (IC100 = 8.6 mM dCO_2, and exponent n = 2.3).

Key takeaways and data gaps

- An IC50 of 6.3 mM was estimated for dCO2, however, more studies are needed to define dCO_2 tolerance levels in CM-relevant cell lines.
- Researchers should control for pCO_2, pH, and osmolality independently to distinguish their effects, as exemplified in (Zhu et al. 2005)
- Larger-scale bioreactor studies are needed to assess the combined impacts of dCO_2 and osmolality on culture performance.

Summary of metabolite inhibition

Across the studies analyzed, metabolite IC50s ranged from ~3–8 mM for ammonia, ~10–80 mM for lactate, ~6.3 mM for dissolved CO_2, and ~465 mOsm/kg for osmolality. The variance in data for some metabolites can be explained by differences in the cell line (i.e., cell type-specificity, primary vs. transformed cells), culture conditions (e.g., suspension vs. adherent), and medium composition (e.g., presence or absence of serum). While inhibition could be modeled mathematically, curves fitted to acute exposure data may overestimate effects in real-world cultures where metabolites accumulate gradually, as some cells have demonstrated the ability to adapt to higher metabolite concentrations. Strategies to reduce metabolite buildup, optimize nutrient feeding, and limit osmotic shifts are critical for improving growth and viability in CM processes. The priorities for future research include acquiring

more data on metabolite inhibition on cell growth and pluripotency for processes requiring differentiation in CM-relevant cell lines, performing studies with gradual metabolite accumulation instead of bolus addition, and designing studies to disentangle the interactive effects between metabolites under different culture conditions.

3.5 Stoichiometry of cell growth, substrate consumption, and metabolite production

While the previous section focused on the factors directly affecting the rate of cell growth and death, this section delves into how much of each primary substrate (oxygen, glucose, and glutamine) is consumed and how much of the key waste metabolites (lactate, CO_2, and ammonium) are produced. Although the consumption and production rates of these metabolites are generally proportional to the growth rate of the cell, their relative amounts can vary due to a number of factors. These amounts, driven by culture conditions and substrate and metabolite concentrations, have significant bearing on process performance. The efficient use of substrates will reduce media costs, while minimizing the accumulation of inhibiting waste products will increase bioreactor productivity and cell viability.

All TEMs published to date assume a static stoichiometry for overall growth, implying that substrate consumption is proportional to biomass produced. This simplification is equivalent to using apparent yields (discussed in Section 2.4), which implicitly include the maintenance requirements of the cells. In other words, the yield factors are constant regardless of growth rate or substrate concentrations present in the extracellular medium. As a result, these models treat growth rate as the sole determinant of substrate use and by-product formation, regardless of the overall conditions. We were interested in evaluating whether this simplifying assumption is justified when modeling bioreactor performance and the overall use of the major carbon and energy substrates.

Methodology for estimating yield factors

To calculate the yield factors for oxygen, glucose, and glutamine, we compiled available consumption data for these substrates under various growth conditions to build a more quantitative understanding of metabolic requirements. In some studies, the specific consumption rates were calculated from cell culture data and reported in graphs or tables. In others, they were estimated from time-series data on substrate and biomass concentrations. For the latter, if a growth profile was provided with the associated metabolite concentrations, specific consumption rates could be calculated.

For a batch culture, Equation 3.5a defines the instantaneous specific consumption rate of a substrate (q_S) as the rate of its disappearance (dS) divided by the cell concentration (X). Using time interval data, this derivative can be approximated by the difference between the substrate concentrations at the two time points divided by the time increment and the average cell concentration over the time interval:

$$q_S = \frac{1}{X}\frac{dS}{dt} = \frac{\Delta S}{\overline{X}\ \Delta t} \qquad \textbf{Equation 3.5a}$$

This approximation is reasonable as long as there is not a very large difference in cell concentration, such as during exponential growth. Very small time increments with only small changes in substrate

concentrations are also prone to error due to inaccuracies in concentration measurements. For fed-batch cultures, this calculation is somewhat more complicated as any substrate additions over the time interval must be accounted for when estimating rates.

For continuous cultures, specific consumption rates can readily be calculated using Equation 3.5b when a steady state has been established:

$$q_S = \frac{(S_{feed} - S)\ D}{X}$$ **Equation 3.5b**

The latter method using a chemostat and Equation 3.5b to determine these specific rates is generally more accurate since the conditions are time-invariant and precise sampling time is not critical.

Where true yield coefficients and cell maintenance requirements were not explicitly reported, they were estimated by fitting Equation 2.4a to the various specific consumption rates as a function of growth rate at the time of the sampling. Apparent yield data were also collected where available.

To compare data between cell lines, we normalized all consumption data on a dry cell weight basis. The rationale for this is that water content and cell size could otherwise skew results (see Section 3.2). The presumption here is that a cell that is twice as large (in volume) with twice as much dry mass would probably consume twice as much substrate under the same conditions. We standardized units for specific consumption rates as mmol substrate consumed per gram of dry cell weight per day (mmol/gDCW/day). Substrate concentrations were kept in molar terms so that molecular flux rates could be directly compared as molar ratios. For reporting yield coefficients and maintenance terms, we used mass-based units (gDCW/g Substrate), which are easier to interpret. The inverse of the apparent yield coefficient is then equivalent to a feed conversion ratio (FCR):

FCR = 1 / Y'

We also noted time delays in cell responses to changing nutrient or environmental conditions, as this information will be needed for modeling dynamic bioreactor behavior.

There is a wealth of data available for cell lines that have been used for biopharmaceutical production. For these lines, maximum achievable cell concentrations were historically of interest, but the productivity of secreted recombinant proteins was the primary thrust. We assessed if the available data regarding the control of metabolism toward cell growth were relevant for emerging CM-relevant cell lines. In the subsections that follow, we present data and analysis on each major substrate-metabolite pair to identify trends, differences, and model-relevant insights. While discussed individually, their mechanisms of metabolic control are often highly interconnected, and the final subsection synthesizes these interactions to provide a more holistic interpretation.

Stoichiometry of oxygen metabolism

Studies conducted by Miller et al. and Ozturk and Palsson offer the most comprehensive analysis of oxygen's influence on the relative consumption of energy substrates (Miller, Wilke, and Blanch 1987, 1988; Ozturk and Palsson 1990). As a key substrate for respiration in aerobic organisms, oxygen is essential for the complete oxidation of carbon substrates into carbon dioxide and water. At a fixed

growth rate, oxygen consumption depends on its availability. If the dissolved oxygen (DO) concentration decreases, both glucose consumption and lactate production increase, indicating a metabolic shift from oxidative phosphorylation to glycolysis. The yield of lactate from glucose ($Y'_{Lac/Glc}$) also increases, reflecting enhanced glycolytic flux.

Figure 3.5a highlights this phenomenon using data from a continuous culture where the growth rate was constant while the oxygen concentration was varied widely.[4] As can be seen, when the oxygen concentration falls below a critical point (to the left of the red line), oxidative phosphorylation can no longer be supported. In response, the cells resort to increasing glycolysis and glutaminolysis to generate the requisite energy needs. This metabolic switch occurred below DO concentrations corresponding to 1% of air saturation at atmospheric pressure (<0.002 mM in the liquid phase), and accelerated as DO decreased further to 0.1%.

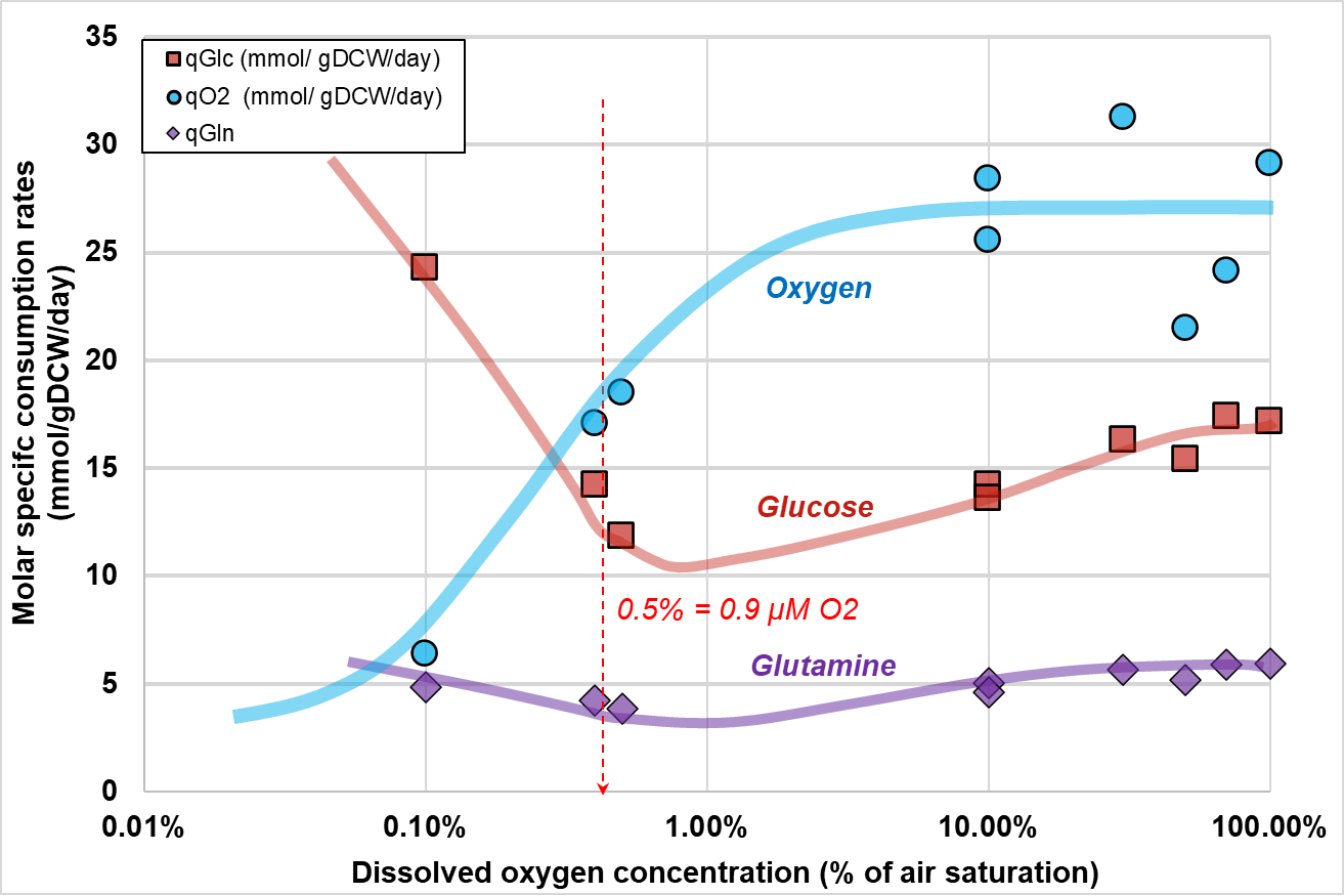

Figure 3.5a: Effect of DO concentration on the uptake of oxygen, glucose, and glutamine in a mouse hybridoma cell line. The x-axis is shown with a logarithmic scale to emphasize the relationships at very low DO concentrations. Data from (Miller, Wilke, and Blanch 1987, 1988; Ozturk and Palsson 1990).

Ozturk and Palsson found a similar threshold at 1.2% of air saturation, resulting in increases in the specific uptake rates of both glucose and glutamine from their respective minima. Interestingly, they

[4] Recall Equation 2.2c, where growth rate in a continuous culture can be held constant by keeping the dilution rate constant.

also observed that very high DO concentrations (above 10%) led to the same effect, likely driven by more complete oxidation and higher overall metabolic activity, both of which demand increased substrate flux (Ozturk and Palsson 1990).

Part of the reason for the dramatic rise in glucose consumption at low DO is because it cannot be fully oxidized in the absence of oxygen. Because glycolysis yields only 2 ATP per mole of glucose consumed, more substrate is needed to fulfill energy demands and more lactic acid is produced. Concomitantly, glutamine consumption and ammonia production also rise at lower DO levels, though less dramatically, suggesting adjustments in amino acid metabolism.

Presumably, with a further reduction in DO, cell death would ensue; however, this appears to be highly cell-line dependent. For example, the murine hybridoma cell line studied by Ozturk and Palsson maintained viability for a prolonged period at zero DO (Ozturk and Palsson 1990). This would suggest that glycolysis and/or glutaminolysis can continue to be catabolized for energy if either substrate is readily available. The continuation of catabolism in the absence of oxygen also has important implications for end-product quality, with initial experiments demonstrating that post-harvest changes resemble postmortem changes in conventional meat production (Mehmood et al. 2025).

Oxygen consumption and growth rate

Oxygen uptake is typically proportional to growth rate, except when below threshold DO concentrations, such as those shown above. However, the bioprocess literature rarely correlates oxygen uptake rate (OUR) with growth rate, presumably due to the relative difficulty in measuring oxygen consumption rates in culture. Much of the original foundational literature used a traditional Clark-type dissolved oxygen electrode to measure oxygen consumption. Newer methods are now available (discussed later in Section 5) but are focused largely on cancer biology. **Figure 3.5b** compiles the limited data available in an attempt to establish a yield coefficient and typical maintenance requirement for this essential nutrient.

The bioreactor-derived data in Figure 3.5b were taken from chemostat experiments at a constant dilution rate, measuring specific OUR (q_{O2}). While actual growth rates can be extracted from cell viability data at each steady-state sample point, the true growth rates still spanned a narrow range. This limited range of growth rates did not allow a robust slope and intercept to be determined. To augment this data set, we used data from Wagner et al., who studied a wide variety of malignant cell types (Wagner, Venkataraman, and Buettner 2011). For the six cell lines they studied, the average specific OUR ranged from 5.8 to 14 mmol/gDCW/day for experiments where the cells were growing exponentially and not artificially stimulated. Neither total cell mass nor exact specific growth rates were reported, but q_{O2} was normalized to cell protein. So, protein was assumed to be 50% of cell dry mass to convert to a cell mass basis. The single point on the graph is the average (9.5 mmol/gDCW/day) and the error bars are the standard deviation across eight measurements at an assumed growth rate corresponding to just under a 24-hour doubling time.

We also indicate the values for oxygen uptake assumed by prior TEMs in Figure 3.5b (Negulescu et al. 2023; Humbird 2021). Humbird differentiated between wild-type and metabolically enhanced cells, the latter consuming more oxygen to model the effects of less lactate and ammonia accumulation.

Nonetheless, all the values fell within a similar range and are roughly in line with the data analyzed from Miller et al. and Ozturk and Palsson, except for the lower values, which likely reflect outliers due to oxygen-limited conditions. The average from Wagner et al. also agrees well with the q_{O2} assumed by Humbird and Negulescu et al. for wild-type cells. These agreements all support the use of specific metabolic rates normalized to dry cell mass, as Wagner et al. also observed a loose correlation between OUR and cell size and protein content.

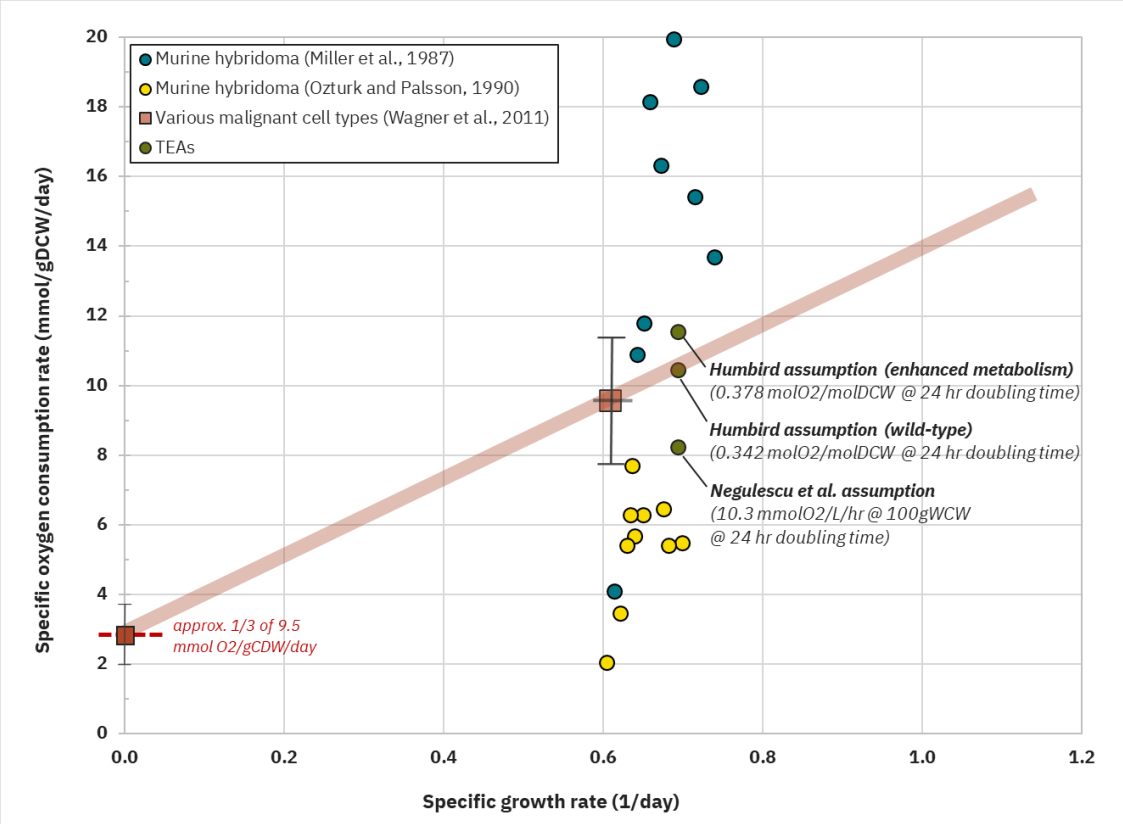

Figure 3.5b: Specific oxygen consumption rate as a function of cell-specific growth rate data that could readily be found. The data from Wagner was aggregated into a single average (n=8) at an assumed growth rate, and the y-intercept of the trend line was approximated from the reduction in q_{O2} when four of the cell lines studied reached the stationary phase. Starred data points indicate values assumed by published TEMs. Data from ((Wagner, Venkataraman, and Buettner 2011)) and mouse hybridoma cells (Miller, Wilke, and Blanch 1987; Ozturk and Palsson 1990).

For four cell lines, Wagner et al. measured q_{O2} when the cells reached stationary phase (i.e., zero growth rate). From these measurements, the oxygen uptakes as a fraction of the values measured during exponential growth ranged from 12 to 67%. An average of 31% was applied to the average growth-associated average to approximate a typical maintenance requirement, as shown by the y-intercept in Figure 3.5b. Using the slope of the trend line, an approximate true biomass yield on oxygen can be estimated at 2.9 gDCW/g O_2. Lastly, an interesting observation by Wagner et al. was that cells in a lag phase had a dramatically (~9-fold) higher q_{O2} than even that measured in exponential growth, reflecting important transients that are at play.

Overall, the lack of data for oxygen consumption under various rates of growth indicates a gap for CM-relevant cell lines under bioreactor conditions and oxygen-related growth phenomena need to be understood for scaling up these aerobic processes.

Key takeaways and data gaps

- Very low DO levels, below ~0.5% air saturation (<0.001 mM), represent a metabolic transition zone where cells switch from oxidative phosphorylation to glycolysis, resulting in significant increases in specific glucose and glutamine uptake rates and subsequent lactate and ammonia formation. This low threshold indicates the efficiency at which aerobic organisms can sequester oxygen, but DO should be kept well above this threshold.
- However, very high DO levels are also not optimal, apparently due to the toxicity of oxygen. The optimal range of DO lies between 1 and 10% air saturation.
- Limited data exist for the relationship between oxygen consumption and cell growth rate, as oxygen consumption, historically, has been challenging to measure accurately. A true yield coefficient of 2.9 gDCW/g O2 (FCR = 0.34 g O2/gDCW) was determined as an initial estimate. However, newer methods are available and should be leveraged for CM development. See Section 5.3 for recommendations.
- Due to its low solubility, oxygen transfer is a likely limiting factor for bioreactor productivity. Since the impact of oxygen deprivation on cell viability (death rates) appears to be cell line dependent, more studies of CM-relevant cell lines are needed, including the timescale of the response.

Stoichiometry of glucose metabolism and lactic acid production

Publications with data on glucose consumption under various conditions were more abundant in the literature. Glucose consumption rates normalized on a DCW basis were plotted against the specific growth rate of the cultures at the time of sampling (**Figure 3.5c**).

On average, most of the data clustered between 8-18 mmol Glc/gDCW/day and showed a general trend of higher glucose consumption rates as growth rate increased. Considerable scatter was observed, especially at low growth rates in small batch cultures and time intervals that may be prone to error. The data clustered well around the more conservative assumptions made in prior TEMs (Negulescu et al. 2023; Humbird 2021). However, our estimations for DCW based on cell type may introduce errors, as only Miller et al. reported a real DCW of 265 pg/cell. For example, if cells weigh more than assumed, the specific consumption rate on a DCW basis would decrease.

This relationship between cell mass and growth rate was summarized previously in Figure 3.2f, which showed that dry mass can change by more than a factor of two over the range of typical animal cell growth rates. This substantial increase would make the trend line appear steeper. Of particular interest was the study by Frame and Hu, who observed a kink in the line at growth rates above 1.2 day^{-1}, where the slope appears to suddenly change (Frame and Hu 1991a). This suggests a shift to lower yields (i.e., a lower efficiency of glucose utilization) at high growth rates. The implications of such phenomena are important to consider for CM processes, which are intended to run at high growth rates aligned with these data. Collectively, this analysis underscores the importance of measuring DCW across different cell lines used in cultivated meat, which can be used to derive a more accurate assessment of the relationship between glucose consumption rate and growth rate.

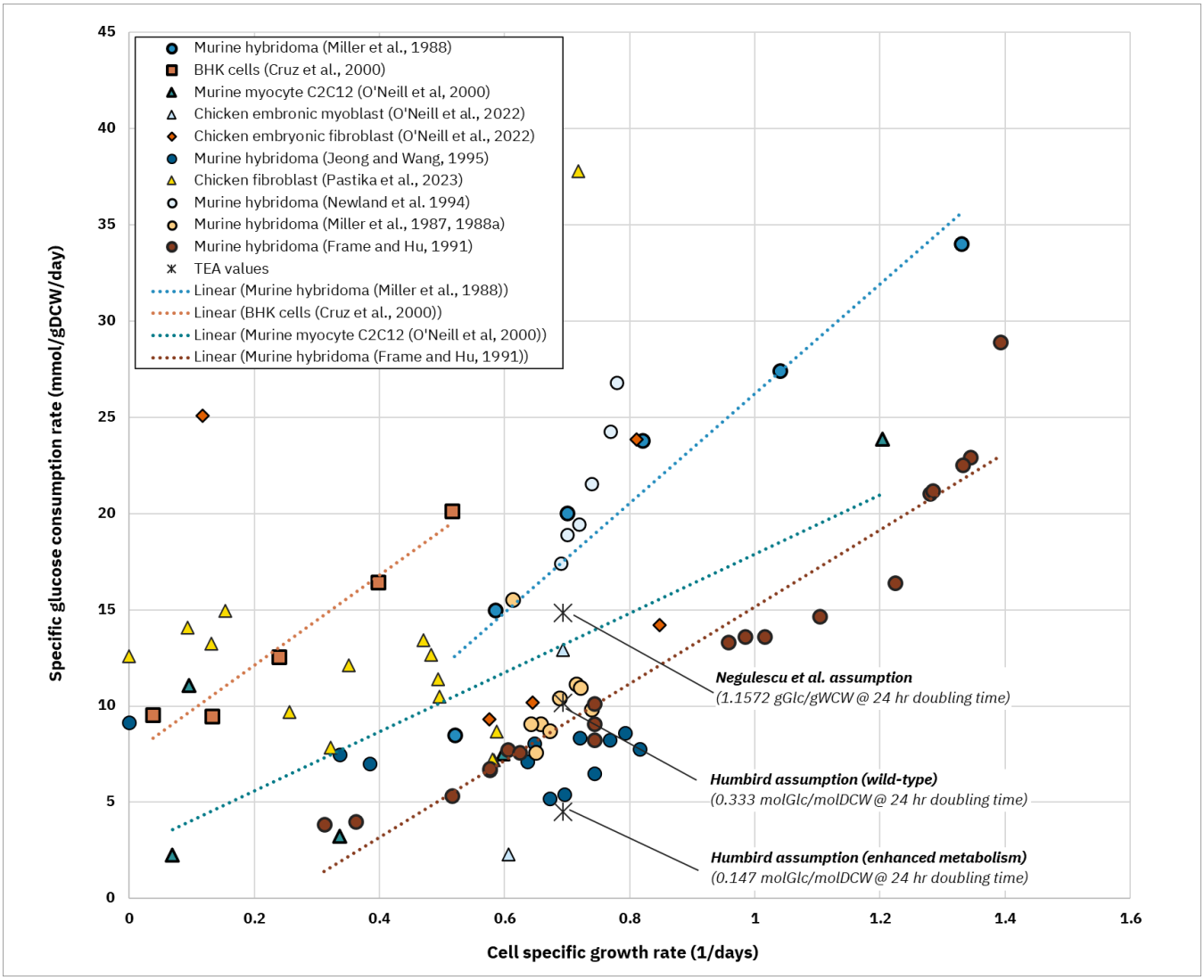

Figure 3.5c: Specific glucose consumption rate as a function of cell-specific growth rate. The size of the points denotes the relative confidence in the data sets—those collected from continuous cultures at steady state or from batch or fed-batch cultures with a substantial differential of cell concentrations over a given time interval were considered higher quality data. Assumptions used in prior TEMs are shown for reference.

Maintenance requirement for glucose

According to the theory explained earlier, the plot of specific growth rate (μ) vs. q_{Glc} should show a positive intercept representing the minimum maintenance requirement. However, most of the discernible trends in Figure 3.5c indicate a maintenance requirement that is very low and in some cases less than zero. While Miller et al. estimated a glucose maintenance requirement of 1.2 mmol/1e^{9}cells/day (4.54 mmol/gDCW/day; (Miller, Wilke, and Blanch 1987)), in a subsequent paper they admitted: "The effect of μ on the glucose metabolic quotient is not adequately described by the maintenance energy model because the amount of glucose going into each of the metabolic pathways depends on the glucose concentration and other factors, such as the pH and glutamine concentration. Deviations in specific growth rate from a modified Monod model may also be due to the path changes. New models . . . that account for these path changes are required."

Whether or not a maintenance requirement is indicated is likely a result of the regimen in which the data were collected. If glucose is acting as the primary carbon source and contributing significantly to the cell's energy maintenance requirement, a positive intercept may well be observed for data collected from a given experiment and medium. The data from Cruz et al. on a BHK cell line appear to indicate a maintenance requirement of ~7.5 mmol Glc/gDCW/day (Cruz, Moreira, and Carrondo 2000). However, where glutamine is contributing significantly, the maintenance requirement for glucose may appear to be close to zero. Also, cells have an absolute requirement for glucose in the absence of any other sugars for the synthesis of the carbohydrate portion of nucleic acids. However, some cell culture media contain other nucleotide precursors.

Data from the literature are summarized in **Table 3.5a** for both the apparent and true biomass yields using assumed maintenance requirements. The average apparent yield across all cell types and conditions is approximately 0.461 gDCW/gGlc $\pm$ 40%. As mentioned above, the FCR can be calculated by taking the inverse of the apparent yield (Y'). Using this estimate, the range of FCRs for glucose roughly spans 1.6 to 3.6 g Glc/g DCW.

Table 3.5a: Glucose biomass yields and maintenance requirements for various cell lines found in the literature.

Reference	Cell type	Apparent Glucose Yield Y' x/Glc (gDCW /gGlc)	Maintenance Requirement mGlc (gGlc /gDCW /day)	Actual Glucose Yield Y x/Glc (gDCW /gGlc)
Miller et al., 1988	Murine Hybridoma	0.228	0.8172	0.3380
Jeong and Wang, 1995	Murine Hydridoma	0.514	0.4504	0.8190
Lao et al., 1997	CHO	0.233		
Cruz et al., 2000	BHK	0.097	1.3332	0.2367
Slivac et al., 2010	Channel Catfish Ovary	1.015		
Lopez-Mesa et al., 2015	CHO	1.185		
	CHO	0.905		
O'Neill et al., 2022	Chicken Embryonic Fibroblast	0.248	0.9008	0.4432
	Chicken Embryonic Myoblast	0.298	0.9008	0.4857
	Murine Myoblast (C2C12)	0.303	0.4504	0.8986
O'Neill et al., 2024	Murine Myoblast (C2C12)	0.160		
Averages		**0.471**	**0.809**	**0.537**
Previous TEM Assumptions				
Humbird, 2020	Model - Wild type	0.3778		
Humbird, 2021	Model - Enhanced	0.8558		
Negulescu et al., 2022	Model	0.2592		

Factors affecting glucose consumption rate

Like oxygen, glucose consumption rates are also clearly affected by the availability of substrate. Several studies have shown that when glucose supply is restricted through fed-batch operation, its consumption and the production of lactate are significantly decreased without compromising growth rate or final cell concentrations (Glacken, Fleischaker, and Sinskey 1986; Ljunggren and Häggström 1994; Kurokawa et al. 1994). This implies that cells make more efficient use of energy-producing substrates when available at limited concentrations.

This phenomenon has been known for some time and is often exploited by the biopharmaceutical industry to increase growth and recombinant protein yields by controlling the addition of the key substrates during fed-batch processes. One such process used the changes in pH induced by the formation or uptake of lactate to control the addition of glucose (high-end pH-controlled delivery of glucose or HIPDOG), resulting in a significant reduction in total lactate accumulation and base addition with an approximately two-fold increase in therapeutic protein titer (Gagnon et al. 2011).

Apparently, the glucose concentration below which this metabolic shift is observed is on the order of 1 mM. However, plotting the available data for biomass yields based on glucose ($Y'_{X/Glc}$) collected during this review did not show a discernible relationship with residual glucose concentration since most data points were above this limit. Additionally, glutamine concentration, as will be described, also impacts energy yields and varied across these studies, contributing to the data scatter. Successful implementation of strategies to increase the efficiency of biomass yield on glucose in manufacturing could reduce its cost contribution to media.

A few studies did attempt to separate these effects by measuring yield coefficients at very low glucose concentrations. One such study by Acosta et al. is shown in **Figure 3.5d**, alongside other data (Acosta et al. 2007). Performed in small-scale batch cultures, only those points where glutamine was not first depleted are included. Under these controlled conditions, a 100-fold increase in $Y'_{X/Glc}$ is clearly observed for this mouse hybridoma cell line as glucose concentrations fall below 1 mM.

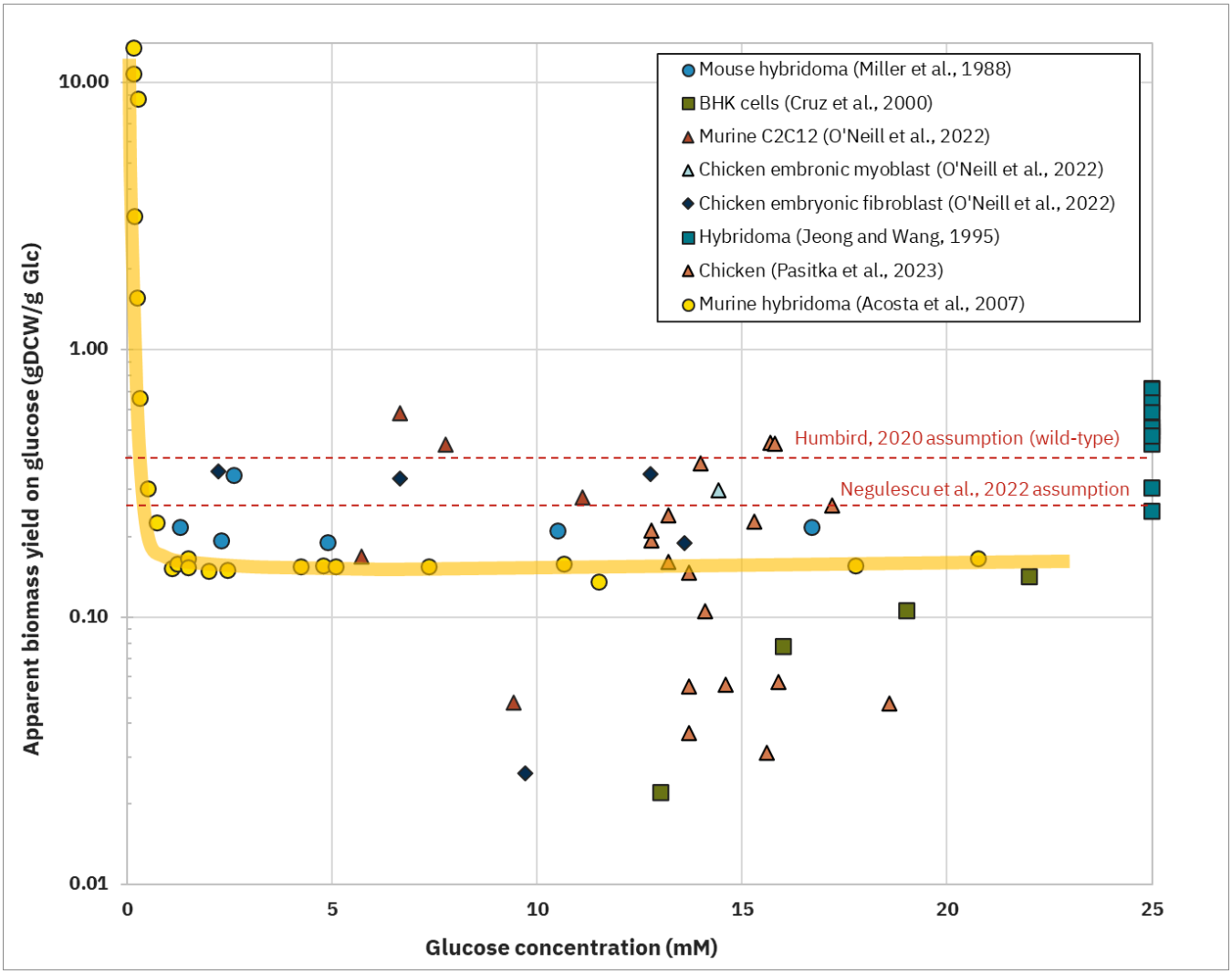

Figure 3.5d: Apparent biomass yields on glucose as a function of glucose concentration. Data from all available studies. Trend line drawn through controlled study by (Acosta et al. 2007) but apparent yields are converted to a dry mass basis from cell number, assuming a cell mass for this murine hybridoma cell line of approximately 271 pg DCW/cell and 75% water. Dotted red lines show the biomass yield assumptions used in prior TEMs.

Lactate formation and yields on glucose

Using many of the same data sets as depicted in Figure 3.5c, lactate formation rates and yields on glucose consumed were also calculated and compared to growth rates and substrate concentrations. **Figure 3.5e** shows cell-specific lactate formation rate as a function of glucose consumption, both in molar units per unit dry cell weight. The dotted line through the origin with a slope of 2.0 represents the maximum ratio of lactate formation to glucose consumed if all the glucose is converted to lactate and does not enter the TCA cycle. While the data are fairly scattered, the trend suggests that glucose is more efficiently used at lower consumption rates with a lactate to glucose ratio of less than 2. At higher consumption rates, lactate formation rates increase to ratios higher than 2. This has been observed by others with the explanation that the catabolism of glutamine can also result in lactate production, leading to lactate:glucose ratios over 2.

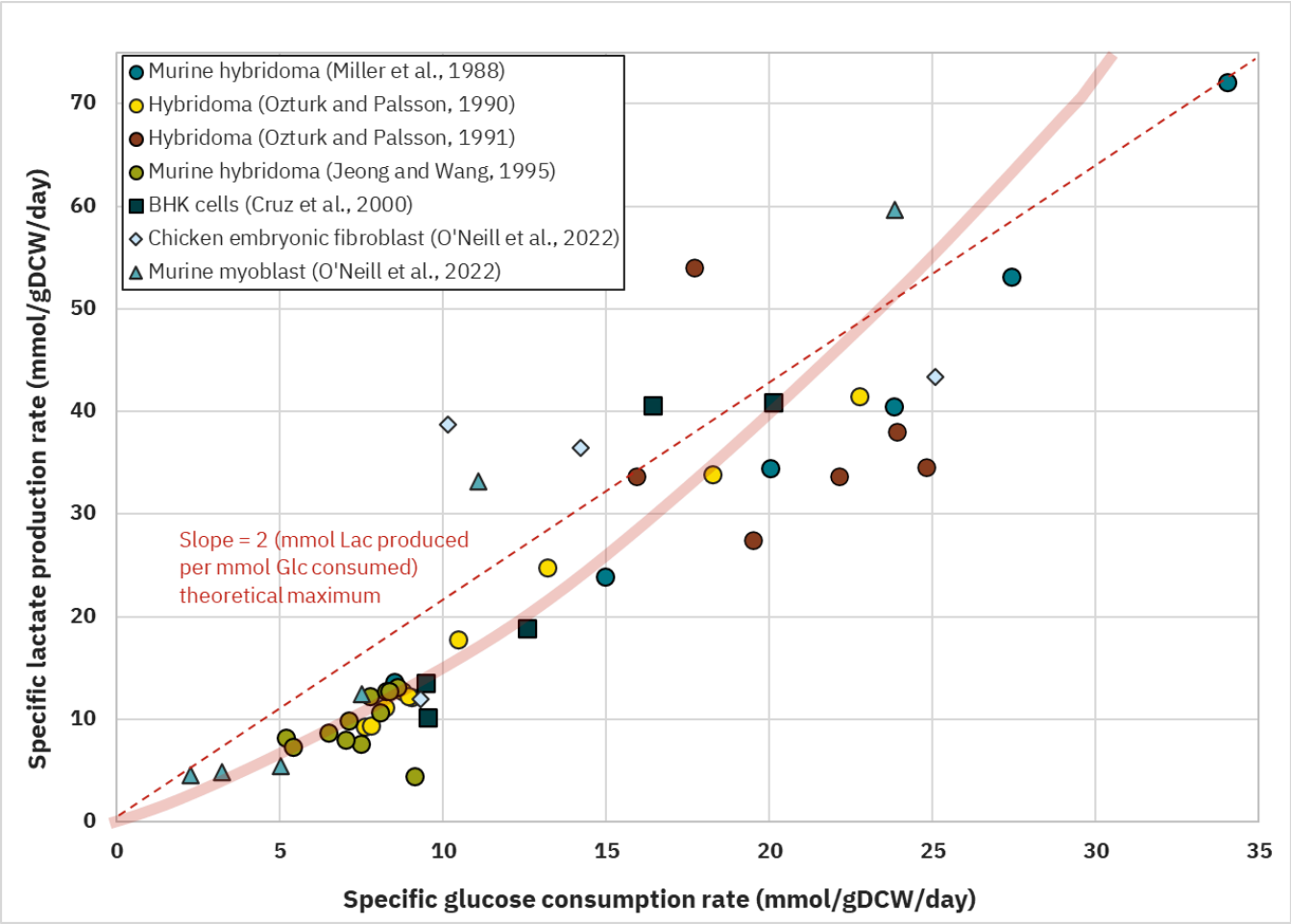

Figure 3.5e: Specific lactate formation rates as a function of glucose consumption rate. The blue dotted line with a slope of 2 indicates the maximum ratio of lactate:glucose if all glucose is converted to lactate and does not enter the TCA cycle.

When the same data are plotted as an apparent molar yield of lactate on glucose (**Figure 3.5f**), the points show a loose correlation with an upward trend, with a global mean slightly below 1.5. The data confirm the apparent molar yield of lactate from glucose observed by Miller et al. of about 1.5, which is 75% of the theoretical maximum. Humbird also selected 1.5 for the wild-type metabolism, whereas the “enhanced” metabolism was set at 0.5.

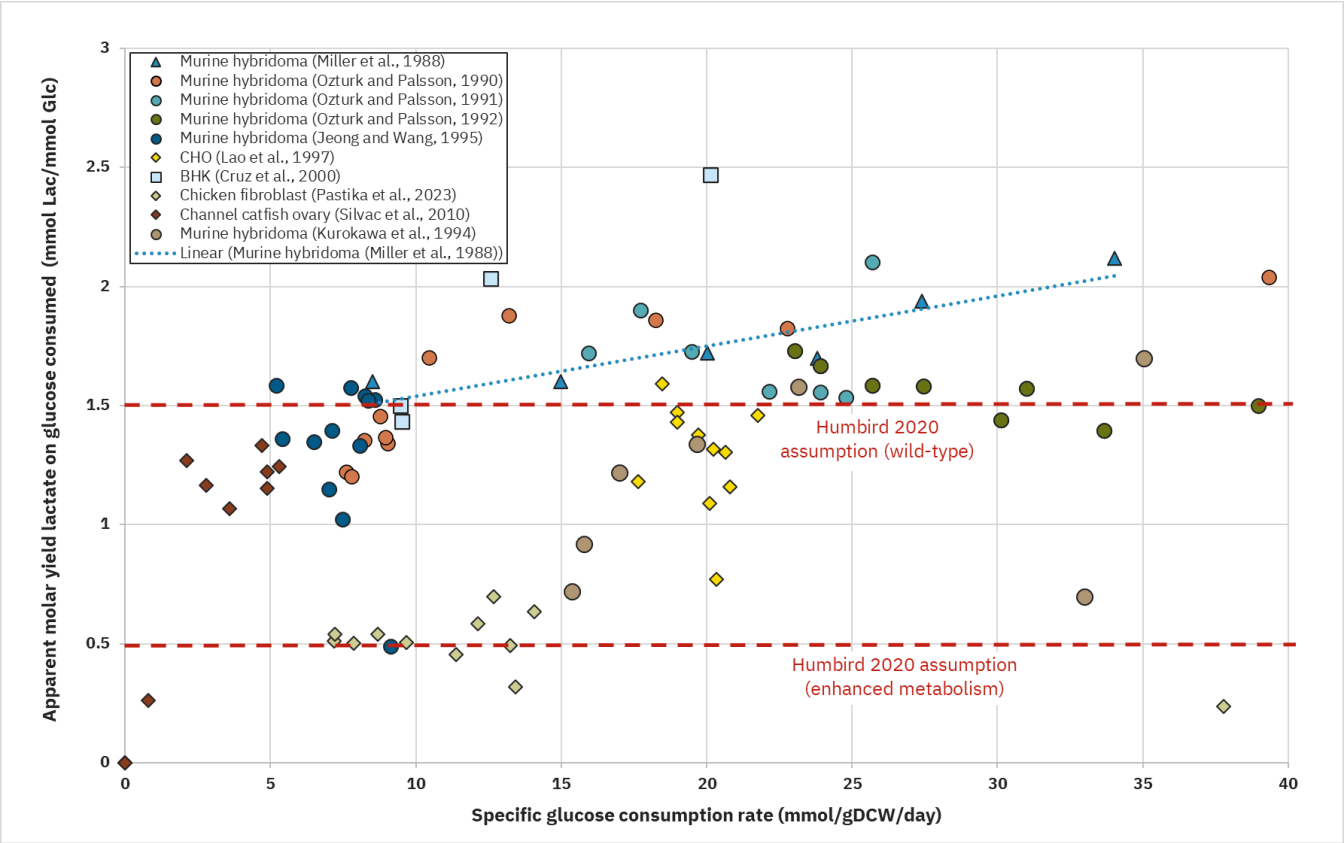

Figure 3.5f: Apparent molar yield of lactate on glucose as a function of glucose consumption rate from all available data. Red dotted lines denote the wild-type and enhanced metabolic quotients assumption used by Humbird 2020.

Given the relatively high lactate yields, the Warburg Effect is clearly at play. Despite the adequate supply of oxygen in these experiments, the majority of the glucose, and some glutamine, are not fully oxidized but instead are shunted to lactate with a far lower energy yield. More recently, the Warburg Effect and lactate production were eliminated using genome editing in CHO and HEK cells (Hefzi et al. 2024). The experiments showed that cells maintained normal growth rates by rewiring their metabolism toward oxidative phosphorylation. Interestingly, data from Believer Meats using chicken fibroblasts clustered around a lactate:glucose ratio of 0.5, suggesting efficient glucose metabolism may be possible without engineering (Laura Pasitka et al. 2024). These experiments, as well as others using alternative substrates such as galactose, point to the many tools that CM manufacturers will have available to achieve favorable lactate:glucose ratios and efficient oxidative metabolism.
Lastly, the vast majority of lactate production rate data has been derived from proliferating cell cultures and there is less known about the metabolism of differentiating cells. Culturing C2C12 murine myoblast cells in a hollow fiber bioreactor operating under batch mode, Tuomisto et al. observed that q_{Lac} during the differentiation phase dropped to about 24% from what it was in the proliferation phase (Tuomisto, Allan, and Ellis 2022). However, this effect could well be attributed to a reduction in growth rate and does not necessarily mean that differentiating cells have very different substrate needs on a

per unit mass basis. This highlights another data gap in the literature that CM researchers can investigate.

Key takeaways and data gaps

- The average apparent biomass yield for glucose (Y'X/Glc) across all cell types and conditions collected is approximately 0.461 gDCW/gGlc + 40%. This range in yield is equivalent to a feed conversion ratio (FCR) for glucose roughly spanning 1.6 to 3.6 g Glc/g DCW.
- Restricting glucose below 1 mM can lead to dramatically increased biomass yields for this key substrate and consequently decreased lactate production. Maintaining low residual glucose concentrations is best achieved with continuous or highly controlled fed-batch cell culture modes, which could decrease glucose's contribution to media costs and may improve bioreactor performance.
- The Warburg Effect can be engineered or at least partially mitigated. Practitioners should build on methods developed in the pharmaceutical sector to reduce lactate:glucose ratios toward 0.5 by shifting cells toward more energy-efficient oxidative metabolism.
- In general, the data for glucose consumption and maintenance requirements were scattered, highlighting the flexibility of metabolism under different conditions and the need for controlled experiments to be conducted in CM-relevant cell lines. Data on glucose consumption during differentiation were largely absent, highlighting a gap that CM researchers can investigate.
- The lack of a clear maintenance requirement is at odds with the known dependency on glucose for the synthesis of nucleic acids for ribose. However, this may be a small demand compared to total energy production and may be obscured if nucleotide precursors are included in the medium.

Stoichiometry of glutamine metabolism and ammonia production

Glutamine is known to degrade spontaneously in cell culture media by deamidation, resulting in free ammonia and pyroglutamate. Most metabolic studies account for this loss by verifying it is minimal or correcting specific consumption rate calculations. Since degradation is pH- and temperature-dependent (and can be accelerated by certain anions like phosphate and bicarbonate), models should include this effect unless a stable glutamine analog such as GlutaMAX is used.

As with glucose, glutamine consumption data were collected and normalized to DCW. **Figure 3.5g** presents the glutamine-specific consumption data as a function of cell growth rate. Though these data also show considerable scatter, most points fall between 0.5 and 7 mmol Gln/gDCW/day, with higher growth rates generally linked to greater consumption. Thus, it appears that CM-relevant cell types have a very similar glutamine uptake as other historic cell lines used for recombinant protein expression, which should be verified through additional experiments.

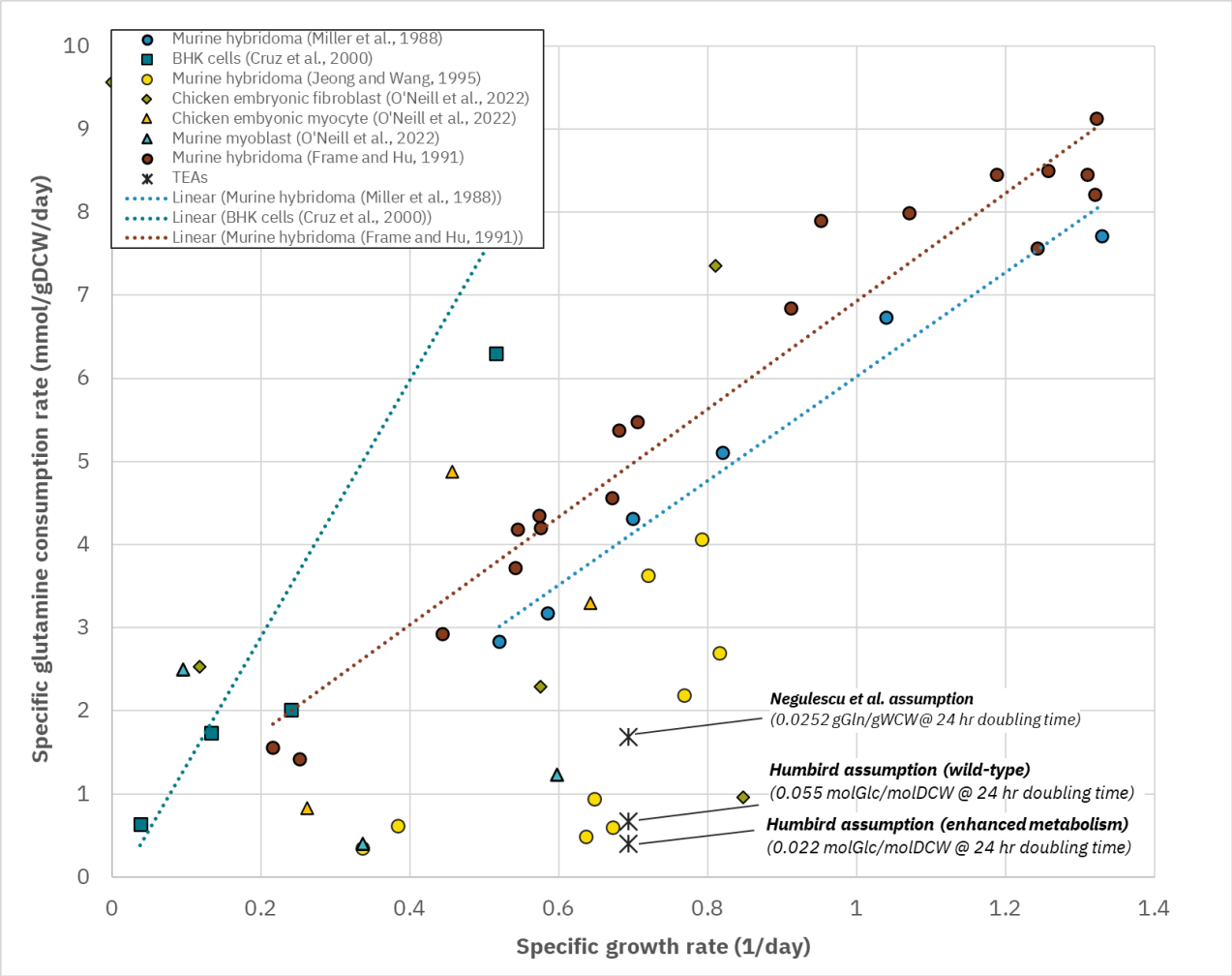

Figure 3.5g: Specific glutamine consumption rate as a function of cell-specific growth rate. Circles are hybridomas, squares are BHK cells, diamonds are fibroblasts, and triangles are fibroblasts. The Xs denote the values assumed in recent TEMs of CM.

Maintenance requirement for glutamine

Data from chemostats again provide the most consistent trends (Frame and Hu 1991a; Miller, Wilke, and Blanch 1988). When fit linearly, the data show positive slopes with slightly negative y-intercepts, suggesting no clear maintenance requirement from glutamine, which is consistent with prior literature. However, all data assume constant DCW across growth rates, which is an oversimplification that may introduce error (see Figure 3.2e). Due to the absence of a maintenance estimate, the summary of glutamine yield coefficients collected in **Table 3.5b** is associated with a zero maintenance term. Therefore, the apparent yields are equal to their corresponding true yields. The average biomass yield for glutamine is about 1.98 gDCW/gGln $\pm$ 23%, which corresponds to an FCR range of 0.4 to 0.65 g Gln/gDCW. The FCR for glutamine is 3 to 5 times less than that for glucose.

While no definitive reason can be offered for the absence of a maintenance requirement for glutamine, it is likely related to the fact that glucose and glutamine are partially substitutable energy substrates. Furthermore, cell culture media are typically rich in other amino acids that can serve as an energy and/or nitrogen source.

Table 3.5b: Glutamine biomass yields for various cell lines found in the literature. No maintenance requirements have been reported and the data plotted in Figure 3.5g reveal a near-zero y-intercept. Therefore, the assumed maintenance terms were set to zero.

Reference	Cell type	Average Apparent (Y' x/Gln) and actual (Y x/Gln) Glutamine Yield (gDCW /gGln)
Miller et al., 1988	Murine Hydridoma	1.157
Jeong and Wang, 1995	Murine Hydridoma	4.355
Frame and Hu, 1991	Murine Hydridoma	0.979
Cruz et al., 2000	BHK	0.564
O'Neil et al., 2022	Chicken Embryonic Fibroblast	1.236
	Chicken Embryonic Myoblast	2.680
	Murine Myoblast (C2C12)	2.880
Averages (all cell types)		**1.979**
Previous TEA Assumptions		
Humbird, 2020	Model - Wild type	2.823
Humbird, 2021	Model - Enhanced	7.058
Negulescu et al., 2022	Model	11.905

Ammonia formation and yields on glutamine

Figure 3.5h shows the molar yield of ammonium from glutamine (mostly) as a function of specific glutamine consumption rate. Similar to data shown previously for glucose, it is known that the faster the cells grow and/or the faster that glutamine is taken into the cell, the more it is deaminated, freeing glutamate to enter into various metabolic pathways. Consistent with this, there is a very clear increase in ammonia yield with an increasing rate of glutamine consumption. This would be expected to level out at the theoretical maximum for ammonia yield on glutamine of 2.0. However, other amino acids can also be deaminated and contribute to ammonia release, which could push ammonia yields even higher.

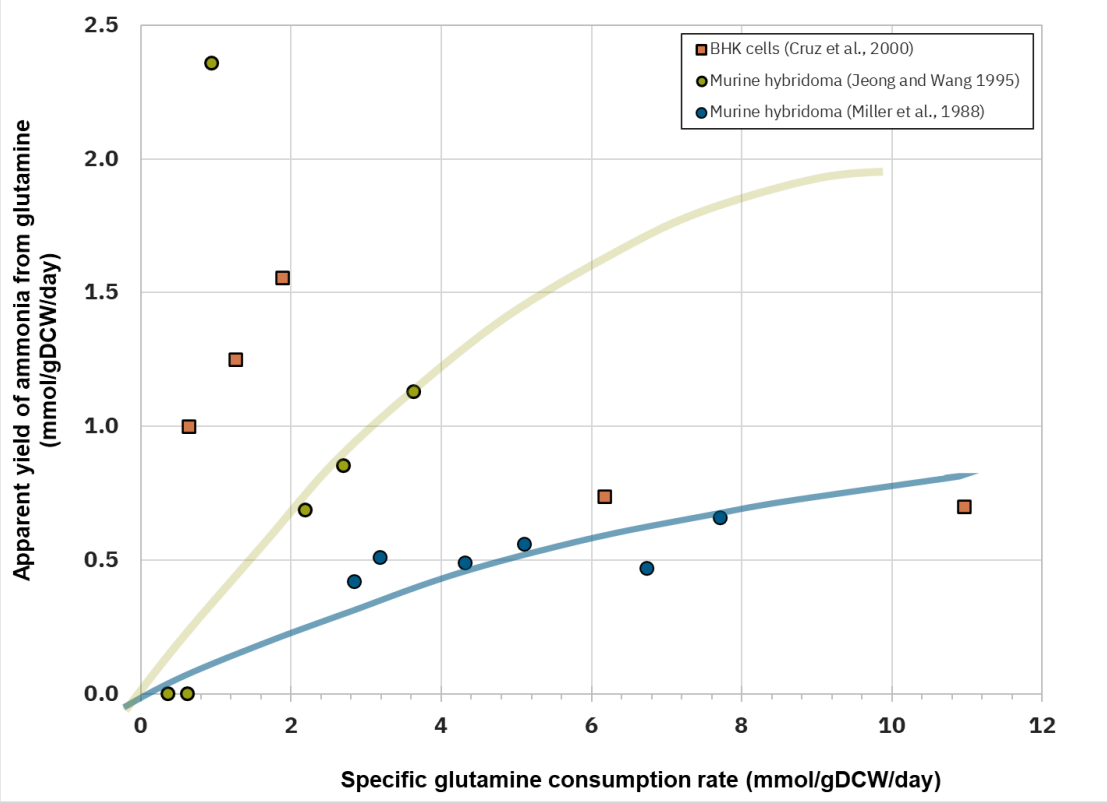

Figure 3.5h: Apparent yield of ammonia from glutamine as a function of extracellular glutamine concentration.

Factors affecting glutamine consumption rate

As with other substrates, the availability of glutamine is also a factor in how it is consumed and metabolized. **Figure 3.5i** confirms that there is a dramatic rise in glutamine efficiency at very low residual concentrations. Similar to glucose (Figure 3.5d), Figure 3.5i shows that there is a threshold below ~0.3 mM where the metabolism switches. This agrees well with the threshold determined by Ljunggren and Haggstrom of 0.2 mM (Ljunggren and Häggström 1994) and others who have concluded that glutamine is used less efficiently at higher concentrations, leading to even more ammonium ion production (Butler and Spier 1984; Miller, Wilke, and Blanch 1988). Successful implementation of this strategy in manufacturing could reduce glutamine's cost contribution to media.

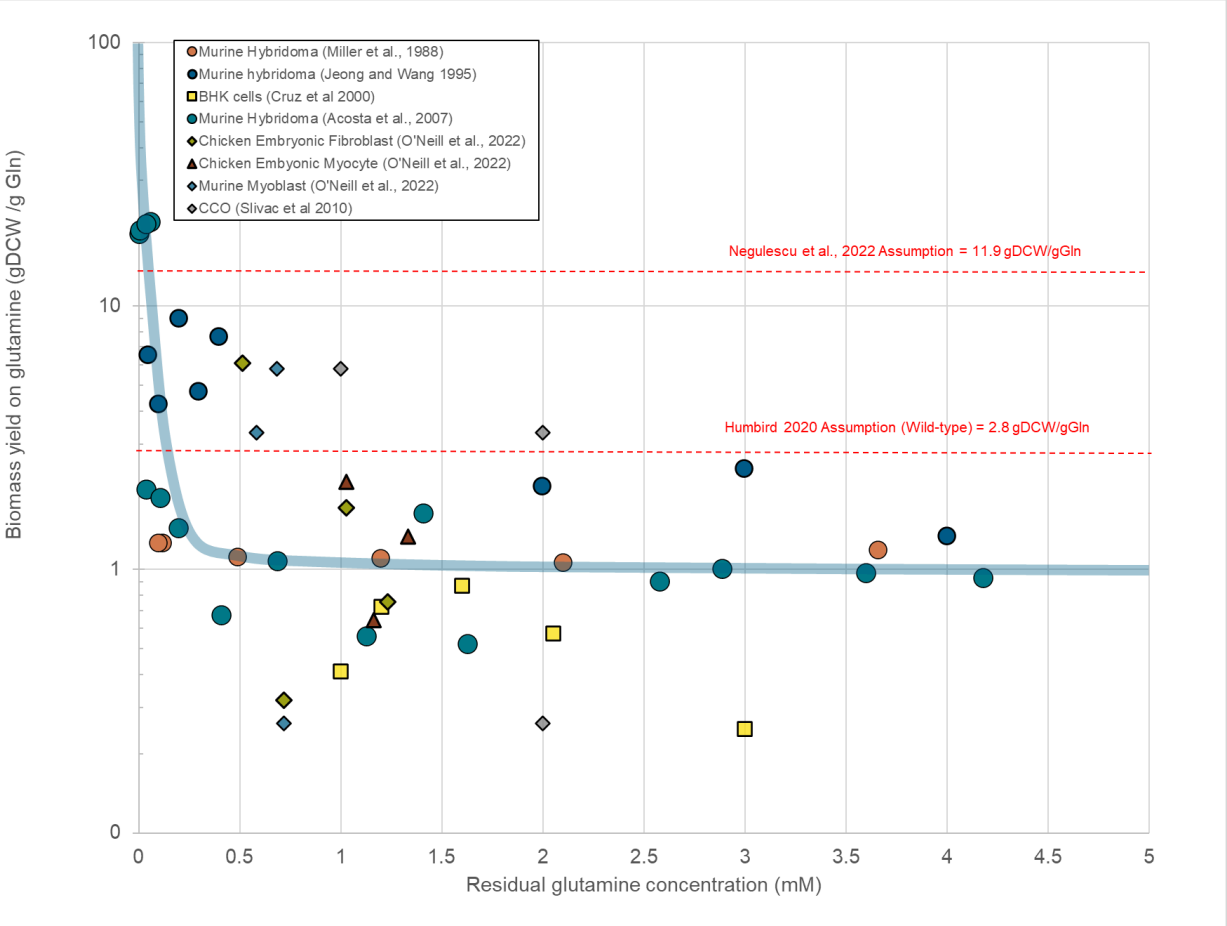

Figure 3.5i: Biomass yields on glutamine as a function of glutamine concentration. Assumptions from previous TEMs by Humbird and Negulescu et al. are included in red.

In addition to specific growth rate and glutamine concentration, glutamine's uptake rate is also influenced by culture mode, serum concentration, and availability of other amino acids. The effects of other amino acids are briefly discussed in the section on interactions, but in general, glutamine metabolism appears tightly linked to the same regulatory pathways that control glucose metabolism. Lactate yields exceeding 2 mol/mol of glucose are often observed, implicating glutamine catabolism in lactate production. As glutamine concentration increases, both ammonium and lactate production tend to rise, suggesting co-regulation of nitrogen and carbon waste metabolite pathways (Jeong and Wang 1995)**. Figure 3.5j** shows the influence of glutamine concentration on $Y'_{Lac/Glc}$ from available data where biomass yields could be extracted.

Jeong and Wang speculated that at extremely low glutamine concentrations (< 0.1 mM), "cells do not waste energy by converting pyruvate to lactate, which is the least energy-efficient pathway. Thus, glucose consumption is not significantly increased until the cells are almost completely starved of glutamine and forced to consume more glucose because they desperately need the energy for survival." Taken together, these data show that lactate formation is strongly influenced by residual glutamine concentration as well as glucose. This helps explain the high degree of variability in biomass yields on the two substrates from various studies.

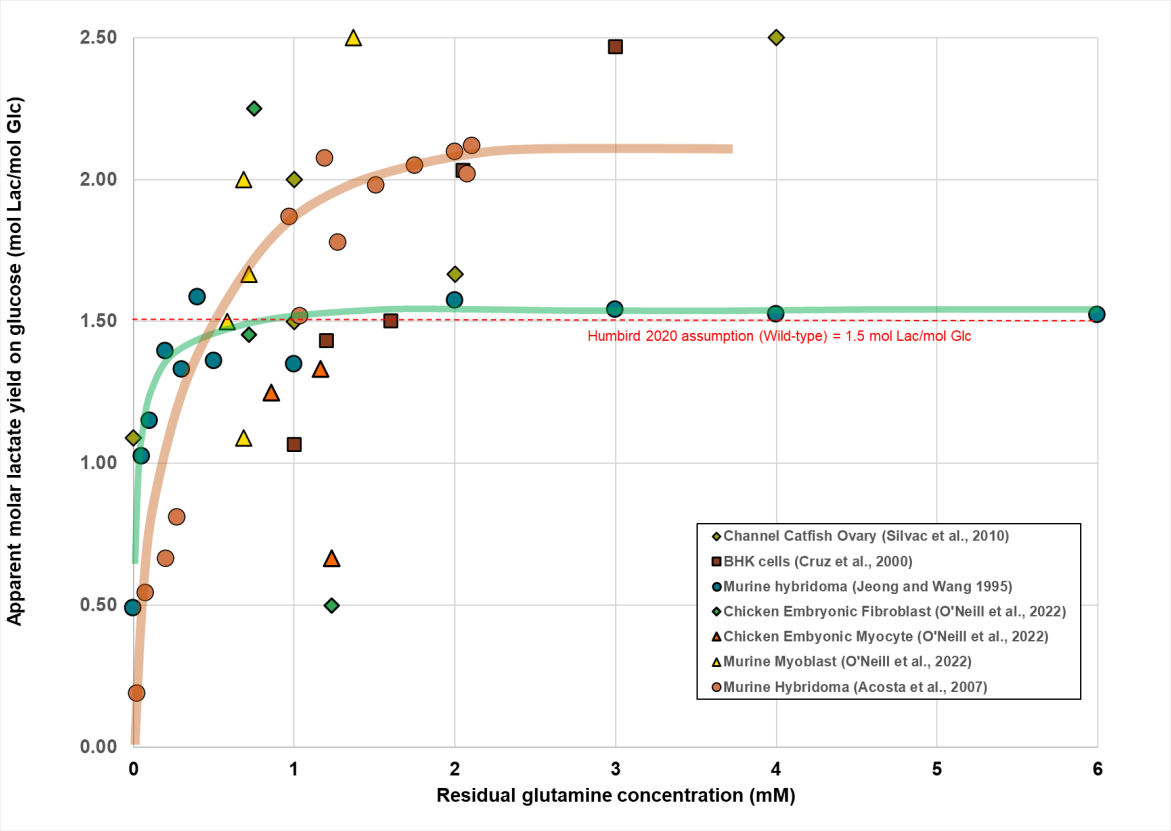

Figure 3.5j: Apparent yield of lactate on glucose as a function of glutamine concentration.

Key takeaways and data gaps

- The average biomass yield for glutamine is about 1.98 gDCW/gGln + 23%. This yield range corresponds to an FCR from 0.4 to 0.65 g Gln /gDCW, which is roughly 3-5 times less than that for glucose.
- No clear maintenance requirement could be established for glutamine, likely due to the fact that glucose and glutamine are partially substitutable energy substrates and that other amino acids can serve as energy or nitrogen sources.
- Restricting glutamine below ~0.3 mM can lead to dramatically increased biomass yields on glutamine. Leveraging this in manufacturing could potentially decrease glutamine's contribution to media costs.
- Lactate formation is strongly influenced by residual glutamine concentration as well as glucose. This helps explain the high degree of variability in biomass yields on the two substrates from various studies.
- Spontaneous degradation of glutamine is a function of temperature and pH, and should be mitigated in manufacturing and accounted for in metabolic studies.

Stoichiometry of carbon dioxide (CO_2) production

CO_2 generation follows from the catabolic fates of glucose and glutamine. Since O_2 is the only substrate involved in this terminal reaction, the rate of CO_2 evolution (carbon evolution rate or CER) is directly proportional to the O_2 uptake rate (OUR). This ratio is typically close to 1.0 and is referred to as the respiratory quotient (RQ).

The RQ can vary with growth rate to some extent but even more so depending on what substrate is being used for energy production. High RQs of approximately 1 indicate glucose is the primary energy source, assuming complete oxidation, whereas an RQ of 0.83 would indicate glutamine catabolism, and an RQ of 0.7 indicates lipid catabolism. However, these values are confounded with growth rate and the degree of oxidation. At low growth rates where glucose is the primary energy substrate, less lactate is produced, which represents a more efficient use of substrate than at higher growth rates. In this case, the RQ may be as low as 0.8-0.9, as some of the oxygen is used for maintenance respiration and NADH oxidation for biosynthetic pathways such as lipid synthesis. At higher growth rates, lactate production rates increase, indicating reduced oxidative phosphorylation and incomplete glucose oxidation. In these cases, the RQ can be greater than 1.2.

From the modeling perspective, the use of RQ offers a convenient shortcut for estimating CO_2 production. Assuming an RQ of 1.0 will not lead to a major error in the calculated rate of CO_2 production. However, if the specific uptake and secretion rates of glucose, glutamine, and other metabolites are available, as proposed in our modeling application, the carbon evolution rate (CER) can be calculated directly using their stoichiometric fates:

$$CER = 6\,q_{GLc} + 5\,q_{Gln} - 3\,q_{Lac} - 2\,q_{Ala} - 3q_{Ser} - C_{biomass}\,X\,u$$ **Equation 3.5c**

Symbol	Definition	Typical units
$C_{biomass}$	Molar content of carbon in dry biomass	mol C/gDCW
$q_{Glc, Gln, Lac, Ala, Ser}$	Specific consumption or production rates	mmol/gDCW/day
X	Dry cell weight concentration	gDCW

If alanine and serine are not included in the model, neglecting these terms should not result in appreciable error since their production is often much lower than the other waste metabolites (Xiu, Deckwer, and Zeng 1999). While CER and RQ can conveniently be measured online for a bioreactor through the use of exhaust gas analyzers, the values obtained by themselves should be used with caution as a clear indication of metabolic efficiency or as a control parameter (Xiu, Deckwer, and Zeng 1999).

Key takeaways and data gaps

- The CO2 released by oxidation is proportional to oxygen consumption. The RQ, which is the ratio between the cell-specific CER and the specific OUR, is typically between 0.9 and 1.2.
- The online measurement of CER and RQ using off-gas analyzers is to be encouraged but should be interpreted along with the other primary metabolites to gain a complete picture of metabolism in real time.
- It is unclear if the presence of CO2 has a significant effect on the stoichiometry of catabolism but some is likely due to its disruption of pH gradients within and around the cells.

Metabolic influence of lactate and ammonia accumulation

Over the years, various phenomena related to the coordinated regulation, metabolic feedback, and cellular control of lactate and ammonia have been observed (see Appendix A3 for further analysis). The degree of the effect can be cell line-dependent and it is recommended that further characterization of these phenomena be performed in CM-relevant cell lines.

For lactate:

- **Feedback inhibition:** Elevated lactate can regulate its own production through glycolysis (Ozturk and Palsson 1991; Cruz et al. 2000; Lao and Toth 1997). Its suppression may decrease lactate yield from glucose ($Y_{Lac/Glc}$) but overall lactate generation may increase. Lactate appears to have only a minor impact on specific rates of glutamine update (q_{Gln}), and the impact on glucose consumption (q_{Glc}) appears to be cell line- or condition-dependent.
- **Adaptive responses:** Cells adapted to high lactate conditions reduced $Y_{Lac/Glc}$ to ~0.39 from 1.4 in control conditions, improving tolerance to high extracellular lactate, productivity, and culture pH stability via reduced requirements for base addition (Freund and Croughan 2018).
- **Culture-stage dynamics:** Cells have demonstrated the capacity to switch from lactate production to lactate consumption during later culture stages, often after glucose depletion (Freund and Croughan 2018).
- **Cross-talk:** Higher lactate levels are correlated with lower ammonia yields, indicating an influence on glutamine metabolism (Miller, Wilke, and Blanch 1988).

For ammonia:

- **Feedback inhibition:** Ammonia yield from glutamine ($Y_{Amm/Gln}$) likewise decreases at high extracellular concentrations of ammonia (Cruz et al. 2000; Ozturk and Palsson 1991; Lao and Toth 1997), with nitrogen being shunted to alanine instead (Miller, Wilke, and Blanch 1988).

- **Cross-talk:** As for lactate, ammonia impinges on glycolytic flux. There is a mild suppression of $Y_{Lac/Glc}$ but overall glucose consumption may increase due to decreased energy yields. Its impact on specific glutamine consumption rates appears to be cell line- or condition-dependent.
- **Adaptive responses:** There is evidence that tolerance to elevated ammonia levels can also occur, but this can take longer than the time of accumulation typical in common batch or fed-batch processes.

These observations suggest that lactate and ammonia are not passive but play active roles in regulating metabolic fluxes, with mechanistic explanations still being active areas of research (Torres et al. 2024). While the forward catabolism of glucose and glutamine can be modeled by the empirical yield equations, accounting for the added layers of interactions and feedback in the backward direction is not as straightforward. Attempting to do so is complex and could quickly become unmanageable. Thus, using an energetics-based model reflecting feedback inhibition of these waste products on energy-producing pathways may be a more tractable modeling approach, as will be discussed in later sections.

The influences of other amino acids on metabolism

Amino acid metabolism is closely tied to the same biochemical pathways that govern energy production and substrate consumption. The consumption and release of specific amino acids depend on the availability of glucose and glutamine and reflect the cell's energy and biosynthetic needs (Mancuso et al. 1998; Cruz et al. 1999). **Table A1.1** in the Appendix summarizes the links between TCA cycle intermediates and groups of structurally related amino acids, highlighting which ones are typically synthesized, consumed, or used for anaplerotic or cateplerotic functions.

In general, essential amino acids cannot be synthesized and must be provided externally, though species-specific differences can exist. For example, most fish and avian species cannot synthesize arginine, while mammalian species are not dependent on its presence in the medium. The nonessential amino acids alanine, glycine, asparagine, and aspartate are often produced and released into the medium. Alanine, in particular, serves as an overflow metabolite and a nitrogen sink. Its production rate can equal or exceed that of ammonium, but it drops significantly in the absence of glucose because it is derived from glutamic acid and pyruvate. Therefore, alanine should perhaps be included in a model for the sake of material balance, but the other amino acids do not typically have a significant effect on growth and metabolism for a given medium.

These patterns shift depending on substrate availability. When glucose or glutamine is lacking, amino acid uptake increases as cells compensate for missing inputs (Mancuso et al. 1998; Cruz et al. 1999). For modelers, it is important to recognize that amino acid metabolism contributes substantially to both biomass formation and energy balance. Interestingly, relatively little of the primary substrates contribute to the carbon content of the cell, confirming their primary role as energy substrates rather than a carbon source. Only 10% of carbon in cell mass is derived from glucose and 20% from glutamine, unless the cell is an adipocyte accumulating lipids. The rest is mainly from the other amino acids provided (Hosios et al. 2016). Understanding this variable stoichiometry is critical from a

bioprocess perspective, as it directly influences key model outputs described in Section 2, including bioreactor productivity and raw material requirements.

3.6 Energy metabolism and the role of energy carriers

Given the complexity and multivariate dependency of the above metabolic and growth processes, many of the papers cited above also present calculations of ATP and NADH generation and consumption as a basis for explaining the various metabolic patterns observed. As noted in Section 2.5, the production of energy carriers and their subsequent oxidation to transfer their energy might offer a better way to account for the metabolic shifts that occur under varying substrate and culture conditions, rather than attempting to model metabolism using strictly empirical correlations. While Section 3.5 focused on the external substrates and waste metabolites, this section delves into what is known of these intracellular substrates and their role in controlling metabolism.

ATP metabolism

Figure 3.6a presents all of the ATP production data that we could find as a function of cell growth rate. While there are a limited number of data sets, the functional relationships are remarkably consistent. The slopes of the trend lines for the three data sets have similar slopes, which represent the inverse of the true (growth-associated) yield (Glacken, Fleischaker, and Sinskey 1986; Dimasi 1992; Miller, Wilke, and Blanch 1989, 1987)(Glacken, Fleischaker, and Sinskey 1986; Dimasi 1992; Miller, Wilke, and Blanch 1989, 1987). Each data set has a distinct y-intercept, representing the cell maintenance requirement (Equation 2.4a) but the three values are roughly within 30% of one another. The data from Ozturk and Palsson are also included but were from a study of the effects of oxygen availability conducted in a chemostat where most of the data points are from steady-state determinations at the same dilution rate and therefore similar growth rates ((Ozturk and Palsson 1990). Thus, no slope or y-intercept could be determined. However, the data scatter falls within the same range as the other studies when normalized by cell mass. Cell mass was not specifically reported in their study, so 271 pgDCW/cell was assumed for this analysis based on the average size of a hybridoma cell.

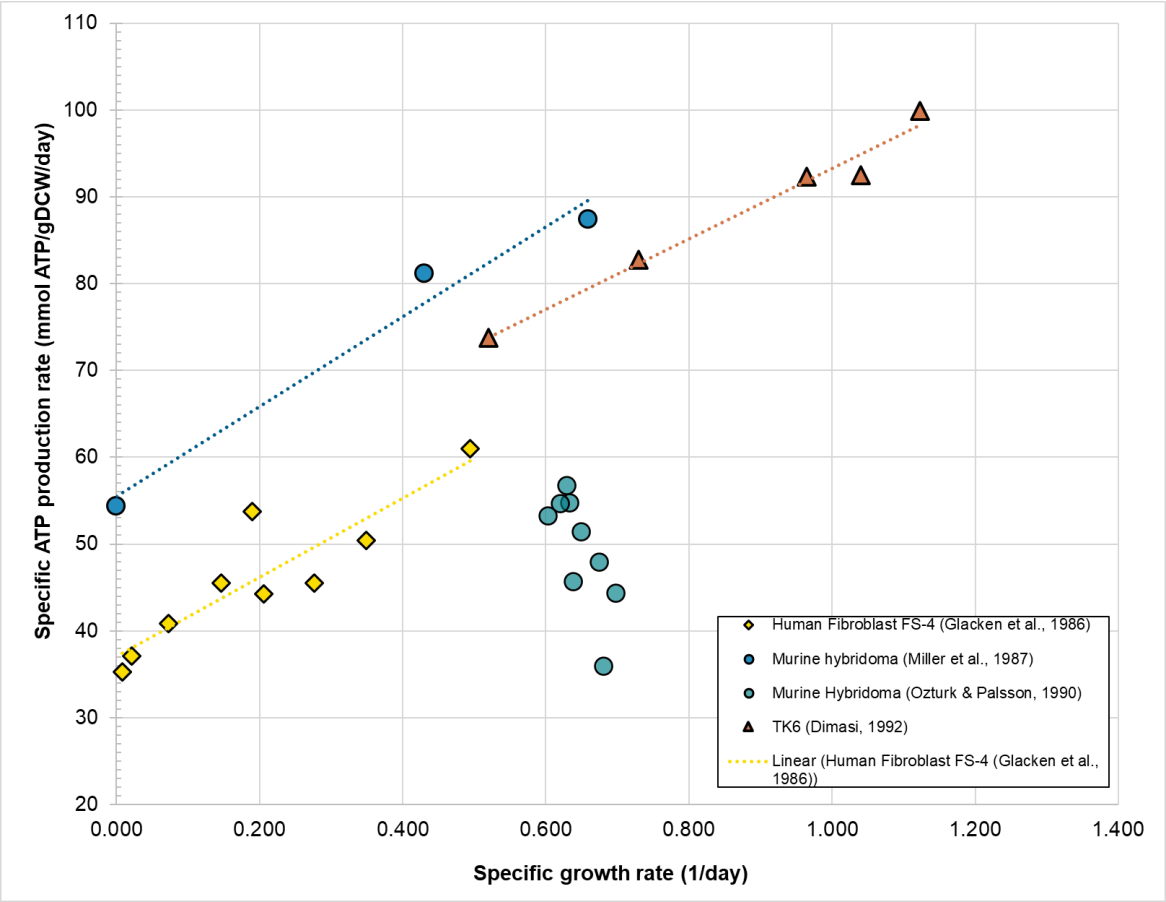

Figure 3.6a: Cell-specific ATP production rates calculated by various authors as a function of growth rate. Calculations are based on observed oxygen uptake rates and metabolite formation rates, mainly lactate. The data from Miller et al. (1987) was a single measurement, but they established an error estimate denoted by the error bar, which overlaps with their later study in 1989.

The yield coefficients determined from this data are summarized in **Table 3.6a**. The true yields calculated from the slopes in Figure 3.6a are indeed very close at approximately 21 gDCW/mol ATP, suggesting that the energy requirement for growth is very similar across these three cell types. The maintenance requirements are not as close to one another but have an average value of 47 $\pm$ 10 mmolATP/gDCW and are clearly non-zero. This difference could be due to different maintenance requirements for the three cell lines or could be partially attributed to the different cell mass assumptions used. However, all three groups apparently measured and reported the dry mass content of the cells they studied.

DiMasi went one step further and measured cell size and mass as a function of growth rate (Dimasi 1992). He observed a significant and strong positive correlation with specific growth rate, which confirms the more qualitative observations in earlier studies by Miller et al. Using the correlation between cell mass and growth rate (shown in Figure 3.2f), each data point in Figure 3.6a was corrected for the actual cell mass at each growth rate. Had this not been possible, the apparent slope would have been significantly higher and is reminiscent of the data for glucose uptake rates at high growth rates measured by Miller (shown in Figure 3.5c above).

Table 3.6a: Apparent and true biomass yields and cell maintenance requirements on ATP (in molar units) from various literature sources. The maintenance terms were deduced from the y-intercepts in Figure 3.6a and the true yields from the slopes according to Equation 3.4a.

Reference	Cell type	Average Apparent ATP Yield Y' x/ATP (gDCW/mol ATP)	Measured or Assumed Maintenance mATP (mmol ATP /gDCW/day)	Actual ATP Yield Y x/ATP (gDCW/mol ATP)
Glacken et al., 1986	Human Fibroblast FS-4	4.90	37.00	19.96
Miller et al., 1987	Murine Hydridoma	5.31		
Miller et al., 1989	Murine Hydridoma	7.55	54.34	21.88
Ozturk & Palsson, 1990	Murine Hydridoma	12.73	45.67	61.61
DiMasi, 1992	TK6	7.32	52.68	24.62
Averages (all cell types)		**7.56**	**47.42**	**32.02**

All the above is consistent with the conclusions of others. Ozturk and Palsson, in their oxygen study, observed that cells obtain ATP at a relatively constant rate of 0.58 µmol per million cells per hour. At the near constant growth rate of 0.645 day^{-1} used in their chemostat study and an assumed cell mass of 169 pgDCW/cell, this production rate translates to an apparent ATP yield of 7.9 gDCW/mol ATP. This apparent yield aligns well with the average value shown in Table 3.6a.

Recall that apparent yield implicitly includes the maintenance requirement as well as the biosynthetic demand for ATP, such that the former is always less than the latter. The large difference between the apparent and true yield coefficients implies that the maintenance requirement represents a significant fraction of the total energy demand of the cells. This is supported by Miller et al., who calculated the fraction of energy metabolism required for non-growth-associated processes (i.e., maintenance) to be 62% of the total specific ATP consumption rate at a specific growth rate of 0.66 day^{-1}. Particularly at low growth rates, animal cells can have maintenance requirements well above half of their total energy demand. This is a hallmark of animal cell metabolism when compared to microorganisms, which have a much lower maintenance requirement and therefore nearly equal true and apparent yields for ATP.

This constant requirement for ATP is supported by studies done with alternative carbon sources. Glacken tested this hypothesis by using galactose and found a consistent 1.7 mmol ATP/gDCW/hr (41 mmol/gDCW/day) as the specific ATP formation rate, whether the human fibroblast FS-4 cells were grown on galactose or glucose at both high and low concentrations (Glacken, Fleischaker, and Sinskey 1986). This constant energy demand was observed despite a much reduced consumption of the substrate and formation of lactate for the galactose case compared to the glucose control.

Interestingly, most of the energy produced with galactose was from oxidative phosphorylation, whereas about two-thirds of the energy from glucose was derived through glycolysis.

NADH Metabolism

Of the several papers that examined the effect of substrate and waste metabolite concentrations on ATP yields, the authors also invoked the role of NADH, another critical energy carrier and reducing agent, to explain observed behavior. A few studies went as far as calculating the yield of this energy substrate based on the consumption patterns (mainly for oxygen) and known catabolic and anabolic pathways active in animal cells. We were not able to find direct biomass yields based on NADH but were able to back some out based on the dissertation of DiMasi, who studied TK6 lymphocytes in continuous culture under several different limiting conditions (Dimasi 1992). When specific NADH consumption (or production) rates were plotted against specific growth rate, the various conditions did not align, and the lines had variable slopes but were relatively flat. Similarly, when apparent yields were plotted against growth rate (**Figure 3.6b,** panel 1), each set of conditions had very different NADH requirements, suggesting that there is no absolute requirement for growth, unlike ATP. Whereas the biomass yields are only mildly dependent on growth rate, likely due to the lack of a discernible maintenance requirement, the biomass yields on NADH do appear to increase with increasing growth rates. When the ratio between the moles of ATP and NADH produced is plotted with growth rate, there is no consistent trend, with yields ranging between 2 to 8.5 mol ATP/mol NADH. However, they do appear to converge at high growth rates toward a ratio between 3 and 5, which is close to the theoretical yield of 3 ATP generated from one NADH molecule. This is likely due to changing relative fluxes between glycolysis and the TCA cycle as growth rates increase.

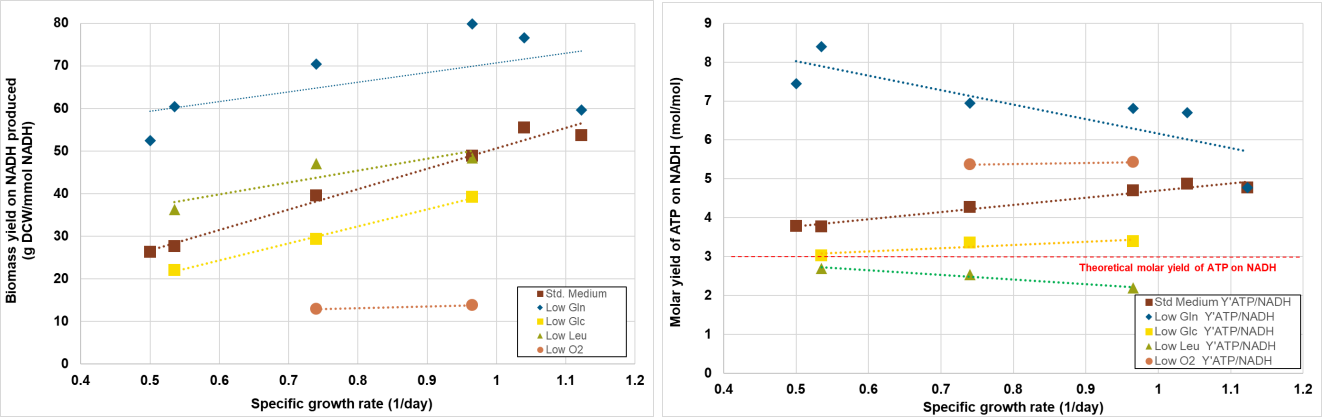

Figure 3.6b: Biomass yields (panel 1) and molar ATP yields (panel 2) on NADH as a function of specific growth rate of TK6 lymphoma cells. Data from (Dimasi 1992). Five conditions were tested in continuous culture at various dilution rates (growth rates): a standard medium with 10.45mM Glc, 3.8mM Gln, 0.382mM Leucine (Leu), and 21% DO (% air saturation); Low Gln, reduced to 0.5mM; Low Glc, reduced to 0.9mM; Low Leu, reduced to 0.0572mM; Low Oxygen, reduced 0.4%.

The effect of oxygen concentration on NADH-based yields sheds further light on the metabolic control of energy production. **Figure 3.6c** shows NADH yields calculated from the specific consumption and production rates observed in studies by Ozturk and Palsson of the impact of oxygen and pH on metabolism (Ozturk and Palsson 1990, 1991). As dissolved oxygen concentrations are decreased, the

production of NADH from glutamine is reduced. NADH levels in the cell increase because they cannot be oxidized, which in turn inhibits any further consumption of glutamine for catabolic purposes. Because less NADH is produced, the energy equivalents need to be produced by other means, primarily by glycolysis, which has a very different ratio of the moles of ATP produced compared to NADH.

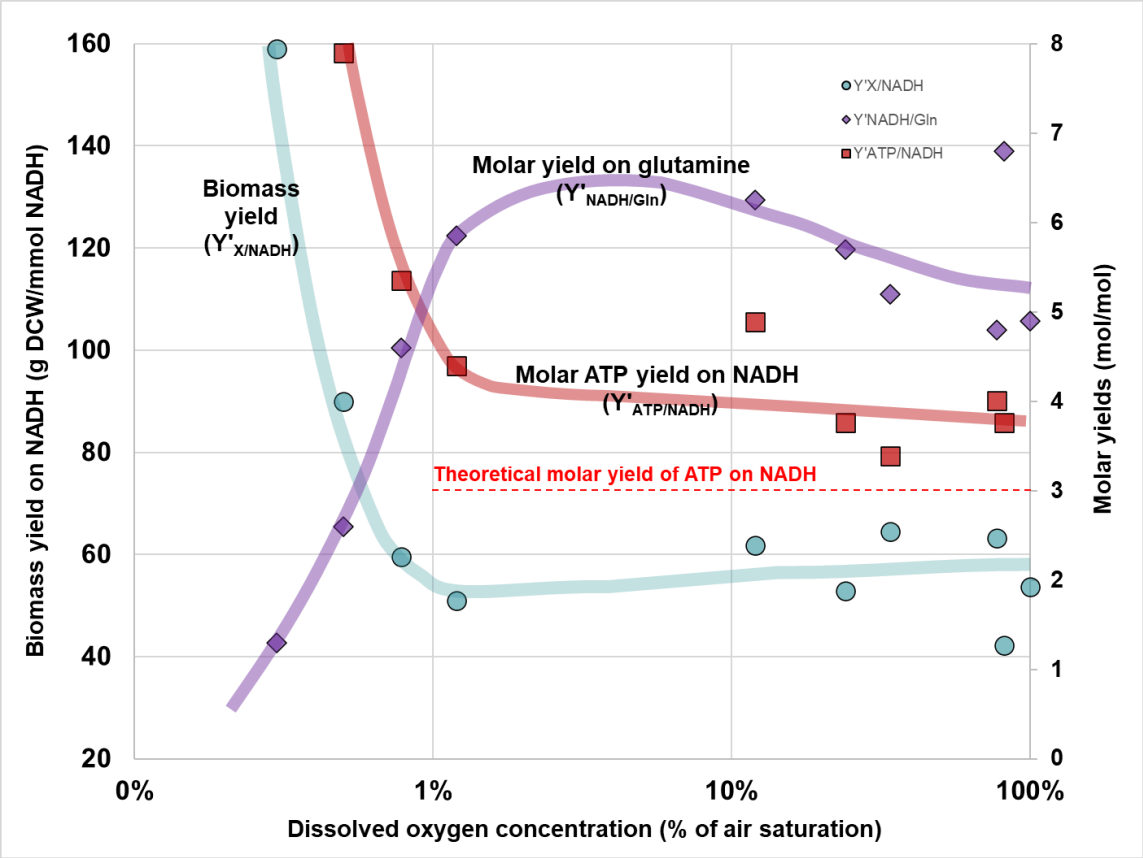

Figure 3.6c: Biomass yields and molar ATP yields on NADH and NADH yields on glutamine consumed as a function of dissolved oxygen concentration ((Ozturk and Palsson 1990)). Interpretation explained in the text.

Consequently, at very low DO concentrations, there is a rapid differential in all parameters noted. The molar ratio of NADH produced per glutamine consumed decreases significantly as DO is dropped below 1%, trending toward zero. Therefore, biomass yield based on NADH rises sharply as does the ratio between ATP molecules produced compared to NADH. However, at DO concentrations above 1%, these metabolic quotients level out as $Y'_{NADH/Gln}$ trends towards 5 and $Y'_{ATP/NADH}$ trends toward its theoretical value of 3.

At the highest point, the NADH yield is approximately 6 moles NADH per mol of glutamine consumed at dissolved oxygen concentrations in the 5-20% air saturation range. Since three ATPs can be reactivated from a single NADH molecule, the total energy yield in terms of ATP would be 18 mol ATP/mol Gln. This would mean that the glutamine is almost completely oxidized through the TCA cycle under these conditions (Ozturk and Palsson 1990).

Key takeaways and data gaps

- The total ATP required to support cell growth is remarkably consistent between cell types under normal conditions when normalized to dry biomass — approximately 8 gDCW/mol ATP consumed.
- A maintenance requirement is evident and thus its ATP's consumption conforms to the semi-empirical model of (Pirt 1965).
- NADH production is not as consistent stoichiometrically and varies with growth rate and the availability of substrates.
- The molar yield of NADH from the consumed glutamine can range from zero to over 8, but tends toward 6 under optimal oxygen concentrations and higher growth rates, indicating that most of the glutamine is fully oxidized.
- The molar ratio of ATP produced to NADH produced can also vary above 3, but also trends toward its theoretical value of three at high growth rates and when sufficient oxygen is present.

Influence of pH on energy metabolism

Since pH is also of interest as a potential optimization parameter, we noted the data from the Ozturk and Palsson study of the effects of medium pH on growth and metabolite kinetics in addition to serum and oxygen concentrations (Ozturk and Palsson 1991). They found that, "medium pH did not alter the cell specific oxygen uptake rates but that ATP production continually increased with increasing pH due to the increased glycolytic activity as measured by glucose uptake rate." This is also supported by the increased lactate-on-glucose yield at higher pH. The yield of NADH on glutamine trended in the opposite direction. Even though glutamine uptake increased slightly with increasing pH above pH 7.2, NADH yield decreased continually over the pH range of 6.8 to 7.8.

It was also noted that oxidative phosphorylation contributed to ATP production at a relatively constant rate over the range of pH studies, except at the lower pH values, when the percentage of this contribution increased. At pH 6.9, cells obtained about 76% of their energy from oxidative phosphorylation, whereas at pH 7.65 this contribution was approximately 25%. Inhibition of glycolysis at low pH is well established and can explain the shift toward oxidative phosphorylation.

Glutamine consumption was at a minimum at pH 7.2, the optimal pH for the growth of this cell line. However, compared to glucose, it was fairly constant. Thus, the glucose/glutamine consumption ratio was a strong function of pH, where glutamine contributed significantly to energy production at low pH. The yields of the other metabolites, including the various amino acids connected to these pathways, were thus affected in a similar manner.

Key takeaways and data gaps

- pH can cause a marked shift in the amount of energy derived from glycolysis compared to oxidative phosphorylation, where the latter is favored by lower pH.
- The impact of pH on energy production is likely related to its impact on proton gradients in the cell and underlies the inhibitory effects of lactate and ammonia.
- Due to these interactions, pH may be an important optimization parameter for future CM processes. The effects of pH and these inhibitors on cellular maintenance requirements should be further studied.

Cellular response to sudden changes in substrate concentrations

In addition to the studies presented above examining the stoichiometry of growth under varying substrate concentrations, a few of the same authors also studied culture dynamics in response to sudden changes. Capturing these transients necessarily required a shorter timeframe. As mentioned, the rate of cellular response is of interest because it may serve as a clue to how cells may react to potential concentration gradients and depletion zones in a large-scale bioreactor. These transient responses also shed light on the regulation of cellular metabolism and energetics. For a rapid change in the concentration of a single substrate, it is useful to observe the associated changes for several of the key substrate and waste metabolites to gauge the approximate sequence of cellular events.

To get a sense of the speed at which animal cells respond to a change in substrate concentrations, the experiments performed by Miller et al. offer significant insight using continuous culture in a chemostat mode (Miller, Wilke, and Blanch 1988). In these studies, once the culture had stabilized at a steady state, the DO concentration was abruptly changed by entering a new DO setpoint into the control system. Immediately after the change, substrate and metabolite concentrations were tracked as a function of time. By keeping the sampling time intervals relatively short, the various metabolic quotients and specific rates could be computed. The study covered DO concentrations from 0.1% to 100% of air saturation with a total culture duration of 25 days (the steady state results were used to generate Figure 3.5a above).

To focus on the transient responses, **Figure 3.6d** covers a time period that spans only two DO concentration transitions: 0.4% to 0.1%, which was the lowest DO concentration studied and induced a severe oxygen limitation, and the change from 0.1% back to 10% DO. As noted in Section 3.3, 10% of air saturation is well above growth-limiting conditions for animal cells. Based on the data points available, we fit a trend line through the points that we felt was a good approximation of the response for each substrate consumption rate and for each metabolite yield. While there are time gaps of about 15 hours when no sample was taken, it is the only data set available with this resolution. Due to the low solubility of oxygen, the control response to a change in DO setpoint would be on the order of seconds to minutes. As can be seen in Figure 3.6d, the most rapid changes appear to be on the order of minutes to hours; however, the resolution post-change was a few hours at best. Nonetheless, the

time profiles do provide an approximation of cause and effect. The two transitions are discussed sequentially below.

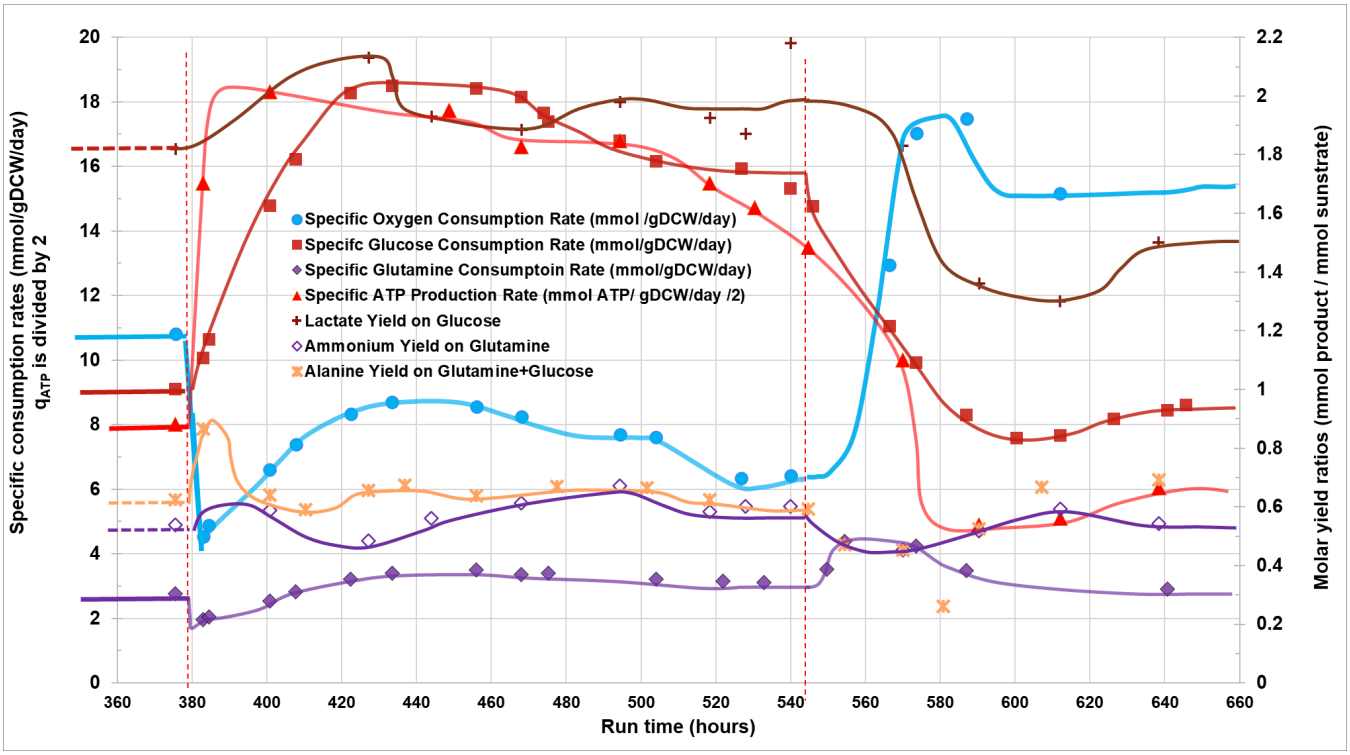

Figure 3.6d: Traces of oxygen, glucose, and glutamine specific consumption rates, calculated ATP specific production rate, and yield factors for lactate, ammonium, and alanine around the transitions in DO concentrations in a continuous bioreactor. The first transition shown in this figure is from 0.4% air saturation to 0.1% at around 380 hours into the run and then from 0.1% to 10% at about 543 hours. The ATP-specific production rate (q_{ATP}) is divided by two to better fit on this graph. Data from (Miller, Wilke, and Blanch 1988).

Sudden transition to growth-limiting oxygen concentrations (0.4% to 0.1% air saturation)

In this case, the DO concentration was already low at 0.4% before the change and thus the lactate yield reactive to glucose ($Y'_{Lac/Glc}$) was already near its theoretical maximum of 2 mol Lac/mol Glc. Once the setpoint was dropped to 0.1%, there was a precipitous drop in specific oxygen consumption. Not surprisingly, due to its low solubility, the oxygen available was quickly used up, which forced a reduction in uptake. Under these conditions of oxygen deprivation, the cells shift to deriving most if not all of their energy from glycolysis because oxidative phosphorylation is not possible through the TCA cycle. This results in a dramatic increase in glucose uptake and in ATP production through glycolysis. Note that the specific ATP production rates were divided by two to fit on the graph. Thus, ATP is being generated at roughly twice the rate of glucose uptake, reflecting the net production of 2 ATP per glucose consumed. Of particular note is that the rise in ATP production rates is almost immediate, whereas the rise in glucose consumption per cell rises more slowly over minutes, initially, to many hours. A maximum is reached in about 50 to 60 hours post-change. There is a spike in $Y'_{Lac/Glc}$ that roughly corresponds with this temporary maximum that is greater than 2.0, meaning that amino acids are also being catabolized through the glycolytic pathways.

The specific consumption of glutamine (q_{Gln}) drops almost as precipitously as q_{O2}, which means that some of the glutamine was contributing to energy production, but if oxygen is scarce, it can no longer be oxidized through the TCA cycle. In general, q_{Gln} follows the q_{O2} trajectory and trends in the opposite direction of glucose consumption (q_{Glc}) because of its dependency on oxygen for catabolism. A rise in residual glutamine concentrations was observed (data not shown) during this transition phase. While both consumption rates drop, q_{Gln} does not fall as far as q_{O2}. It is speculated that biosynthetic intermediates previously derived from glucose must now be provided by glutamine. Increased glutamine consumption at lower values of q_{O2} would be expected to increase the mitochondrial NADH/NAD ratio. This would inhibit a number of the TCA cycle reactions and lead to increased concentrations of TCA cycle intermediates. Such a build-up of TCA cycle intermediates would provide additional precursors for aspartate and asparagine synthesis and might also be expected to reduce the consumption of amino acids that are metabolized to acetyl CoA or TCA cycle intermediates. Higher q_{Gln} also provides more nitrogen for biosynthesis and may be expected to result in higher specific production rates for alanine and ammonia. As can be seen in Figure 3.6d, the average yields of ammonium and alanine are higher at 0.1% DO than they are at 10% DO.

Changes in the metabolism of other amino acids were also noted when oxygen was limited. Additional aspartate and asparagine were produced at low DO due to an apparent increase in TCA cycle intermediates that resulted from the higher glutamine consumption rates required to replace metabolic intermediates previously derived from glucose (data not shown). Miller et al. also speculated that high NADH levels directly inhibit the oxidation of glutamine as well as glycine and branched-chain amino acids (Miller, Wilke, and Blanch 1988).

Sudden transition to non-growth-limiting oxygen concentrations (0.1% to 10% air saturation)

The transition from a condition of oxygen deprivation to one of excess results in a reversal of the responses observed in the previous case. With the sudden availability of oxygen, there is a rapid if not immediate decline in q_{Glc}. The lactate yield ($Y'_{Lac/Glc}$) follows but with a substantial lag, suggesting that glycolysis continues at the pre-change rate for many hours even after the drop in glucose consumption. It only levels out at about 1.5 mol/mol as q_{Glc} also reaches a new steady state. Before this, a minimum in $Y'_{Lac/Glc}$ is observed, which may reflect the increased use of glycolytic intermediates for biosynthesis during the increase in cell concentration. The cell concentration profile is not shown in the graph because the main objective of Figure 3.6d is to show the metabolic interactions, but the cell concentration also varies during these changes in an attempt to balance the nutrient supply rate.

Interestingly, there appears to be a lag in the rebound of oxygen and glutamine uptake (q_{O2} and q_{Gln}) after the sudden increase in DO. Despite the availability of oxygen, the uptake of oxygen and the catabolism of glutamine appear to be inhibited, perhaps because of the high ATP production rates and its availability. During this phase, glutamate yields were seen to increase (data not shown) transiently when q_{Gln} increased in response to the increase in the oxygen supply, and then decreased at the 10% DO steady state. Glutaminase is activated by many effectors, including ATP, which could explain the

initial increase in q_{Gln} at 10% DO. Also, the maximum in q_{O2} lagged behind that of q_{Gln}, which illustrates the buffering effect of the TCA cycle and connecting pathways.

In general, specific ammonia and alanine production rates follow those of q_{Gln}; however, there are more pronounced oscillations in the yields of both end products around the transition points. The increase in q_{Amm} lagged behind the other two and the overshoot for ammonia is larger than that for glutamine. These differences between q_{Gln} and q_{Amm} indicate that the fate of glutamine is changing during the oxygen transients. The dip in ammonium and alanine yields after the increase to 10% DO suggests that much of the nitrogen from glutamine was being used for biosynthetic reactions in preparation for rapid cell division.

The yield for alanine shown in Figure 3.6d is the sum of the yields calculated for the alanine produced from glucose as well as glutamine. Notably, the production of alanine is at least as prevalent as the production of ammonium and, therefore, from a material balance perspective, should be included in modeling efforts. In fact, on average, the total alanine produced is 20% higher than ammonium, indicating that the pathway via transamination of pyruvate is a significant one. The generation of alanine from glucose is roughly a third of that produced from glutamine but is not insignificant. It may be worth noting that the portion of alanine generated from glucose rose from roughly 27% of the total at 0.1% DO to an average of 41% when the DO was increased to 10% air saturation, probably as a result of the generally higher glycolytic flux when oxygen is not limiting growth.

In a similar set of studies, Miller et al. also measured changes in metabolism in response to sudden changes in glucose (Miller, Wilke, and Blanch 1989). These studies are instructive in showing the control over energy production. Also, measurements were done on a shorter timescale than the ones described above for the oxygen concentration study and thus give a better sense of the speed at which animal cells respond to a change in substrate concentrations. **Figure 3.6e** presents the results of a glucose pulse experiment where the concentration was abruptly increased in a chemostat from a residual concentration of 0.1 mM to 6.6 mM. At the pre-pulse concentration (0.1 mM), the culture was almost certainly limited by glucose. Various metabolite yield coefficients are plotted to show the timing of their response as the glucose falls with washout following the sudden increase. Only those species that showed a significant shift are shown in the figure.

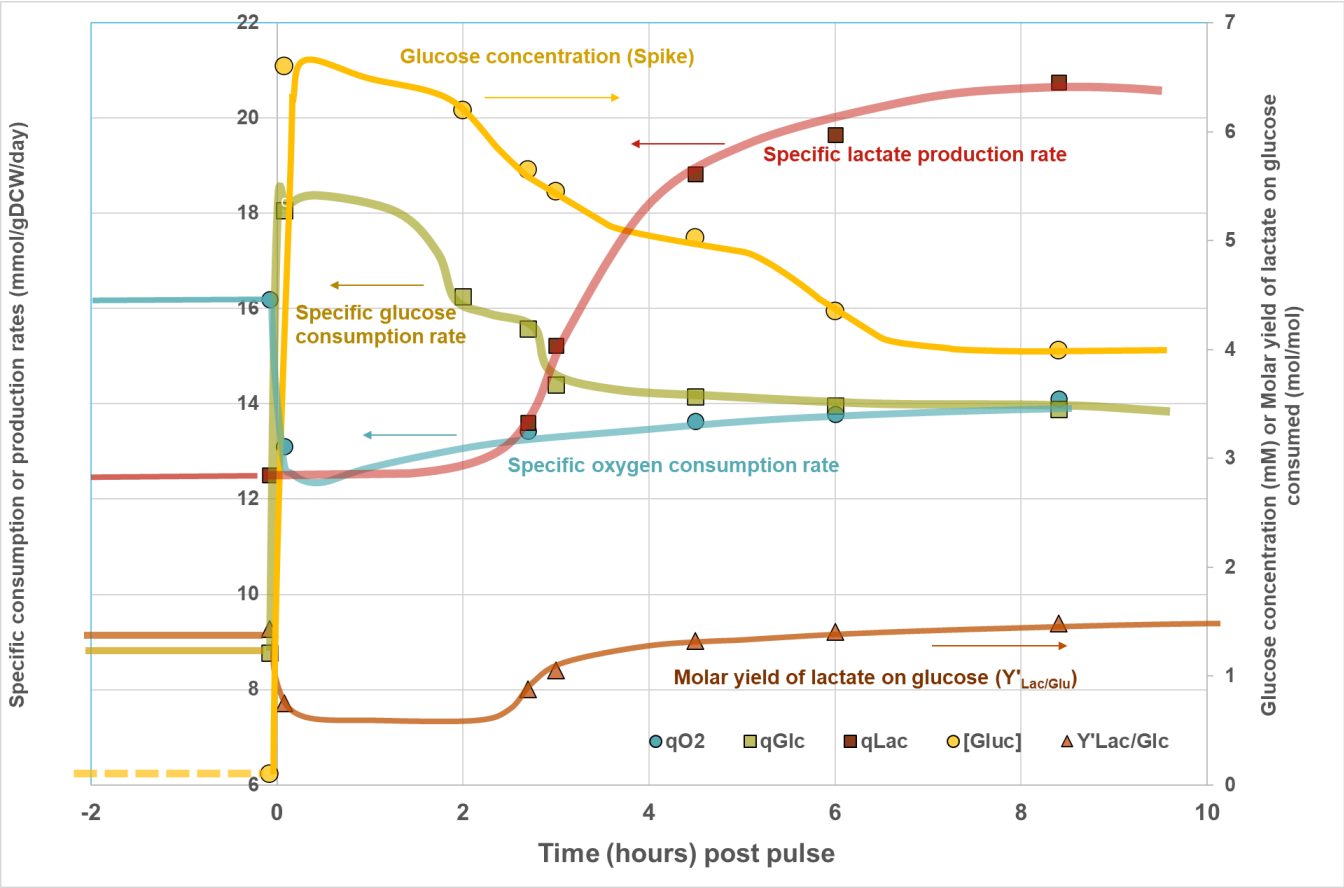

Figure 3.6e: Response of a murine hybridoma cell line in a continuous culture to a pulse change in glucose concentration. The simultaneous response profiles of glucose concentration and the specific rates of glucose and oxygen consumption and lactate production are superimposed. Data from (Miller, Wilke, and Blanch 1989). ATP production rates are not included in the graph because they were relatively constant during this experiment, except for a slight dip immediately after the pulse.

The specific glucose consumption rate (q_{Glc}) increased by 100-200% immediately after glucose was added to the reactor (t=0). This response was on the order of minutes if not seconds; the time resolution of the experiment was inadequate to distinguish absolute response rates. Concurrently, there was an immediate decrease in the specific oxygen consumption rate, followed by a slow climb to pre-pulse levels over the course of 40-50 hours. The sudden drop in oxygen consumption occurred even though plenty of oxygen was available and total ATP production also appeared to experience a short dip before regaining its original rate after about 8 hours. The authors attributed this response to a shift from oxidative energy production to increased glycolytic ATP production.

As expected, the specific lactic acid production also increased after the pulse but lagged behind the immediate increase in q_{Glc}. This can explain why the specific ATP production rate was below the pre-pulse value during the first few hours (data not shown), because the initial increase in glycolytic ATP production was not immediately sufficient to offset the decrease in q_{O2}. However, it should be noted that ATP and NADH were not measured directly in these experiments. They were calculated from the consumption rates of the other substrates (primarily oxygen) and the production rates of

lactate and ammonium. Therefore, if there is a lag in their response to changing conditions, the response of energy metabolism may appear to be delayed.

Interestingly, the lactate-on-glucose yield in the above glucose pulse experiment was at first inhibited to almost half of its prior value (1.43 to 0.75 mol Lac/mol Glc) and took several hours to regain full glycolytic activity. While glycolysis and oxidative phosphorylation are both major sources of ATP production, their relative importance depends on the cell line and growth conditions. At high glucose concentrations, the oxidation of glucose, glutamine, and other amino acids is inhibited and glycolysis accounts for a majority of the ATP generated. Glucose oxidation via the TCA cycle is always low, but at low glucose concentrations and for sugars other than glucose, most of the ATP generation has been attributed to glutamine oxidation (Miller, Wilke, and Blanch 1988).

Key takeaways and data gaps

- The above works by Miller et al. (1988 and 1989) are good examples of how the dynamic control of metabolism can be determined in real time.
- More experimentation like this, with greater time resolution, is needed to give a more accurate determination of response times.
- Such studies can give important clues to how cells may behave in a bioreactor with heterogeneous conditions, as well as provide meaningful insight into the dynamics of cellular metabolism.

3.7 Summary and discussion

We have concluded a comprehensive review of the foundational scientific literature from the 1980s to the present of what is known about the growth and metabolism of animal cells. Starting with the cells in Section 3.2, we reviewed available data on cell composition for as many cell types as we could find, including some that are relevant to CM. By virtue of its composition, cell type is a key determinant of the final CM product's nutritional profile. Its mass, more specifically its dry mass, is what ultimately defines output and cost, but there is little data available, even less so for CM-relevant cell lines. In fact, it appears that recent CM TEMs overestimated the mass of a typical cell, as size does not correlate directly with mass (Figure 3.2c). Furthermore, not only do cells of different types vary in mass and size, the same cell line's size is a significant function of growth rate (Figure 3.2f).

Cell type also informs the maximum specific growth rate, which is a function of temperature and pH. In Section 3.3, we reviewed what is known about the kinetics of cell growth and death with respect to these major control variables as well as the availability of substrates. Unfortunately, very little data was available on cells undergoing differentiation. Monod constants, used to quantify the reduction in growth rate as a substrate is depleted, varied by over an order of magnitude for the same cell types. This variability is likely due to a number of factors, including serum concentrations and mode of culture as well as temperature and pH. These half-saturation constants appear to be different for similar cell types grown under batch or continuous conditions, suggesting a time factor. Apparently, there can be multiple transporters, each with a different affinity for the same substrate, and that may be expressed under different conditions (Bosdriesz et al. 2015). Stationary versus suspension culture also seems to affect the growth kinetics.

The direct effect of waste metabolites on cell growth and death was reviewed in Section 3.4. Almost all the experiments attempting to quantify the degree of growth inhibition or death rate as a function of the metabolite's concentration were done under conditions of acute and sudden exposure through the spiking of various concentrations of the inhibitor. We now know that the IC50s determined from such studies likely overestimate the inhibitory properties of the metabolite. The individual conditions were not always adjusted for osmolality as a result of the addition of the biochemical as a salt and the resulting pH differences. Both of these can affect growth rate in addition to the metabolite being studied. More exciting is the observation that cells can better tolerate these inhibitory substances if they are given the time to adapt, suggesting genetic-level regulation and an opportunity to mitigate inhibitory effects.

In Section 3.5 on the stoichiometry of growth, we found that the quantitative consumption of substrates and the associated formation of inhibitory metabolites are highly variable. The complex coordination of glucose and glutamine uptake is a function of their availability (i.e., their concentration in the extracellular medium). The variability in their consumption also leads to a highly variable output of lactate and ammonium. However, this dependency can be used as an advantage. Ljunggen and Haggstrom showed that when both glucose and glutamine are restricted, the hybridoma cells displayed an even higher metabolic efficiency than if either substrate was restricted individually (Ljunggren and Häggström 1994). Similarly, Kurokawa et al. found biomass yields ($Y_{X/Glc}$) increased

more than two-fold for glucose, and lactate was reduced by one-third, seemingly as a result of intracellular lactate dehydrogenase (LDH) activity being halved (Kurokawa et al. 1994).

The coordinated consumption of these primary energy substrates is also closely tied to the energy status of the cell, which can be represented by the intracellular concentrations of the primary energy carriers ATP and NADH. As the end products of catabolism, these energy carriers, along with lactate and ammonia, control their generation through direct feedback inhibition of major biochemical pathways by direct interaction with the allosteric enzymes that catalyze them (see Figure A1.2 in Appendix). Thus, substrate concentrations dictate how they and the products of their catabolism are consumed.

Animal cells generally have a higher maintenance energy requirement than microorganisms, but energy generation is exacerbated by the Warburg Effect, which further increases substrate demand due to incomplete oxidation. However, a key finding during this review is that cells of very different lineages appear to adjust their utilization of metabolic pathways to maintain a constant q_{ATP} even under varying nutrient conditions. Thus, using a fixed energy demand provides a unifying currency on which to base mathematical models of substrate utilization.

Still more needs to be understood about the Warburg Effect but the leading hypothesis for its origin is that it allows cells to grow more quickly. More recently, there is evidence that the mitochondria themselves are involved. They may be altered biochemically, up- or down-regulated in terms of the number per cell and the speed at which active transport systems can shuttle key metabolites between the mitochondrial millieux and the cytoplasm (Martins Pinto et al. 2023; Bouchez et al. 2020).

Together, all the above mechanisms reveal how animal cells flexibly regulate substrate use based on the demand for ATP, redox balance, and biosynthesis. This multidirectional and multifaceted control system is a consequence of many interactions. Taking the Warburg Effect as an example, there appears to be a time element, possibly involving transcriptional and translational controls. On the shortest timescale, these interactions are nowhere more evident than in the perturbation experiments mentioned in Section 3.5, where certain metabolites or substrates are suddenly spiked into a culture. The speed at which cells respond gives an indication of the more immediate control mechanisms. Responses on the order of seconds can only be accomplished by enzymes either through allosteric control, direct competition, or inhibition of substrate binding (i.e., Crabtree effect). However, responses on the order of minutes may be controlled by diffusional or transport limitations or the time it takes internal reservoirs of certain metabolites to be depleted or replenished.

Amino acid metabolism, while not the central focus of this review, is closely tied to the same biochemical pathways that govern energy production and consumption. As noted in Section 3.5, the consumption and release of specific amino acids depend on the availability of glucose and glutamine and reflect the cell's energy and biosynthetic needs. When glucose or glutamine is lacking, amino acid uptake increases as cells compensate for missing inputs *(Mancuso et al. 1998; Cruz et al. 1999)*. In general, amino acids contribute substantially to both biomass formation and energy balance. There may be instances where their inclusion in a model mechanistically would be of interest, however, their respective consumption or accumulation extracellularly appears to be relatively consistent for a given medium.

Section 4. Challenges and opportunities for cell growth modeling

In support of the original objective of this work, Sections 2 and 3 set the groundwork for the construction of more predictive models of animal cell culture process performance, which in turn can better inform experimental work in cultivated meat and future TEMs. Our review led us to conclude that predictable, scalable, and cost-effective processes are within reach through integrated modeling.

4.1 The case for modeling to support bioprocess design and TEMs

A unique aspect of this proposed model system is that it is aimed specifically at bioreactor-based process development and scale-up. This application lies at the intersection of cell behavior, media optimization, and bioreactor design and operation. Most modeling applications cater to one or the other but not both. Our approach to join a Cell Model with another model representing the physical aspects of a bioreactor and its control system (Figure 1.3) means that overall complexity needs to be managed from the perspective of both the level of technical input required and the computational demands.

As mentioned earlier, we believe that no single model can satisfy all future needs as CM technology continues to develop. As much as we would like to establish a single definitive approach to modeling cell behavior in bioreactor systems, the needs of the industry are sure to change as the anticipated variety of CM and hybrid products approach commercialization. However, the core model of cell behavior, we believe, can be based on the concepts reviewed in this paper.

Unfortunately, due to the large number of interactions identified in this review, a purely empirical model does not seem practical. To model such a system empirically, a functional relationship would be required for at least the most prominent interactions. Such a model is likely to quickly become intractable if it includes all the necessary details to be predictive. However, by invoking energetics and specifically the role of ATP and NADH, a more mechanistic depiction is possible. The observation that biomass yield across multiple cell types can be based on a constant energy input is unifying. The moles of ATP required for cells to grow and maintain homeostasis provides a basis for normalization even though the consumption of the primary carbon and energy substrates vary widely. Thus, using energetics may be a more manageable way of accounting for metabolic shifts than relying on empirical functions describing specific substrate consumption based on various factors. We believe this key observation will allow a model to be constructed without resorting to very large reaction networks as those used in metabolite flux models.

This underserved need will require careful balancing of complexity with predictive ability. This balance may be different between specific applications but the ultimate yardstick is whether important process trade-offs can be evaluated to enable comparison of performance-to-cost ratios (PCRs) and assessment of the impact of various cost drivers as they relate to overall performance.

As examples, the following questions illustrate the type of performance and cost trade-offs that could be supported by the appropriate model.

1. Should all nonessential amino acids be included in the growth medium in addition to the essential ones or does the elimination of expensive ones outweigh the sacrifice in maximal growth rates? The current belief is that their reduction or elimination would be counterproductive. Maximal growth rates would likely be lower and additional inhibition may occur because of the cells' increased ammonium production due to their reliance on glutamine to support the synthesis of these amino acids for protein formation.
2. Do changing factors such as pH, temperature, and osmolality benefit physical bioreactor performance that may outweigh a deviation from the optimal conditions at small scale?
3. What type of bioreactor is best suited to proliferating cells in a suspension mode? An airlift bioreactor may have a somewhat lower volumetric productivity but a higher PCR (at the bioreactor level) due to its lower fabrication cost. It could require higher gas input to provide comparable motive force for mixing and aeration (i.e., higher utility costs) and may require greater structural support in its installation, lowering the PCR at the facility level (Table 1.1).
4. A bioreactor designed for suspension culture is unlikely to be the best choice for differentiating cells into a tissue in a stationary matrix. Cell-type dependencies will also be factors, with some companies developing custom bioreactors for adherent fat cell culture as a means to avoid their buoyancy issues in suspension.
5. Different reactor designs or materials of construction may have different setup, sterilization, and/or cleaning requirements. When comparing such designs, cycle-averaged volumetric productivities should be compared, which account for the differential durations of these operations when the bioreactor is not actively producing product.

The digital twin

Digital twins are already in development and used in the biopharmaceutical sector (Ranpura et al. 2025), and they can offer a clear opportunity for CM to accelerate development while minimizing risk. These tools enable predictive modeling, reduce experimental burden, and help identify failure points early in process design. Given the scale required for CM to reach cost targets and compete with conventional meat, relying on trial-and-error or isolated experimental results is not a viable approach. Several companies have already faced setbacks after scaling too early without a sufficient understanding of process constraints. These outcomes highlight the importance of integrated modeling approaches that reflect the complexity of real production systems.

The construction of useful digital twins will necessarily be an evolution, but the alternative is to proceed by trial and error. Given the scale and cost of the required bioreactor systems, such an approach could discourage further investment if it is deemed high-risk. We are not advocating for a blind trust in such models. Rather, we encourage an iterative process whereby initial models are gauged against real-life data to build confidence in their predictive capabilities and to incrementally improve them.

Harnessing artificial intelligence

The emergence of artificial intelligence (AI) and machine learning offers an unprecedented opportunity for model development and improvement. Perhaps even more exciting is harnessing AI to streamline experiments needed to determine model parameter values. There is already a precedent in the biopharmaceutical industry over the last five years of deploying such hybrid digital twins to help identify the most important factors influencing a process's overall performance. Mathematical models have already been coupled with machine learning to augment predictive power and assimilate new data. This has the potential to shorten the time and work required to define process design space as well as to speed the design and scale-up of cost-effective bioreactors desperately needed by the emerging CM industry.

By interpreting data patterns and shedding light on the underlying phenomena, hybrid models have the potential to guide the development and optimization of the tools needed for the development and deployment of CM manufacturing infrastructure and ongoing TEAs. In this way, they can accelerate their own evolution. Going forward, the number of models in the toolbox may also have to be expanded as new innovations arise and to fully understand the major cost drivers, including overall metabolic efficiencies, feed conversion ratios, and waste product generation.

4.2 Choosing the appropriate modeling tool

Computational modeling can serve several needs in designing bioprocesses and evaluating their economics. However, the model used should depend on the objectives of the practitioner. The model most appropriate for an engineer designing a novel bioreactor will not be the same as the one used by a process scientist developing the bioprocess or by a molecular biologist creating a new cell line. The best model will allow quantitative evaluation of the parameters of interest with sufficient accuracy to be predictive without resorting to overly burdensome computational and/or theoretical complexity. For example, modeling can also be applied to the development and optimization of cell culture media that consist of many components. While not the focus of this review, the latter application can be served with genome-scale metabolic models and multi-component metabolic flux analyses (Gomez Romero, Spielmann, and Boyle 2025). However, such a model will likely be too intensive to couple to the evaluation of bioreactor design or how best to operate it. It is imperative to match the application with the model of appropriate complexity such that the model serves the application rather than the other way around.

Types of models

Figure 4.2a depicts the different types of models with respect to both their mathematical complexity and computational intensity. These model type definitions are well established in the biochemical engineering field; the reader is encouraged to read published reviews that discuss the multi-scale aspects of biological systems (Schaffer and Ideker 2021). As an overview, there are empirical models and mechanistic ones that require an understanding of the underlying principles governing a cell's behavior. However, a model can make use of both approaches. In the modeling context, a structured

model regards a cell as having a distinct boundary and distinguishes intracellular components and processes from extracellular ones. Actual cell size may or may not be accounted for.

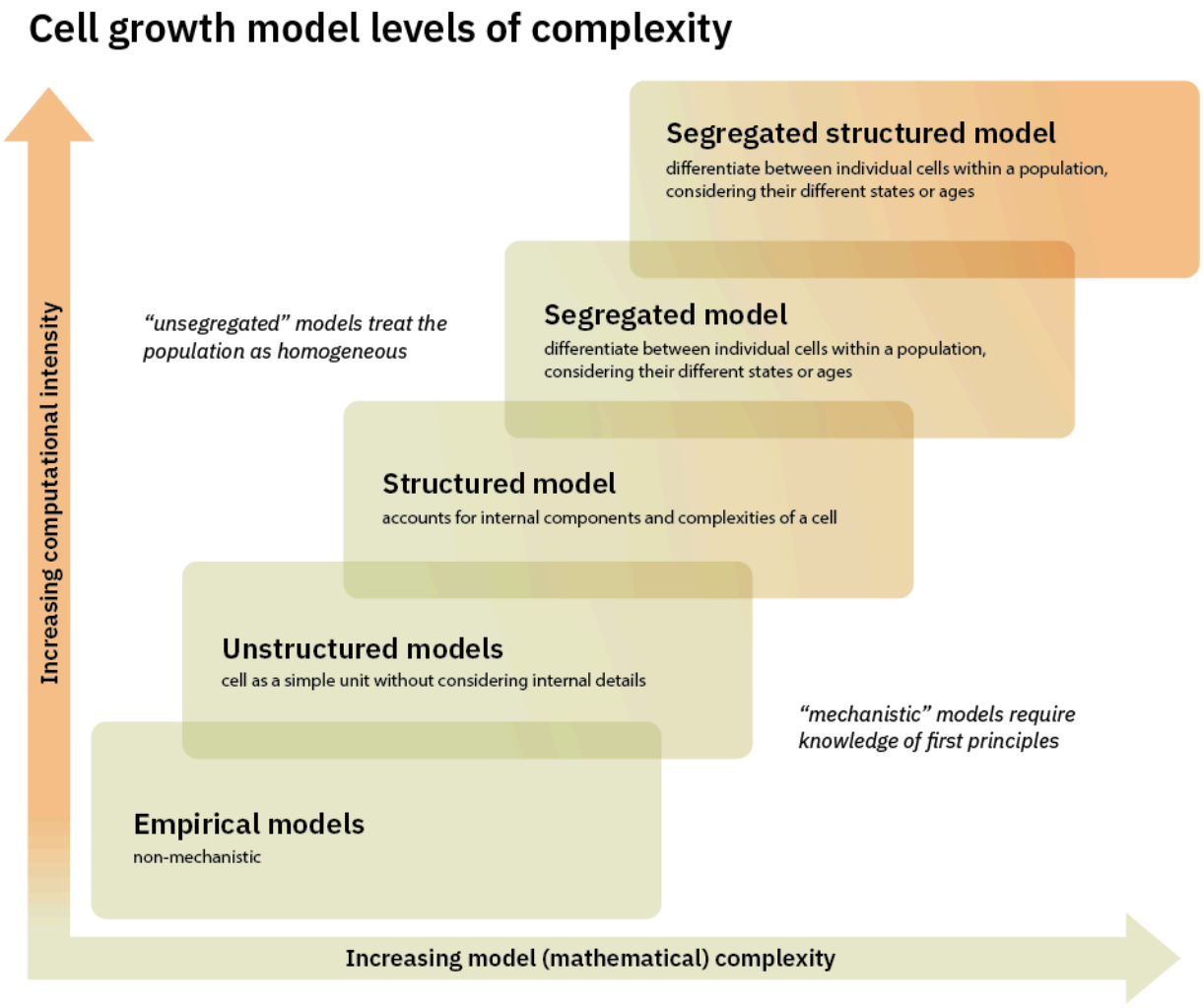

Figure 4.2a: Relative mathematical complexity and computational intensity of different biological model types.

Segregated models are less common but are used when there are different cell populations with respect to one or more characteristics. This is a stochastic approach to account for shifting distributions of cell phenotypes and even genotypes depending on the application. For more complex applications, these two model types can be combined. But in general, segregated models are more complex and use statistical principles, while structured models are less intensive. However, this depends on how many components are included and whether they are media constituents, internal metabolites, specific enzymes, and/or cellular compartments.

Empirical models

In simpler applications, empirical models such as the ones reviewed in this study may suffice. A model may be able to predict the impact on substrate consumption as growth rates vary and/or simulate responses to the concentrations of a single limiting substrate. It could also be argued that most CM

applications would strive toward maximum growth rates to generate biomass as quickly as possible. Thus, modeling growth and metabolic effects at low growth rates may not add much value. However, it will be important to understand that their application is relevant to a limited set of conditions.

Empirical models require data sets that cover the range of conditions in which they will be deployed. The model will need to be fit to the data using arbitrary mathematical functions because these relationships are not founded on first principles. However, some of the relationships outlined in this report can serve as a starting point for testing model construction and a scaffold for summarizing the relationships found.

While many of the functional relationships described in this review can certainly be modeled empirically, the overall model for a bioreactor process will likely become too complex due to the many interactions involved. Furthermore, circular dependencies representing feedback mechanisms may lead to computational or numerical instability and may become problematic in terms of ensuring mass balance closure. Thus, moving toward a more mechanistic approach using structured biological models may well be preferable to adding non-intuitive complexity to an empirical model.

Structured models

Empirical models cannot predict outcomes if other cellular processes are involved and/or the conditions are outside the range characterized because they are not mechanistic. Structured models, on the other hand, can account for some of the cell's dynamic behavior by separating intracellular and extracellular substrate or metabolite species. This decouples substrate uptake (usually by active transport) from substrate utilization. Building an internal reservoir of a certain substrate or metabolite makes the cell less responsive to external concentrations over shorter time frames. This depiction is closer to reality because intracellular pools of metabolites can continue to support cellular processes for a certain amount of time, even though the extracellular environment may have suddenly changed.

Also, where growth limitations can occur with more than one substrate, we have found that the typical semi-empirical model of a yield coefficient and a maintenance term does not apply. Therefore, where there are complex feeding strategies and/or trade-offs in raw material consumption, such simpler models will not be sufficiently predictive. Treating key intermediates, including energy carriers, as a global species (i.e., as an average concentration across the cell culture milieu) is meaningless unless presented as a ratio to cell mass or volume concentration. Representing them instead as internal constituents is more mechanistic and intuitive. An example of an energetically structured model is presented in Section 4.3.

Metabolic flux models

Metabolic flux analysis, including flux balance analysis, has proliferated extensively over the last 20 years due to the parallel advances in computational power and multivariate algorithms. In essence, models using these techniques could be classified as structured models since they usually refer to many intracellular constituents in order to simulate the cell's internal environment. Because they can simultaneously represent many parallel reactions, they are well-suited to the design of media that typically have many components. However, these models are complex, have many parameters, and

are likely not well suited to couple with a bioreactor model other than the simplest possible representation. While these types of models were not the emphasis of this review, the reader is encouraged to leverage the abundant literature on this subject if earlier stage development is the focus of their work (Quek et al. 2010; Gomez Romero and Boyle 2023; Sacco and Young 2021). A recent review offers a comprehensive view of the state of the art. The review is focused on CHO as the workhorse of the biopharmaceutical industry but it can serve as a roadmap for CM process development (Ranpura et al. 2025).

Segregated and cell memory models

To explore new bioreactor designs and the limits of their performance, the industry needs models that can account for spatial and/or temporal variations in conditions. An example where a segregated model may describe a CM application is in cell differentiation, in which cells may be at various discrete stages (phenotypes) along the way to a terminal state. Another application may be in simulating the different zones in a bioreactor. As a cell traverses the environs of a very large-scale bioreactor, it will experience different extracellular conditions and media concentrations. The degree to which cells react to these changes will influence the bioreactor's overall productivity. Thus, understanding the rate of a cell's response to these changing conditions may be important when simulating such an environment.

Part of a cell's transient response to changes in its environment can be represented by structured models. However, there may be instances where certain conditions have a cumulative effect on a cell. This response can be viewed as a memory effect and would apply to only those cells exposed. Accounting for varying populations of cells falls into the segregated model category. How such cell memory models will be constructed is beyond the scope of this review but there is some precedence in the literature on microbial systems that could be leveraged (Amirian, Irwin, and Finkel 2022). Also, the adaptation response of cells to more extreme conditions may require accounting for the genomic responses to changing environments. These responses may be on a longer time scale but are important for exploring adaptation strategies to high-waste metabolite concentrations, for example.

Similarly, it may be desirable to understand the impact of various bioreactor design scenarios on performance. Can less intensive agitation (i.e., longer mixing times) be tolerated without appreciable deterioration of performance, particularly in light of the potential adverse effects of hydrodynamic shear on cells? Structured and/or segregated models may be better equipped to predict the effects of bioreactor scale and design on cell culture processes. These types of models will be further explored in subsequent work that will address the heterogeneous environments of a large-scale bioreactor.

Hybrid models

There is no limitation as to how or which model types are employed for a given application. Model types can be combined to address different aspects of the process and/or cell response. Such hybrid models are not restricted to formal mathematical equations. Combining mechanistic models with AI algorithms, as mentioned in Section 4.1, offers additional opportunities to represent complex design spaces as well as guide process scale-up and the determination of scale-relevant parameters.

However, while structured models combined with AI offer real potential, that potential will only be realized if models are trained with high-quality data.

4.3 Using structured energetics to model cellular metabolic control

We have seen that a cell's ATP requirements do not change appreciably over a wide range of conditions as long as the cells are not under stress. Furthermore, the role of NADH is also important in explaining metabolic patterns and its complementary role to ATP's in cellular energetics. A hallmark of animal cell metabolism is the coordinated consumption of glucose, a carbohydrate, and glutamine, an amino acid, for both energy production and anabolic processes. The depletion or abundance of one influences the metabolism of the other. Their relative importance appears to vary with cell type as well as other factors such as their physical environment, including temperature and pH. From these observations and careful study of the catabolic pathways, we conclude that a structured model based on cellular energetics is the most promising for future CM applications.

As a concrete example, we describe the model proposed by DiMasi and Swartz (DiMasi and Swartz 1995). Although such models were first described about 30 years ago, few models have been developed since that attempt to simplify the mechanisms of mammalian cell growth and metabolism to be tractable for bioreactor design and simulation without resorting to complex metabolic flux analyses involving many equations representing tens of metabolic pathways. Batt and Kompala's model was adapted from microbial systems modeling and was one of the first to represent glucose and glutamine as partially substitutable precursors of various pools that comprise the cell mass (Batt and Kompala 1989). Their model is briefly described in Appendix A3. DiMasi and Swartz built on this and the Cornell single-cell model (Wu, Ray, and Shuler 1992), where glucose and glutamine are substitutable precursors and contribute to intracellular metabolite pools. They postulated that only a model that is structured based on energetics can describe the coordinated substrate utilization and concomitant oxygen consumption in animal cells, which are of primary interest in designing culture media and in developing bioreactor technology and feed strategies.

The interested reader is referred to (Dimasi 1992) and (DiMasi and Swartz 1995) for a comprehensive description of the model's construction and inherent assumptions, but **Figure 4.3a** is offered as an overview of the model's structure. Instead of using the four main macromolecular precursors (amino acids, nucleic acids, protein, and lipids) as in Batt and Kompala's model, they structured their four-component model on monomer pools, including ATP and NADH. They defined four internal pools of pseudo-metabolites: (1) precursors associated with the glucolysis of glucose to pyruvate (G_i), (2) precursors associated with glutaminolysis of glutamine (Q_i), and the energy carriers associated with (3) ATP cycling (ATP_i) and (4) NADH cycling ($NADH_i$). These are pseudo-metabolites because they do not represent the concentration of a single metabolite but an average of many. For example, ATP_i represents the actions of AMP, ADP, GDP, etc. in addition to fully charged ATP. The low-energy forms of these carriers are known to also regulate pathways by activation of energy-producing pathways, but to simplify the model, these interactions are represented by feedback inhibition of a single pseudo-metabolite (ATP_i) instead. Here, the use of ATP_i avoids using the adenylate energy charge described earlier.

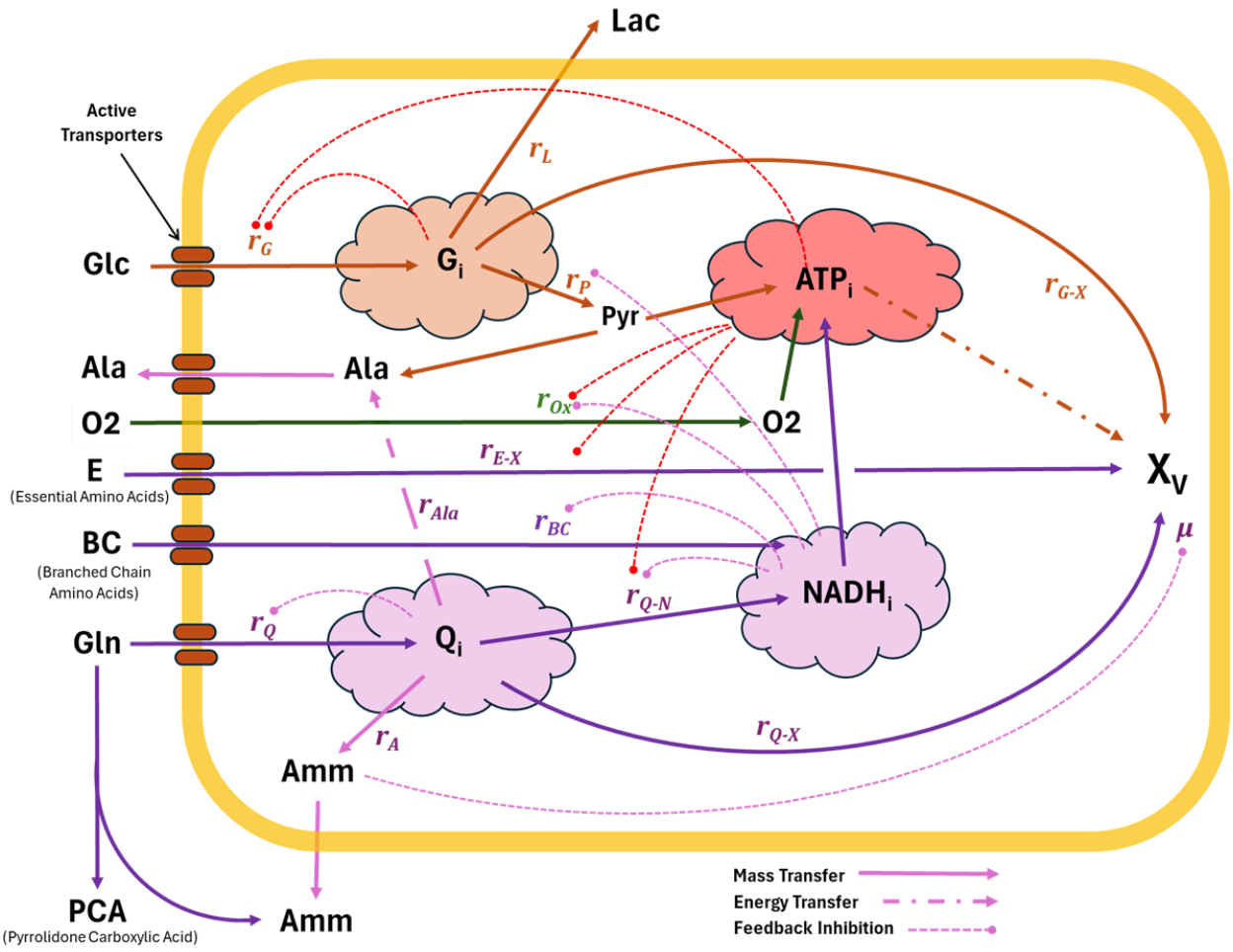

Figure 4.3a: Diagrammatic representation of the Energy Structured model of DiMasi and Swartz (1994). Solid lines represent a transfer of mass such as transport of a substrate or a reaction. Dash-dot lines denote energy transfer and the thin dashed lines indicate feedback inhibition on a reaction.

In the diagram, reaction rates are indicated with the small letter r with a subscript identifying the pathway. Many of these rate expressions include a Monod–type factor representing the availability of the reactant. Feedback inhibition, indicated by the dotted lines, is expressed as reverse Monod expressions using an exponent of 4, similar to those described earlier to simulate a sharper control action.

Representations for both ATP and NADH were incorporated since they have somewhat different influences on critical biochemical pathway branch points. For example, the fate of glutamine and its associated metabolites is very much governed by the relative need for NADH in its reduced (high-energy) form. The size of each pseudo energy metabolite is governed by its overall production and consumption. Thus, the rate of change in the ATP_i pool is the difference between its rate of production either by glycolysis or oxidative phosphorylation and the rate of its consumption, depending on the cell's energy needs for ATP-requiring processes, as shown by Equation 4.3a.

$$r_{ATP} = r_{ATP}^{Production} - r_{ATP}^{Consumption} = \left[2\,r_G + 2\,(P/O)\,r_{OX}\right] - \left[\mu\,Y_{ATP} + m_{ATP}\right]$$

Equation 4.3a

Note the consumption term uses the same linear semi-empirical model as discussed earlier, using a constant yield coefficient and a maintenance term (Pirt 1965). This is justified by the earlier observations that ATP needs appear to be constant and dependent on these two quantities. The ATP production term is represented by the true molar yields of ATP from glycolysis and oxidative phosphorylation, respectively. It is also governed by typical saturation kinetics by virtue of the expressions for r_G and r_{OX} that are dependent on the availability of glucose and oxygen, respectively. The appearance and disappearance of NADH is determined from the known stoichiometric ratios associated with its production and consumption for each of the major pathways.

In this version of their model, DiMasi and Swartz included branched-chain amino acids independently from other essential amino acids since they can play a significant role in energy production should the culture be depleted of the primary carbon and energy sources. These three amino acids (leucine, isoleucine, and valine) are also essential but are assumed to make up a negligible portion of the total essential amino acid pool and, therefore, are not subtracted. This is an example of adjustments that can be made to such a model to make it more sensitive to certain aspects of a process. This version also includes an inhibitory factor for ammonium using an expression similar to those described in Sections 2 and 3.

Another example of model adaptability is that the nonessential amino acids are not mathematically represented in the energy-structured model. Similar to our original assertion, it is assumed that the nonessential amino acids do not become growth-rate-limiting and are supplied in the medium and available in excess so that the yields of cell mass on the nonessential amino acids are constant. The extracellular essential amino acids, on the other hand, are represented as a lumped quantity. If the nonessential amino acids were not exogenously supplied, but rather derived from the essential amino acids, a more complicated version of the model, including additional intracellular variables, would be required, but certainly possible if the study of the contributions of nonessential amino acids to the overall process PCR is desired.

It remains to be seen whether a model like this, where metabolites are aggregated into pools, will have sufficient range and predictive power to be of use when coupled to a model of the bioreactor environment. In his work, DiMasi simulated the extensive data sets from Miller et al. that have been cited in much of this review, along with data he collected on an entirely different type of cell line. The model predictions were superior to any others published up to that point and beyond, with the exception of much larger flux balance models.

4.4 Model development and evolution

The word model is a ubiquitous term because there are many types and applications that can be brought to bear on the development of CM biomanufacturing. As in the development of any process, there are multiple stages, each with unique needs and challenges. It will be critical to properly define each application, though boundaries will be blurred. Analogous to the process development lifecycle,

the models will follow a similar evolution where one stage will overlap the next in a semi-iterative manner. What is learned in the prior stage and model will inform the next stage and its model, with the aim of simplifying and focusing on the most critical aspects for the upcoming stage.

Quiroga-Campano et al. provide a good example of how model building can fit into the bioprocess development workflow and even serve as an aid to the quality-by-design paradigm in biopharmaceutical manufacturing (Quiroga-Campano, Panoskaltsis, and Mantalaris 2018). At an early stage, models design an energy-based model based on ATP homeostasis to characterize the cell line as Step 1. This feeds into a model designed to assist in media development (Step 2). Step 3 uses a simplified version of the media development model to guide the design of a fed-batch process, which is then optimized in Step 4.

Similarly, genome-scale and metabolite flux analyses are used in earlier stages of bioprocess development, primarily cell line and media development. What is learned at these stages will feed into the model to support bioprocess development and bioreactor design. Only those metabolites would be included from the basal medium that would have an interactive effect with other primary substrates and/or growth processes. In this way, the basal media formulation is an input to this model rather than an output by virtue of the assumed basal composition supporting a maximum measured specific growth rate.

We emphasize that the model will need to be adapted to the application, which includes the medium that is used to grow the cells. However, a key objective for bioprocess and bioreactor design is to make the model as simple as possible. A key premise of the DiMasi and Swartz model formulation is that only key nutrients and waste products have a dominant effect on cell growth. Less critical nutrients or media components that are not inhibitory or don't result in significant inhibitory by-product formation can be supplied in excess of the growth requirements, and so these less critical components essentially behave as if they are at steady state and do not significantly impact culture dynamics. Using a disaggregated model would involve biochemical reaction measurements that are intractable or impractical in a dynamic cultivation situation.

As an example of this feature, nucleotide precursors such as hypoxanthine and thymidine have been shown to increase rates of cell growth and are often included in the medium. In this case, the maximum specific growth rate and the biomass yields on glucose will reflect the medium's composition. If, however, nucleotide precursors are not included, potentially limiting, or otherwise growth-impactful, the model could be appropriately augmented to include them as separate model components, but likely with different yield coefficients.

Similarly, if a specific amino acid or alternative substrate is important from the performance-to-cost perspective, then it may need to be added to the mechanistic portion of the model. For this, its conversion pathways and energy yield would need to be included. The use of pyruvate as a supplemental substrate is almost certain to be further explored by CM companies. Pyruvate can be used as a substrate for ATP generation, allowing for (under the right conditions) glucose to be used for biomass generation rather than ATP. One of the key anabolic uses of glucose is for upstream nucleotide synthesis. This is already assumed by the structured energetics model of DiMasi and Swartz described above because nucleotides making up RNA/DNA are defined and stoichiometric

components of cell mass. A model for this scenario would include pyruvate as a substrate but otherwise should not dramatically alter the model's structure.

Model validation

Finally, at some point, both physical and mathematical models need to be verified and validated. Larger-scale data are not always available to compare to small-scale results and model outputs until later in the development lifecycle. However, model confirmation will be an important and necessary aspect of CM process development under this paradigm to build the necessary confidence that these tools can be used to design larger, bespoke bioreactor systems. Larger-scale data, when available, do not need to be from an ideal setup or design, or even a design resembling what will ultimately be built. It could even be from similar cell lines. Inputting the associated design specifications, cell characteristics, and process particulars into the model and then comparing predictions with actual results will foster confidence with these tools, even if the process itself is not optimal or for the directly relevant application of CM production.

Section 5. Report summary and calls to action

This review was drawn from over 40 years of animal cell culture literature. Much work was done in the 1980s and 90s at the dawn of recombinant DNA technology and applied to the production of biopharmaceuticals and vaccines. Our fundamental understanding of animal cell behavior and metabolism was vastly improved as a result, and much of this experience can be leveraged for the benefit of CM. In general, we have found that many of the quantitative aspects for growth and metabolism of animal cells can be materially transferred to CM applications or at least offer a convenient starting point to model more CM-relevant cell lines.

5.1 Key conclusions

What we have learned from a thorough review of the literature underscores the inherent inefficiencies of animal cell metabolism with respect to converting substrates into energy and cell mass and the high energy requirements to support cellular processes compared to microorganisms. The well-recognized Warburg Effect exacerbates the large substrate demand due to incomplete oxidation, even in the presence of sufficient oxygen. The possible mechanisms and biological rationale of this effect, some described in Section 3.6, are still being debated, however, the phenomenon appears to be associated with higher growth rates (Vander Heiden et al. 2010). This raises the question of whether using animal cells with wild-type metabolic control and conventional substrates can ever achieve cost-competitiveness with commoditized conventional meat. As Humbird alluded to in his early but comprehensive analysis of CM feasibility, modifying (or adapting) cells to enhance their metabolic efficiency may be a prerequisite for the industrialization of CM.

Secondly, animal cells use more than one energy substrate. The two typical substrates are only partially substitutable as they provide unique biosynthetic precursors. This fact and the high degree of coordinated control over their joint metabolism make for a complicated picture. The traditional semi-empirical models used in biochemical engineering do not apply to dual substrates. Thus, we will need a higher-level model for our purposes. Fortunately, the energy carriers of most cells, ATP and NADH, can act as a unifying currency on which to base a model without resorting to very large reaction networks *in silico*. While some data are available for proliferating cells, almost none have been collected for cells undergoing differentiation.

Third, the adaptability of animal cells to adverse conditions appears to be somewhat underappreciated. It has long been known that animal cells are subject to growth inhibition and death if suddenly exposed to toxic substances or even their own waste metabolites. However, there are promising data that cells pre-adapted to otherwise damaging conditions can increase their tolerance. Due to their evolution toward survival under many possible conditions, we can leverage their plasticity through the use of alternative substrates, some of which have been successfully used in cell proliferation. What remains in those cases is to determine whether the cost of the alternative substate, if more expensive than the typical ones, justifies their use. Our prediction is that they will be justified if the accumulation of inhibitory waste metabolites can be reduced.

Lastly, amino acids are also a major component of cell culture media and contribute to the overall cost. While a detailed review of their metabolism was not a focus of this work, the inclusion of some of the essential and/or nonessential amino acids in a model may be needed in certain applications. Certainly, they should be included in the material balance as a pool because their uptake contributes significantly to overall biomass production in most cell culture media. However, incorporating specific amino acids into the equations to account for variable substrate consumption will add to model complexity. If specific amino acids are particularly expensive like serine and histidine, contribute to metabolic shifts, or can partially substitute for others, the added complexity may be worthwhile.

Harnessing all the above knowledge through the use of mathematical models, we assert, will focus attention on the aspects of a process that are most influential on performance and cost. Moreover, combining a cell model with a physics-based bioreactor model will enable quantitative assessments of trade-offs between competing phenomena such that an optimum balance can be identified. Even indirectly, models can help point out strategies that will have a meaningful impact on overall economics. For example, knowledge of the key aspects of metabolism limiting a given cell line's growth can suggest targets for genetic modifications in addition to the more immediate mitigations such as substrate restriction or substitution.

5.2 Overview of gaps and recommendations to modelers

This work was undertaken to help fulfill the vision presented above by identifying a starting point and highlighting gaps. In light of current and future needs, **Table 5.2a** reflects on the same six proposed model functions outlined in Section 2 in terms of what remains to be done to make modeling a useful reality for CM. A predominant theme that runs throughout the gaps is the need for further characterization of cellular energetics and high-flux biochemical pathways toward our main recommendation of building an energetically structured model. More data are needed to understand quantitatively how energy pathways are controlled to maintain high growth rates and how cell maintenance requirements may shift depending on stress conditions. In addition to the transformational work by Hefzi et al. on engineering out the Warburg Effect of a CHO cell line, similar work on CM-relevant cell lines is needed to benefit economical biomass production (Hefzi et al. 2025).

	Modeling needs	Current limitations, challenges, and actions needed

1.	**Prediction of bioreactor performance.**
	• Calculation of volumetric productivity
	• Accounting for:
	  ○ Controlled growth conditions
	  ○ Availability of oxygen, primary carbon, energy, and nitrogen substrates
	  ○ Accumulation of inhibitory waste metabolites
	  ○ Impact on the formation rate of inhibitory metabolites.
	• Identification of factors restricting a bioreactor's performance envelope
	• Relating system productivity to both capital and operating costs for
		• More characterization of CM-relevant cell lines and measurement of key model parameters needed, including cellular biomass content.
		• Standardized quantification of bioreactor performance, including volumetric productivity in terms of biomass and/or key nutritional components needed.
		• Current TEMs assume binary thresholds for inhibitors that can not be exceeded. In reality, there is an optimum to be found that pushes on the boundaries of mixing homogeneity and exposure to toxic metabolites.
		• Most metabolite inhibition studies used sudden additions of test metabolites to cells not previously exposed, which is not representative of typical culture process dynamics. More data are needed on the effect on cells after prolonged exposure to lactate and ammonia since it is apparent that they can adapt to these adverse conditions.
		• Related to the previous point, few detailed inhibition data are available from perfusion or other continuous culture systems on these metabolites, and even less for dissolved carbon dioxide and elevated osmolality.
		• There are almost no data on the rates of cell death of CM-relevant cell lines due to various stressors. Similar to inhibition studies, exposure was immediate, resulting in the highest

	Modeling needs	Current limitations, challenges, and actions needed
	determining and comparing performance-to-cost ratios	death rates, which is not representative of cell culture conditions.
2.	**Optimization of bioreactor feeding strategies and operating modes** • With respect to raw material costs and bioreactor performance • Accurate prediction of performance, substrate consumption efficiency, and feed conversion ratios as a function of the rate and timing of substrate addition • Evaluation of the quantitative trade-offs between the cost of medium components and their relative contribution to overall productivity	• Greater understanding is needed of the factors leading to the metabolic shift from lactate production to lactate consumption for CM-relevant cell lines. • Current TEMs use a single apparent yield for each substrate. This static stoichiometry is an oversimplification since substrate consumption depends on their residual concentrations and their metabolic interactions with each other. • Minimally variable yields should be determined as a function of their concentrations under representative conditions. A structured model based on energetics where substrate fluxes can be deduced could better serve this need. This requires more measurement of energy (e.g., ATP) yields for each substrate under a range of conditions. • Maintenance terms should also be used and measured as a function of the same conditions and in the presence of various concentrations of inhibiting metabolites. • Additional amino acids may need to be included in the mechanistic portion of the model, depending on the media design and their relative cost. • The specific metabolism for differentiating cells is largely unexplored, including for the substrates preferred and their corresponding growth yields (and feed conversion ratios). • Data from studies of substrate deprivation (including oxygen) are highly variable, probably due to many other conditions and/or nutrient concentrations not being controlled. Death kinetics will be important for CM processes consisting of two stages. If cells are proliferated (expanded in number) in the first stage, only live cells will appropriately attach and mature in the second stage.

	Modeling needs	Current limitations, challenges, and actions needed

3.	**Enabling bioreactor design and design evaluations**
	• Thorough capture of the effects of heterogeneous conditions on overall performance, such as insufficient mixing, oxygen transfer, or control overshoot
	• Estimate impact of:
	  ○ Localized depletion of substrates, including oxygen
	  ○ Concentration gradients or transients
	  ○ Other potential non-idealities inherent in large bioreactor systems.
		• All models to date assume well-mixed ideal conditions where the concentrations of substrates and metabolites are the same everywhere in the bioreactor. This will likely not be the case in large-scale bioreactors.
		• Few data have the time resolution to inform such models. Concentration fluctuations are likely to occur on the order of minutes to seconds — possibly less.
		• Cellular responses may need to be measured on this timescale. Single events are unlikely to have a measurable effect; however, intermittent or oscillating conditions may indeed have an effect over time. This could be simulated at small scale using an appropriately designed physical scale-down model of a large-scale bioreactor.
		• Structured models are likely required to account for these effects through the representation of internal metabolite pools such that intracellular concentrations are not immediately affected by an external change.
		• Such structured models will also likely need to be based on energetics since depletion of energy reserves or an increase in maintenance as a result of stressors would help predict some of these transient responses.
		• Current models are woefully inadequate for simulating differentiation stage bioreactors. Very little quantitative information is available on the rate at which specific cell types differentiate, their associated mass gain, or compositional changes.

4.	**Improving and optimizing bioprocesses** • Models should support study of performance trade-offs between various physical and biochemical conditions. • Ideally, include temperature and pH on overall system performance in addition to substrate feeding strategies and	• Data are needed for the effects of temperature and pH on the growth, differentiation, and metabolism of CM-relevant cells. This knowledge will enable the assessment of trade-offs with physical parameters in the bioreactor, potentially leading to more optimized cell culture processes at large scale. It is quite possible that an overall process optimum exists that does not necessarily coincide with the temperature and pH that maximizes growth rate for a given cell line. • Characterization of CM-relevant cell lines should include the impact of these key variables at

	Modeling needs	Current limitations, challenges, and actions needed
	operating modes.	least over a limited range around the growth rate optimum. • The addition of these parameters to a biological model will add another level of complexity since each of the mathematical expressions used to represent control of metabolic pathways and flux will also have to be a function of temperature and or pH. Fitting these relationships will likely require complex empirical functions since several factors are likely involved with changes in these key process variables. • Similar to Function #2, other amino acids may need to be included in the mechanistic portion of the model if they interact appreciably with the primary substrates and/or contribute significantly to cost.
5.	**Evaluation of cellular adaptation strategies** • Time-based adaptation to inhibitory metabolites • Comparison to pre-adapted cell lines • Use of alternative substrates such as pyruvate and alpha-ketoglutarate and their impact on performance-to- cost ratio • Model must be adaptable to incorporate other pathways	• The phenomenon of lactate uptake needs characterization for CM-relevant cell lines. This has significant implications for both the control of growth inhibition by lactate and the efficiency of substrate energy conversions. • While some semi-empirical models exist that provide excellent simulation of the relative consumption of conventional animal cell substrates, they are not intuitive or mechanistic enough to allow easy reconfiguration for other potential substrates. • By understanding how alternative substrates are metabolized, particularly with respect to energy generation, internal energy yield coefficients can be adjusted in a straightforward and intuitive manner. • The change in waste metabolite yields should also be quantifiable based on the known catabolism of the alternative substrate. • A time component may need to be added to the model to account for adaptive responses. • More study of the adaptation mechanisms is needed, along with time-resolved measurements.

	Modeling needs	Current limitations, challenges, and actions needed
6.	**Predicting the quantitative benefit of altered biochemical pathways** • as a result of adaptation • and/or genetic manipulation. • This benefit would be in the context of large-scale bioreactor operation.	• Much of such cell line improvement work would first be done in more sophisticated biological models, such as comprehensive metabolic flux analyses, to understand the consequences on cellular processes and flux distribution. • Various pathways and/or feedback mechanisms would be blocked or bypassed *in silico* simply by modifying their mathematical representations. • Once understood, the proposed simplified model would be adjusted to account for the salient effects of the biological modification and inserted into the larger bioreactor model. • This is where a model needs to be sufficiently mechanistic such that it is clear how to modify the equations to represent an altered pathway.

Table 5.2a: Outstanding gaps and needs for each of the desired modeling functions outlined in Section 2.

5.3 Model parameter determination and recommendations to experimentalists

To leverage models, CM production needs a systematic approach to obtaining the necessary mathematical parameters. With greater diligence in how experiments are conducted, manufacturers can make more progress in both process technology and fundamental understanding. Many of the same approaches used by previous researchers studying biopharma-relevant cell lines, as described earlier in this review, can now be followed for CM-relevant cells with the above caveats. Not only does a model provide a method of performance prediction, its framework also organizes causes and effects, highlights influential parameters, suggests the types of experiments needed to measure these parameters in the model, and provides a quantitative and structured summary of results. Moving forward, several priorities are clear. The following list offers some more specific recommendations regarding parameter measurement.

1. **Normalization of cell growth and bioreactor productivity data to dry cell weight.** This removes the variables of cell size and moisture content. Too much of cell culture research and current modeling still rely on cell number, despite the fact that biomass is what ultimately defines output and cost. Experiments, even with the same cell line, should be tracked by dry mass since it varies with growth rate and conditions. Moreover, data can be compared between cell lines with the potential that some results are transferable. Thus, accurate mass-based measurements of biomass and product yields must become standard practice. Methods using computationally enhanced quantitative phase microscopy (ceQPM) to populations of proliferating cells show much promise, as it enables highly accurate measurement of cell dry mass throughout the cell cycle ((Liu, Yan, and Kirschner 2022)).
2. **The chemostat as a measurement tool.** Maintaining culture conditions long enough to get a reliable measurement is a challenge with batch-like cell cultivations. Substrate concentrations can change rapidly under exponential growth, metabolites accumulate, and growth rates do not remain constant. By contrast, using continuous culture in which measurements can be made at a steady state removes the urgency and immediacy of sampling from non-steady state systems. Even the study of transient responses can be well supported with a chemostat by perturbing the system and then tracking deviations from steady state conditions. This recommendation is not to be confused with scale-down modeling. Rather, the chemostat is a tool for measuring biological parameters, even though it may not be the operating mode intended for the final process.
3. **Use of physical scale-down models.** There is still a fundamental disconnect between small-scale experiments and large-scale needs. Without designing experiments that reflect the conditions at commercial scale, it will be difficult to scale up these processes and generate results that will translate to performance and cost at scale. However, not all parameter measurements need to be made in a scaled-down version of the final bioreactor process. This only pertains to scale-relevant parameters. For isolated scale-dependent parameters, a specialized physical model might be designed to simulate a singular effect. For example, the

exposure of cells to a rapidly oscillating condition, such as a substrate (e.g., oxygen), metabolite concentration, or shear-rate distributions to simulate larger-scale heterogeneity could be conducted at small scale with an appropriately designed culture system. However, whenever possible, a cultivation system should be used that is as close to the final bioreactor and bioprocess design as possible. This includes the use of media, including serum concentrations, representative of the final process.

4. **Focus on cellular energy metabolism, yields, and maintenance requirements.** Based on what we have reviewed, much of the cell's response to changing conditions has ramifications for its energy status or balance. This is why we have recommended using energetics as the underlying structure for a model. Thus, even if culture attributes like growth rate and metabolite concentrations are measured, energy yields and maintenance requirements should also be measured when possible. There is likely a correlation between them and more will be learned about how to model the studied effects in terms of energy metabolism. For example, it is highly likely that the inhibitory effects of both lactate and ammonium on cell growth rate manifest by increasing the energy demand on the cells, taking it away from supporting growth.

5. **Measurement of cellular bioenergetics.** To support the previous recommendation, measurements of energy-related parameters are challenging in real time due to the rapid changes that can occur even in a sample withdrawn from a steady state culture. ATP and NADH yields have historically been inferred from oxygen uptake and lactate formation rates using conventional oxygen sensors in a bioreactor. This method, while practical, is not conducive for small-scale cultures used in high-throughput investigations. Using equipment like Agilent's Seahorse Bioanalyser (Desousa et al. 2023; Yoo et al. 2024) and Oroboro's O2k (Walsh et al. 2023; Gnaiger 2020) will give much better resolution of substrate and oxygen use on small samples. Indeed, the recent seminal work by (Hefzi et al. 2025) used the Seahorse analyzer for some of its measurements of lactate production. Also relevant to CM, others used the same instrument to measure oxygen consumption rates in muscle stem cells (Hong and Muñoz-Cánoves 2023). There are also more methods of measuring the total intracellular ATP content rather than ATP production rates using fluorescent or bioluminescent-based assays (Ley-Ngardigal and Bertolin 2021).

6. **Time-resolved measurements.** The bioprocess development scientist should be cognizant of the appropriate timescale relevant to the parameter or situation being studied. The latency of cellular responses to short timescale changes in nutrient availability (particularly oxygen) will be important for simulating bioreactor environments. Experiments should then be designed with a representative timescale and samples collected at a corresponding frequency. For example, in metabolite inhibition studies, we have seen the resulting cell response change with the duration of exposure. Sudden additions of test metabolites to cells not previously exposed lead to the most dramatic effects and are not representative of typical culture dynamics, even in a batch mode. Looking at adaptation kinetics is almost impossible with batch-like experiments with rapidly changing conditions, even if the test metabolite is held constant. This is further support for using chemostat cultures as a study tool (see #2 above).

7. **Use of comprehensive analytical tools.** Modern tools such as metabolomics should be used to collect as much information as possible from time-consuming cell culture experiments. With the availability of advanced analytical methods, it is often an insignificant investment in time and expense compared to the labor-intensive culture work. As we have learned, amino acids are inextricably linked to key catabolic and anabolic pathways and may have interactive effects with the primary substrates that may otherwise not have been predicted. Amino acids are typically assayed as a panel, so in measuring one, the others might as well also be measured. Going one step further, submitting results to metabolomic software to identify operative pathways would be a valuable extension of work.

5.4 Implications for CM Process Development

While modeling will support and guide process development going forward, aspects learned during this review already point toward process recommendations. Below, we attempt to collect the relevant findings and what implications they have for first-generation CM manufacturing process technologies.

The advantages of continuous cultivation

We have seen how substrates are consumed is dictated by their own concentrations and by the concentrations of their accumulated catabolic products. The amount of substrates consumed has a direct impact on the formation of these autoinhibitory waste metabolites. Therefore, the manner in which the substrates are fed to the bioreactor can significantly impact the growth rates and maximal cell concentrations achieved. From the biopharmaceutical world, it is well known that in fed-batch cultures, a controlled feed of glucose and glutamine that maintains low residual concentrations leads to significantly higher bioreactor productivities for cell mass and recombinant protein product yields.

Even though batch and fed-batch processes have been the staple method in the biopharmaceutical industry for many years, continuous cell culture seems well suited to CM manufacturing (Laura Pasitka et al. 2024). With greater scales required and lower cost margins, efficiency will be paramount. Just as importantly, the need to restrict the residual concentrations of the primary energy substrates is most easily accommodated by a continuously fed bioreactor. An actively growing culture at steady state will inherently keep residual substrate concentrations down as fresh medium is fed into the bioreactor as long as the substrate(s) is growth-limiting.

To achieve the high cell concentrations that are targeted to maximize bioreactor productivity, perfusion cell culture is possibly the only option. Perfusion consists of a nutrient medium being fed to the culture while the spent medium is removed from the culture and while the cells are held in the bioreactor. The cells are held in place by means of a cell retention device, which permits the washout of inhibitory substances without losing the cells from the reactor. A perfusion medium should be properly tuned to balance nutrient delivery with waste and inhibitor removal and culture osmolality. While a perfusion system will almost certainly be required for stationary cultures to produce tissue-like CM, perfusion should also be applied to the preceding proliferation step for the same reason. However, a different cell retention device may be required for a suspension culture than for a fixed bed using a scaffold.

Perhaps an even bigger advantage of continuous culture is from the observation that cells can adapt to inhibitory levels of metabolites if given enough time. In batch and fed-batch cultures, waste metabolites accumulate over a relatively short amount of time and while many other conditions are also changing, ending in a death phase. A continuous culture, on the other hand, maintains the same conditions over an indefinite period of time. This feature allows the cells to adapt, thereby reducing their sensitivities and possibly shifting their metabolism in a favorable direction, such as the reuptake of lactate.

Lastly, among the most critical parameters, temperature and pH have not been fully explored as means of process optimization. Examining the trade-offs between biological parameters and physical processes that occur in the bioreactor, including mass transfer, gas dispersion, and viscosity, may offer unique opportunities for overall bioprocess performance improvements.

Mitigation of waste metabolite inhibition

Prior researchers aimed to reduce lactate and ammonium buildup in CHO cells and compiled them in a summary table ((Freund and Croughan 2018)). They found that strategies such as nutrient replacement, amino acid modulation, media reformulation, and adaptation protocols were all employed with varying success. Such strategies have not been completely characterized and are sure to be of use in CM applications. Strategies to mitigate ammonia toxicity include glutamine substitution or reduction and the use of alternative nitrogen sources (e.g., alanine, glutamate, or dipeptides) as methods not requiring genetic intervention. Physical approaches such as dialysis-based perfusion, two-compartment reactors, and membrane-based ammonia extraction have also been investigated (Van EikerenJohn M. Radovich 1990). More recently, co-culture systems involving recombinant cyanobacteria capable of ammonia uptake and assimilation have shown promise in improving media quality and supporting long-term mammalian cell proliferation (Chu et al. 2024; Haraguchi et al. 2024).

Alternative substrates

As suggested by the literature, the use of substrates that are intermediates of glycolysis and the TCA cycle can generate energy equivalent to or approaching that of the native carbon, energy, and nitrogen sources while also avoiding the excessive discharge of inhibiting waste metabolites like lactate and ammonium. In fact, a few industry stakeholders have already explored the use of pyruvate as a partial substitute for glucose or the use of alpha-ketoglutarate as a substitute for glutamine (Hubalek et al. 2023). It remains to be seen if these strategies can improve the overall PCR of CM processes but such analyses and comparisons can be supported using mathematical models.

5.5 Implications for cell line development

Similar to the recommendations for cell culture process development offered in the preceding section, our review of the literature has also made apparent some early recommendations for the development of new cell lines for CM. Achieving some of the performance improvements already mentioned may be best accomplished by direct modification of wild-type metabolism. As alluded to in the summary above, the adaptability and flexibility of natural animal cell metabolism come at the expense of

substrate consumption efficiency. This trait might pose extensive economic challenges for CM if wild-type cells are used. However, genetic engineering approaches have already proven effective. For example, genetic modifications aimed at upregulating pyruvate carboxylase or downregulating LDH-A have shown promise in reducing lactate formation and improving culture longevity. The main challenge with this approach may be nontechnical: seeking regulatory approvals for the use of genetically modified organisms in the production of human food. Currently, there are parts of the world that are not ready to accept this approach.

As progress continues to be made in understanding the Warburg Effect, which appears to be characteristic of all animal cell lines, not just transformed ones, additional strategies for genetic engineering will reveal themselves. The recent work of (Hefzi et al. 2025) the energy efficiency of animal cells. Their approach to knock out both LDH and pyruvate dehydrogenase succeeded in eliminating lactate production, forcing more oxidation of glucose without reducing growth rates. This approach focuses on the most immediate level of metabolic control. However, recent discoveries indicate the involvement of mitochondria as part of the Warburg phenomenon, suggesting additional possible strategies for more efficient cell lines.

The potential use of alternative substrates was mentioned in the previous section. If the biochemical is a natural metabolite that can be utilized by a wild-type cell, no genetic modification is necessary. However, non-natural substrates could be conceived and may offer some advantages. While this approach may have negative implications for a food product, it should be given some consideration at least for potential substrates that are considered food safe (i.e., GRAS designated).

Other less invasive approaches are also possible by pre-adaptation of cell lines before banking them for use in the actual production process. What remains is to acquire the data to evaluate the quantitative benefit of such strategies coupled with modelling to assess cost-benefit and other performance trade-offs.

References

Acosta, María Lourdes, Asterio Sánchez, Francisco García, Antonio Contreras, and Emilio Molina. 2007. "Analysis of Kinetic, Stoichiometry and Regulation of Glucose and Glutamine Metabolism in Hybridoma Batch Cultures Using Logistic Equations." *Cytotechnology* 54 (3): 189–200.

Al-Fageeh, Mohamed B., and C. Mark Smales. 2006. "Control and Regulation of the Cellular Responses to Cold Shock: The Responses in Yeast and Mammalian Systems." *The Biochemical Journal* 397 (2): 247–59.

Alhuthali, Sakhr, Pavlos Kotidis, and Cleo Kontoravdi. 2021. "Osmolality Effects on CHO Cell Growth, Cell Volume, Antibody Productivity and Glycosylation." *International Journal of Molecular Sciences* 22 (7): 3290.

Amirian, Mohammad M., Andrew J. Irwin, and Zoe V. Finkel. 2022. "Extending the Monod Model of Microbal Growth with Memory." *Frontiers in Marine Science* 9 (December). https://doi.org/10.3389/fmars.2022.963734.

Batt, B. C., and D. S. Kompala. 1989. "A Structured Kinetic Modeling Framework for the Dynamics of Hybridoma Growth and Monoclonal Antibody Production in Continuous Suspension Cultures." *Biotechnology and Bioengineering* 34 (4): 515–31.

Boraston, R., P. W. Thompson, S. Garland, and J. R. Birch. 1983. "Growth and Oxygen Requirements of Antibody Producing Mouse Hybridoma Cells in Suspension Culture." *Developments in Biological Standardization* 55:103–11.

Bosdriesz, Evert, Stefanía Magnúsdóttir, Frank J. Bruggeman, Bas Teusink, and Douwe Molenaar. 2015. "Binding Proteins Enhance Specific Uptake Rate by Increasing the Substrate-Transporter Encounter Rate." *The FEBS Journal* 282 (12): 2394–2407.

Bouchez, Cyrielle L., Noureddine Hammad, Sylvain Cuvellier, Stéphane Ransac, Michel Rigoulet, and Anne Devin. 2020. "The Warburg Effect in Yeast: Repression of Mitochondrial Metabolism Is Not a Prerequisite to Promote Cell Proliferation." *Frontiers in Oncology* 10 (August):1333.

Bree, M. A., P. Dhurjati, R. F. Geoghegan Jr, and B. Robnett. 1988. "Kinetic Modelling of Hybridoma Cell Growth and Immunoglobulin Production in a Large-Scale Suspension Culture." *Biotechnology and Bioengineering* 32 (8): 1067–72.

Brunner, Matthias, Jens Fricke, Paul Kroll, and Christoph Herwig. 2017. "Investigation of the Interactions of Critical Scale-up Parameters (pH, pO2 and pCO2) on CHO Batch Performance and Critical Quality Attributes." *Bioprocess and Biosystems Engineering* 40 (2): 251–63.

Butler, M., and R. E. Spier. 1984. "The Effects of Glutamine Utilisation and Ammonia Production on the Growth of BHK Cells in Microcarrier Cultures." *Journal of Biotechnology* 1 (3-4): 187–96.

Chu, Shanga, Yuji Haraguchi, Toru Asahi, Yuichi Kato, Akihiko Kondo, Tomohisa Hasunuma, and Tatsuya Shimizu. 2024. "A Serum-Free Culture Medium Production System by Co-Culture Combining Growth Factor-Secreting Cells and L-Lactate-Assimilating Cyanobacteria for Sustainable Cultured Meat Production." *Scientific Reports* 14 (1): 19578.

Cooper, Julia Promisel, and Richard J. Youle. 2012. "Balancing Cell Growth and Death." *Current Opinion in Cell Biology* 24 (6): 802–3.

Cruz, H. J., A. S. Ferreira, C. M. Freitas, J. L. Moreira, and M. J. Carrondo. 1999. "Metabolic Responses to Different Glucose and Glutamine Levels in Baby Hamster Kidney Cell Culture." *Applied Microbiology and Biotechnology* 51 (5): 579–85.

Cruz, H. J., C. M. Freitas, P. M. Alves, J. L. Moreira, and M. J. Carrondo. 2000. "Effects of Ammonia and Lactate on Growth, Metabolism, and Productivity of BHK Cells." *Enzyme and Microbial Technology* 27 (1-2): 43–52.

Cruz, H. J., J. L. Moreira, and M. J. Carrondo. 2000. "Metabolically Optimised BHK Cell Fed-Batch Cultures." *Journal of Biotechnology* 80 (2): 109–18.

Darzynkiewicz, Z., D. Evenson, L. Staiano-Coico, T. Sharpless, and M. R. Melamed. 1979. "Relationship between RNA Content and Progression of Lymphocytes through S Phase of Cell Cycle." *Proceedings of the National Academy of Sciences of the United States of America* 76 (1): 358–62.

De la Fuente, Ildefonso M., Jesús M. Cortés, Edelmira Valero, Mathieu Desroches, Serafim Rodrigues, Iker Malaina, and Luis Martínez. 2014. "On the Dynamics of the Adenylate Energy System: Homeorhesis vs Homeostasis." *PloS One* 9 (10): e108676.

Desousa, Brandon R., Kristen Ko Kim, Anthony E. Jones, Andréa B. Ball, Wei Y. Hsieh, Pamela Swain, Danielle H. Morrow, et al. 2023. "Calculation of ATP Production Rates Using the Seahorse XF Analyzer." *EMBO Reports* 24 (10): e56380.

Dezengotita, V. M., R. Kimura, and W. M. Miller. 1998. "Effects of CO2 and Osmolality on Hybridoma Cells: Growth, Metabolism and Monoclonal Antibody Production." *Cytotechnology* 28 (1-3): 213–27.

Dhir, S., K. J. Morrow Jr, R. R. Rhinehart, and T. Wiesner. 2000. "Dynamic Optimization of Hybridoma Growth in a Fed-Batch Bioreactor." *Biotechnology and Bioengineering* 67 (2): 197–205.

Dimasi, Don. 1992. "A Mechanistic Analysis of Mammalian Cell Metabolism in Continuous Culture." PhD, Medform, MA: Tufts University.

DiMasi, D., and R. W. Swartz. 1995. "An Energetically Structured Model of Mammalian Cell Metabolism. 1. Model Development and Application to Steady-State Hybridoma Cell Growth in Continuous Culture." *Biotechnology Progress* 11 (6): 664–76.

Dohmen, Richard G. J., Sophie Hubalek, Johanna Melke, Tobias Messmer, Federica Cantoni, Arianna Mei, Rui Hueber, et al. 2022. "Muscle-Derived Fibro-Adipogenic Progenitor Cells for Production of Cultured Bovine Adipose Tissue." *NPJ Science of Food* 6 (1): 6.
Dorrity, Michael W., Lauren M. Saunders, Madeleine Duran, Sanjay R. Srivatsan, Eliza Barkan, Dana L. Jackson, Sydney M. Sattler, et al. 2023. "Proteostasis Governs Differential Temperature Sensitivity across Embryonic Cell Types." *Cell* 186 (23): 5015–27.e12.
Eagle, H. 1973. "The Effect of Environmental pH on the Growth of Normal and Malignant Cells." *Journal of Cellular Physiology* 82 (1): 1–8.
Eigler, Tamar, Giulia Zarfati, Emmanuel Amzallag, Sansrity Sinha, Nadav Segev, Yishaia Zabary, Assaf Zaritsky, et al. 2021. "ERK1/2 Inhibition Promotes Robust Myotube Growth via CaMKII Activation Resulting in Myoblast-to-Myotube Fusion." *Developmental Cell* 56 (24): 3349–63.e6.
Frame, K. K., and W. S. Hu. 1991a. "Kinetic Study of Hybridoma Cell Growth in Continuous Culture. I. A Model for Non-Producing Cells." *Biotechnology and Bioengineering* 37 (1): 55–64.
———. 1991b. "Kinetic Study of Hybridoma Cell Growth in Continuous Culture: II. Behavior of Producers and Comparison to Nonproducers." *Biotechnology and Bioengineering* 38 (9): 1020–28.
Freund, Nathaniel W., and Matthew S. Croughan. 2018. "A Simple Method to Reduce Both Lactic Acid and Ammonium Production in Industrial Animal Cell Culture." *International Journal of Molecular Sciences* 19 (2). https://doi.org/10.3390/ijms19020385.
Frontera, Walter R., and Julien Ochala. 2015. "Skeletal Muscle: A Brief Review of Structure and Function." *Calcified Tissue International* 96 (3): 183–95.
Gagnon, Matthew, Gregory Hiller, Yen-Tung Luan, Amy Kittredge, Jordy DeFelice, and Denis Drapeau. 2011. "High-End pH-Controlled Delivery of Glucose Effectively Suppresses Lactate Accumulation in CHO Fed-Batch Cultures." *Biotechnology and Bioengineering* 108 (6): 1328–37.
Gillooly, James F., Eric L. Charnov, Geoffrey B. West, Van M. Savage, and James H. Brown. 2002. "Effects of Size and Temperature on Developmental Time." *Nature* 417 (6884): 70–73.
Glacken, M. W., E. Adema, and A. J. Sinskey. 1988. "Mathematical Descriptions of Hybridoma Culture Kinetics: I. Initial Metabolic Rates." *Biotechnology and Bioengineering* 32 (4): 491–506.
Glacken, M. W., R. J. Fleischaker, and A. J. Sinskey. 1986. "Reduction of Waste Product Excretion via Nutrient Control: Possible Strategies for Maximizing Product and Cell Yields on Serum in Cultures of Mammalian Cells." *Biotechnology and Bioengineering* 28 (9): 1376–89.
Gnaiger, E. 2020. "Residual Oxygen Consumption: Baseline Correction Mitochondrial Respiration." *Mitochondr Physiol Network*.
Gomez Romero, Sandra, and Nanette Boyle. 2023. "Systems Biology and Metabolic Modeling for Cultivated Meat: A Promising Approach for Cell Culture Media Optimization and Cost Reduction." *Comprehensive Reviews in Food Science and Food Safety* 22 (4): 3422–43.
Gomez Romero, Sandra, Isabella Spielmann, and Nanette Boyle. 2025. "Genome-Scale Metabolic Models in Cultivated Meat: Advances, Challenges, and Future Directions." *Current Opinion in Biotechnology* 94 (103313): 103313.
Goodwin, Corbin M., William R. Aimutis, and Rohan A. Shirwaiker. 2024. "A Scoping Review of Cultivated Meat Techno-Economic Analyses to Inform Future Research Directions for Scaled-up Manufacturing." *Nature Food*, October. https://doi.org/10.1038/s43016-024-01061-3.
Gray, David R., Su Chen, William Howarth, Duane Inlow, and Brian L. Maiorella. 1996. "CO2 in Large-Scale and High-Density ClIO Cell Perfusion Culture." *Cytotechnology* 22:65–78.
Gupta, Priyanka, Kerry Hourigan, Sameer Jadhav, Jayesh Bellare, and Paul Verma. 2017. "Effect of Lactate and pH on Mouse Pluripotent Stem Cells: Importance of Media Analysis." *Biochemical Engineering Journal* 118 (February):25–33.
Hanga, Mariana Petronela, Fritz Anthony de la Raga, Panagiota Moutsatsou, Christopher J. Hewitt, Alvin W. Nienow, and Ivan Wall. 2021. "Scale-up of an Intensified Bioprocess for the Expansion of Bovine Adipose-Derived Stem Cells (bASCs) in Stirred Tank Bioreactors." *Biotechnology and Bioengineering* n/a (n/a). https://doi.org/10.1002/bit.27842.
Haraguchi, Yuji, Yuichi Kato, Ayaka Tsuji, Tomohisa Hasunuma, and Tatsuya Shimizu. 2024. "Recombinant Lactate-Assimilating Cyanobacteria Reduce High-Concentration Culture-Associated Cytotoxicity in Mammalian Cells." *Archives of Microbiology* 206 (11): 425.
Harsini, Faraz, and Elliot Swartz. 2024. "Trends in Cultivated Meat Scale-up and Bioprocessing: A Summary of a 2023 Industry-Wide Survey." The Good Food Institute. https://gfi.org/wp-content/uploads/2024/05/Trends-in-cultivated-meat-scale-up-and-bioprocessing.pdf.
Hauser, Michelle, Amit Zirman, Roni Rak, and Iftach Nachman. 2024. "Challenges and Opportunities in Cell Expansion for Cultivated Meat." *Frontiers in Nutrition* 11. https://doi.org/10.3389/fnut.2024.1315555.
Hefzi, Hooman, Iván Martínez-Monge, Igor Marin de Mas, Nicholas Luke Cowie, Alejandro Gomez Toledo, Soo Min Noh, Karen Julie la Cour Karottki, et al. 2024. "Multiplex Genome Editing Eliminates the Warburg Effect without Impacting Growth

Rate in Mammalian Cells." *Bioengineering*. bioRxiv. https://www.biorxiv.org/content/10.1101/2024.08.02.606284v1.full.pdf.
———. 2025. "Multiplex Genome Editing Eliminates Lactate Production without Impacting Growth Rate in Mammalian Cells." *Nature Metabolism* 7 (1): 212–27.
Hong, Xiaotong, and Pura Muñoz-Cánoves. 2023. "Measuring Oxygen Consumption Rate (OCR) and Extracellular Acidification Rate (ECAR) in Muscle Stem Cells Using a Seahorse Analyzer: Applicability for Aging Studies." *Methods in Molecular Biology (Clifton, N.J.)* 2640:73–88.
Hosios, Aaron M., Vivian C. Hecht, Laura V. Danai, Marc O. Johnson, Jeffrey C. Rathmell, Matthew L. Steinhauser, Scott R. Manalis, and Matthew G. Vander Heiden. 2016. "Amino Acids Rather than Glucose Account for the Majority of Cell Mass in Proliferating Mammalian Cells." *Developmental Cell* 36 (5): 540–49.
Hubalek, S., J. Melke, P. Pawlica, M. J. Post, and P. Moutsatsou. 2023. "Non-Ammoniagenic Proliferation and Differentiation Media for Cultivated Adipose Tissue." *Frontiers in Bioengineering and Biotechnology* 11 (July):1202165.
Humbird, David. 2020. "Scale-Up Economics for Cultured Meat: Techno-Economic Analysis and Due Diligence." https://doi.org/10.31224/osf.io/795su.
———. 2021. "Scale-up Economics for Cultured Meat." *Biotechnology and Bioengineering* 118 (8): 3239–50.
Hwang, Leroy N., Zhiya Yu, Douglas C. Palmer, and Nicholas P. Restifo. 2006. "The*in Vivo*expansion Rate of Properly Stimulated Transferred CD8+ T Cells Exceeds that of an Aggressively Growing Mouse Tumor." *Cancer Research* 66 (2): 1132–38.
Jeong, Yeon-Ho, and Shaw S. Wang. 1995. "Role of Glutamine in Hybridoma Cell Culture: Effects on Cell Growth, Antibody Production, and Cell Metabolism." *Enzyme and Microbial Technology* 17 (1): 47–55.
Konige, Manige, Hong Wang, and Carole Sztalryd. 2014. "Role of Adipose Specific Lipid Droplet Proteins in Maintaining Whole Body Energy Homeostasis." *Biochimica et Biophysica Acta* 1842 (3): 393–401.
Kurokawa, H., Y. S. Park, S. Iijima, and T. Kobayashi. 1994. "Growth Characteristics in Fed-Batch Culture of Hybridoma Cells with Control of Glucose and Glutamine Concentrations." *Biotechnology and Bioengineering* 44 (1): 95–103.
Lao, M. S., and D. Toth. 1997. "Effects of Ammonium and Lactate on Growth and Metabolism of a Recombinant Chinese Hamster Ovary Cell Culture." *Biotechnology Progress* 13 (5): 688–91.
Letcher, Sophia M., Olivia P. Calkins, Halla J. Clausi, Aidan McCreary, Barry A. Trimmer, and David L. Kaplan. 2024. "Establishment & Characterization of a Non-Adherent Insect Cell Line for Cultivated Meat." *bioRxiv*. https://doi.org/10.1101/2024.10.18.618906.
Ley-Ngardigal, Seyta, and Giulia Bertolin. 2021. *Emerging Methods Technologies Approaches Monitor ATP Levels Living Cells: Where Do We Stand?*
Li, Qian, and Kirsty L. Spalding. 2022. "The Regulation of Adipocyte Growth in White Adipose Tissue." *Frontiers in Cell and Developmental Biology* 10 (November):1003219.
Liu, Xili, Seungeun Oh, Leonid Peshkin, and Marc W. Kirschner. 2020. "Computationally Enhanced Quantitative Phase Microscopy Reveals Autonomous Oscillations in Mammalian Cell Growth." *Proceedings of the National Academy of Sciences of the United States of America* 117 (44): 27388–99.
Liu, Xili, Jiawei Yan, and Marc W. Kirschner. 2022. "Beyond G1/S Regulation: How Cell Size Homeostasis Is Tightly Controlled throughout the Cell Cycle?" *Cell Biology*. bioRxiv. https://www.biorxiv.org/content/10.1101/2022.02.03.478996v2.full.pdf.
———. 2024. "Cell Size Homeostasis Is Tightly Controlled throughout the Cell Cycle." *PLoS Biology* 22 (1): e3002453.
Li, Xinxin, Khin Thu Lwin, Hirunika U. Kumarasinghe, Lilianne Iglesias-Ledon, Eesha Bethi, Yushu Wang, Colin Fennelly, et al. 2024. "Quantifying Biomass and Visualizing Cell Coverage on Fibrous Scaffolds for Cultivated Meat Production." *Current Protocols* 4 (12). https://doi.org/10.1002/cpz1.70076.
Ljunggren, J., and L. Häggström. 1994. "Catabolic Control of Hybridoma Cells by Glucose and Glutamine Limited Fed Batch Cultures." *Biotechnology and Bioengineering* 44 (7): 808–18.
Lohr, Verena, Oliver Hädicke, Yvonne Genzel, Ingo Jordan, Heino Büntemeyer, Steffen Klamt, and Udo Reichl. 2014. "The Avian Cell Line AGE1.CR.pIX Characterized by Metabolic Flux Analysis." *BMC Biotechnology* 14 (1): 72.
López-Meza, Julián, Diana Araíz-Hernández, Leydi Maribel Carrillo-Cocom, Felipe López-Pacheco, María Del Refugio Rocha-Pizaña, and Mario Moisés Alvarez. 2016. "Using Simple Models to Describe the Kinetics of Growth, Glucose Consumption, and Monoclonal Antibody Formation in Naive and Infliximab Producer CHO Cells." *Cytotechnology* 68 (4): 1287–1300.
Mancuso, A., S. T. Sharfstein, E. J. Fernandez, D. S. Clark, and H. W. Blanch. 1998. "Effect of Extracellular Glutamine Concentration on Primary and Secondary Metabolism of a Murine Hybridoma: An in Vivo 13C Nuclear Magnetic Resonance Study." *Biotechnology and Bioengineering* 57 (2): 172–86.
Martins Pinto, M., P. Paumard, C. Bouchez, S. Ransac, S. Duvezin-Caubet, J. P. Mazat, M. Rigoulet, and A. Devin. 2023. "The Warburg Effect and Mitochondrial Oxidative Phosphorylation: Friends or Foes?" *Biochimica et Biophysica Acta. Bioenergetics* 1864 (1): 148931.

Mattick, Carolyn S., Amy E. Landis, Braden R. Allenby, and Nicholas J. Genovese. 2015. "Anticipatory Life Cycle Analysis of In Vitro Biomass Cultivation for Cultured Meat Production in the United States." *Environmental Science & Technology* 49 (19): 11941–49.
McQueen, A., and J. E. Bailey. 1990. "Growth Inhibition of Hybridoma Cells by Ammonium Ion: Correlation with Effects on Intracellular pH." *Bioprocess Engineering* 6 (1-2): 49–61.
Mehmood, Waris, Martin Krøyer Rasmussen, Polina Rabinovich-Toidman, Neta Lavon, Jette Feveile Young, and Margrethe Therkildsen. 2025. "Postharvest Changes in Bovine Satellite Cells in Vitro Resemble Postmortem Conversion of Muscle to Meat." *Food Chemistry* 483 (144292): 144292.
Miettinen, Teemu P., Kevin S. Ly, Alice Lam, and Scott R. Manalis. 2022. "Single-Cell Monitoring of Dry Mass and Dry Mass Density Reveals Exocytosis of Cellular Dry Contents in Mitosis." *eLife* 11 (May). https://doi.org/10.7554/eLife.76664.
Miller, W. M., H. W. Blanch, and C. R. Wilke. 2000. "A Kinetic Analysis of Hybridoma Growth and Metabolism in Batch and Continuous Suspension Culture: Effect of Nutrient Concentration, Dilution Rate, and pH." *Biotechnology and Bioengineering* 67 (6): 853–71.
Miller, W. M., C. R. Wilke, and H. W. Blanch. 1987. "Effects of Dissolved Oxygen Concentration on Hybridoma Growth and Metabolism in Continuous Culture." *Journal of Cellular Physiology* 132 (3): 524–30.
———. 1988. "Transient Responses of Hybridoma Metabolism to Changes in the Oxygen Supply Rate in Continuous Culture." *Bioprocess Engineering* 3 (3): 103–11.
———. 1989. "Transient Responses of Hybridoma Cells to Nutrient Additions in Continuous Culture: I. Glucose Pulse and Step Changes." *Biotechnology and Bioengineering* 33 (4): 477–86.
Mitić, Rada, Federica Cantoni, Christoph S. Börlin, Mark J. Post, and Laura Jackisch. 2023. "A Simplified and Defined Serum-Free Medium for Cultivating Fat across Species." *iScience* 26 (1): 105822.
Muralidharan, Naveenganesh, Emma Bolduc, and Mark Davis. 2024. "Characterizing Oxygen Mass Transfer and Shear During Cell Culture: Calculating the Maximum Cell Density Supported By a 20,000-Liter Stirred-Tank Bioreactor." February 6, 2024. https://www.bioprocessintl.com/bioreactors/characterizing-oxygen-mass-transfer-and-shear-during-cell-culture-calculating-the-maximum-cell-density-supported-by-a-20-000-liter-stirred-tank-bioreactor.
Negulescu, Patrick G., Derrick Risner, Edward S. Spang, Daniel Sumner, David Block, Somen Nandi, and Karen A. McDonald. 2023. "Techno-Economic Modeling and Assessment of Cultivated Meat: Impact of Production Bioreactor Scale." *Biotechnology and Bioengineering* 120 (4): 1055–67.
Newland, M., M. N. Kamal, P. F. Greenfield, and L. K. Nielsen. 1994. "Ammonia Inhibition of Hybridomas Propagated in Batch, Fed-Batch, and Continuous Culture." *Biotechnology and Bioengineering* 43 (5): 434–38.
O'Toole, Angela. n.d. "An Investigation into Factors That Cause Inhibition of the Growth of Animal Cells in Vitro." Accessed October 30, 2024. https://doras.dcu.ie/19265/1/Angela_O'Toole_20130718083840.pdf.
Ozturk, S. S., and B. O. Palsson. 1990. "Effects of Dissolved Oxygen on Hybridoma Cell Growth, Metabolism, and Antibody Production Kinetics in Continuous Culture." *Biotechnology Progress* 6 (6): 437–46.
———. 1991. "Growth, Metabolic, and Antibody Production Kinetics of Hybridoma Cell Culture: 2. Effects of Serum Concentration, Dissolved Oxygen Concentration, and Medium pH in a Batch Reactor." *Biotechnology Progress* 7 (6): 481–94.
Ozturk, S. S., M. R. Riley, and B. O. Palsson. 1992. "Effects of Ammonia and Lactate on Hybridoma Growth, Metabolism, and Antibody Production." *Biotechnology and Bioengineering* 39 (4): 418–31.
Pasitka, Laura, Guy Wissotsky, Muneef Ayyash, Nir Yarza, Gal Rosoff, Revital Kaminker, and Yaakov Nahmias. 2024. "Empirical Economic Analysis Shows Cost-Effective Continuous Manufacturing of Cultivated Chicken Using Animal-Free Medium." *Nature Food* 5 (8): 693–702.
Pasitka, L., M. Cohen, A. Ehrlich, B. Gildor, E. Reuveni, M. Ayyash, G. Wissotsky, et al. 2022. "Spontaneous Immortalization of Chicken Fibroblasts Generates Stable, High-Yield Cell Lines for Serum-Free Production of Cultured Meat." *Nature Food*, December, 1–16.
Pattison, R. N., J. Swamy, B. Mendenhall, C. Hwang, and B. T. Frohlich. 2000. "Measurement and Control of Dissolved Carbon Dioxide in Mammalian Cell Culture Processes Using an in Situ Fiber Optic Chemical Sensor." *Biotechnology Progress* 16 (5): 769–74.
Pirt, S. J. 1965. "The Maintenance Energy of Bacteria in Growing Cultures." *Proceedings of the Royal Society of London. Series B, Containing Papers of a Biological Character. Royal Society (Great Britain)* 163 (991): 224–31.
Pörtner, R., and T. Schäfer. 1996. "Modelling Hybridoma Cell Growth and Metabolism--a Comparison of Selected Models and Data." *Journal of Biotechnology* 49 (1-3): 119–35.
Quek, Lake-Ee, Stefanie Dietmair, Jens O. Krömer, and Lars K. Nielsen. 2010. "Metabolic Flux Analysis in Mammalian Cell Culture." *Metabolic Engineering* 12 (2): 161–71.
Quiroga-Campano, Ana L., Nicki Panoskaltsis, and Athanasios Mantalaris. 2018. "Energy-Based Culture Medium Design for Biomanufacturing Optimization: A Case Study in Monoclonal Antibody Production by GS-NS0 Cells." *Metabolic*

Engineering 47 (May):21–30.
Ranpura, Sandeep, Vishwanathgouda Maralingannavar, Alexandra-Gabriela Gheorghe, Edward Ma, James Morrissey, Michael J. Betenbaugh, and Deniz Demirhan. 2025. "Wheels Turning: CHO Cell Modeling Moves into a Digital Biomanufacturing Era: Subtitle: CHO Metabolic Modeling." *Computational and Structural Biotechnology Journal* 27 (June):2796–2813.
Ravikumar, Maanasa, Dean Powell, Elliot Swartz, and Claire Bomkamp. 2023. "Cell Line Development and Utilisation Trends in the Cultivated Meat Industry." The Good Food Institute.
Rubio, Natalie, Isha Datar, David Stachura, David Kaplan, and Kate Krueger. 2019. "Cell-Based Fish: A Novel Approach to Seafood Production and an Opportunity for Cellular Agriculture." *Frontiers in Sustainable Food Systems* 3:43.
Sacco, Sarah A., and Jamey D. Young. 2021. "13C Metabolic Flux Analysis in Cell Line and Bioprocess Development." *Current Opinion in Chemical Engineering* 34 (100718): 100718.
Sanderson, C. S., J-D Jang, J. P. Barford, and G. W. Barton. 1999. "A Structured, Dynamic Model for Animal Cell Culture Systems: Application to Murine Hybridoma." *Biochemical Engineering Journal* 3 (3): 213–18.
Schaffer, Leah V., and Trey Ideker. 2021. "Mapping the Multiscale Structure of Biological Systems." *Cell Systems* 12 (6): 622–35.
Sinke, Pelle, Elliot Swartz, Hermes Sanctorum, Coen van der Giesen, and Ingrid Odegard. 2023. "Ex-Ante Life Cycle Assessment of Commercial-Scale Cultivated Meat Production in 2030." *International Journal of Life Cycle Assessment* 28 (3): 234–54.
Straathof, Adrie J. J. 2023. "Modelling of End-Product Inhibition in Fermentation." *Biochemical Engineering Journal* 191 (108796): 108796.
Sunley, Kevin, Tharmala Tharmalingam, and Michael Butler. 2008. "CHO Cells Adapted to Hypothermic Growth Produce High Yields of Recombinant Beta-Interferon." *Biotechnology Progress* 24 (4): 898–906.
SuperMeat. 2024. "A Deep Dive Into Cost-Effective Cultivated Meat Production." SuperMeat.
Széliová, Diana, David E. Ruckerbauer, Sarah N. Galleguillos, Lars B. Petersen, Klaus Natter, Michael Hanscho, Christina Troyer, et al. 2020. "What CHO Is Made of: Variations in the Biomass Composition of Chinese Hamster Ovary Cell Lines." *Metabolic Engineering* 61 (September):288–300.
Taylor, D. M., A. Los, and M. F. Robinson. 1984. "The Effect of pH on the Growth of a Human Myeloma Cell Line in Vitro." *British Journal of Cancer* 49 (2): 193–201.
Thrower, Thomas, Susanna E. Riley, Seungmee Lee, Cristina L. Esteves, and F. Xavier Donadeu. 2024. "A Unique Spontaneously Immortalised Cell Line from Pig with Enhanced Adipogenic Capacity - a Foundational Tool for Cellular Agriculture." *Research Square*. https://doi.org/10.21203/rs.3.rs-5128082/v1.
Thyden, Richard, Tanja Dominko, Pamela Weathers, Antonio Carlos Freitas dos Santos, Luke Perreault, David Reddig, Jack Kloster, and Glenn Gaudette. 2024. "Recycling Spent Animal Cell Culture Media Using the Thermally Resistant Microalga Chlorella Sorokiniana." *Systems Microbiology and Biomanufacturing*, June. https://doi.org/10.1007/s43393-024-00280-w.
Torres, Mauro, Ellie Hawke, Robyn Hoare, Rachel Scholey, Leon P. Pybus, Alison Young, Andrew Hayes, and Alan J. Dickson. 2024. "Deciphering Molecular Drivers of Lactate Metabolic Shift in Mammalian Cell Cultures." *Metabolic Engineering*, December. https://doi.org/10.1016/j.ymben.2024.12.001.
Tuomisto, Hanna L., Scott J. Allan, and Marianne J. Ellis. 2022. "Prospective Life Cycle Assessment of a Bioprocess Design for Cultured Meat Production in Hollow Fiber Bioreactors." *The Science of the Total Environment* 851 (Pt 1): 158051.
Tuomisto, Hanna L., and M. Joost Teixeira de Mattos. 2011. "Environmental Impacts of Cultured Meat Production." *Environmental Science & Technology* 45 (14): 6117–23.
Tzimorotas, Dimitrios, Nina Therese Solberg, R. Christel Andreassen, Panagiota Moutsatsou, Vincent Bodiou, Mona Elisabeth Pedersen, and Sissel Beate Rønning. 2023. "Expansion of Bovine Skeletal Muscle Stem Cells from Spinner Flasks to Benchtop Stirred-Tank Bioreactors for up to 38 Days." *Frontiers in Nutrition* 10 (August):1192365.
Vander Heiden, Matthew G., Jason W. Locasale, Kenneth D. Swanson, Hadar Sharfi, Greg J. Heffron, Daniel Amador-Noguez, Heather R. Christofk, et al. 2010. "Evidence for an Alternative Glycolytic Pathway in Rapidly Proliferating Cells." *Science (New York, N.Y.)* 329 (5998): 1492–99.
Van EikerenJohn M. Radovich, Paul. 1990. Ammonia removal from mammalian cell cultures. *Patent*, issued 1990.
Wagner, Brett A., Sujatha Venkataraman, and Garry R. Buettner. 2011. "The Rate of Oxygen Utilization by Cells." *Free Radical Biology & Medicine* 51 (3): 700–712.
Walsh, Maureen A., Robert V. Musci, Robert A. Jacobs, and Karyn L. Hamilton. 2023. "A Practical Perspective on How to Develop, Implement, Execute, and Reproduce High-Resolution Respirometry Experiments: The Physiologist's Guide to an Oroboros O2k." *FASEB Journal: Official Publication of the Federation of American Societies for Experimental Biology* 37 (12): e23280.
Wang, Zheyu, Caixia Wang, and Gong Chen. 2022. "Kinetic Modeling: A Tool for Temperature Shift and Feeding Optimization in Cell Culture Process Development." *Protein Expression and Purification* 198 (106130): 106130.
Watanabe, I., and S. Okada. 1967. "Effects of Temperature on Growth Rate of Cultured Mammalian Cells (L5178Y)." *The*

Journal of Cell Biology 32 (2): 309–23.
Wu, P., N. G. Ray, and M. L. Shuler. 1992. "A Single-Cell Model for CHO Cells." *Annals of the New York Academy of Sciences* 665 (1): 152–87.
Xing, Zizhuo, Zhengjian Li, Vincent Chow, and Steven S. Lee. 2008. "Identifying Inhibitory Threshold Values of Repressing Metabolites in CHO Cell Culture Using Multivariate Analysis Methods." *Biotechnology Progress* 24 (3): 675–83.
Xiu, Z. L., W. D. Deckwer, and A. P. Zeng. 1999. "Estimation of Rates of Oxygen Uptake and Carbon Dioxide Evolution of Animal Cell Culture Using Material and Energy Balances." *Cytotechnology* 29 (3): 159–66.
Xu, Jianlin, Peifeng Tang, Andrew Yongky, Barry Drew, Michael C. Borys, Shijie Liu, and Zheng Jian Li. 2019. "Systematic Development of Temperature Shift Strategies for Chinese Hamster Ovary Cells Based on Short Duration Cultures and Kinetic Modeling." *mAbs* 11 (1): 191–204.
Yamano-Adachi, Noriko, Rintaro Arishima, Sukwattananipaat Puriwat, and Takeshi Omasa. 2020. "Establishment of Fast-Growing Serum-Free Immortalised Cells from Chinese Hamster Lung Tissues for Biopharmaceutical Production." *Scientific Reports* 10 (1): 17612.
Yang, Ming, Ning Xiang, Yunan Tang, Yue Li, and Ximing Zhang. 2025. "Layered Sodium Zirconium Phosphate Adsorbent for Ammonia Removal in Cell Culture Media for Cultivated Meat Application." *Separation and Purification Technology* 364 (132415): 132415.
Yoo, Inhwan, Ihyeon Ahn, Jihyeon Lee, and Namgyu Lee. 2024. "Extracellular Flux Assay (Seahorse Assay): Diverse Applications in Metabolic Research across Biological Disciplines." *Molecules and Cells* 47 (8): 100095.
Zagury, Yedidya, Iris Ianovici, Shira Landau, Neta Lavon, and Shulamit Levenberg. 2022. "Engineered Marble-like Bovine Fat Tissue for Cultured Meat." *Communications Biology* 5 (1): 927.
Zeng, A. P., and W. D. Deckwer. 1995. "Mathematical Modeling and Analysis of Glucose and Glutamine Utilization and Regulation in Cultures of Continuous Mammalian Cells." *Biotechnology and Bioengineering* 47 (3): 334–46.
Zheng, Zaiyu, Bin Chen, Xiaodong Liu, Rui Guo, Hongshu Chi, Xiuxia Chen, Ying Pan, and Hui Gong. 2024. "Novel Eel Skin Fibroblast Cell Line: Bridging Adherent and Suspension Growth for Aquatic Applications Including Virus Susceptibility." *Biology* 13 (12): 1068.
Zhu, Marie M., Asti Goyal, Douglas L. Rank, Sunil K. Gupta, Thomas Vanden Boom, and Steven S. Lee. 2005. "Effects of Elevated pCO2 and Osmolality on Growth of CHO Cells and Production of Antibody-Fusion Protein B1: A Case Study." *Biotechnology Progress* 21 (1): 70–77.

Appendices

A1. Overview of animal cell metabolism

The energy required for animal cell growth is naturally provided by the catabolism of carbon and energy substrates, glucose, a sugar, and glutamine, an amino acid. Under conditions of rapid growth, glycolysis is the primary contributor to energy production from the consumption of glucose, resulting in the production of lactic acid. Glycolysis occurs even though the greatest energy is produced via oxidative phosphorylation through the TCA cycle, ending in the formation of carbon dioxide. This phenomenon is known as the Warburg Effect, which occurs even if oxygen is available in excess. Glucose also has an anabolic role in contributing 5-carbon sugars (pentoses) to the synthesis of nucleotides.

Glutamine is typically the main contributor to the nitrogenous base of nucleotides and to the synthesis of nonessential amino acids and protein synthesis more generally, but can also be consumed as an energy substrate, resulting in the release of free ammonia. It is well established that glucose and glutamine are partially substitutable as energy sources in mammalian cell culture media (DiMasi and Swartz 1995). Each provides unique biosynthetic precursors but is complementary for the production of other metabolites and energy (Miller, Wilke, and Blanch 1989). Thus, glycolysis and glutaminolysis are jointly regulated to provide sufficient energy required by cells, depending on the availability of these major energy substrates (Jeong and Wang 1995).

The rate of glucose and glutamine consumption directly determines the production rates of their main waste products of lactic acid, ammonium, and carbon dioxide. It is also well established that all three of these metabolites can inhibit the growth of most animal cells and can even result in cell death at higher concentrations.

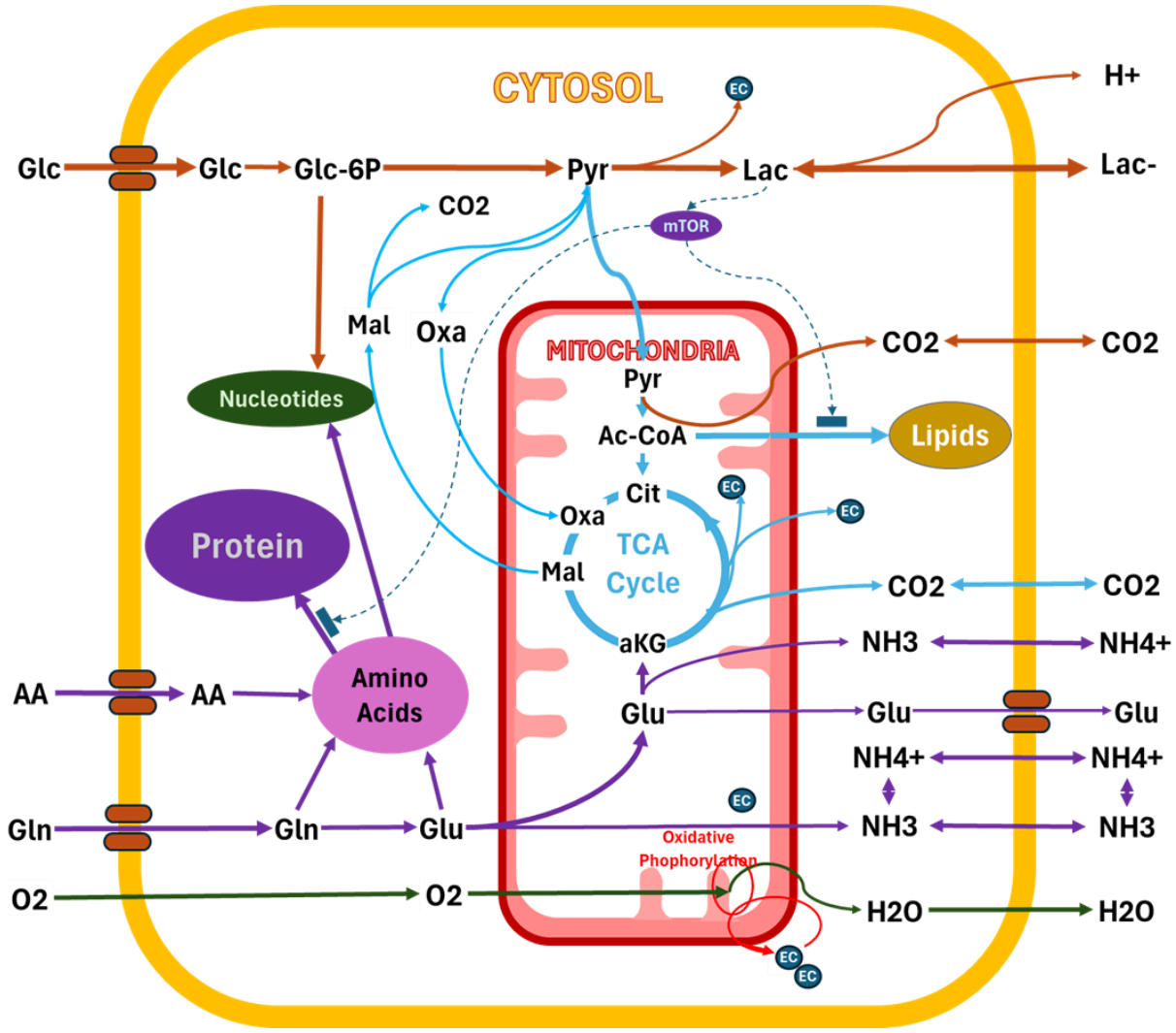

Figure A1.1: Overview of primary pathways that have the greatest flux during active cell growth. Thus, concentrations of the substrates and metabolites shown change to the greatest extent during batch growth.

The role of energetics in the control of metabolism is best explained by examining the actual biochemical pathways involved. A detailed diagram of the relevant biochemical pathways is provided in **Figure A1.2**, showing the enzymes that catalyze each reaction step in glycolysis, glutaminolysis, and the TCA cycle. The most critical regulatory enzymes, typically located at the start or end of each pathway, are colored in red in the diagram. These enzymes are allosterically regulated by the concentrations of energy carrier molecules. Regulation at these points allows the cell to commit to or bypass entire pathways depending on the demand for the end products, particularly the energy carriers produced through these pathways.

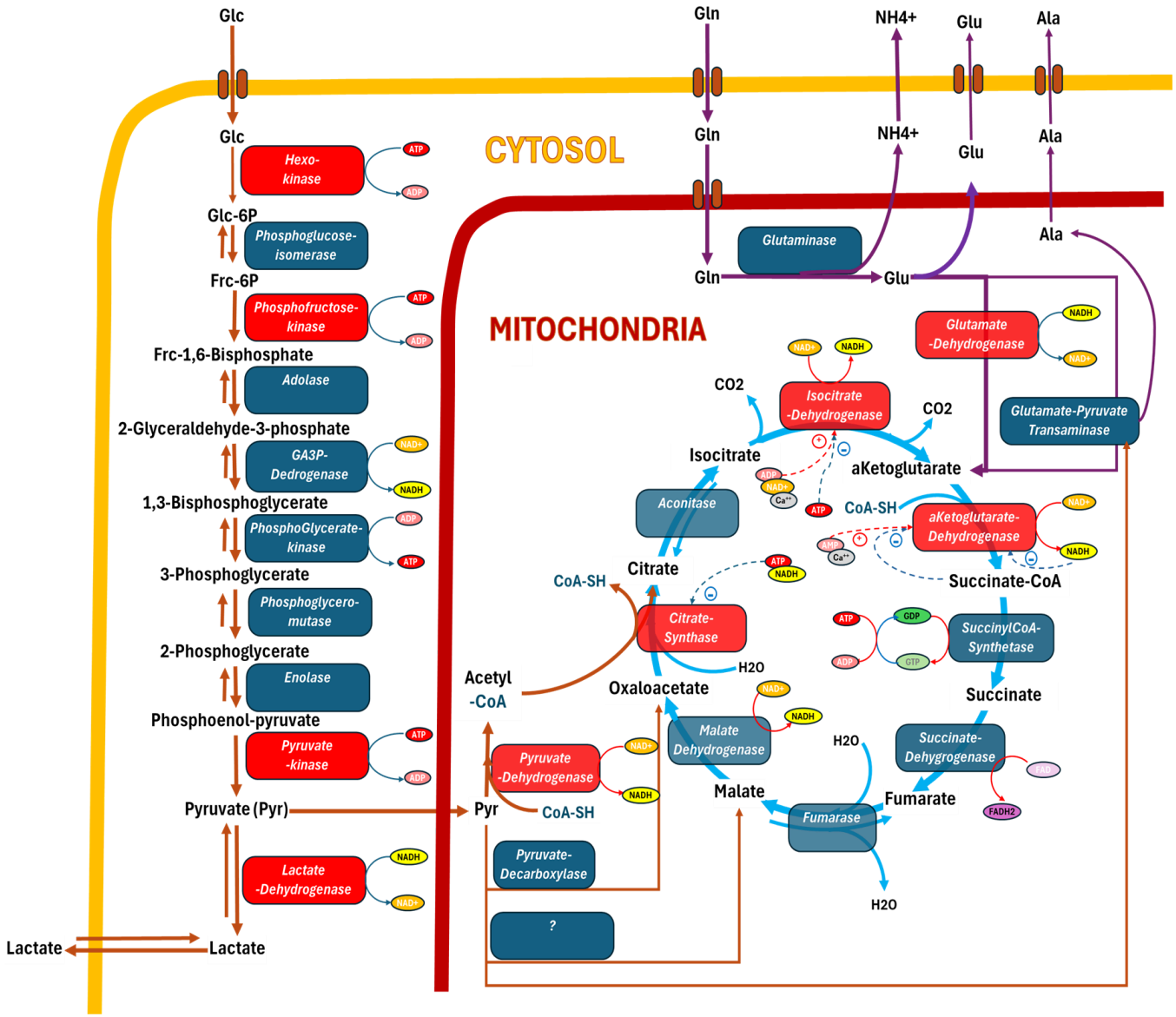

Figure A1.2: Diagram of catabolic pathways, including the enzymes that catalyze each reaction. The key enzyme control points are shown in red for each of the primary pathways: glycolysis, glutaminolysis, and the TCA cycle.

Together, these pathways reveal how animal cells flexibly regulate substrate use based on the demand for ATP, redox balance, and biosynthesis. Glucose mainly supports ATP and NADH generation through glycolysis, while glutamine feeds the TCA cycle to supply biosynthetic precursors (anaplerosis) and support redox homeostasis. The balance of glucose and glutamine determines how much pyruvate is oxidized versus reduced to lactate. When glucose is abundant but glutamine is limited, the TCA cycle lacks sufficient anaplerotic input, and pyruvate is diverted to lactate production to regenerate NAD^+. This leads to a high lactate-to-glucose yield ($Y'_{Lac/Glc}$), often approaching or exceeding 1.5 mol/mol. When glutamine is sufficient, it supports TCA activity and biosynthesis, allowing more pyruvate to be oxidized and lowering lactate output. In this way, lactate production reflects a broader metabolic strategy shaped by nutrient availability and the cell's energy and biosynthetic needs.

When ATP demand is high and oxygen is available, glucose can be fully oxidized. But in rapidly dividing cells, glycolysis often dominates even in the presence of oxygen. This is known as the Warburg Effect, leading to lactate accumulation, and which appears to be a characteristic of most animal cells, including the ones we have evaluated. Animal cells generally have a higher maintenance energy requirement than microorganisms, but energy generation is exacerbated by the Warburg Effect, which further increases substrate demand due to incomplete oxidation. However, a key finding during this review is that cells of very different lineages appear to adjust their utilization of metabolic pathways to maintain a constant q_{ATP} even under varying nutrient conditions. Thus, using a fixed energy demand provides a unifying currency on which to base mathematical models of substrate utilization.

Though discovered over 100 years ago in cancer cell lines, the Warburg phenomenon still perplexes scientists. The mechanisms and biological rationale of this effect are still being unraveled; however, considerably more is known today than 10 years ago. The leading hypothesis for its origin is that it allows cells to grow more quickly. It is therefore no longer surprising that the effect was first discovered in cancer cells, which grow more quickly than the surrounding normal cells.

It is now understood that many normal cell types display this same phenomenon, possibly as a strategy to boost growth or counteract stresses. Several explanations have been offered. Glucose uptake is increased significantly in part because it is also an important contributor to nucleotide synthesis. By supplying the ribose portion, nucleotides can be assembled, more of which are required under conditions of rapid proliferation. However, much of the glucose is also wasted (energetically speaking) by being converted to lactate. Another explanation is that for cells to recruit oxidative phosphorylation at high growth rates for their growth energy needs, they would need to invest significantly in the construction of mitochondria. This investment may not be worth the expenditure (Bouchez et al. 2020; Martins Pinto et al. 2023).

Also, the use of mitochondria requires active transport systems to shuttle key metabolites between the mitochondrial millieux and the cytoplasm. The aspartate-malate shuttle is a key example and may not be compatible with high growth rates. Since glycolysis is a cytoplasmic process, it may be faster and be able to provide energy in the form of ATP, albeit less efficiently, and maintain redox balance by the reduction of NAD by means of the energy-rich pyruvate to lactate enzymatic conversion. As a consequence, it is possible that mitochondrial expression can be down-regulated under conditions of high growth rate and/or when glucose is available in excess.

The pathways diagram also reveals that amino acids are intimately tied to this network of energy-producing reactions. It was noted in Section 3.5 that certain amino acids were either consumed or produced depending on which primary substrate was most available. The fate of many amino acids can be deduced from the cell's need for energy relative to its needs for biosynthetic precursors. **Table A1.a** reflects the control points associated with the TCA cycle intermediates leading to the synthesis or consumption of groups of structurally related amino acids. The common essential amino acids cannot be synthesized by most animal cells but can be used for anaplerotic purposes. The nonessential amino acids can also enter the TCA cycle through certain branch points or be synthesized by withdrawing the appropriate precursors. The removal of these intermediates is essentially the opposite of anaplerosis, known as cateplerosis.

Table A1.1: Control points associated with the TCA cycle intermediates.

TCA Cycle-associated Intermediates (Branch points)	Nonessential Amino Acids (Consumption or Synthesis)	Essential Amino Acids (Consumption Only)
Pyruvate (via Acetyl-CoA or Oxaloacetate)	Alanine Cysteine Glycine Serine	Threonine Tryptophan Threonine
Acetyl-CoA (via Acetoacetate)	(none)	Leucine Lysine Tryptophan Tyrosine
alpha-Keto Glutarate	Arganine Glutamine Proline	Histidine
Succinyl-CoA	(none)	Isoleucine Methionine Threonine Valine
Fumarate	Aspartate	Phenylalanine
Oxaloacetatae	Aspartate Asparagine	(none)
Glutamate (Amine group donor)	Glutamine and by transamination to all other nonessential amino acids	(can be deaminated)

A2. Additional models for cell growth, substrate consumption, and metabolite production

Over the past four decades, several models have been proposed to address metabolic dynamics that go beyond the semi-empirical model (Equation 2.4g) based on Pirt (1965). Since then, it has been found that structured models are better able to capture these dynamics in general, but they increase model complexity significantly. One of the first such models distinguishes between intracellular and extracellular substrate concentrations (Batt and Kompala 1989). To simplify the metabolic transformations, four intracellular component pools were included in the model: amino acids, including TCA cycle precursors (A), nucleotides, including DNA and RNA (N), proteins (P), and lipids (F). The model was structured such that it accounted for specific pools of metabolites within the cell. The sum of these lumped metabolite pools represents the total dry mass of the cell. Thus, the total rate of their increase is equal to the growth rate in mass units.

The synthesis rates of the internal pools are functions of the extracellular substrate concentrations of glucose (G) and glutamine (Q), as the only potentially limiting substrates. For example, Equation A2a represents the total rate of change of the internal concentration amino acid pool with terms for the individual synthesis and consumption of pool A.

$$r_A = k_{AG}^{max} NF_G * IF_A + k_{AQ}^{max} NF_Q * IF_A + k_{AAe}^{max} NF_{Ae} * IF_{Ae} - a_{AP} r_P - a_{AN} r_N - a_{AF} r_F - \mu A$$

Equation A2a

Where:

- r_A, r_A, r_A, r_A = Rates of synthesis of the internal pools, A, N, P, and F, respectively
- k^{max}_{AG} , k^{max}_{AQ} , k^{max}_{AAe}, k^{max}_{AG} = Maximum amino acid synthesis rates from glucose (G), glutamine (Q), and external amino acid concentration (Ae)
- NF_G , NF_Q ,NF_{Ae} = Nutrition factors for the contributions of G, Q, and Ae to the synthesis of amino acids
- a_{AP} ,a_{AN} a_{AF} = Stoichiometric coefficients for the production of pools P, N, and F from the pool (A) of amino acids

The final term (μA) represents the dilution of the internal pool A due to expansion of the growing cells. When this system of equations was applied to the data from Miller et al., a reasonable fit was achieved for both batch and continuous culture modes.

As an improvement to the four-component model of (Batt and Kompala 1989; DiMasi and Swartz 1995) built a structured model also with four intracellular components, but not the macromolecular precursors and cellular constituents. They included the internal concentration of glucose (G_i), glutamine (Q_i), pseudo-metabolites ATPi and $NADH_i$ representing the intracellular pools of energy carriers associated with ADP/ATP cycling and NAD/NADH cycling. Two energy metabolites were incorporated because they exert somewhat different influences on the critical biochemical pathway branch points; for instance, pyruvate can either be shunted to lactate or be used for other purposes. As an example of the model construction, Equation 2.4i represents the overall oxidation rate of NADH based on the availability of dissolved oxygen and reduced NADH, but inhibited by the end product ATP. The rate of change in the ATPi pool is then the difference in the rate of its production either by glycolysis or oxidative phosphorylation and the rate of its consumption, depending on the cell's energy needs for ATP-requiring processes (Equation 2.4j).

$$r_{ox} = k_{NADH}^{max} \left[\frac{O2}{K_{O2} + O2}\right]\left[\frac{NADHi}{K_{NADHi} + NADHi}\right]\left[\frac{1}{1 + (ATPi / K_{ATPi})^4}\right]$$

Equation A2b

$$r_{ATP} = r_{ATP}^{Production} - r_{ATP}^{Consumption} = \left[2 r_G + 2 (P/O) r_{OX}\right] - \left[\mu Y_{ATP} + m_{ATP}\right]$$

Equation A2c

Where:

- r_{ox} = Total oxidation of NADHi in the cell by means of oxidative phosphorylation needed to produce ATP
- K_{NADHi} = Monod-type saturation parameter depending on the availability of NADHi

Note the consumption term uses the same linear consumption model as already shown in Equation 2.4h. ATP production is modeled with typical saturation kinetics. DiMasi and Swartz also applied their model to the data from (Miller, Wilke, and Blanch 1988) and were able to demonstrate a superior fit of the data.

Another model proposed by (Zeng and Deckwer 1995) does not directly invoke cellular energy requirements. Building off an earlier model developed for microorganisms growing on multiple limiting substrates, they applied it to the dual substrates for animal cells (glucose and glutamine). Instead, it suggests that the specific consumption rate is made up of a minimum amount, as if the substrate were limiting cell growth, and an additional amount associated with the degree to which the substrate is in excess of this amount. However, if another substrate is available in excess, it will influence the uptake of the first. Thus, in the case of glucose, there is an additional term in the expression for the excess metabolism.

$$q_{Glc} = q^{*}_{Glc} + q^{E}_{Glc} = q^{*}_{Glc} + \left(\Delta q^{Glc}_{Glc} + \Delta q^{Gln}_{Glc} \right) \quad \text{Equation A2d}$$

Where:

- q_{Glc} = Total specific consumption rate of glucose
- q^{*}_{Glc} = Minimum specific consumption rate of glucose under substrate-limiting conditions
- q^{E}_{Glc} = Additional specific consumption rate of glucose associated with the excess availability of substrates, in this case, glucose and glutamine.
- Δq^{Glc}_{Glc} = Additional specific consumption rate of glucose due to excess of glucose
- Δq^{Gln}_{Glc} = Additional specific consumption rate of glucose due to excess of glutamine

The first term describing consumption under substrate limitation can be described with the (Pirt 1965) linear model presented above, which includes a maintenance quantity representing the absolute minimum consumption to maintain cell viability.

$$q^{*}_{Glc} = (\mu / Y^{max}_{Glc}) + m_{Glc} \quad \text{Equation A2e}$$

Where:

- q_{Glc} = Total specific consumption rate of glucose
- Y^{max}_{Glc} = Maximum biomass yield of glucose (minimum consumption) under substrate-limiting conditions

- m_{Glc} = Maintenance requirement for glucose

The terms describing the excess metabolism use a Monod-type saturation model.

$$\Delta q_{Glc}^{Glc} = \Delta q_{Glc}^{Glc(max)} \left[\frac{\Delta Glc}{\Delta Glc + K_{Glc}^{Glc}} \right] = \Delta q_{Glc}^{Glc(max)} \left[\frac{(Glc - Glc^*)}{(Glc - Glc^*) + K_{Glc}^{Glc}} \right] \quad \text{Equation A2f}$$

$$\Delta q_{Glc}^{Gln} = \Delta q_{Glc}^{Gln(max)} \left[\frac{\Delta Gln}{\Delta Gln + K_{Glc}^{Gln}} \right] = \Delta q_{Glc}^{Glc(max)} \left[\frac{(Gln - Gln^*)}{(Gln - Gln^*) + K_{Glc}^{Glc}} \right] \quad \text{Equation A2g}$$

Where:

- $\Delta q^{Glc(max)}{}_{Glc}$ = Maximum additional specific consumption rate of glucose due to excess of glucose
- ΔGlc = Differential glucose concentration between the limiting concentration and the actual concentration in the extracellular medium
- $K^{Glc}{}_{Glc}$ = Half-saturation constant associated with additional consumption of glucose due to the excess glucose
- Glc* = Concentration of glucose at which it becomes limiting.

Equation A2g represents the cross-over influence of glutamine on the consumption of glucose. The consumption model for glutamine is analogous to the above equation set for glucose. A term for the cross-over influence of excess glucose on glutamine consumption can be included if glucose does affect glutamine metabolism. Using this model, Zheng and Deckwer (1995) were able to predict glucose and glutamine consumption rates over a wide variety of animal cell culture data.

In general, the more complex the model, the more parameters are required. These parameters then need to be determined from experimental data, requiring a significantly greater investment in laboratory-based work and model construction. The challenge then remains to build a model that will adequately simulate the cell culture process to be of value in assessing bioreactor performance while minimizing the effort.

A3. Detailed effects of lactate and ammonium on cell metabolism

As further evidence of the complexity of metabolic interactions, it has been shown that the main end-products of glucose and glutamine catabolism, namely lactate and ammonia, have a feedback effect on the cells' metabolic quotients. Several studies have measured the response of various cell types when exposed to elevated levels of these waste metabolites.

Figure A3.1 illustrates the effect of lactate concentration on both glucose- and glutamine-specific consumption rates. A few studies looked at concentrations as high as 68 mM. Despite this large range, the impact on both substrates was relatively mild. However, the trend appears to depend on the cell line, but most probably on other differences in the media and conditions used in the studies.

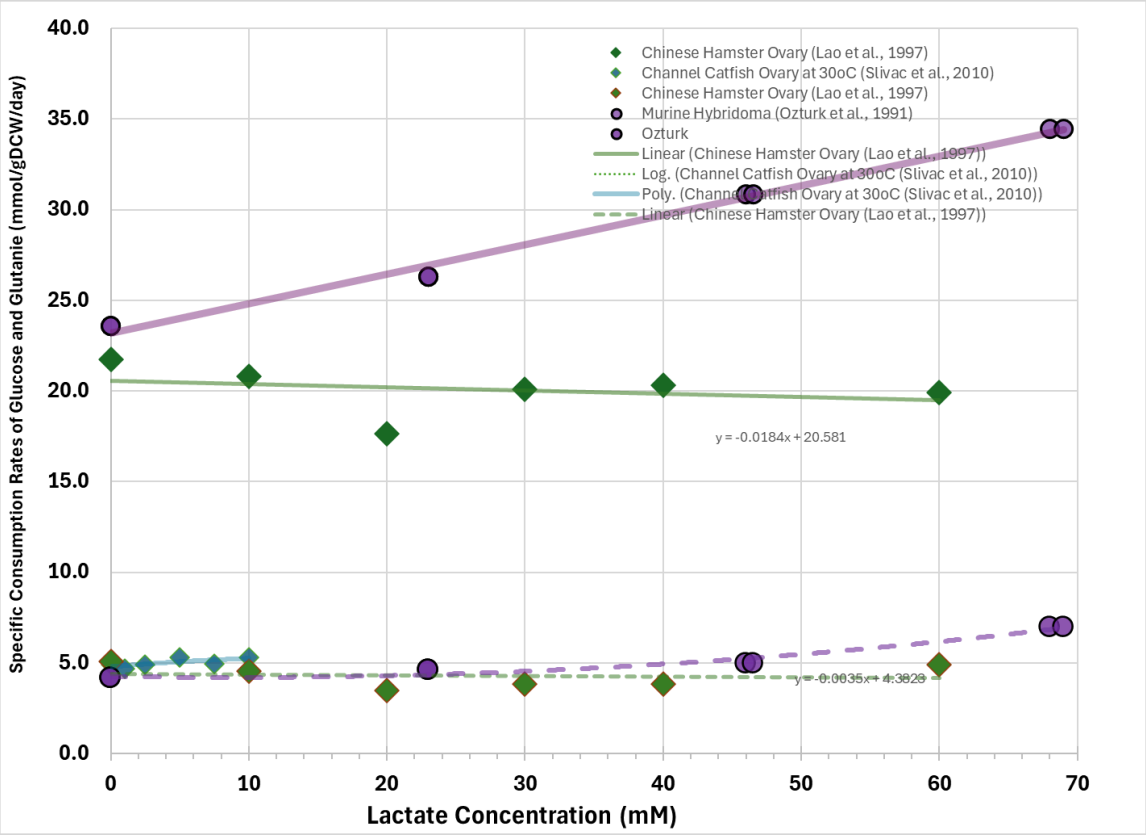

Figure A3.1: Effect of lactate concentration on glucose- and glutamine-specific consumption rates. Solid lines show glucose response and dashed lines show glutamine.

The impact on glutamine uptake was negligible, while glucose consumption increased for a hybridoma cell line but slightly decreased for a CHO cell line. **Figure A3.2**, on the other hand, shows a very strong effect of lactate concentration on its molar yield from glucose. The trend is distinctly negative for all three cell lines included, a clear sign of feedback inhibition of lactate on its own production through glycolysis.

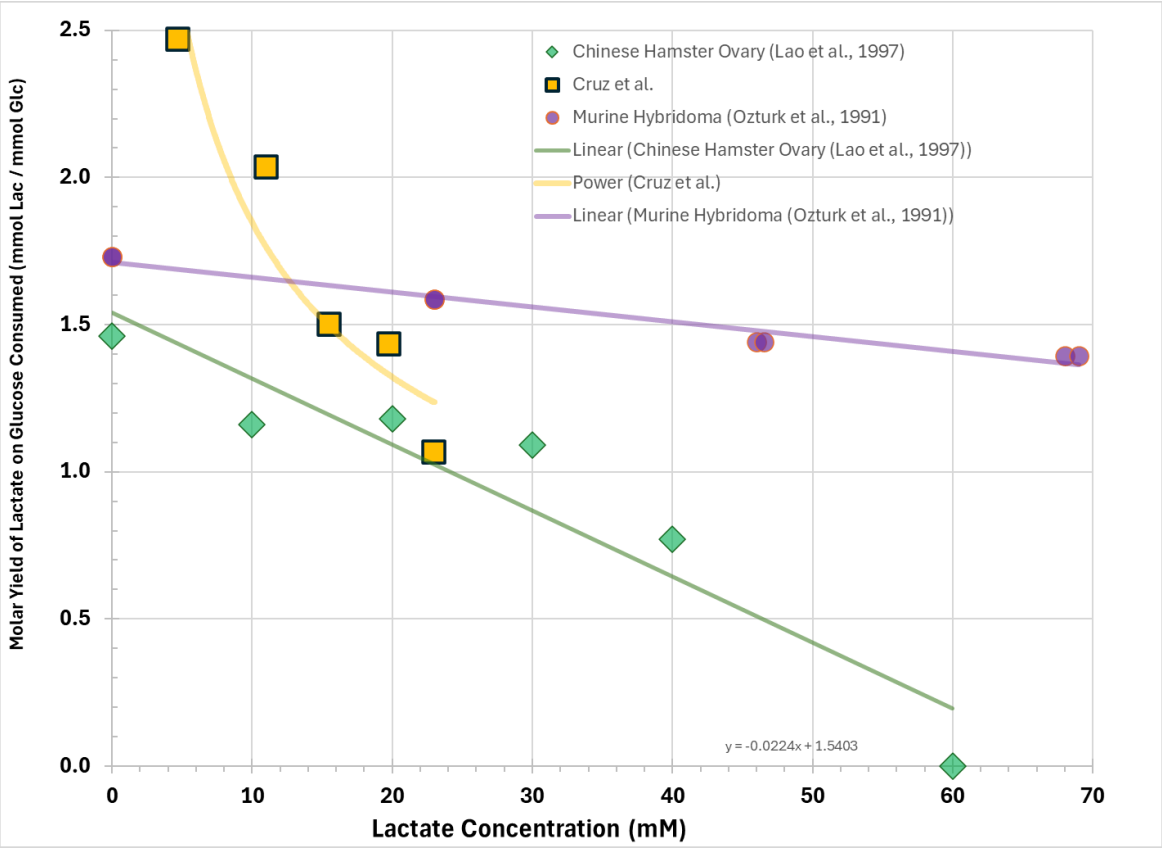

Figure A3.2: Effect of lactate concentration on the lactate yield on glucose.

The trend in **Figure A3.3**, showing the impact of lactate on the molar yield of ammonia produced on the glutamine consumed, is less clear. There appears to be a gentle downward trend with increasing lactate concentration, suggesting that less glutamine is needed for energy if glucose is being used more efficiently. The data with trend lines associated with them were from continuous culture experiments, while the data on the BHK cells were derived from a batch culture with many more factors changing at the same time.

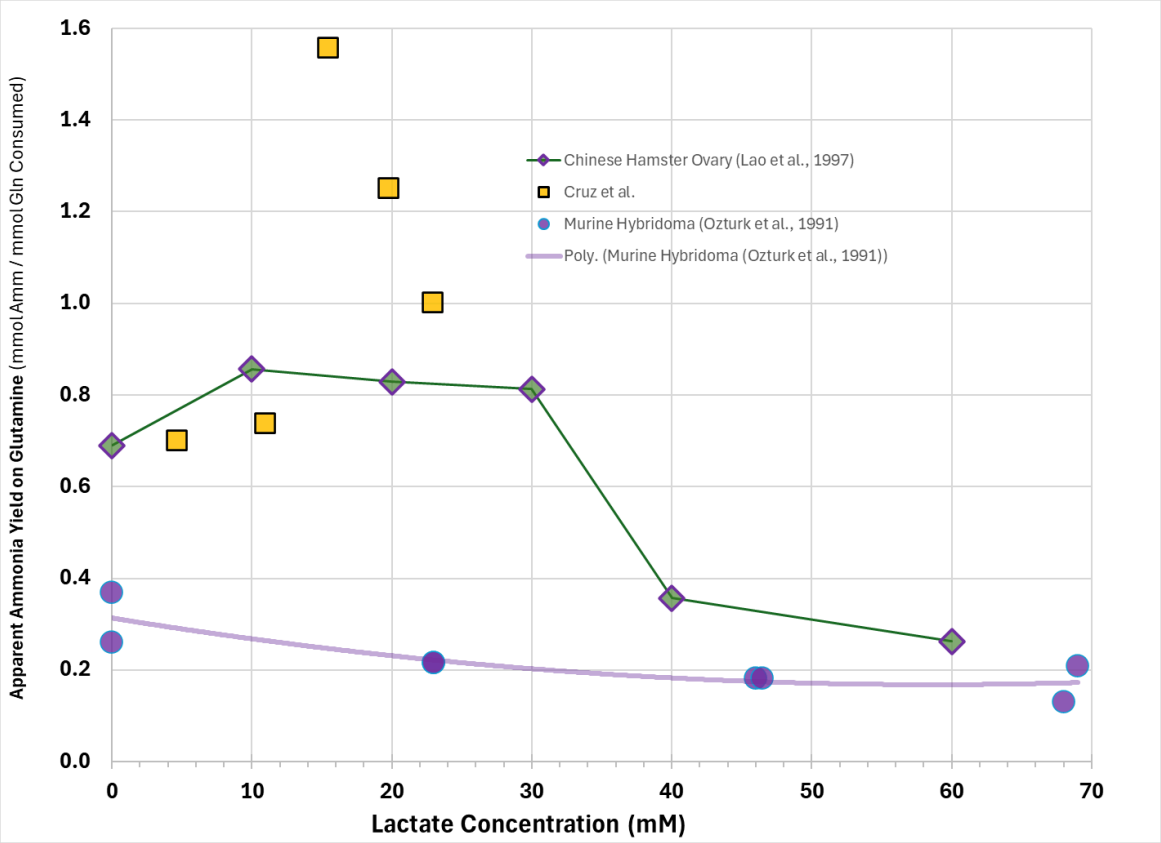

Figure A3.3: Effect of lactate concentration on the molar yield of ammonia on glutamine consumed.

In addition to studying the effect of lactate on steady-state metabolic quotients, Miller et al. also studied the impact of sudden changes in lactate concentration (Miller, Wilke, and Blanch 1988). For this, they subjected a chemostat culture at steady state to pulse and step changes of lactate concentration. **Figure A3.4** shows the culture's response to a pulse of lactate when its concentration was suddenly increased from the steady state level of 25 mM to 44 mM by spiking the culture with a concentrated solution of sodium lactate. Catabolic end-product formation rates were traced as the excess lactate was slowly washed out of the bioreactor.

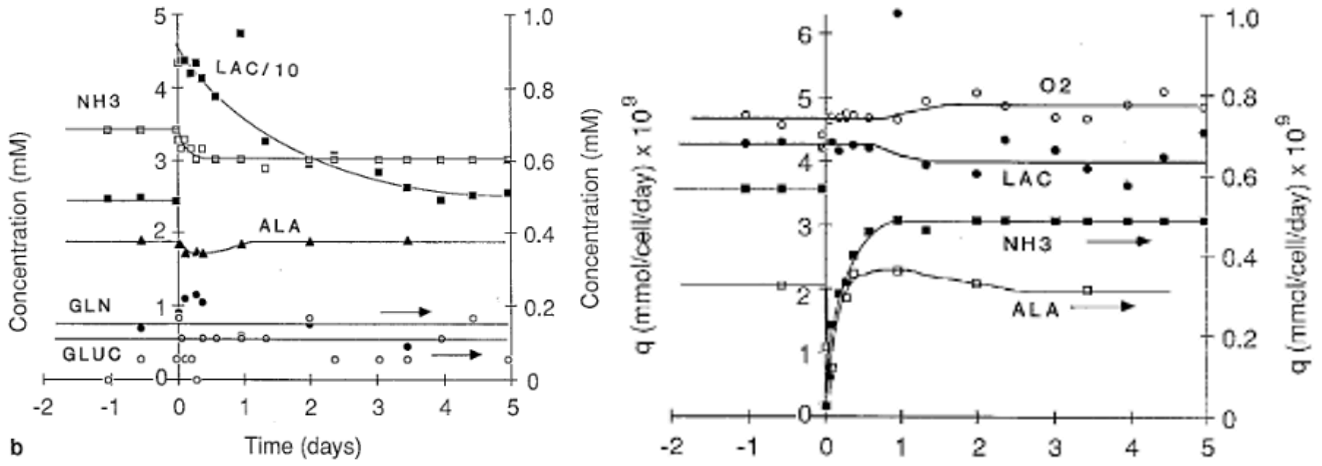

Figure A3.4: Response of a murine hybridoma cell line to a pulse change in lactate concentration. The time courses included are for ammonium concentration, and lactate-, ammonium-, and alanine-specific production rates.

Immediately after the pulse, there was a slight decrease in cell concentration, which might be expected due to the inhibitory effect that lactate (and osmolality) can have on growth rate. The specific consumption rates of glucose and glutamine did not change appreciably, while there was a modest increase in oxygen uptake and a decline in the specific lactate formation rate, again suggesting feedback inhibition of the elevated lactate concentration on glycolysis. Much more pronounced was the rapid change in the formation rates of glutamine's main catabolic end products, ammonium and the amino acid alanine. There was an immediate drop in the specific production rates of both metabolites, followed by a rebound within hours of the pulse. Alanine, another by-product of catabolism, was also tracked. Its specific production rate returned to its pre-pulse level within roughly 8 hours; however, ammonium production did not return to its original level for days post-pulse, remaining about 15% below its prior rate. The authors suggest that more of the glutamine was oxidized after the pulse, presumably to make up for the decrease in energy derived from glycolysis.

As pointed out in Section 3.4 regarding waste metabolite inhibition on cell growth, cells are able to adapt to prolonged exposure to these same metabolites. The above lactate pulse experiment was clearly an acute and sudden exposure. However, cell lines adapted to higher lactate concentrations showed a dramatic reduction in the buildup of this metabolite. For lactate-adapted CHO cells, Freund and Croughan showed that the corresponding lactate yield per glucose ($Y_{Lac/Glc}$) could be reduced to approximately 0.39 (Freund and Croughan 2018). In contrast, osmotically adapted CHO cells maintained the higher $Y_{Lac/Glc}$ of 1.41. Moreover, the lactate-adapted CHO cells not only produced less lactate but also showed improved tolerance to high extracellular concentrations, and even evidence of lactate reuptake during the later stages of culture. The result was higher cell concentrations and culture productivity, and about an 8-fold reduction in base addition to maintain pH. Interestingly, ammonia production was also suppressed.

Metabolic Influence of Ammonia Accumulation

The accumulation of ammonium in culture influences metabolic fluxes to a similar degree as lactate, albeit at significantly lower concentrations. This difference is likely related to the same reasons ammonium has a greater inhibitory effect on cell growth, particularly when the exposure is acute. **Figure A3.5** shows the impact of ammonium concentration on the specific consumption rates of both glucose and glutamine. Unlike lactate, the impact on glutamine uptake is more pronounced; however, the trend is different for the cell lines included. Glutamine uptake is unchanged with a CHO cell line and increases with a hybridoma.

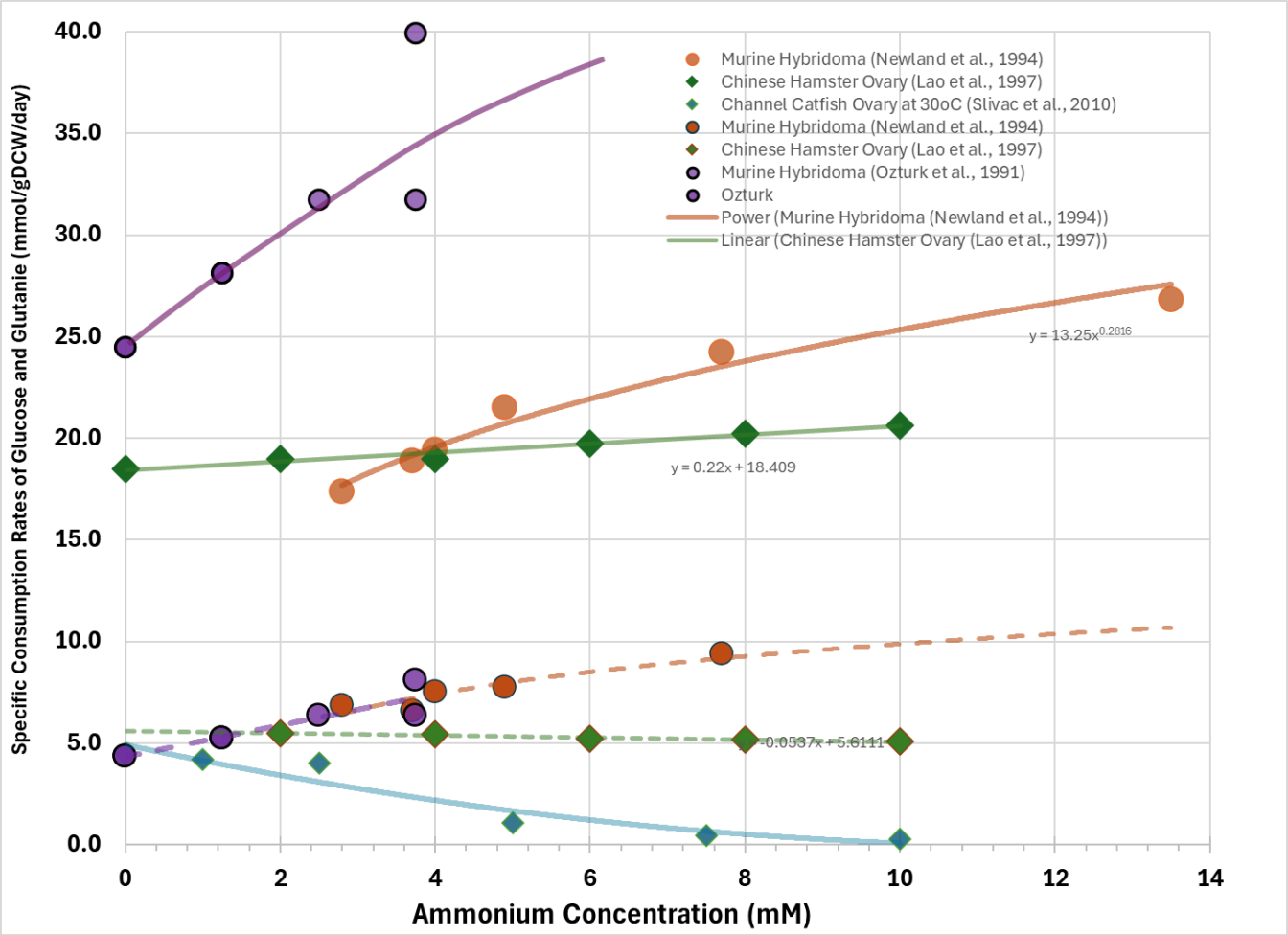

Figure A3.5: Effect of ammonium concentration on the specific consumption rates of glucose and glutamine. The solid lines show the suggested relationship for glucose and the dotted lines for glutamine.

Cruz et al. observed that in BHK cultures, the interplay between lactate and ammonium is highly dynamic (**Figure A3.6**). They observed the shift from lactate production to reuptake, discussed in the lactate section, occurred in parallel with decreasing ammonium levels, supporting the view that coordinated regulation of both metabolites is central to achieving high cell density and productivity (Cruz et al. 2000). Like Freund and Croughan for lactate-adapted CHO cell lines, Cruz et al. also

observed a reduction in specific ammonia production rates, indicating that metabolic engineering or selective pressure can reduce ammonium output while maintaining productivity.

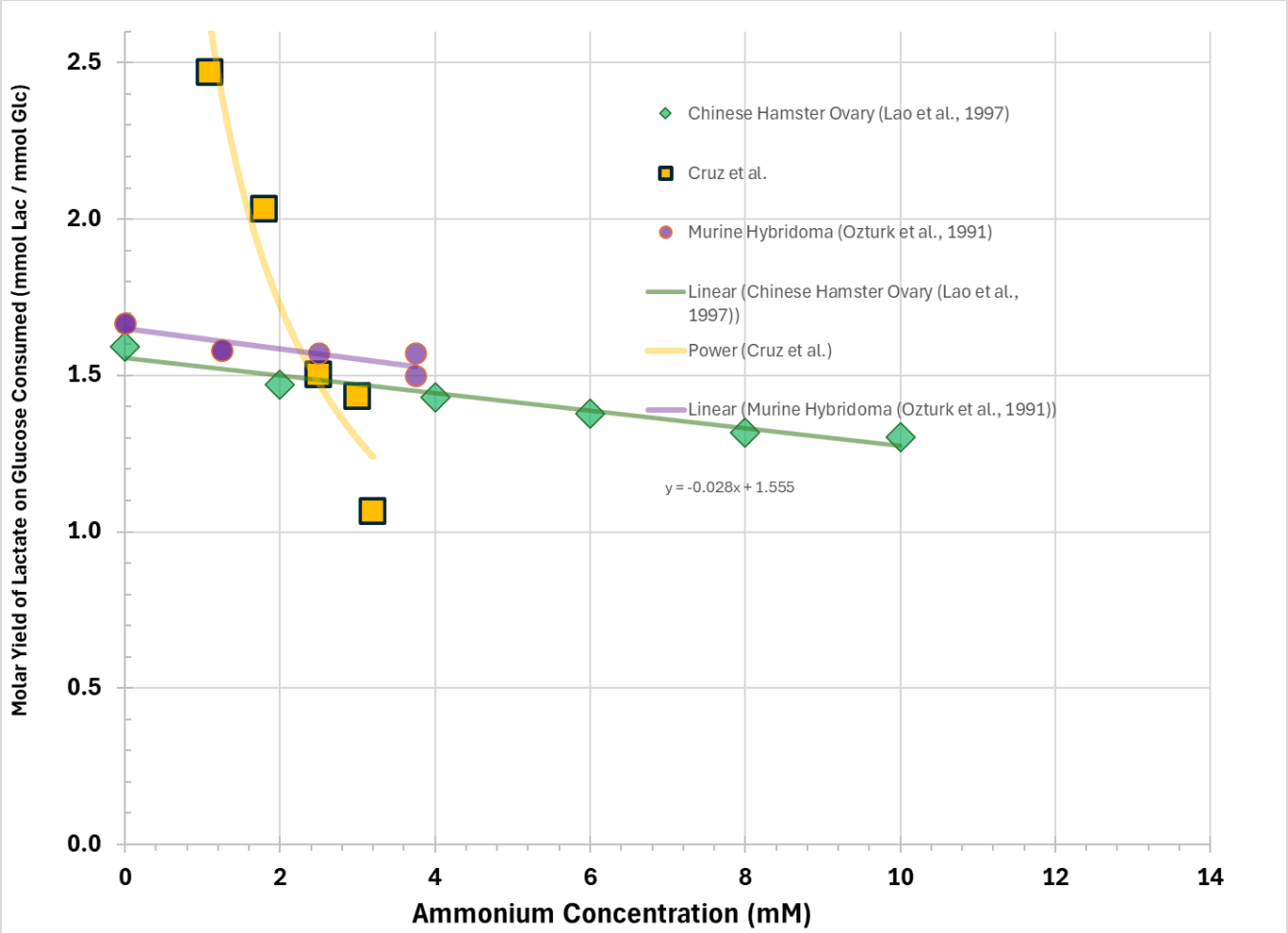

Figure A3.6: Effect of ammonium on the molar yield of lactate from glucose

In terms of glucose consumption, all three cell lines show an increase with increasing ammonium concentrations, but at different slopes. The hybridoma is the most sensitive and the CHO is relatively unaffected. The specific glucose consumption is dramatically lower for an aquatic species than for the other three lines, possibly due to the lower growth temperature and the consumption of other substrates. Not surprisingly, increased ammonia concentrations have a feedback effect on the metabolite's own formation, shifting glutamine metabolism toward alanine production. In the study by Ozturk et al., ammonia levels as low as 4 mM halved the growth rate of hybridoma cells and triggered metabolic shifts that included decreased glutamine-to-ammonia conversion and increased alanine production (Ozturk, Riley, and Palsson 1992). **Figure A3.7** shows the impact of ammonium on the total yield of ammonia as a ratio to glutamine consumption for some other cell lines. All show a decline in ammonium yields with increasing ammonium concentration.

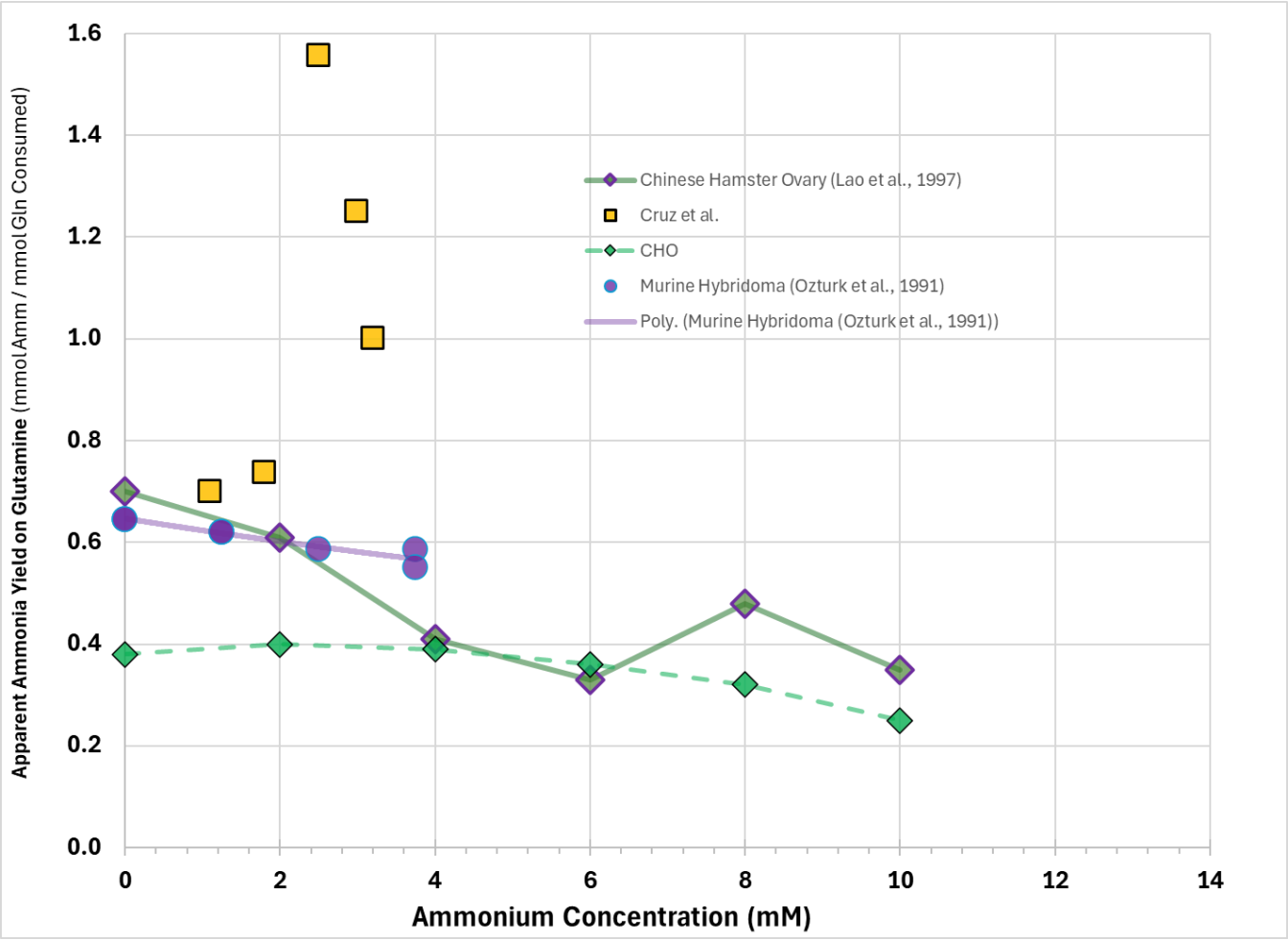

Figure A3.7: Effect of ammonium concentration on the molar yield of ammonia from glutamine.

Using the same methodology explained above for lactate, Miller et al. also studied the impact of sudden changes in ammonium concentration on metabolic yields. After subjecting a chemostat culture to a pulse of ammonium, a similar set of substrate consumption and metabolite production profiles, with the exception of alanine, was observed as the spiked ammonium washed out of the continuous bioreactor. Whereas both ammonium and alanine dropped precipitously immediately after the pulse of lactate, alanine did the opposite when the culture was spiked with ammonium. Its production increased rapidly at first and then declined back to its steady state value as the excess ammonium was removed. These transient dynamics underscore the interconnected control of catabolism. In this case, the higher ammonium concentration inhibited the pathway to its own formation, pushing the excess amine moieties towards alanine instead.